APPLICATION OF MODERN CONTROL TECHNIQUES TO A DISTILLATION COLUMN

Volume 1

TAOFEEK OLADIRAN FOLAMI (BSc, MSc)

Doctor of Philosophy

THE UNIVERSITY OF ASTON IN BIRMINGHAM

April 1989

THE UNIVERSITY OF ASTON IN BIRMINGHAM

APPLICATION OF MODERN CONTROL TECHNIQUES TO A DISTILLATION COLUMN

Taofeek Oladiran Folami

PhD 1989

SUMMARY

Modern control techniques have been applied to a distillation column. Three control techniques were selected for evaluation. These are; a decoupling and disturbance rejection control scheme; an estimator aided control techniques using a Kalman filter; and an implicit generalised minimum variance self tuning control. A 10 tray pilot scale binary distillation column, interfaced with a microcomputer, was used for investigation of the process control techniques. A non-linear model of the column was developed. The reliability of this model was demonstrated. The model was therefore used for the design, analysis and screening of control systems for the pilot plant distillation column.

The results of extensive simulations on linearised state variable models of the column simulator demonstrate that the decoupling and disturbance rejection controller works in the presence of load disturbances and setpoint changes. The proper choice of the values of a diagonal matrix in the precompensator of the controller required for accurate setpoint tracking has also been shown. By analogy with PI control, integral and derivative modes have been introduced into the controller to equip it with the ability to remove offsets. Simulation results demonstrate that the sensitivity of the controller to non-linear effects makes the controller inoperable on the column simulator, as well as on the pilot plant. Therefore, the use of an adaptive form of the controller is necessary to compensate for the non-linear effects and other model errors for on-line application to be practical on the pilot plant.

On-line implementation of the Kalman filter algorithm using a linear state variable model of the column simulator as the filter model, was not possible because of the large memory requirement of the software, long execution time and the inability to produce satisfactory estimates of all the tray compositions.

Simulated and experimental studies for both single temperature control and dual temperature control of the distillation column, demonstrated that self tuning control can provide tighter control of the products of distillation columns than PI control.

An algorithm, called the Simplified Correction (SPC) method, has been implemented to prevent the parameters of a self tuning controller from reaching unsatisfactory values when the closed loop system is not sufficiently excited. Simulations show that the SPC can provide significant improvements even when only a subset of the controller parameters are prevented from attaining bad values.

The findings in this work verify the degrading effects that model errors have on controller performance. Areas for future work have been suggested in the case of the on-line implementation of the control schemes selected in this work.

Key Words: Self tuning control, Decoupling and Disturbance Rejection control, Parameter Correction, Simplified parameter Correction, Distillation Column.

This thesis is dedicated to my mother, Rashidat Olayinka Folami, to my late brother, Salmon Ayodeji Folami, and to the rest of my family; Sabitu Olaore Folami, Muyibat Wonuola Folami, Alhaja Nofisat Idewu, Sabitu Olayinka, Abubakar Oladotun, Uthman Oluwakemi, Hakeem Oludare, Kamal Ademola, Sarata, Yewande, Bolakale, Rotimi

Acknowledgements

I wish to thank Dr J.P. Fletcher for his supervision of this research work, and for his patience and valuable suggestions on this thesis.

I wish to Dr A.P.H. Jordan for his assistance and encouragement during the course of the research work.

I would also like to thank

Dr B. Gay for allowing me to use the computing facilities at the Depertment of Computer Science α Applied Mathematics;

The University of Aston in Birmingham for financing me and for providing all necessary equipment;

Diane Stretton for her typing of part of this thesis;

Phillipa Forde for her help in preparation of this thesis;

My friends, Numfor Ajongwen, Sama Nwana, Mohammed Sarki and all my colleagues in the Department of Chemical Eingineering and the Department of Computer Science and Applied Mathematics for their encouragement throughout the course of this work.

Finally, I should thank my family for their support throughout my education.

List of Contents
Volume 1

List of Contents
Volume 2

List of Figures
Volume 1

List of Figures
Volume 2

List of Tables
Volume 2

List of Plates
Volume 1

This page is left intentionally blank

CHAPTER ONE

Introduction

1.1 Introduction

The control of a physical system involves taking action to counteract any disturbances that may have adverse effects on the state of the system. The disturbances could be due to changes in the environmental conditions or may be introduced by an operator if a change in the state of the system is desired. In the chemical industry process control is central to the smooth and safe operation of plant as well as improving plant economy.

Any equipment designed to effect the change of physical or chemical properties of the raw materials on a commercial scale can be considered as a chemical plant. Often such plants consist of arrangements of connected units such as chemical reactors, heat exchangers, pumps and distillation columns, all arranged in a systematic manner in order to convert raw materials into desired products. The products of the plant are to be made to the desired specification in a safe and environmentally acceptable manner, using the available energy sources in the most economical manner. During plant operation, the physical limitations of the equipment must not be exceeded, nor should some process variables exceed some specified bounds for reasons of safety and environmental regulations. Account must also be taken of external disturbances such as noise, weather changes and changes in the raw material compositions. The operation of chemical plant must therefore be continuously monitored and controlled to ensure all the operational objectives are being satisfied. The control of the entire chemical plant is the culmination of the control of the primary variables of the individual processing units. The primary variables will influence the final product and each unit will have its own operational objectives and physical limitations which must be satisfied.

In the face of a disturbance, one approach to control is to wait for the effect of the disturbance to manifest itself and then take proper corrective, or control, action. This is known as *feedback* control since the output of the process is "fedback" to the

controller as expressed schematically in Figure 1.1a. This brings into being a *closed loop* system The control action is based on the amount of deviation of the output from the desired value. The input that is manipulated in order to bring about this effect is the *manipulated*, or *control*, input; the output that is under control is called the *controlled* output.

Feedback is the most commonly used approach in all fields of engineering. Another approach to control is to perform the corrective action before the disturbance materializes on the output of the process. This is achieved by anticipating the effects of the disturbance using a model of the process and measurement of the disturbance. This is *feedforward* control and is expressed schematically in Figure 1.1b. Both feedback and feedforward methods can be combined in order to improve the quality of control of the system. The intent is that the feedforward counteract most of the effects of the disturbances and the feedback provide residual control and setpoint tracking (Rinard (170))

One of the earliest control methods include the flyball governor and the most common early control methods were based on manual adjustment of the inputs of the process. The development of measurement devices and automatic control valves has permitted automatic control, where control is performed continuously by mechanical, electrical and pneumatic devices. These are commonly referred to as analogue controllers. The methods commonly used to obtain the controller settings, which determine how much the input is to be changed subject to the deviation of the output from the desired values, are classified generally as "classical design theory". These design methods are called classical, or sometimes, conventional design methods and they include those of Cohen and Coon (203) Ziegler and Nichols (191), Nyquist, and Bode, which are all treated in Stephanopoulos (116). The methods are based on the assumption that the process is linear and is described by simple transfer functions. They are suitable for designing single loop controllers which have one control, or manipulated, input and one controlled output, both of which must be paired appropriately. Each control loop is designed independently, without taking into

account of interactions that may exist between the controllers when they are in operation.

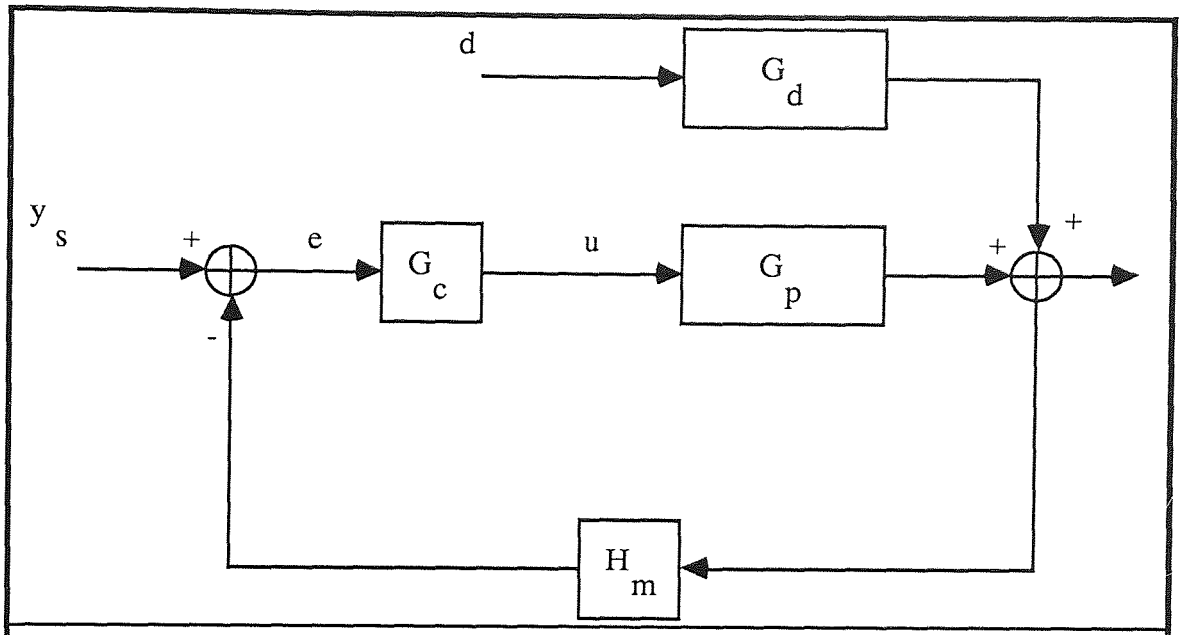

Figure 1.1a General structure of a feedback controlled system

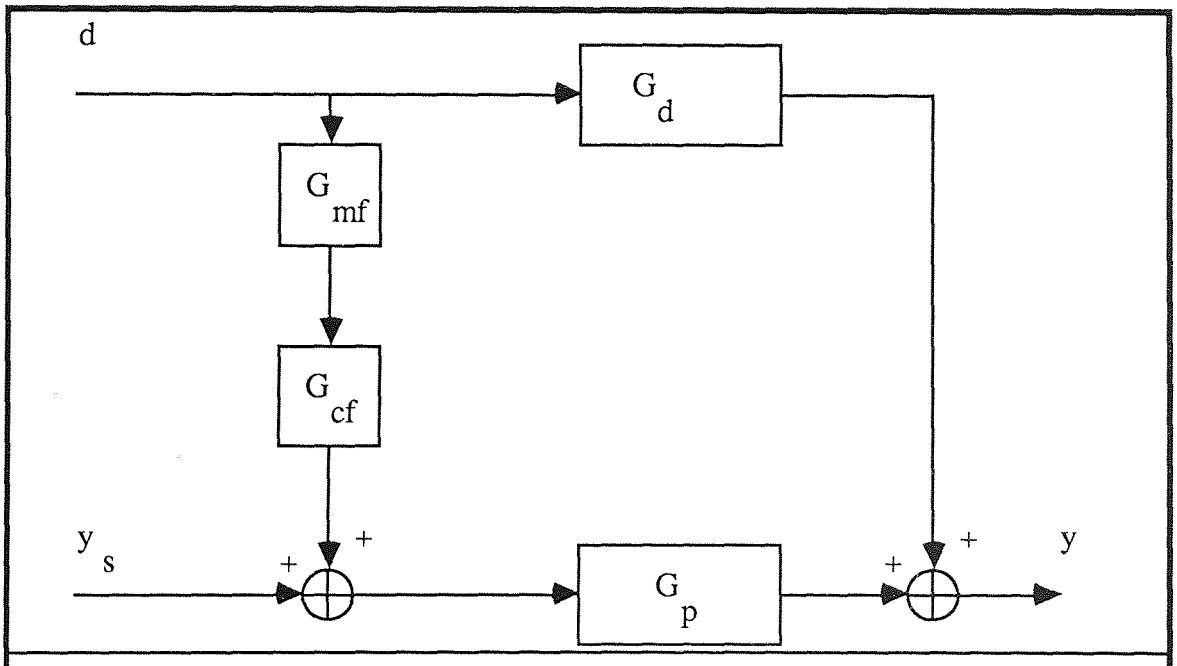

Figure 1.1b General structure of a feedforward control system

Notation

d is disturbance, u is the input, e is the error signal y is the output and y_s is the setpoint. G_p, G_d are the process transfer functions relating the input to the output and the disturbance to the output. H_m, G_{mf}, G_{cf}, G_c and are the feedback measurement, disturbance measurement, the feedforward controller and the feedback controller transfer functions

1.2 Requirements of a control system

An important step to control systems design is to determine what the control system is meant to do and what performance is expected of it. Practical process control criteria generally belongs to types involving product quality, economic, safety and equipment limitations and the paramount requirement of the control system is to maintain stability of the closed loop system.

The qualities of an ideal control system are perfect disturbance rejection and perfect setpoint tracking, in other words "perfect" control; this is where the output tracks the desired trajectories perfectly and where the effects of disturbances are not evident in the closed loop response. This is, however, an idealistic feature which can rarely be attained in practice due to various reasons such as material holdups in the process, delays due to mass and energy transport, measurement delays and various limitations of the equipment. The desirable qualities of a control system are, thus, good regulatory control and quick and smooth setpoint tracking capabilities. Other desirable qualities of a control system include, (1) robustness to errors in the model used to design the controller, since it is usually the case that a model of the process is involved at the design stage, (2) robustness to instrument failure (3) insensitivity to changes in operating conditions (4) avoidance of excessive control action and (5) avoidance of controller saturation. Some of these requirements will result in conflicting controller designs. It is therefore usually the case that a compromise must be met to satisfy various criteria. For example, in the high performance case with the requirement of fast setpoint tracking and fast disturbance rejection, the control action will generally be required to be fast in order to bring the system to the new state quickly. This would usually require excessive control actions and oscillatory response of the output and easy saturation of the manipulated input. Robustness is usually achieved by slowing down the control action.

1.3 Previous industrial practice and motivation for change

The most widely used conventional feedback controller is the proportional-integral-derivative (PID) controller which the conventional design methods are commonly used to assist their tuning. The PID algorithm is widely used in industry. It has a long and proven history of applications such that it has become the standard by which all other forms of controller designs are assessed (Shaffii (115)). Ray (104) pointed out that in the 1960s simple control schemes like the PID, in analogue form, were commonly used for automatic control. Installation of the hardware was costly, so that only a limited number of control loops could be justified on a chemical plant. According to Ray, these simple control schemes worked well because industrial processes were large, slow responding systems and were usually stable even without a controller. Plants were generally overdesigned and intermediate storage tanks were widely used to dampen out fluctuations and, therefore, helped to compensate for inadequate control. Product specifications and safety specifications were loose and energy efficiency was permitted. Ray concluded that the incentive for improving control were therefore quite low.

In the last 20 years there have been new developments that have provided the incentive to develop better ways of designing chemical plants and their control systems. Most chemical companies have been under pressure to operate their plants more efficiently, increase their productivity, reduce their operating cost and energy consumption. The market also demand for consistently high quality products. The main objective of these companies is to achieve financial benefits, be competitive in the market and thus stay in business. There are also stricter safety and environmental regulations that must be met. For these reasons, capital investment has gone into the construction of many large and continuously operated plants to replace the older ones, and to increase the integration between the processing units in order to make better use of the energy and raw materials. The consequence of this is the increased complexity of plant and a more complex and interconnected control structure for the plant. This in turn gives an increased possibility of failure of instruments and control systems; the consequence of which could be severe to the environment due to the large scale and

continuous nature of chemical plant. The incentive therefore exists for developing reliable high quality, high performance and robust control systems for modern chemical plants.

1.4 The use of digital computers in process control

Digital computers are now available to perform automatic control. In computer control the computer replaces the hardware and, since the control is then done in digital form. The control laws can be programmed in the computer and the control performed cheaper and more efficiently than hardware. There is also the opportunity to use more complex control schemes which would be difficult to apply with mechanical, pneumatic and electrical devices. The performance of real time process computer and microcomputers has improved greatly while prices have fallen significantly over the last 15 years. This has made it possible to easily justify the installation of computers to monitor, schedule, and control the chemical plant on the basis of improved safety, reduced labour costs and reduced cost of controller hardware (Ray (104), Benson (148)). There have also been significant improvements in on-line measuring devices such a flowmeters, composition analysers and thermocouples (Gunderlach (186)). There is evidence that many plants are now under computer control and financial benefits have been obtained (Stephanopoulos(116)).

1.5 Inadequacies of conventional methods and the need for new approaches to control systems design

Conventional controller design methods frequently cannot provide control systems that meet the demand for high performance, robust and more reliable control systems required for modern chemical plant. In the first place, the methods assume that the process is linear. Linear models are only valid approximately since chemical processes are usually non linear. Therefore, if the operating conditions of the system change significantly, new controller parameters may need to be found or control action slowed so as to ensure good control at the new operating point. The presence of significant time delays and time lags between the input change and the output response will have a

destabilizing effect on the controlled system. Such delays and lags may be due to fluid transport in pipelines, measurement delays and measurement lags. For example, the presence of time delays in the system will reduce the maximum controller gain of a PID controller that can be used before the system becomes unstable. If measurements of the variables needed for control are not directly available, because the variable may be difficult, expensive or even impossible to measure, a conventional controller cannot be applied directly. In such a case a method must be devised in order to infer accurate values of the variables needed for control from secondary measurements which relate, in some way, to the required variables.

When more than one variable of a process is to be controlled, interaction between the control loops will exist due to interations between the process variables.The classical design methods do not take account of interactions that may exist between the variables of the process as the methods are suitable for designing SISO controllers only. Therefore, when more that one process variable is controlled by conventional SISO controllers the combined performance of the multiple loop control system may be poor and non linearities and time delays will simply make the situation worse. The selection of the appropriate pairing of the manipulated and controlled variables is also very important in such situations, so that the designer must use his knowledge about the process to select the appropriate control configuration. In the presence of interactions among the control loops, it is, strictly speaking, not satisfactory to consider each control loop as independent. A design method that handles several variables is required. This is known as multivariable control.

The various inadequacies of classical controller design methods provided the incentive for developing better methods of performing control in all fields of engineering. The result is that significant progress has been made in the development of new control techniques and there is now a wide variety of advanced control techniques available as alternatives to the classical design methods. In general, any method that departs from the classical design methods is called an advanced control technique. Advanced control systems design methods range from simple feedforward control to multivariable control through to adaptive control where the controller

parameters are changed according to changes in operating conditions. Many of these design methods, particularly the multivariable design methods, are classified under the general heading of " Modern Control Theory". Many have arisen from fields of engineering such as the aerospace and electronics industry (Bell and Griffin (15), Ray (144)). Some methods are extensions of single loop frequency domain design methods, such as Nyquist and Bode methods, to multivariable systems. Advanced control techniques can, in principle, solve many of the problems encountered in chemical process control, but there is a wide range of problems to be addressed and no single technique can solve them all (Foss (33)).

Compared with conventional controllers such as the PID, advanced control techniques usually involve more complex calculations to obtain the controller parameters and implement the resulting control policy. On-line digital computers are needed for their implementation since to design mechanical, pneumatic or electrical hardware for there implementation would be difficult, or even impossible to do. The basis of most advanced control techniques is a mathematical model of the process, therefore, mathematical modelling and process identification techniques are valuable tools for the design, analysis and implementation of advanced control systems. In fact, with the complexity now required for the overall control system of modern chemical plant, a good knowledge about the behaviour of the processes over a wide range of operating conditions is required by the control systems designer. This means that the first stage in the design of a control system for a process usually involves building a mathematical model of the process that will be valid over a wide operating range. The availability of cheaper and powerful computers has made the task of process simulation easier, as large complex calculations can be performed much more easily. This has increased the scope for applying advanced control techniques.

1.6 The extent of application of advanced control in the chemical industry

Despite the theoretical advantages of advanced control methods and the availability of cheaper, powerful and flexible computers and microcomputers, the application of

advanced control schemes to industrial chemical processes has been, and still is, limited. The PID algorithm is still the most widely used in industry (Benson (148), Rinard (170) and Clarke and Gawthrop (22)) and computers have been mainly used to make their implementation more cost effective and reliable (Clarke and Gawthrop (22)) . Computer simulations using process models have been frequently used to demonstrate the benefits of most advanced control schemes.

Several factors are responsible for this state of events. One is because advanced control techniques involve complex calculations for controller design and implementation of the control policy and this complexity tends to discourage their use. This is particular true if the plant engineer is not familiar with the calculations, which, it can be said, is often the case.

The practicability of many advanced control schemes have also been question. Critics such as Foss (33) have criticised several multivariable controller design methods that do not address the real problems such as non linearities, control loop pairing and estimation of unmeasurable variables in chemical systems. He gives examples of situations were failures have occurred and are likely to occur in the direct applications of multivariable design methods that assume linearity of the process. The assumption of linearity of the process can rarely be valid for chemical systems which are inherently non linear with parameters that change unpredictably: while such models can adequately describe a large number of mechanical and electrical systems even if high performance control systems is required (Ydstie et al. (146)). While this is true in many cases, there are a significant number of methods which, in theory, do not fall in this category, but are still not widely used. An example is adaptive control design methods based on continuous on-line identification of a model of the process which is then used to update the controller parameters. The availability of more flexible and powerful computers that make their real time implementation relatively easy. The superiority of many of adaptive control methods over conventional methods have been demonstrated, but they have not had extensive application at industrial level; they are still perceived difficult to use in industry (Dumont (176)).

A major contributory factor to the limited use of advanced control systems in industrial processes has been attributed to the reluctance of industrial practitioners to adopt new ideas. This is the point of view of some including Bell and Griffin (15) and Shaffii (115). According to Shaffii, industrial practitioners are usually not interested in applying new control methods unless the methods have had a long and proven history of applications, reliability and satisfactory performance. This is strongly supported by the fact that some industrial processes like distillation and absorption columns are still controlled manually, according to Skogestad and Morari (153).

There is now wider opportunities to bring advanced control into practice in the process industries. According to Asbjornsen (2), many companies now regard improved process control as a significant contributor to plant economy in the future. One reason he gives for this is that these companies perceive that the exploitation of increased integration of processing units and exploitation of economies of scale to increase productivity and plant economy as a whole, will soon be exhausted. Ray (104) gives another reason, which is that engineers trained in advanced process control are now reaching positions of responsibility. They can, therefore, assess the practical advantages of these advanced control methods in industrial environment and influence their wider applications on the industrial processes.

Furthermore, there are many older plants which still have significant operating life and where it may be more cost effective to invest in improving control rather than building a new plant. Increasing knowledge about the operation of such processes has been gained over the past years so that adequate steady state and dynamic models for many chemical processes can now be developed to the point were they can be used for control systems design and detailed analysis by computer simulation. This will make the analysis of advanced control methods by computer simulations more realistic and convincing so that they will be useful in determining the practicality of the methods. It is also important the the synthesis of the control system can be done conveniently. Even though the calculations may be lengthy and complex, the control engineer should be carried along the synthesis and the implementation of the control scheme with relative ease, as this will help promote the use of the design method. This factor has

greatly promoted the development and the use of interactive computer packages for control systems design and analysis over the last decade.

1.7 This Research

Having given some factors responsible for the limited use of advanced control systems, it is true that not all the methods would be practical to chemical systems. There are many methods which have not been evaluated on realistic process models and in practical situations. This provides the incentive to test applicability of some design methods on practical systems, preferably on real plant, to assess their practicality, benefits and limitations. Furthermore, the robustness of any control scheme to various factors such as model errors and instruments failures, are important requirements of the control system. Such desirable property of a control system when demonstrated in a real environment, would contribute significantly in promoting the use of the control system in real systems.

The aim in this research work is to select some advanced controller design methods and apply them on a practical chemical engineering system with the use of a microcomputer for direct digital control. Three methods were selected on the basis of three different criteria, so that each method primarily addressed a particular problem. It was aimed to consider a reasonably wide class of advanced control methods so as to address a reasonably wide range of problems. A binary distillation column was chosen to assess the design methods.

The criteria for selecting the design methods, and the methods selected, are given as follows:

1) One multivariable controller design method that addresses the problem of control loop interactions. A method called the Disturbance Rejection and Decoupling Control originally proposed by Falb and Wolovich (179) is chosen. The method assumes the the process is linear and is described by a set of linear ordinary differential equations, that is, in state variable form. The control objective is to decouple the control loops so that the closed loop response of each output variable will be independent of the others.

2) One method that is applicable in the situation were direct measurements of the controlled variables are not available. A method called the Estimator Aided FeedForward (EAFF) control scheme proposed by Daie (26) is selected. The method employs an Extended Kalman Filter as an estimator to generate the controlled variables of the process using a non linear model of the system combined with secondary process measurements.

3) One method that addresses the problem of changes in operating conditions of the plant. The adaptive control system design method called the generalized minimum variance (GMV) Self Tuning Controller (STC) is selected. This basis of this method is the single step optimisation of a quadratic cost function and was developed by Clarke and Gawthrop (156). The design method adapts the controller to changes in the process environment by adjusting the controller parameters based on the parameters of an assumed model of the process. The parameters of the model is identified on-line using process input and output data and a recursive parameter estimation law.

These design methods, the synthesis of the control policies and their applications to chemical processes, will be treated in more detail in the next chapter. In order to achieve the goals of this research work, the first task was to develop a dynamic model of the column used in this work, after the construction of the pilot plant distillation column used in this work. This model was used for studying the dynamic behaviour of the column and to design and analyse the control systems for the column. The decision to proceed with on-line application of the control schemes selected for evaluation was based on the performance on the dynamic model. The next section deals with the importance of distillation columns in the chemical industries and why they are good examples to illustrate application of advanced control systems.

1.8 Reasons for studying distillation column control

The purpose of a distillation column is to split the feed into two or more products: A conventional binary distillation column splits the feed into two products, the tops and the bottoms products. Heat is used to bring about the separation and the amount of heat input is strongly linked to the degree of separation that is achieved. Distillation is

an important fundamental chemical engineering process found in a majority of chemical and petrochemical plants. Distillations systems are complex non linear multivariable systems with strongly interacting variables. They generally consume large amounts of energy and it is usually the case that the quality of the products from a distillation column strongly influences the quality of the final product of the plant. This is particularly the case when the column is towards the end of the processing line, where it will be subject to many load disturbances from processing units in upstream.

The usual control objective of a column is to maintain the product quality, at one or both ends, at desired levels subject to many adverse load disturbances and product demand changes. Another desirable operating objective is to reduce the energy consumption of the column since they usually consume a lot of energy. Numerous studies on the dynamics and control of distillation columns have been carried out (10, 44, 57, 169, 188, 192, 199). It is generally agreed (199, 57, 169, 188) that improving the control of distillation columns would make it possible to operate the column closer to the product specification, reduce off specification periods, increase the rare of recovery of products and hence achieve more economical operation of the column. The recent article by Skogestad and Morari (153) point out that many distillation columns are still controlled manually, and , in most cases, only the product at one end is under control.

The problems in the control of an average industrial, and even a pilot scale distillation process, is typical of the major problems in chemical process control. These include the presence of significant time lag between the response of the product compositions to changes in the inputs. These lags are usually introduced by the large liquid holdups in the column and by composition analyzers used for direct measurement of the product compositions. The selection of the proper location in the column were composition should be measured to achieve effective product composition control is frequently encountered. There are also many manipulatable inputs in a distillation column that strongly influence most of the primary variables of the entire column including the product compositions. Therefore, selecting the best input to control a particular product can be difficult. It is also usually the case that

direct measurements of the compositions are not available as on-line composition analyzers can be very expensive and unreliable. Furthermore, as distillation is a complex nonlinear multivariable process, the assumption of linearity in controller design means the resulting controller will be subject to robustness and stability problems as operating conditions change.

Numerous simulated and experimental results (73, 57, 169, 161) have shown that the dual composition control of the top and bottoms of distillation columns can provide substantial benefits in terms of reduced energy consumption. This has been reported (199, 205) to have industrial support. Dual composition control is, however, known to pose problems due to the strong interactions that exists between the variables of the distillation column. The control loop interactions in distillation columns can sometimes be considerable. A control loop at one end will affect the control loop at the other end because the manipulated inputs have significant influence in the entire column. The combined performance of independently designed conventional SISO controllers may become very bad as they will interact with each other. Stability problems are likely to arise and the nonlinear characteristic of the column will worsen the case. In such situations the controllers will have to be detuned to maintain stability and robustness with the loss of performance since longer response times and large deviations of the product quality from the desired levels will result. This type of control loop interactions has been cited (Marchetti et al. (82), Tham et al. (131) and Skogestad and Morari (153)) as one of the main reasons why multiproduct control of distillation columns is difficult. The incentive, therefore, exists to develop techniques which can deal more effectively with such interactions than conventional control methods.

In the face of load disturbances such as feed flow and feed composition disturbances, feed forward control can be beneficial to distillation column control if the disturbances can be measured and a model which adequately predicts the effects of the diturbances on the product composition can be developed. The advantage of such a scheme is that the disturbances can be nullified before they have significant effect on the product composition and also avoid significant lags due to the hold ups in the column. Significant saving in off-specification products and in energy consumption

can be achieved (Jafarey and McAvoy (57)). Combinations of feedback and feedforward control schemes have been shown (Luyben (76) and Coppus et al. (25)) to offer significant improvements in the control of distillation columns.

In view of all the control problems in distillation column control, distillation columns are regarded as good examples for illustrating advanced control techniques (Rys (169). In fact, it can be assumed that an advanced control strategy that can tackle some of the major problems in distillation column control has a promising future in becoming widely applied in the chemical industry.

1.9 The Thesis

The rest of this thesis is arranged as follows.

Chapter 2 reviews some recent developments in control systems design, analysis and the selection of control configurations. It surveys some modern controller design methods including those that have been selected for evaluation in this work. The review extends to the applications of the control schemes there benefits, and limitatations as reported in the lterature.

Chapter 3 follows on from the literature review. It states the issues addressed in this work as regards each of the control techniques selected for evaluation.

Chapter 4 describes the pilot plant binary distillation column and the interfacing of the column with the microcomputer, System96, for investigating process control techniques.

Chapter 5 describes the steady state and dynamic modelling of the column as well as the verifications of the models.

Chapter 6 describes and discusses the results obtained from applying the Disturbance Rejection and Decoupling Control scheme by simulation on linearised state variable models of the non-linear model of the column and on the non linear dynamic model of the distillation column.

Chapter 7 describes the Kalman filtering studies performed in an effort to assess the feasibility of applying the EAFF control scheme of Daie (26) to the distillation column.

Chapter 8 describes the design of self tuning controllers for single variable and multivarible control of the column.

Chapter 9 discusses performance the self tuning control systems on the on the non-linear model of the column and compares the results with PI control.

Chapter 10 discusses the results obtained from computer control of the pilot plant distillation column and

Chapter 11 gives the general discussions, conclusions and future work recommended of this work.

1.10 Chapter Conclusion

This chapter has introduced the need, approaches and the motivations for developing new control schemes. It has given a brief description of the aim of this work.

CHAPTER TWO

Literature Review

2.1 Introduction

The purpose of this review is to survey the state of the art of control systems design, analysis and structuring with reference to distillation. A review of some advanced control techniques and some reported applications to chemical engineering systems is made. The review does not survey every development in advanced control theory. Rather it surveys some design methods which have been receiving significant interest during the last 15 years and some methods that have been demonstrated as practical by laboratory and industrial applications. Also the review of the design approaches that were selected for evaluations in this research work is made.

2.2 Recent developments in control systems design and analysis

2.2.1 Control loop pairing

The development of control systems generally involves the formulation of the control objectives, the selection of the appropriate pairings of the controlled and manipulated variables; that is loop pairing, and the determination of the appropriate control law (Lau et al. (75)). The interconnections between the manipulated inputs and controlled outputs, or loop pairing, is referred to as the controller structure while the manipulated and controlled variables is called the control configuration, or sometimes the control structure (Arkun (165)).

Lau et al. (75) argue that the selection of the manipulated and controlled variables and pairing them appropriately is worth more attention than it previously has had. They base this on the need for efficient and reliable control structures for complex highly interconnected modern chemical plants. The argument is that since these plants have to show high performance and the incentives for improved control are great the choice of

the various manipulated and controlled variables and their pairings become important in achieving good control.

Choosing the proper manipulated and controlled variables and there pairings is usually more involved for multivariable systems with single input single output control loops since it may be necessary to pair the loops to minimise interactions between the control loops. Interaction analysis in multivariable systems is thus an important consideration in the design and analysis of control systems for multivariable systems. Numerous studies have therefore been carried out (Jensen et al. (59), Witcher and McAvoy (194) and Lau et al. (75)) on providing measures of the degree of interactions in multivariable systems.

Multiple loop and Multivariable control systems: It is appropriate here to mention the distinction between what is meant by a multiple loop control system, as used in this review, and a multivariable control system, as regards the necessity for control loop pairings. A set of single loop controllers controlling the outputs of a multiple-input multiple-output (MIMO) system can be referred to as a multiple loop control system. The single loop controllers may be conventional or advanced controllers; each is designed independently without considerations of the interactions that may exist between them. After selecting the manipulated and the controlled variables, it is then is necessary to determine the proper control structure for the multiple loop control system.

By contrast a multivariable controller design method takes into account of the interactions between the control loops of the MIMO systems since, strictly speaking, implicit in the controller design is the ability to handle several variables. There is no need to specify the proper control structure; the multivariable controller will consist of a matrix relating the manipulated inputs and the controlled outputs. Thus, strictly speaking, if there are no interactions among control loops there will be no need for a multivariable controller design method to be used since each loop could be treated

independently. Control loop pairing is therefore primarily concerned with either single loop and multiple loop control systems.

2.2.2 The Relative Gain Array method for control loop pairing

In industrial practice the control loop pairings is commonly done by experience of the plant operators. For systems that require multiple control loops, it is usually more difficult to select the best loop pairings when interactions between the variables are severe. A method called the relative gain array (RGA) technique is one method for selecting the control configuration for MIMO systems. This method is treated in books on distillation column control by Shinskey (142) and Desphande (168). The method indicates the control configuration that will give the minimum interactions between the control loops. Each element in the RGA represent the relative gain of a pairing of controlled and manipulated variables. Scali et al. (111) have defined the relative gain is the ratio between the steady state gain relating the manipulated and controlled variables when the MIMO system is in open loop condition and the steady state gain when all the other loops are closed. The quantity is given as;

$$\pi_{ij} = \frac{\text{steady state gain with all control loops open}}{\text{steady state gain with all other control loops closed}} \qquad 2.1$$

$$= (dy_i/du_j)_{uk,k\neq j} \; / \; (dy_i/du_j)_{yk,k\neq i} \qquad 2.2$$

where π_{ij} corresponds to the relative gain between the output i, y_i, and the input j, u_j. The i and j correspond to the i-th row and j-th column in the RGA. Qualitatively, the RGA is an index of how much the system is influenced when control loops change from open to closed loops. If there are no interactions between a manipulated variable u_i and the other controlled variables, y_j where $j \neq i$, the corresponding relative gain π_{ij} will be 1. The elements in each row, or in each column, of the RGA must also add up to 1.

The RGA is a measure of the strength of interactions in the system and it indicates the proper pairings for the minimum steady state interaction among the control loops. It is

easy to compute because it requires only the knowledge of the steady state gains of the process system. Since the elements in each row and in each column of the RGA must add up to 1 for a process with 2 manipulated inputs and 2 controlled outputs (a 2 x 2 system) only one relative gain need to be determined. The other elements can be obtained by appropriately summing up to make the row elements and column elements add up to 1. The RGA may, however, be computed directly from the process gain matrix rather than perform actual experiments, or simulations. Given the process gain matrix for a 2×2 system as

$$Gp = \begin{bmatrix} g_{11} g_{12} \\ g_{21} g_{22} \end{bmatrix} \qquad 2.3$$

the RGA is computed as (Skogestad and Morari (119), Marlin et al. (98))

$$RGA = \begin{bmatrix} \pi_{11} \pi_{12} \\ \pi_{21} \pi_{22} \end{bmatrix} = \begin{bmatrix} \pi_{11} 1-\pi_{11} \\ 1-\pi_{11} \pi_{11} \end{bmatrix} \qquad 2.4$$

where $\pi_{11} = (1 - (g_{12}g_{21})/(g_{11}g_{22}))^{-1}$

For a process gain matrix of size n x n the RGA is

$$RGA = Gp \times (Gp^{-1})^T \qquad 2.5$$

Ideally, it is desirable to have pairings which have relative gains close to 1 as this indicates minimum interactions of the corresponding loop with other loops. Shinskey (142) has used the RGA to compare control configurations for dual composition control of distillation columns and suggested some recommendations which has been interpreted by Skogestad and Morari (153) as pairings with relative gains between 0.9 and 4 should be used.

The drawback of the steady state formulation of the RGA is that the degree of interactions between the control loops may vary significantly during operation and these may dictate a different control configuration than that predicted at steady state (Lau et al. (75)). The RGA can be computed at different frequencies of practical importance to the system. The significance of this is that an indication of variations of the strength of interaction during the transient behaviour of the system could be

Please note

page 111 (Sect. 2.7.9) is

missing from

this thesis

and no copy

can be obtained.

obtained. The RGA is therefore defined in the frequency domain as (Skogestad and Morari (119), Scali et al. (111))

$$RGA = Gp(\omega) \times (Gp(\omega)^{-1})^T \qquad 2.6$$

The magnitude of the dynamic relative gain elements and the phase angles can then be plotted against frequency similar to the Bode plots in frequency response analysis used for analysing SISO systems. Frequencies of practical importance in a particular system may be the crossover frequency and the ultimate frequency. The variations in the dynamic relative gains around the ultimate frequency, for example, may be obtained. If the variations are significant then this discloses that the degree of interactions would vary greatly and control may be poor (Deshpande (168)). An adequate compensator or a different controller design could then be sought for in order to avoid poor controller performance. Analysis and evaluations of relative gains of multivariable systems have also been extended to non linear multivariable systems (Mijares et al. (83)). Steady state RGA analysis has also found use in analysis of the operability of chemical processes and the prediction of process control performance (Marlin et al. (98))

2.2.3 The Singular Value Decomposition applied to loop pairing

The singular values of a system are related to the eigenvalues of the system. Given a matrix, Gp, the singular values of the matrix are the square roots of the eigenvalues of matrix

$Gp^+ \times Gp$, where superscript + denotes the complex conjugate transpose of Gp, that is

$$\sigma_n = \lambda_n^{1/2}(Gp^+ \times Gp) \qquad 2.7$$

where σ_n is the singular value which is the square root of the eigenvalue λ_n. The singular values are thus the spectral norms of the matrix. In numerical analysis the spectral norm of a matrix is the Euclidean norm, represented as $\|Gp\|_2$,which is the 2-norm of the matrix Gp. It is defined (Grosdidier et al. (204)) as the maximum singular value given by

$$\sigma_{max} = \lambda_{max}^{1/2}(Gp^+ \times Gp) \qquad 2.8$$

In the context of control the singular values are also known as the principal gains of the plant matrix (Shimizu et al. (189)).

Another quantity that can be derived from the singular values is the condition number of the system matrix. The condition number, $\gamma(Gp)$, is the ratio of the maximum and minimum singular values, σ_{max} and σ_{min}, respectively, and is given by

$$\gamma(Gp) = \sigma_{max} / \sigma_{min} \qquad 2.9$$

In numerical analysis, the condition number of a matrix indicates the extent of illconditioness of a matrix.

The singular value decomposition of Klema and Laub (160) is another method of obtaining the singular values of a matrix. It involves the decomposing the plant matrix, whether square or non-square, into three matrices. These are given as ;

$$Gp = VQW^T \qquad 2.10$$

where $Q = \text{diag}(\sigma_1, \sigma_2, \ldots\ldots, \sigma_n)$

σ_i are the singular values of the Gp matrix of rank n

$V = (v_1, v_2, \ldots\ldots)$ - the matrix of the left singular vectors v_i

$W = (w_1, w_2, \ldots)$ - the matrix of the right singular vectors w_i

$V^TV = I$

$W^TW = I$

where I is the identity matrix. This relationship is given in the articles by Lau et al. (75) and Levien and Morari (152).

According to Lau et al. (75), by performing SVD on the plant matrix it is possible to make direct relationships between the input and outputs of the MIMO system and extract much more information about the characteristics of the system. They point out that the singular values are measures of the sensitivity of the MIMO systems in the same manner as the amplitude ratio is used in SISO systems. Yu and Luyben (137) have also combined the singular values and the singular vectors to select the controlled and manipulated variables of systems and pair them appropriately, since the singular vectors disclose the extent at which an input affects the outputs of the system.

In the work of Lau et al. this SVD technique of Klema and Laub (160) was shown to be an efficient method for selecting the control structure MIMO systems with SISO controllers. Lau et al. extended the SVD to the frequency domain to enable analysis to be carried out over a range of frequencies of practical significance to the given process, in a similar way as the Bode plots is used in the frequency response analysis of SISO systems (Stephanopoulos (116)). By formulating the SVD in the frequency domain, they were able to define new measures of dynamic interactions among the control loops of the MIMO system. This interaction measure was then combined with the condition number of the process matrix to assess the control properties of some example model systems which included a distillation column. These quantities were plotted against frequency and the information the plots provided were used to assess the need and the feasibility of designing compensators to minimise interactions among the multiple SISO control loops.

The ability of the SVD analysis to identify aspects such as model uncertainties which can affect performance of the control structures selected was also demonstrated. They found that the SVD analyses indicated that a closed loop system with larger dominant time constant (slow responding system) can tolerate model errors than a system which has smaller dominant time constant (faster responding system). This result conforms with practical experience and engineering judgement since the universal way to improve the robustness and the stability properties of a control system is to reduce the control actions; for example, reducing the proportional gain of the PID controller will reduce the closed loop response of the controlled system. Hammarstrom et al. (47) investigated the effects of model errors on the performance of a multivariable optimal linear quadratic gaussian (LQG) controller on a distillation column with time constants as large as 16.6 minutes. There investigation showed that errors of up to 30% in the time constants had no significant effects on the controller performance.

Yu and Luyben [137], in their work which involved the design of rigorous composition estimators for multicomponent distillation systems, employed the SVD to locate the best tray temperature measurement for product composition estimation, and

to select the control configuration for control of the product compositions of the column. The criteria for selecting the control configuration is given in the article. In summary the criteria is as follows;

1) Select the largest singular value and the the largest element corresponding left singular vector v_1 .

2) The location of this element is the location of the controlled variable.

3) The appropriate manipulated variable is the largest element in the corresponding vector w_1.

They found that resulting control structures based on this criteria were reasonably insensitive to changes in the operating conditions. They also used the SVD to determine which tray temperature can infer feed composition disturbance best, using a similar criteria to that given above.

In recent years the RGA and SVD have found extensive use as tools for assessing the effects of plant characteristics, such as model errors, on the properties of multiple loop and multivariable control systems (Morari (159), Grosdidier et al. (204)). The topic of the next section concerns these areas.

2.2.4 Model uncertainty and controller performance

A view held by Doyle and Morari (177) and Morari (150) is that for any controller design procedure to yield a control algorithm which works satisfactorily, the following need to be specified:

(1) Process model and model uncertainty bounds.

(2) Types of inputs (set point changes, load disturbances).

(3) Performance objectives.

These considerations are from the point of view of Internal Model Control (IMC), which will be introduced in the next section. According to them, the omission of any of these procedures may eventually lead to bad controller performance because every controller design or tuning method is centred around a process model. In particular, they emphasize that the presence of uncertainty in the model can adversely affect the

performance of the resulting control system. They base this on the fact that processes can seldom be modelled exactly so that there is always a mismatch between the plant and the best model available. This mismatch is referred to as model uncertainty. The sources of uncertainties in process models include incorrect estimates of the process parameters such as rate constants and time constants, the neglect of non-linearities and higher order dynamics, and errors in the input and output measurements due to noise and faulty measuring instruments.

Doyle and Morari (177) and Morari (150) claim that model uncertainty is one of the major problems that face the control systems designer in the development of reliable and robust control systems. They pointed out that neglecting uncertainty in the models could lead to a controller that is too tight which will cause oscillatory closed loop response of the system or even instability. Simple examples were used to illustrate how errors in the assumed process time delay can seriously affect the performance of a control system that is based on compensating for the time delay, and how errors in the manipulated inputs can deteriorate the control of an MIMO system with controllers aimed at compensation for control loop interactions (i.e decoupling control).

Doyle and Morari also claim that one reason for the lack of use of advanced control techniques in the chemical industry is because these techniques often do not address practical issues such as model uncertainties. They emphasised that the control engineer in industry needs efficient and robust controller synthesis procedures rather than having to embark on time consuming and usually expensive procedures of analysis either by simulation or by experimentation.

In recent years, aspects of model uncertainties on controller performance have been receiving a great deal of attention. Some definitions now commonly used to indicate the closed loop system performances will be given. These are, nominal performance, robust performance and robust stability. These are defined more fully in the articles by Doyle and Morari (177) and Morari (150) and only simple forms of the definitions will be given here.

Robustness is defined as a measure for the effect of uncertainty on plant stability when under control (Morari (150)). Robustness is put in a simpler manner by Grosdidier et al. (204) as the ability of a closed loop system to remain stable in the presence of errors in the plant model used for the controller design. Grosdidier et al. (204) define a closed system which becomes unstable due to model mismatch as "sensitive". *Nominal performance* is stable performance of the controller on the process model. The terms *robust stability* and *robust performance* are used to indicate that a closed loop system is stable and meets the performance specifications, for example, fast set point tracking, even though the model used for controller design is associated with errors.

Arkun et al. (1) also noted that a common criticism levied at various controller design methods is the lack of considerations of model uncertainties in the design procedures. If model uncertainty considerations are not considered at the controller design stage, then tuning of the controller to compensate for model uncertainties so as to improve the robustness of the closed loop system can only be done when the controller is in operation. In the case of simulation this will be done by trial and error simulations. However, it is not straightforward to quantify model uncertainties and predict their effects on controller performance. This is probably one of the major reasons that model uncertainty considerations have been excluded from control systems design and analysis procedures for chemical systems. It can thus be said that this difficulty provided the incentive for some workers such as Grosdidier et al. (204), Morari (159) to concentrate on finding methods of quantifying model uncertainties and predict their effects on controller performance. Workers such as Arkun et al. (1), Doyle and Morari (177), Morari (150) and Shinnar (100), have addressed the issues of describing model uncertainties and include model uncertainty considerations and robustness features into controller design. A new theory and representation of control systems has thus emerged in recent years and has been useful in assessing the effects of model uncertainties and other plant characteristics on controller performance. This is

the Internal Model Control introduced by Garcia and Morari (200, 201, 202) and is treated in brief in the next section.

2.2.5 The Internal Model Control structure

Garcia and Morari (200, 201, 202) proposed a general structure called the Internal Model Control (IMC) structure for the design of feedback controllers. This IMC structure is equivalent to the conventional feedback loop structure as expressed in Figures 2.1a and 2.1b. The name Internal Model Control is pointed out by Morari (150) to have arisen because the IMC structure includes a plant model, Gp, explicitly in the control loop. An advantage offered by using the IMC is that many control systems can fit into the structure (Ray 104). However, the controller designs considered by Garcia and Morari (200, 201, 202) using the IMC are based on the controller being the inverse of an approximate plant model, i.e;

$$Gc = 1/Gp \qquad 2.11$$

If the model is exact, that is, Gp = G, then "perfect" control can be achieved. Morari (159) emphasized that any feedback controller provides an approximate inverse of the plant transfer matrix. The full theory on the IMC can be found in the articles of Garcia and Morari (200, 201, 202) mentioned above, therefore only a summarised review of these articles will be given in the following.

In practice, perfect control cannot be achieved because certain plant characteristics will limit the achievable performance of the controller. The model Gp is, therefore, factorized as shown by Garcia and Morari (200) into

$$Gp = G_- G_+ \qquad 2.12$$

where G_- contains the invertible part of the plant and G_+ contain the non-invertible parts. The IMC controller is then assumed to be the obtainable and stable parts of the system inverse, G_-^{-1}. The G_+ holds the parts of the plant that limit the controller performance. The IMC controller is then given as

$$Gc = Gp^{-1}G_+ = G_-^{-1} \qquad 2.13$$

Considering a multivariable system the closed loop transfer function for the IMC structure in Figure 2.1b is

$$\mathbf{y} = GGc[I + (G - Gp)Gc]^{-1}(y_s - \mathbf{d}) + \mathbf{d} \qquad 2.14$$

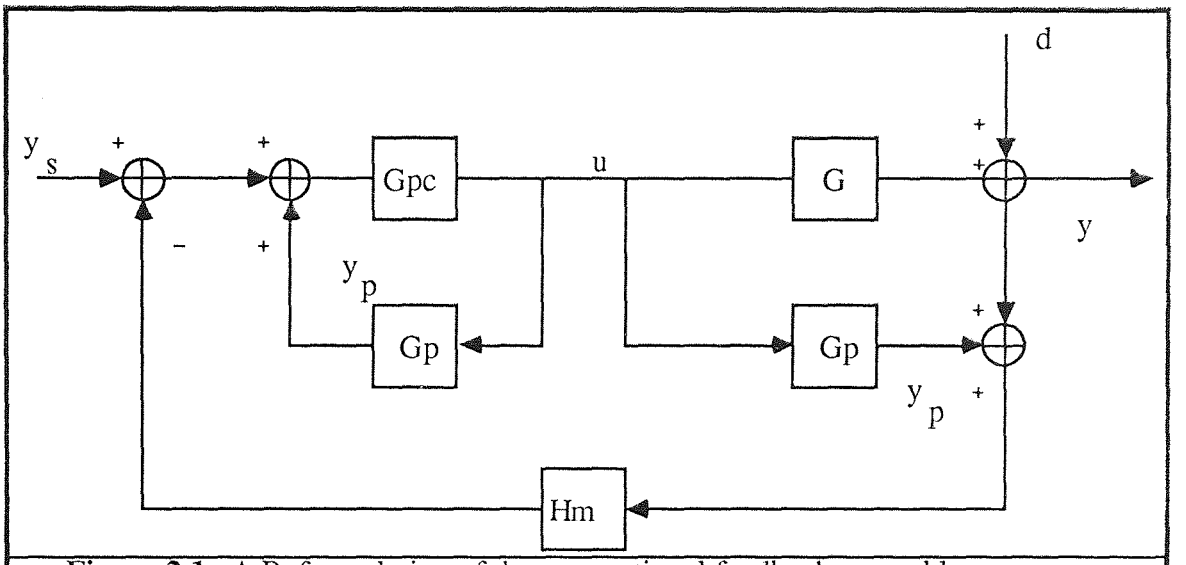

Figure 2.1a A Reformulation of the conventional feedback control loop

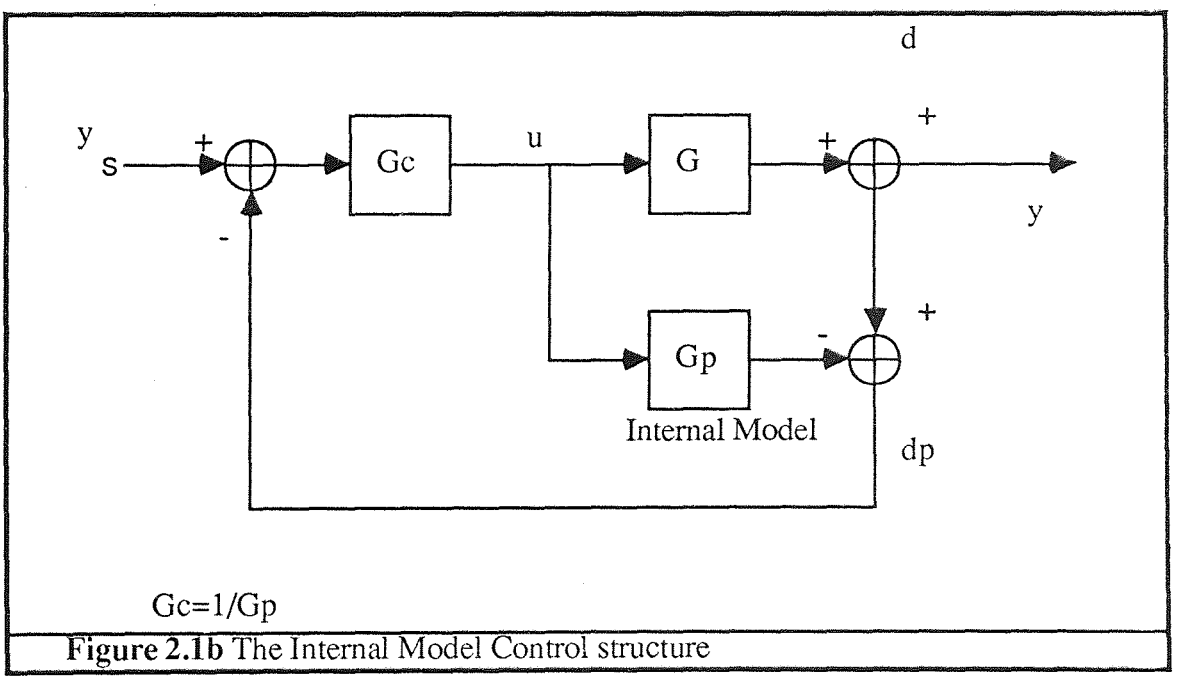

Figure 2.1b The Internal Model Control structure

The control input is

$$\mathbf{u} = [I + Gc(G - Gp]^{-1}Gc(y_s - \mathbf{d}) \qquad 2.15$$

If the model Gp is exact then the control input will be

$$\mathbf{u} = Gc(y_s - \mathbf{d}) \qquad 2.16$$

The IMC design strategy is, therefore, to find a stable approximation to the inverse of the plant model since if controller Gc is stable then the closed loop system is stable. The controller parameters and the control structure are given directly so that control loop pairing is not necessary. This property is claimed to be one major advantage of using the IMC structure instead of the conventional feedback controller structure; the conventional feedback controller has to be chosen to achieve closed loop stability.

From Figure 2.1b, if no disturbances enter the system, that is, y_s and **d** are zero, then the feedback signal **dp** given as

$$\mathbf{dp} = \mathbf{d} + [G - Gp]\mathbf{u} \qquad 2.17$$

becomes zero. Hence, the IMC becomes a feedback controller only when it is necessary .

Garcia and Morari (201) explained that a system equipped with a controller $Gc = Gp^{-1}$ can be very sensitive to modelling errors. They mentioned that even when Gc is stable, if a pole of its discrete time transfer function Gc(z) is close to -1, the manipulated variables can exhibit oscillatory behaviour which may produce undesirable responses in the outputs. There is, however, another feature of the IMC which allows the inclusion of robustness as a design objective. This is achieved by designing an appropriate filter, F, shown in Figure 2.1c, which is capable of improving the robustness to modeling errors. Garcia and Morari (201) addressed the issue of the design of the filter F. They give a necessary condition that must be satisfied for design of a diagonal exponential filter for a multivariable system that would give a stable closed loop system. A diagonal filter implies one filter for each control loop; an exponential filter implies a filter having the form of a first order transfer function.

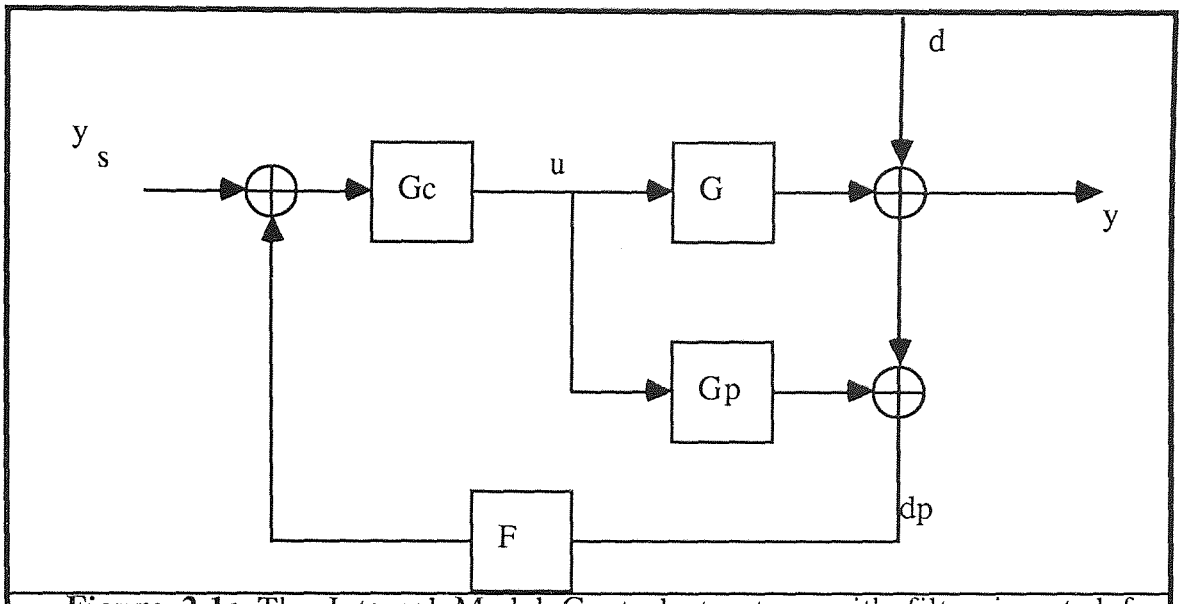

Figure 2.1c The Internal Model Control structure with filter inserted for robustness design

Morari (159) used the IMC philosophy to identify the plant characteristics that are likely to limit the performance of a controller; in terms of perfect control, this implies the characteristics that will prevent perfect control to be achieved. The goal was to find these characteristics without imposing any constraints or structure on the controller. The IMC structure provided this feature. The characteristics that where found to prevent perfect control from being achieved where sensitivity to model uncertainties, time delays in the process, constraints on the manipulated inputs and inverse response behaviour of the output.

Inverse response is the case where the initial response of the output of the system is in the opposite direction to where it eventually ends up. This usually occurs due to opposing effects in the system. When a plant output exhibits inverse response behaviour it is said to have nonminimum phase (NMP) behaviour. This occurs in plants which have positive zeros and time delays in their continuous time transfer function. In the case of the discrete time transfer function, a nonminimum phase system has zeroes outside the unit circle, that is zeroes which have magnitudes greater than one.

Taking the inverse of the system, time delays will require prediction. The inversion of zeroes which are positive in Laplace domain and greater than 1 in discrete time, will result in an unstable controller. These characteristics are therefore included in G_+ to represent the characteristics that prevent perfect control from being achieved. Garcia and Morari (200) point out that these plant characteristics are inherent in the system and cannot be removed by any control system. Their effects can only be suppressed by designing appropriate compensators: for example, time delay compensator and inverse response compensators.

2.2.6 Assessing the effects of model uncertainties on controller performance

Morari (159) investigated techniques for assessing the effects of time delays, nonminimum phasedness, and sensitivity to model errors on the performance of multivariable control systems. These techniques are also summarised in the articles of Levien and Morari (152) and Skogestad and Morari (119, 153). The effects of model uncertainties on controller performance have been assessed using tools, or indices, provided by SVD analysis and RGA analysis.

Morari (159) proposed the SVD analysis to predict model uncertainty effects on controller performance. The other quantity is provided by SVD analysis is the condition number, $\gamma(Gp)$, of the process gain matrix. In matrix algebra the condition number of a matrix is a measure of illconditioness of the matrix. One example of an illconditioned matrix is one were the magnitude of the elements in the diagonal differ by orders of magnitude. Another example is were the matrix is singular, or near singularity. Matrices with high condition numbers thus have high degree of illconditioness.

Shimizu et al. (189) have used the SVD analysis to assess the ability of a closed loop system to compensate for disturbances. Grosdidier et al. (204) showed the norm of the matrix from the steady state RGA analysis can also be used to assess effects of

model uncertainties on controller performance. How all these techniques are applied is summarized here.

Compensating for Disturbances

Performing SVD on the plant matrix enables the control input, **u**, to be related to the minimum singular value, σ_{min}, of the plant matrix as is shown by Shimizu et al. (189). Their analysis is as follows. From SVD analysis the plant gain matrix Gp becomes $Gp = VQW^T$ from Equation 2.10. Substituting into Equation 2.16 then gives

$$\mathbf{u} = WQ^{-1}V^T (\mathbf{y}_s - \mathbf{d}) \qquad 2.18$$

and hence they obtain the relationship

$$\|\mathbf{u}\| = \sigma_{min}^{-1} \|\mathbf{y}_s - \mathbf{d}\| \qquad 2.19$$

From this relationship the size of the disturbance that can be controlled without saturation of the manipulated variable can be determined. The significance of this is that it is important to avoid cases where σ_{min} is small because the manipulated variable will easily hit a constraint. Whenever a manipulated variable hits a constraint it is no longer useful for control and poor, even unstable, controller performance is likely to result. Furthermore, in the cases where there are several manipulated inputs to choose from, a small σ_{min} could indicate those manipulated inputs that should be avoided since if they have small ranges they will easily hit a constraint to small disturbances.

Sensitivity to Modelling Errors

The magnitude of the condition number of the plant matrix, $\gamma(Gp)$, is a measure the effects of model errors on controller performance. In general the magnitude of $\gamma(Gp)$ indicate the closed loop system sensitivity to model uncertainties. This directly links the degree of illconditioning of the plant matrix to the controller performance. Grosdidier et al. (204), Shimizu et al. (189) explain this from the following relationship :

$$\|G-Gp\| \|Gp^{-1}\| < 1/(\|Gp\| \|Gp^{-1}\|) = \gamma(Gp)^{-1} \qquad 2.20$$

It can be observed that $\|Gp\| \|Gp^{-1}\|$ is the definition of the condition number of the matrix Gp, i.e $\gamma(Gp) = \sigma_{max}/\sigma_{min}$ (Equation 2.9). Regarding the control of the plant, G, the above relationship has been interpreted as to imply the following. For the

controller $Gc = Gp^{-1}$, stability is guaranteed only when the relative modelling error, $\|G-Gp\| \|Gp^{-1}\|$, does not exceed the inverse of the condition number, $\gamma(Gp)^{-1}$, of the plant model. For example, $\gamma(Gp(0)) = 10$ implies that a steady state relative modelling error of as little as 10% might lead to instability, where Gp(0) is the steady state process gain matrix. Hence a very large $\gamma(Gp(0))$ implies the system is "uncontrollable" by the IMC controller $Gc = Gp^{-1}$ as error is implicit in the plant model Gp.

Grosdidier et al. (204) showed that the size of the norm of the RGA, $\|\Lambda\|$, at steady state, can be used to indicate control properties in a similar way to the condition number. They found that a very large $\|\Lambda\|$ also discloses potential difficulties in feedback control as indicated by a large condition number. A system whose plant matrix has large $\gamma(Gp)$ or $\|\Lambda\|$ is termed an illconditioned system. In the context of control, such an illconditioned system is one where the plant gain in certain directions of input change is much larger than in other directions, and when under closed loop control, will be very sensitive to model uncertainties (Skogestad and Morari (153)). Skogestad and Morari (119, 153) also point out that high purity distillation columns usually have this characteristic and that this is one reason why they are usually more difficult to control than low purity columns.

Only MIMO systems can exhibit this sensitivity to model uncertainties. This type of sensitivity cannot be exhibited by SISO systems since, for example, the system cannot be described by a gain matrix. This has been used (Garcia and Morari (201)) to explain why MIMO systems are in general more difficult to control than SISO systems.

Doyle and Morari (177) and Morari (150) illustrate the sensitivity of MIMO systems using a high purity distillation column model under control. They used two control structures; one a set of SISO PI controllers and the other a set of SISO controllers with steady state decoupling. To represent model errors a 20% error in the computed changes in the manipulated variables was introduced. The results of there simulations led them to conclude the following. For multivariable systems the dynamic

responses for different input directions are different and a control system, such as decoupling control, which attempts to change the natural directions makes the dynamic behaviour worse. A small $\gamma(Gp)$ or $\|\Lambda\|$ implies less sensitivity and less difficulty in controlling the system.

2.2.7 The relationship between the RGA and the condition number of a process matrix

Skogestad and Morari (119) noted that the $\|\Lambda\|$ is usually preferred to $\gamma(Gp)$ because SVD involves more complex computations than the computations required for the RGA. Moreover, the value of the condition number depends on the scaling of the process matrix. For example, if the matrix is scaled such that the largest element on each row, or column, has the value of 1 the the condition number will be reduced as shown by Grosdidier et al. (204). These workers thus pointed out that the condition number is a useful measure of sensitivity only when the process matrix have been scaled by the above mentioned procedure to minimise the condition number. They defined this as the minimised condition number, $\gamma_m(Gp)$. They observed relationships between the minimised condition number, $\gamma_m(Gp)$ and $\|\Lambda\|_1$ for 2 x 2 and n x n systems. These are as follows. For 2 x 2 systems

$$\gamma_m(Gp) = \|\Lambda\|_1 + (\|\Lambda\|_1^2 - 1)^{1/2} \qquad 2.21$$

and

$$\gamma_m(Gp) = 2\|\Lambda\|_1 \text{ as } \|\Lambda\|_1 \text{ tends to } \infty \qquad 2.22$$

For n x n systems

$$\gamma_m(Gp) = 2 \max(\|\Lambda\|_1 , \|\Lambda\|_\infty) \qquad 2.23$$

where $\|\Lambda\|_1$ and $\|\Lambda\|_\infty$ are the 1-norm and the ∞ - norm of the RGA matrix.

2.2.8 Applications of Singular Value Decomposition and the RGA analysis to chemical process control

Using the SVD and RGA analysis, it is possible to predict many properties of the multivariable control systems before the controllers are commissioned. The

significance of these predictions is that, in practice, the number of trial and error simulations and pilot plant tests necessary for the detailed analysis of the control system can be significantly reduced (Levien and Morari (152)). This means that significant savings can be obtained.

Levien and Morari (152) employed the SVD technique to test the "resilience" of a 3 × 3 process system which was a coupled distillation system. The term "resilience" was introduced by Morari (159) and is defined by Levien and Morari (152) as the ability of a process to move quickly and smoothly from one operating condition to another, and to reject effects of disturbances effectively; complete resilience implies prefect regulatory and servo control, i.e. "perfect" control. Levien and Morari examined the effects of non-minimum phase characteristics, input constraints and model uncertainties on the performance of multivariable control systems based on IMC structure. They performed their analyses on three 3 x 3 MIMO linear laplace transform models selected from various models all obtained from experimental step response results. They observed that (i) a system with a larger minimum singular value, σ_{min}, could handle larger load disturbances better, (ii) a system with a large condition number $\gamma(Gp)$ was sensitive to model uncertainties when under closed loop control and that (iii) a system with $\gamma(Gp)$ close to 1.0 was insensitive to direction of disturbances under control, indicating that any disturbance (load or setpoint changes) can be handled regardless of the direction of the change. Sensitivity to model uncertainties was found to be the most significant factor that affected the controller performance. It was also shown how steady state SVD alone could lead to misleading conclusions as they found significant variations with frequency in the condition number of one of the MIMO models.

The effects of using a filter in the feedback loop of an IMC controller structure, as shown Figure 2.1c, was also demonstrated by Levien and Morari. They reported simulated and experimental results which show that an exponential filter, a first order lag, in the feedback loop, provides significant improvements in the controller performance by improving the robustness of the system. As the filter time constant is

increased the closed loop response of the system becomes more sluggish since control action is slower. The results showed that, by appropriate selection of the filter time constant, the IMC controlled system that is unstable could be made stable.

2.2.9 Guidelines for selecting control configurations for binary distillation column

The SVD and RGA techniques have been used to explain practical experience and observations that have been made in the control of chemical process systems. One such analysis is that of Skogestad and Morari (153). They used RGA analysis to explain the observations on the dual composition control of distillation columns made by Shinskey (142).

In the dual composition control of distillation columns the recommendation of Shinskey (142) is to choose control loop pairings with relative gains between 0.9 and 4. As this represents relatively small RGA elements, Skogestad and Morari (153) point out that their observations that systems with large RGA elements are difficult to control justifies the recommendations of Shinskey.

Skogestad and Morari (119, 153) applied the SVD and RGA analysis to distillation column control and their work has culminated into good guidelines for selecting control configurations for the multiple loop control of distillation columns. In general, they suggested that a control configuration with large $\gamma(Gp)$ or $\|\Lambda\|$ should be avoided since it implies greater sensitivity to model uncertainties. They also suggested that decoupling control should be avoided for a process with large $\gamma(Gp)$ or $\|\Lambda\|$ as instability may result. An example of the destabilising effect induced by incorporating decoupling into the dual composition control loop of a high purity distillation column was demonstrated in the article of Morari (150). It was shown that the closed loop dynamics could be degraded significantly if decoupling is introduced into the closed loop system consisting of SISO controllers.

This type sensitivity properties induced by decoupling was also explained by RGA analysis. The explanation is given as follows. Without decoupling control the multiple

loop control system is a diagonal controller, that is, a set of independent SISO controllers. The RGA of the control structure, the controller matrix, will have diagonal elements equal to 1. There is then no possibility of an illconditioned control system resulting. If decoupling is introduced, the control matrix is then not a diagonal matrix since the matrix will now have off-diagonal elements. Therefore, the RGA of the MIMO controllers can have elements greater than 1. There is then the possibility of having an illconditioned control matrix which will induce its own instability properties into the closed loop system.

Skogestad and Morari (153) carried out a comprehensive investigation of the characteristics of the various possible control configurations for dual composition control of a binary distillation process. They used the RGA in their investigations. In a distillation column as shown in Figure 2.2 the variables that are usually available for manipulation are the reflux flow, L, vapour boilup, V_N, distillate flow, D, and bottoms flow, B. They used L and V, instead of L and V_N, as notation. The observations and conclusions arrived at include the following.

(1) If uncertainties are present then configurations with small RGA elements will work better than others as they will be more robust to model uncertainties. The LV configuration which uses reflux to control the top product and vapour boilup to control the bottoms product, gave the largest RGA elements. All configurations using D or B for composition control have small RGA elements and hence are insensitive to uncertainties.

(2) If a diagonal controller, such as two single loop PI controllers, is used a control configuration with large RGA elements may not be very sensitive to input uncertainty, for reasons already discussed above. For disturbance rejection a diagonal controller may also deliver acceptable performance if the disturbance condition number is small for all possible expected disturbances and tight setpoint tracking is not required.

(3) For fast initial response, the LV configuration should be used. The $\left(\frac{L}{D}\ \frac{V}{B}\right)$ configuration also has this feature but configurations with D or B for composition control are not preferable since the initial response is slow.

(3) Configurations with D or B for composition control are insensitive to disturbances in reflux flow, vapour boil-up and feed enthalpy, but do not reject disturbances in feed flow. The $\left(\frac{L}{D}\ \frac{V}{B}\right)$ configuration is the best for disturbance rejection. It is insensitive to disturbances in feed flow rejects other flow disturbances as well as provided reflux is large.

The $\left(\frac{L}{D}\ \frac{V}{B}\right)$ configuration was found to be the best choice for servo and regulatory control and pointed out that this agrees with the recommendations of Shinskey (142). It is claimed that all the recommendations agree well with engineering judgement. This, therefore, makes them good guidelines for the design of control systems for distillation columns and other similar processes such as absorption columns as well.

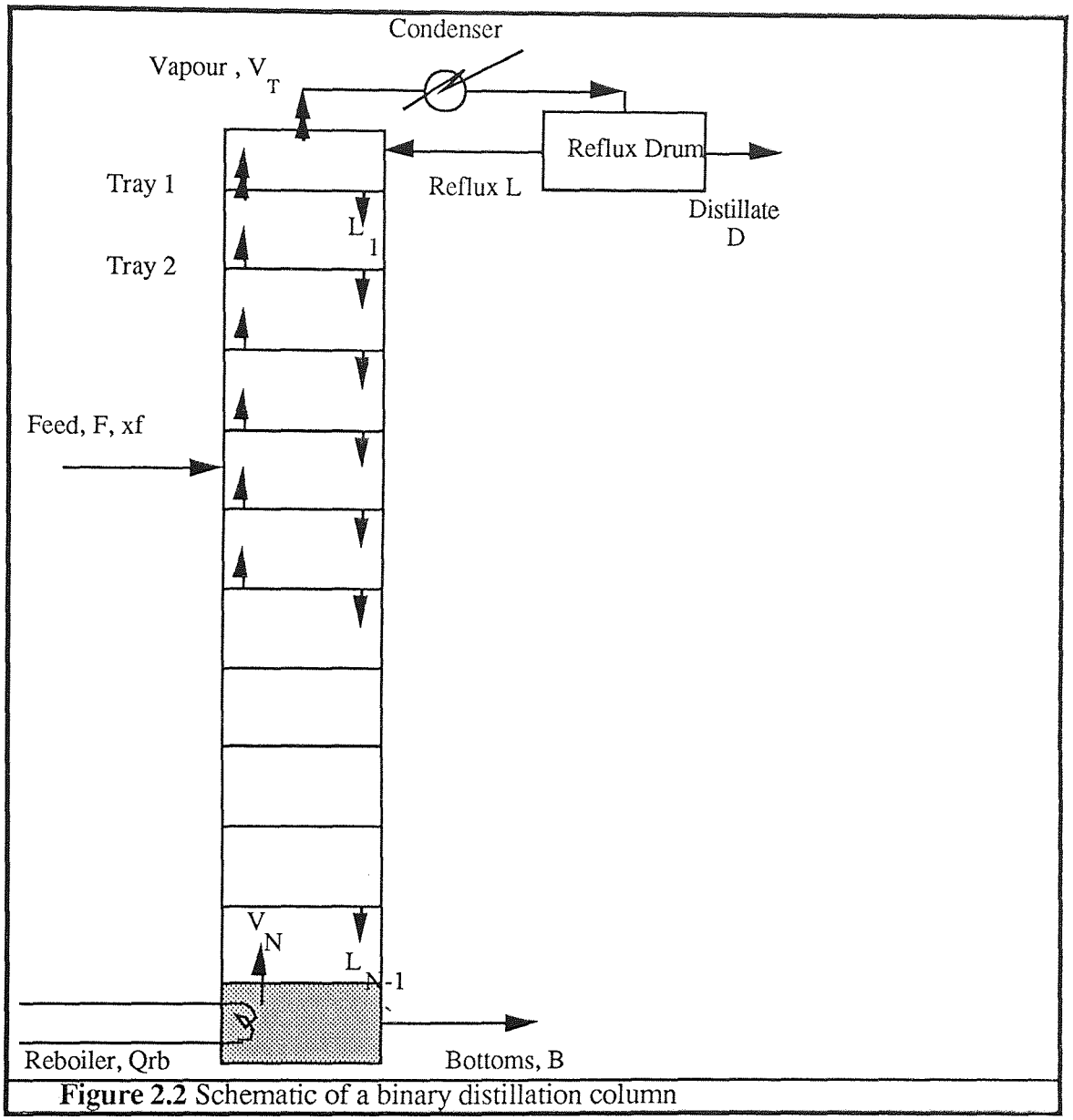

Figure 2.2 Schematic of a binary distillation column

2.3 Introduction to Advanced Control systems

It was mentioned in Chapter 1 that any controller design method that departs from the conventional classical feedback controller design methods is generally classed as an advanced controller design method. Advanced control systems range from feedforward control schemes to state variable feedback control schemes where the system is described by a set of ordinary differential equations. The various methods include the following:

(1) Multivariable Controller design methods such as the Inverse Nyquist Array (INA) method, Direct Nyquist Array (DNA) method and the Characteristic Loci Method. These methods are extensions of SISO frequency domain design methods, such as the frequency domain method of Nyquist, that have been extended to the MIMO case (Nawari (193)). Jensen et al. (59) have recently demonstrated that the DNA method is a useful method for interaction analysis and the method handles control loop pairing and interaction compensation directly.

(2) Multivariable controller design methods based on state variable description of the process system. One such method is Modal Control techniques (Ray (144)) where the poles or eigenvalues of the system can be placed at desired locations in order to speedup the response of the system or stabilise the system. Another method is Optimal Control (Ray (144)), which is defined in various ways. One approach to optimal control is where the control inputs are calculated as a function of the state variables in order to optimise the time required to bring the process to a new state, and another is to determine the feedback and feedforward gains that minimise a quadratic cost functional of the process state variables and the control inputs.

(3) Multivariable controller design methods based on decoupling the control loop of the system. The simplest form is simplified decoupling control where decoupling compensators are inserted into the multiple loop control system in order to directly cancel out the effects of the control loops from each other. A more complicated form of decoupling is called the Decoupling and Disturbance Rejection Control method by Shimizu and Matsubara (113) which is based on the work of Falb and Wolovich (179)

and Morgan (196). In this method, closed loop poles can also be assigned in order to achieve desired closed loop response.

(4) Estimator Aided Control methods, which use the available process measurements and a model of the process to produce estimates of the variables required for control. These methods are used in the cases where direct measurements of the control variables are either not available, corrupted by noise or errors in the measuring instruments or the measurement is subject to long time delays.

(5) Time delay compensation techniques which are used in the situations where there are significant time delays in the system. These methods attempt to directly cancel the time delays using a model of the process and the Smith Dead Time Compensator (172, 173) is one such approach.

(6) Adaptive controller design approaches (Goodwin & Sin (39)) where the controller parameters are continually changed to correspond with changes in the operating conditions and the process environment. The usual approach to adaptive control is to use an identification technique to continually estimate the parameters of an assumed model of the process on-line using process input and output measurements. The model is then used to calculate new controller parameters for the control algorithms.

Standard texts on the various advanced control theory are available for reference. These include Ray (144), Astrom and Wittenmark (206), Stephanopoulos (116) and Bell and Griffin (15). Critical reviews of the applications of advanced control algorithms are given by Foss (33) and by Nawari (193).

In this review two multivariable controller design approaches based on the state variable feedback approach will be reviewed first. These are the Modal Control approach of Rosenbrock (105) and the Decoupling and Disturbance Rejection Control design approach based on the work of Falb and Wolovich (179). Both methods are multivariable controller design methods which result in control systems with decoupling control properties. However, a drawback of the methods is that they do not have integral action so that they cannot address the problem of offsets.

2.4 State variable representation of systems, Controllability and Observability

When a set of first order differential equations is used to describe the dynamic behaviour of a system these equations can be written in the form

$$\mathbf{dx}(t)/dt = A(t)\mathbf{x}(t) + B(t)\mathbf{u}(t)$$

$$\mathbf{y} = C(t)\mathbf{x}(t) \qquad 2.24$$

This is referred to as the state variable or state space formulation of the system dynamics. The **x** is the vector of the state variables, **u** is the vector of the system inputs and **y** is the vector of the outputs. The A is the state, or system, matrix, B is the input driving matrix and t denotes time. Assuming the numbers of the state variables and the number of inputs are n and m, respectively, then the dimension of **x** is $n \times 1$, **u** is $m \times 1$, **y** is $r \times 1$ A is $n \times n$, B is $n \times m$ and C is $r \times n$. If A, B and C do not vary with time then the t can be dropped from A(t), B(t) and C(t) to give

$$\mathbf{dx}(t)/dt = A\mathbf{x}(t) + B\mathbf{u}(t) \qquad 2.25a$$

$$\mathbf{y}(t) = C\mathbf{x}(t) \qquad 2.25b$$

This equation is called a linear time-invariant state variable model.

2.4.1 Controllability and Observability

There are two important issues that arise in the analysis and control of dynamic systems. One is whether it is possible to steer a system from a given initial steady state to another state; this introduces the issue of controllability. The other consideration is whether it is possible to determine the state of the dynamic system from observations of the inputs and outputs; this raises the question of observability. Controllability and Observability are very important particularly in the design of control systems based on state variable representation of the system. The definitions given by Astrom and Wittenmark (206) will be presented here.

Consider the linear time invariant state variable system of Equation 2.25. The discrete time equivalent of the system is given as (Astrom and Wittenmark (206))

$$\mathbf{x}(t_{k+1}) = \Phi(t_{k+1},t_k)\mathbf{x}(t) + \Gamma(t_{k+1},t_k)\mathbf{u}(t_k) \qquad 2.26a$$

$$y(t_k) = Cx(t_k) \qquad 2.26b$$

where

$$\Phi(t_{k+1},t_k) = \exp(A\,\Delta T)$$

$$\Gamma(t_{k+1},t_k) = \int_{t_k}^{t_{k+1}} \exp\,(A\,(t_{k+1}-\tau))d\tau B\mathbf{u}(t_k)$$

$\Delta T = t_{k+1} - t_k$ and k denotes the sampling instant.

A controllability matrix Wc is defined as

$$Wc = [\Gamma,\ \Phi\Gamma,\ \Phi^2\Gamma,.....\Phi^{n-1}\Gamma] \qquad 2.27$$

According to Astrom and Wittenmark, the system of Equation 2.26 is controllable if it is possible to find a control sequence such that the origin can be reached from any initial steady state in finite time. This is possible if the rank of Wc is n.

The observability matrix Wo is defined

$$Wo = [C,\ C\Phi,\ C\Phi^2,\ C\Phi^{n-1}]^T \qquad 2.28$$

The system is observable if there is a finite k , sampling steps, such that the a knowledge of the inputs u(0), u(1),.....u(k-1) and outputs y(0), y(1),.....y(k-1) is sufficient to determine the initial state of the system. This implies that the system is observable if and only if Wo has rank n.

Observability considerations are important in the estimation of the state and parameters of systems, particularly in situations where control depends on the estimates of the state. A good example is in Kalman filtering when applied to estimate the state of the system by combining the measurements and a process model. If observability is lost then the estimates may become unstable, and so will the filter algorithm (Daie (26)).

Russel and Perkins (149) present a review on the various controllability problems frequently encountered in chemical plant. They point out that controllability analysis techniques have isolated major factors that affect the controllability of chemical plant and that this has enabled better assessment of the benefits and limitations of various control systems and control structures for chemical plant. Controllability considerations are very important particularly in applications of control systems which

are based upon state variable representation of the process. Since it is seldom the case that all the states of the process will be available, it is important to ensure, prior to on-line application, that the system will be controllable with the incomplete state vector. Techniques to overcome such problems include using observers or estimators to reconstruct the unmeasured states; thus adding the issue of observability. In fact as, indicated by Russel and Perkins (149), controllability techniques based on using input-output representations of the processes rather are more beneficial for analysis of chemical plant than those based on state space representation of the processes. One reason they give is that it is neither necessary nor practical to measure all the states of the process.

2.5 Modal Analysis and Modal Control

There are many multivariable controller design methods that are based on the assumption that the system is described by a linear state variable model. One of these design methods is the Modal Control technique which was first proposed by Rosenbrock (105).

2.5.1 Modal Analysis

The main procedure in the design of a modal control system is modal analysis of the model. This involves the decomposition of the system matrix, A, into its eigenvalues, λ_i, and associated eigenvectors, v_i, such that

$$Av_i = \lambda_i v_i \qquad 2.29$$

where i = 1 to n and n is the order of **A**. The **A** matrix can be written as

$$A = \Gamma\Lambda\Omega \qquad 2.30$$

where Λ is the diagonal matrix of the system eigenvalues which are real, distinct and negative,

$$\Lambda = \text{diag}(\lambda_1, \lambda_2, \ldots\ldots, \lambda_n) \qquad 2.31$$

Γ and Ω are the right and left eigenvectors of A where

$$\Gamma = (v_1, v_2, \ldots\ldots, v_{n-1}, v_n)$$

$$\Omega=(v_1, v_2, \ldots\ldots, v_{n-1}, v_n)$$

and $\Omega = \Gamma^{-1}$

The modes of the system are the directions in the state space that correspond to the right eigenvectors, v_i. Each mode is associated with an eigenvalue, λ_i. The eigenvalues are also the poles of the system and their negative reciprocals are the time constants of the corresponding modes. A stable system will have negative eigenvalues. An unstable system will have at least one positive eigenvalue.

The eigenvectors discloses the extent at which the other modes affect each other. The sizes of the elements in the eigenvector disclose the phenomenon that accounts for the existence of that mode. For example, Levy et al. (74) found that the slowest mode of a binary distillation column comprised of the accumulation and the transfer of chemical species in the column. The smaller eigenvalues disclose the dominant modes which determine the dynamic behaviour of the system and the larger eigenvalues disclose the faster modes. Modal analysis is therefore useful in providing deeper insight into the dynamic behaviour of the system.

Many multistage processes like distillation columns have a wide spectrum of time constants. In a distillation column each tray has composition, hydraulic and heat dynamics taking place simultaneously. The composition dynamics are usually the slowest. The fast modes decay rapidly leaving the only the slower modes which are important in determining the process dynamics. Modal analysis can provide knowledge about these modes and, therefore, guide the selection of the proper tray location for measuring composition for control. Levy et al. (74) and Shimizu and Mah (117) have used modal analysis in this way to examine the response modes of distillation systems.

One important quantity provided by modal analysis is the activation of the modes (Rosenbrock (105)). The activation, η_{ij}, of a mode i by the j-th input is defined by

$$\eta_{ij} = v_i^T b_j u_j \qquad 2.32$$

where b_j is the j-th column of B and v_i is the left eigenvector of A. The activation is a measure of the extent at which an input affects a mode. Thus, the importance of a

mode can be judged by the activation of that mode relative to the other modes. Furthermore, the activation can indicate the best input to use to manipulate the state variable that is selected as the controlled variable. This has been exploited by Davison (30) in the control of a distillation column using a modal controller.

2.5.2 Modal Control

Modal control is, in general, a technique where the system closed loop eigenvalues can be placed in any desired location using a state variable feedback. This means that the speed of response of the modes of the system, and, therefore, the speed of the system response, can be increased or decreased by a state variable feedback. Consider a system modelled by

$$dx/dt = Ax \qquad 2.33$$

According to Rosenbrock (105), the following feedback controlled system can be adopted;

$$dx/dt = (A + YK\Theta)x \qquad 2.34$$

where Θx is referred to as the measuring vector (Davison (30)), Y is the control matrix and K is a diagonal matrix consisting of feedback loop gains. The control problem is to find Y and Θ. As explained in Rosenbrock (105) and in Davison (30), suppose that $Y = \Gamma$ and $\Theta = \Omega$ and assuming Y and Θ are square matrices and non - singular. Then $YK\Theta = \Gamma\Lambda\Omega$ and the controlled system becomes

$$dx/dt = Y(\Lambda + K)\Theta x \qquad 2.35a$$

The eigenvalues of the controlled system are $\lambda_i + \kappa_i$. So by choosing κ_i large and negative these eigenvalues can be made large and negative as desired. Thus, the speed of response of the closed loop system can be made as fast as desired.

Equation 2.35a is artificial because, in practice, it is usually impossible to make up a control matrix $Y = \Gamma$. Furthermore, it is usually the case that all the state variables in x are not available due to various practical and economic reasons. Rosenbrock considered this difficulty and then suggested a procedure which will enable only the

dominant eigenvalues of the system to be eliminated. This procedure is given as follows.

It is assumed that $\lambda_n < \lambda_{n-1} < \lambda_{n-2} < \ldots\ldots\ldots < \lambda_2 < \lambda_1 < 0$. Rosenbrock suggests chosing $\Theta = U$ which is a n x z matrix having as its columns the first z vectors of Ω and $Y = H$, which is a n x z matrix having as its columns the first z vectors of Γ. The z represents the number of variables or modes that are measured. Then let K be a z x z diagonal matrix with elements $-\kappa_1, -\kappa_2, \ldots, -\kappa_z$ on the principal diagonal. The corresponding controlled system is now

$$dx/dt = (A+YK\Theta^T)x \qquad 2.35b$$

and is represented schematically in Figure 2.3. The eigenvalues of the closed loop system are $\lambda_1 + \kappa_1, \lambda_2 + \kappa_2, \ldots\ldots, \lambda_z + \kappa_z, \lambda_{z+1}, \lambda_n$. Rosenbrock also considers this controlled system to be artificial because it will usually not be possible to choose the control matrix Y which has as its columns exactly as the first z vectors of Γ.

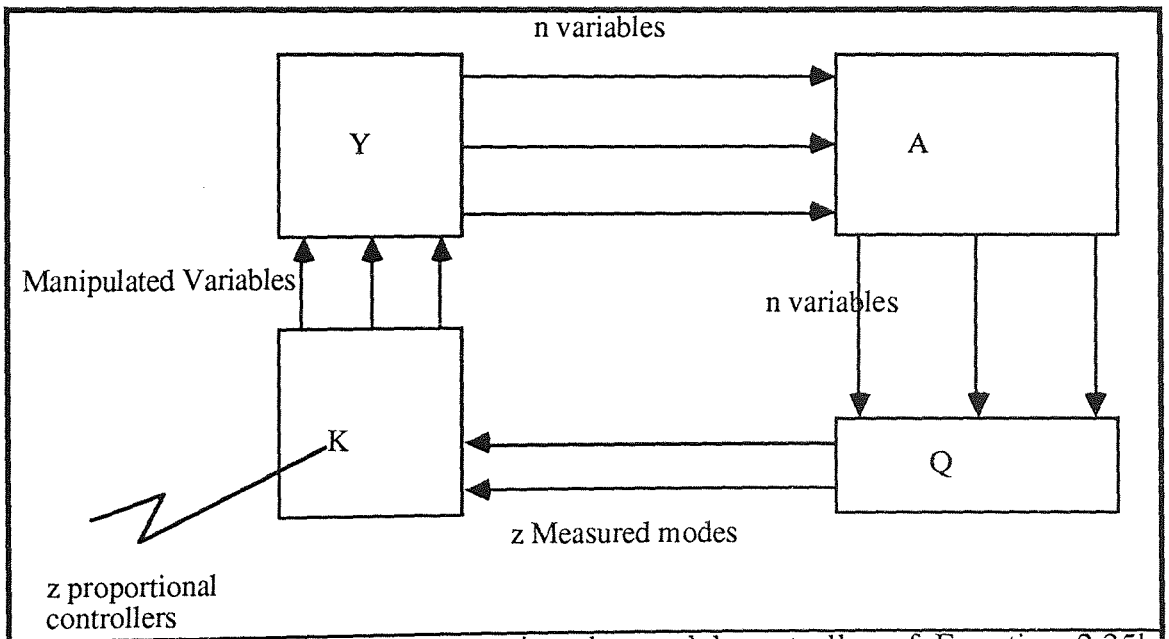

Figure 2.3 Schematic representing the modal controller of Equation 2.35b (Rosenbrock (105))

Following the work of Rosenbrock, Davison (30) designed a modal controller to control a binary distillation column with pressure variations inside the column. His studies were performed on an 8 plate distillation column model via computer simulation and the modal analysis procedure of Rosenbrock was used to select the

proper control configuration for the column. Davison showed that by maximising the smaller eigenvalues, that is, minimising the dominant time constants of the distillation column, the offsets of the state variables from steady state will be minimised. The modal controller was found to deliver better control compared with conventional control. The modal controller greatly reduced the settling time of the column and the offsets in the outputs of the column from steady state when subjected to disturbances in the feed composition, reflux, and reboiler temperature and condenser temperature.

A modal controller called the Pole Assignment technique was proposed by Crossley and Porter (195). The objective of the approach is to speed up the response of a system, or stabilise an unstable system, by shifting either some or all of the system poles to desired locations. To speed up the system the poles are shifted further to the left; that is the eigenvalues are made larger in the negative direction. To stabilise an unstable system the poles are also shifted to the left, but must be made negative. According to Crossley and Porter, the method is applicable to systems having real or complex eigenvalues. They demonstrated that the technique makes it possible to modify both the real and imaginary parts of any number of complex conjugate eigenvalues and any number of real eigenvalues using a single loop. This can only be achieved when all the system modes are controllable and measurements of all the state variables are available.

The synthesis procedure for the pole assignment technique is also presented in the article by Shimizu and Mah (118). The required specifications for the design of the controller are

1) the poles to be shifted and where they must be shifted to

2) the manipulated inputs that are to be used for pole shifting

3) the measurements that need to be fedback to the controller

Shimizu and Mah (118) used the technique to successfully control control a binary secondary reflux and vapourisation (SRV) distillation column. Using modal analysis they found that reflux flow is the best input for pole shifting in the SRV distillation column.

The primary drawbacks of modal control techniques have been noted by Foss (33). They are given as;

1) the controllers do not have integral action and so cannot address the problem of offset.

2) the technique does not address closed loop zeroes which also influence the system behaviour; for example positive zeroes mean nonminimum phase behaviour.

3) the assumption of linear system will not be valid for many systems. This is particularly true of chemical processes which are usually nonlinear systems.

2.6 Decoupling Control

To deal with the problem of interaction between control loops in a multivariable system, the theory of decoupling control emerged. The philosophy behind decoupling control is to eliminate the interactions of the control loops so that a change in the setpoint of one control loop will only affect the corresponding output. If this can be achieved then the control loops can be treated as separate single loops. There are two main approaches that have been proposed for decoupling control. These are the compensator approach and the state variable feedback approach. The compensator approach will be introduced first.

The compensator approach is most popular and the simplest form is called Simplified Decoupling by Luyben (71). The design procedure involves obtaining compensators that would directly cancel out the effects of each manipulated variable on the other outputs. Figure 2.4a gives a schematic of a 2 × 2 MIMO system under control with interacting control loops and Figure 2.4b shows the same system under simplified decoupling with two decoupling compensators D_1 and D_2. The method of obtaining these compensators is given in Stephanopoulos (116) as

$$D_1 = - G_{12}/G_{11} \qquad 2.36$$

$$D_2 = - G_{21}/G_{22} \qquad 2.37$$

Figure 2.4a Schematic of a process with 2 controlled outputs and 2 manipulated inputs

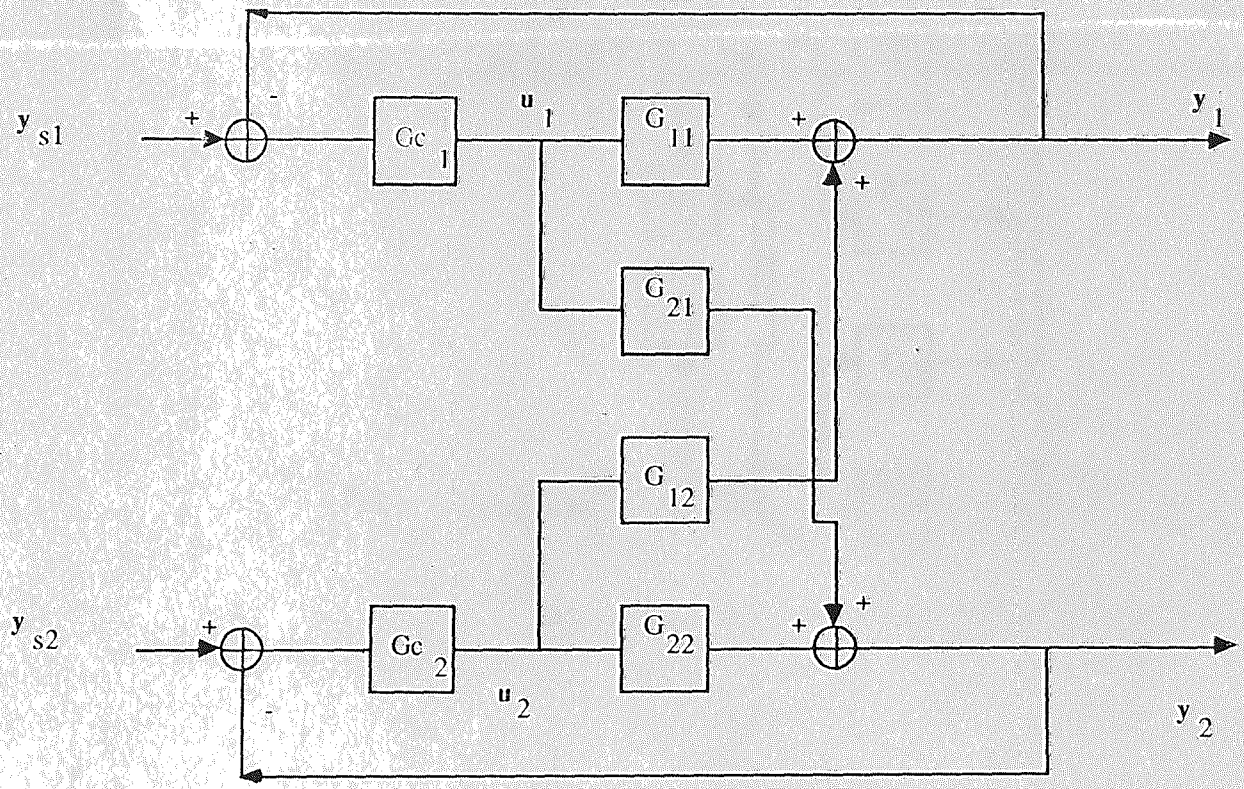

Figure 2.4b Schematic of a process with 2 controlled outputs and 2 manipulated inputs with simplified decoupling

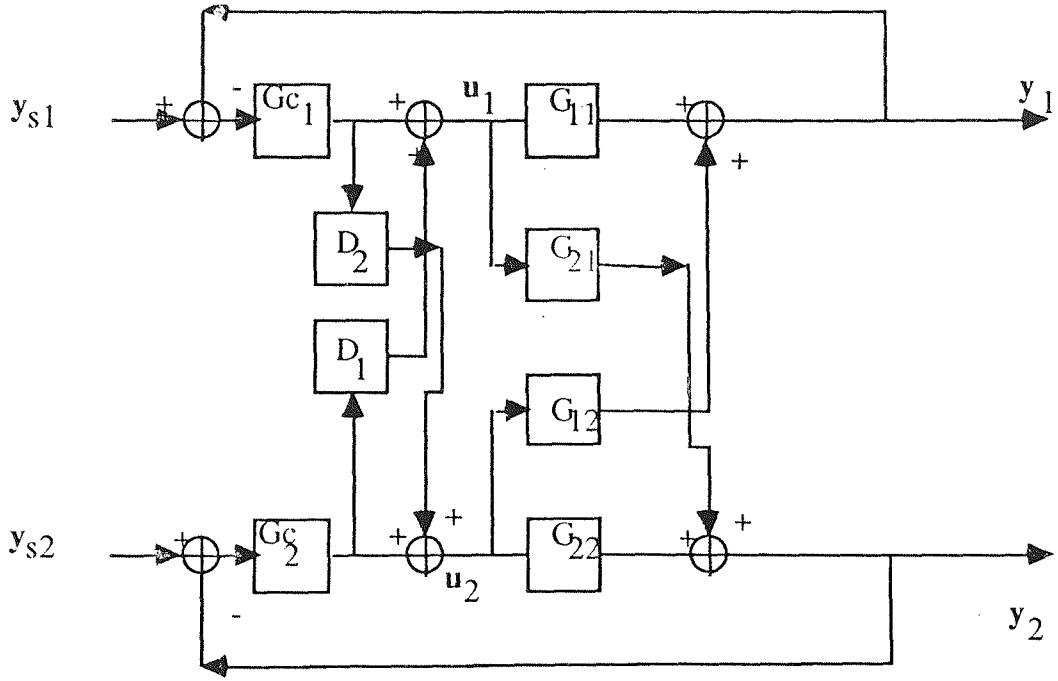

for the system described by

$$y_1 = G_{11}u_1 + G_{12}u_2 \qquad 2.38a$$

$$y_2 = G_{21}u_1 + G_{22}u_2 \qquad 2.38b$$

where $\mathbf{y}$ and $\mathbf{u}$ are the controlled output and manipulated input vectors and G_{ij} is the transfer function relating output y_i and input u_j. The control inputs then become

$$\begin{bmatrix} u_1 \\ u_2 \end{bmatrix} = \begin{bmatrix} 1 & D_1 \\ D_2 & 1 \end{bmatrix} \begin{bmatrix} u_1^c \\ u_2^c \end{bmatrix} \qquad 2.39$$

Luyben (71) applied simplified decoupling in the dual composition control of a binary distillation system by conventional PI controllers. The LV control configuration was used and the studies were performed by computer simulation. He reported that stable effective control could be achieve but noted non-linearities and inaccuracies incurred in approximating the compensators due to the errors in the process models will limit the achievable performance of the control scheme. Therefore, perfect decoupling may not be possible. As mentioned earlier, recent investigations, Skogestad and Morari (119, 153), Doyle and Morari (177) have shown that for dual composition control of distillation columns using the LV configuration, decoupling should be avoided as this configuration usually has large RGA elements which indicate an illconditioned system. Introducing decoupling into the multiple loop control system could degrade the quality of control significantly due to the greater sensitivity of the closed loop system to uncertainties in the model used for the controller and compensator design. High purity columns have higher degree of illconditioness and Morari (150) and Doyle and Morari (177) show how the dynamics of a high purity column under dual composition control is degraded by introducing decoupling into the control loops.

Foss (33) has criticised the notion of decoupling applied to process control. His argument is that since it is natural for most chemical processes to have strongly interacting variables, the interaction between the variables should be exploited rather

than eliminated. He noted that modal control is one such multivariable controller design method.

The state variable feedback approach to decoupling was first proposed by Morgan (196). He derived a feedback controller

$$\mathbf{u} = \mathbf{F}\mathbf{x} + \mathbf{G}\mathbf{w} \qquad 2.40$$

for the system

$$d\mathbf{x}/dt = A\mathbf{x} + B\mathbf{u}$$

$$\mathbf{y} = C\mathbf{x} \qquad 2.41$$

where **y** is the output vector, **u** is the input vector and C is the matrix relating the output **y** to the state **x**. The **w** is the vector of the desired values of the outputs, **F** is a feedback gain matrix and **G** is a precompensator gain matrix. The vectors are deviations from a steady state. Figure 2.5 is a block diagram showing the corresponding closed loop system.

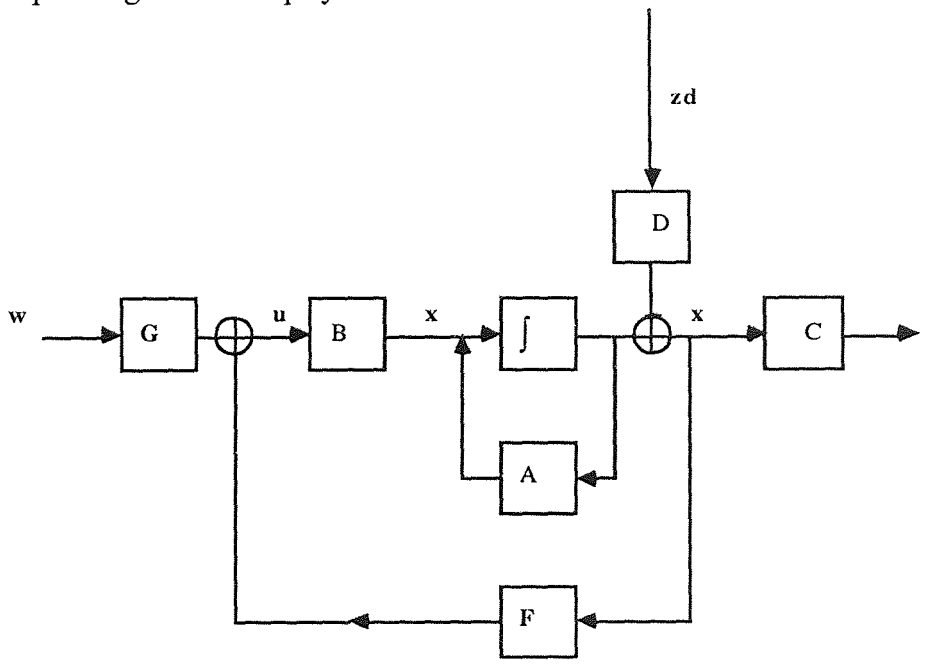

Figure 2.5 Schematic of a closed loop system under control by **u = Fx + Gw** (Shimizu and Matsubara (113))

Falb and Wolovich (179) investigated the approach of Morgan and found that the conditions under which decoupling control of linear state variable systems can be achieved were not well established. They subsequently derived the necessary and sufficient condition for decoupling of general linear multivariable systems described in state variable form. Wonham and Morse (178) also used the state variable approach the multivariable control problem. They called it the "Geometric Approach". The theoretical details are examined in Takamatsu et al. (130). The most recent investigations in these areas regarding application to chemical engineering systems are due to Takamatsu and Kawachi (129), Takamatsu et al. (130) and Shimizu and Matsubara (113,114).

Takamatsu et al. (130) employed the geometric approach to design a multivariable controller for disturbance rejection of the effects of disturbances on the outputs. The controller has the form

$$\mathbf{u} = \mathbb{K}\mathbf{x} \qquad 2.42$$

where $\mathbb{K}$ is the feedback matrix which is designed to reject the effects of disturbances from the outputs of the system described by

$$d\mathbf{x}/dt = A\mathbf{x} + B\mathbf{u} + D\mathbf{z}\mathbf{d}$$

$$\mathbf{y} = C\mathbf{x} \qquad 2.43$$

where the **zd** is the nd x 1 disturbance vector. The works Takamatsu & Kawachi (129) and Shimizu & Matsubara (113, 114) culminate into a control scheme called the Decoupling and Disturbance Rejection control scheme. This is treated in the next section.

2.6.1 Decoupling and Disturbance Rejection for distillation column control

Takamatsu & Kawachi (129) and Shimizu & Matsubara (113) used the formulation of Morgan (196) and Falb and Wolovich (179) to design a multivariable decoupling control scheme which is called the Decoupling and Disturbance Rejection control scheme by Shimizu and Matsubara. Both group of workers use distillation columns as

examples to evaluate the decoupling control scheme. This control scheme has the form of Equation 2.40,

$$\mathbf{u} = \mathbf{F}\mathbf{x} + \mathbf{G}\mathbf{w}$$

The decoupling control problem is to find the matrices **F** and **G** that will reject the effects of disturbances from the outputs and achieve non-interacting control of the outputs such that a change in the setpoint w_i will only affect output y_i.

An important feature of the design is that closed loop poles can be specified to achieve desired output responses while simultaneously decoupling the system. Falb and Wolovich (179) determined the number of closed loop poles that can be assigned and provided a synthesis procedure for obtaining the desired closed loop pole configurations. The number of poles that need to be assigned are partly determined by quantities called decoupling indices and each output is associated with a decoupling index. The synthesis and application of control scheme is reviewed in some detail in the next section with reference to distillation column applications.

2.6.2 Synthesis of the Decoupling and Disturbance Rejection controller

Consider a conventional binary distillation column modelled by Equation 2.43. The **zd** is a nd × 1 vector of the disturbances and D is the n × nd disturbance matrix. This model can obtained by linearising the nonlinear model of the column at a steady state. Consider that the vectors as **x**, **u**, **zd** and **y** as

$$\mathbf{x} = (x_1, x_2, \ldots\ldots, x_n)^T$$

$$\mathbf{u} = (Lr, Vb)^T$$

$$\mathbf{zd} = (F, xf)^T$$

$$\mathbf{y} = (x_1, x_n)^T$$

$$\mathbf{w} = (x_{1s}, x_{ns})^T$$

The Lr, Vb, F and xf denote reflux rate, vapour boilup, feed rate and feed composition, respectively. The control objective is to maintain the outputs **y** at the desired values **w** by manipulating the inputs **u**. The objective of the decoupling controller is to achieve input-output noninteracting control of **y** using a constant

feedback gain matrix, **F**, and a precompensator matrix, **G**. Figure 2.5a shows a block diagram of the decoupling controlled system. Substituting Equation 2.40 into Equation 2.43, the equation of the decoupled system is is obtained

$$\mathbf{dx/dt} = (\mathbf{A}+\mathbf{BF})\mathbf{x} + \mathbf{BGw} + \mathbf{Dzd}$$

$$\mathbf{y} = \mathbf{Cx} \qquad 2.44$$

Before presenting the synthesis procedure of the decoupling control method it is appropriate to say that the mathematical proofs of the design method is quite involved. In fact, Falb & Wolovich (179) and Morgan (196), who have contributed much in this area are not in the field of chemical engineering. Falb is a mathematician and Wolovich is in the disciplines of mathematics and electrical engineering. The mathematical proofs and theorems that culminate in the decoupling control design method involve advanced mathematics and thus are quite complex. Thus, only the synthesis procedure will be given here.

The synthesis procedure for obtaining the controller matrices, **F** and **G**, can be found in the articles of Falb and Wolovich (179), Shimizu & Matsubara (113) and Takamatsu and Kawachi (129). It is summarized here as follows;

A decoupling index, d_i, is defined as

$$d_i = \min (j : \text{for } C_iA^jB \neq 0 \text{ , } j = 0, 1, 2 ,..., n-1)$$

$$= n-1 \text{ (if } C_iA^jB = 0 \text{ for all } j \text{)} \qquad 2.45$$

where i denotes the control inputs, i = 1 to m

Two matrices, A* and B*, are also defined as

$$A^* = \begin{bmatrix} C_1A^{d_1+1} \\ C_2A^{d_2+1} \\ . \\ . \\ C_mA^{d_m+1} \end{bmatrix} \qquad 2.47a$$

$$B^* = \begin{bmatrix} C_1A^{d_1}B \\ C_2A^{d_2}B \\ . \\ . \\ C_mA^{d_m}B \end{bmatrix} \qquad 2.47b$$

where C_i is the i-th row of matrix C. Falb and Wolovich (179) established that the nonsingularity of B* is the necessary and sufficient for decoupling of the system to be achieved.

The **F** and **G** matrices of the controller are obtained as follows

$$\mathbf{F} = \left(\sum_{k=0}^{k=\partial} \mathbf{M}_k C A^k - A^* \right) \quad \text{..... m x n matrix} \qquad 2.48$$

where $\partial = \max_i(d_i)$

$$\mathbf{G} = (B^*)^{-1}\mathbf{K}^* \quad \text{.....} \qquad \text{m x m matrix} \qquad 2.49$$

The $\mathbf{M}_k$ is a diagonal matrix

$$\mathbf{M}_k = \text{diag}(\varsigma^{(1)}_k, \varsigma^{(2)}_k, ..., \varsigma^{(m)}_k)$$

$$\varsigma^{(i)}_k = 0 \text{ for } k > d_i, \text{ for } i = 1 \text{ to m.}$$

The $\varsigma^{(j)}_k$ are used to arbitrarily assign

$$m + \sum_{i=1}^{i=m} d_i$$

closed loop poles to achieve desired closed loop response. The diagonal matrix, **K***, is

$$\mathbf{K}^* = \text{diag}(k_1^*, k_2^*, ..., k_m^*) \qquad 2.50$$

This matrix was introduced by Falb and Wolovich. According to them, if a pair of matrices **F** and **G** decouples the system Equation 2.41 then there is a diagonal matrix **K*** such that

$$\mathbf{G} = (B^*)^{-1}\mathbf{K}^*.$$

This diagonal matrix **K*** is interpreted in Shimizu and Matsubara (113), as manipulating the m decoupled systems. Specific guidance for chosing **K*** is not given.

If no poles are assigned then $\mathbf{M}^{(i)}_k = 0$, i = 1 to m, k = 1 to d_i and the feedback gain matrix, **F**, then becomes

$$\mathbf{F} = (B^*)^{-1}A^* \qquad 2.51$$

The closed loop system is referred to as an "integrator decoupled" system by Takamatsu and Kawachi (129).

The following algebra gives the analysis provided by Falb and Wolovich. Assuming $\mathbf{zd} = \mathbf{0}$, then from Equation 2.43 and 2.44 and using Equation 2.45 then

$$C_i(A+BF)^k = C_iA^k \qquad k = 0,1,\ldots,\ d_i$$

$$C_i(A+BF)^k = C_iA^{d_i}(A+BF)^{k-d_i} \qquad k = d_i+1,\ldots,\ n \qquad 2.52$$

because $C_iA^kB = 0$ for $k = 0$ to $d_i - 1$

Application of the state variable feedback Equation 2.40 and repeated differentiation together with Equation 2.52 results in the following relations

$$y_i = C_ix = C_i(A+BF)^0x$$

$$y_i^{(1)} = C_iAx = C_i(A+BF)x + C_iA^0BGw = C_i(A+BF)x$$

$$y_i^{(2)} = C_iA^2x = C_i(A+BF)^2x + C_iABGw = C_i(A+BF)^2x$$

. . . .

. . . .

$$y_i^{(d_i)} = C_iA^{d_i}x = C_i(A+BF)^{d_i}x + C_iA^{d_i-1}BGw = C_i(A+BF)^{d_i}x$$

The second terms in the above relations cancel out as can be verified from Equation 2.45, which gives the decoupling indices.

$$y_i^{(d_i+1)} = C_i(A+BF)^{d_i+1}x + C_i(A+BF)^{d_i}BGw$$

. . . . . .

. . . . . .

. . . . . .

$$y_i^{(n)} = C_i(A+BF)^nx + C_i(A+BF)^{n-1}BGw + \ldots + C_i(A+BF)^{d_i}BGw^{(n-d_i-1)}$$

where $y_i^{(j)}$ represents the j-th differential of the i-th output, i-th member of $\mathbf{y}$. This implies that

$$y_i^{(d_i+1)} = C_i(A+BF)^{d_i+1}x + C_i(A+BF)^{d_i}BGw$$

$$= C_i(A+BF)^{d_i+1}x + C_iA^{d_i}BGw \qquad 2.53$$

From Equation 2.52, $C_i(A+BF)^{d_i+1} = C_iA^{d_i+1} + C_iA^{d_i}BF$, then the above gives

$$y_i^{(d_i+1)} = C_iA^{d_i+1}x + C_iA^{d_i}BFx + C_iA^{d_i}BGw$$

Since $C_iA^{d_i+1}$ is the i-th row of A* and $C_iA^{d_i}B$ is the i-th row of B*, it can be written that

$$\mathbf{y}^* = (A^* - B^*\mathbf{F})\mathbf{x} + B^*\mathbf{G}\mathbf{w} \qquad 2.54$$

where $\mathbf{y}^*$ is the vector containing the $y_i^{(d_i+1)}$. Substituting Equation 2.48 and 2.49 into Equation 2.54 and assuming $\mathbf{K}^* = I$, where I is the identity matrix, gives

$$\mathbf{y}^* = \Sigma \mathbf{M}_k C A^k \mathbf{x} + \mathbf{w}$$

$$= \Sigma \mathbf{M}_k \mathbf{y}^{(k)} + \mathbf{w} \qquad 2.55$$

or , equivalently,

$$y_i^{(d_i+1)} = \Sigma \mathbf{M}_k\, y_i^{(k)} + w_i. \qquad 2.56$$

A one-to-one correspondence is accomplished. Hence, the i th input, w_i, affects only the i-th output, y_i. In the case with no poles assigned, $\mathbf{M}^{(i)}_k = 0$, i = 1 to m, k = 1 to d_i, Equation 2.56 becomes

$$y_i^{(d_i+1)} = w_i. \qquad 2.57$$

It is claimed in Falb and Wolovich (179) that, for the "control loop" i some suitable values of $\varsigma^{(i)}_k$ can be chosen such that any desired closed loop pole assignment can be achieved. With the poles assigned, the transfer function matrix $\mathbf{G}(s)$ is expressed, according to Shimizu and Matsubara (113) and Takamatsu and Kawachi (129), as

$$\mathbf{G}(s) = \{\ 1/(s^{d1+1} - \Sigma \mathbf{M}_k^{(1)} s^k)\ ;.....;\ 1/(s^{dm+1} - \Sigma \mathbf{M}_k^{(m)} s^k)\ \} \qquad 2.58$$

assuming $\mathbf{K}^* = I$, where I is the identity matrix. In the case with no poles assigned $\mathbf{G}(s)$ becomes

$$\mathbf{G}(s) = \mathrm{diag}\{\ 1/s^{d_1+1}, ...,\ 1/s^{d_m+1}\ \} \qquad 2.59$$

The resulting closed loop system is referred to as an "integrator decoupled" system.

Falb and Wolovich showed that the number of poles, $m + \Sigma d_i$, that can be arbitrarily assigned can never exceed n, where n is the number of state variables, as well as the number of system poles. They claimed that it may sometimes be possible to assign more than $m+\Sigma d_i$ poles, when the number of free parameters, f_p, in the $\mathbf{F}$ matrix is more than $m + \Sigma d_i$. In simple terms, f_p is the number of columns in $\mathbf{F}$ that have at least one non-zero entry.

Feed forward compensation can also be used for disturbance rejection. For a completely observable system, Shah (207) proved that there exists a feedforward compensator which achieves the disturbance rejection if R(D) is a subset of R(B), where R(.) denotes the range of (.). The article by Shimizu and Matsubara (113) gives the feedforward compensator, $\mathbf{T_f}$, which attains disturbance rejection as

$$\mathbf{T_f} = -(B^T B)^{-1} B^T D \quad m \times nd \text{ matrix} \qquad 2.60$$

so that the feed forward control is of the form

$$\mathbf{u} = \mathbf{T_f} \times \mathbf{zd} \qquad 2.60b$$

It is stated in Shimizu and Matsubara (113) and in Shah (207) that, if $m < n$, that is, if the number of control inputs is less than the number of states, the $\mathbf{T_f}$ obtained by Equation 2.60 does not completely reject the disturbances, but suppresses them to some extent.

The mathematical computations involved to obtain the $\mathbf{F}$, $\mathbf{G}$ and $\mathbf{T_f}$ matrices are at least an order of magnitude more complex than those necessary for conventional controller design methods. The synthesis procedure involves many matrix manipulations including matrix inversion. Therefore, as the order of the system increases, i.e n become larger, the computational requirements for obtaining the controller matrices will become more demanding. Numerical problems are likely to occur from computer roundoff errors because of the many floating point calculations that are involved in the synthesis procedure. This could strongly affect the matrix inversion results. The problems will be much more acute if the system is itself illconditioned, that is, if any or all the A, B and D matrices are illconditioned matrices. In this case, the results of the synthesis procedure could become very sensitive to small errors due to roundoff and in the A, B and D matrices. The problem will be more severe with computers using short wordlengths. The use of extended precision can alleviate the problems to some degree.

2.6.3 Minimum number of measured state variables for feedback.

A common problem in the control of chemical plants concerns the availability of measurements vital to control. The decoupling and disturbance rejection control method discussed above is no exception.The feedback controller given by Equation 2.40 presumes that all the state variables are measured for feedback. In practice measuring all the state variables will usually not be possible for various practical and economic reasons. For example, it will not be economical to measure all the tray compositions of a distillation column as composition analysers are expensive. It may be that only a few state variables can be measured. The problem of how many and what state variables should be measured to achieve the control objectives will therefore arise. In simple terms, this implies what state variables must be measured for the system to remain controllable when all the state variables are not available. One way of overcoming this problem would be to use the Kalman filter approach to reconstruct the state variables of the system. The controller synthesis can also be based on an approximate model which considers only the state variables that are, or can be, measured. A drawback of using the Kalman filter approach is the computational requirements will be large, particularly if the order of the system is large. In the case of basing the controller synthesis on an approximate model, there is also a problem. If the process model is simplified, then structural information may be lost since the controller depends on the structure of the model (Shimizu and Matsubara (114)). The possible consequence is the loss of controller performance.

Takamatsu and Kawachi (129) proposed a different approach. The approach aims at finding the minimum number of state variables, and the choice of the variables, that must be measured in order to achieve complete decoupling of the system. They introduced a diagonal matrix, **H**, in which each diagonal element has the value of 1 if the corresponding state variable is measured, and 0 otherwise. The matrix **H** is chosen to satisfy the relationship

$$C_i A^k (I-H) = 0,\ k = 0 \text{ to } d_i+1,\ i = 1 \text{ to } m \qquad 2.61$$

To do this, the diagonal elements of I - **H** which have to be 0 are those that are multiplied by non zero elements of C_iA^k. The corresponding diagonal elements of **H** have to be 1. The state variables are then the minimum number of state variables that must be measured to achieve decoupling control of the system. This procedure implies that, for each input, i, an **H**, called $\mathbf{H}_i$, can be uniquely determined so as to decouple the i-th input-output relationship. The overall $\mathbf{H}_{OV}$ indicating all the state variables to be measured is the logical sum of all the $\mathbf{H}_i$`s.

The feedback control law then becomes

$$\mathbf{u} = \mathbf{F}\mathbf{H}_{OV}\mathbf{x} + \mathbf{G}\mathbf{w} \qquad 2.62$$

and the closed loop equation of the decoupled system now becomes

$$d\mathbf{x}/dt = (\mathbf{A}+\mathbf{B}\mathbf{F}\mathbf{H}_{OV})\mathbf{x} + \mathbf{B}\mathbf{G}\mathbf{w} + \mathbf{D}\mathbf{z}\mathbf{d} \qquad 2.63$$

Figure 2.6 is an illustration of the corresponding closed loop system, with the **H** in this figure corresponding to $\mathbf{H}_{OV}$ in Equation 2.63; Figure 2.7 gives the flowchart for finding $\mathbf{H}_{OV}$.

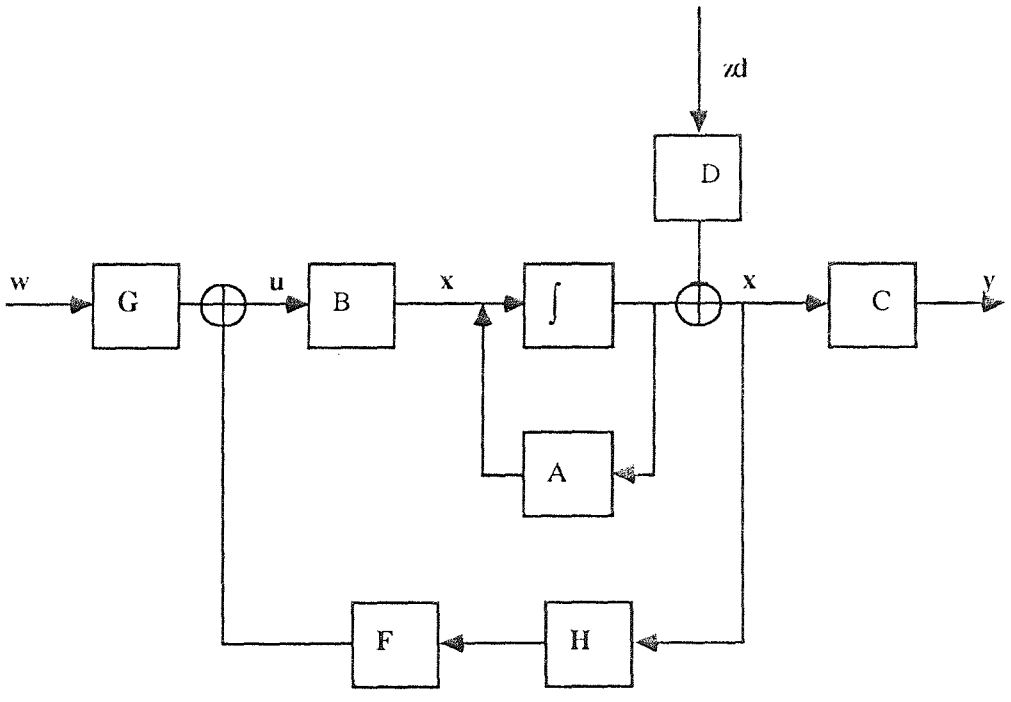

Figure 2.6 Schematic of a closed loop system under control by **u = Fx + Gw** with incomplete state feedback (Takamatsu and Kawachi (129))

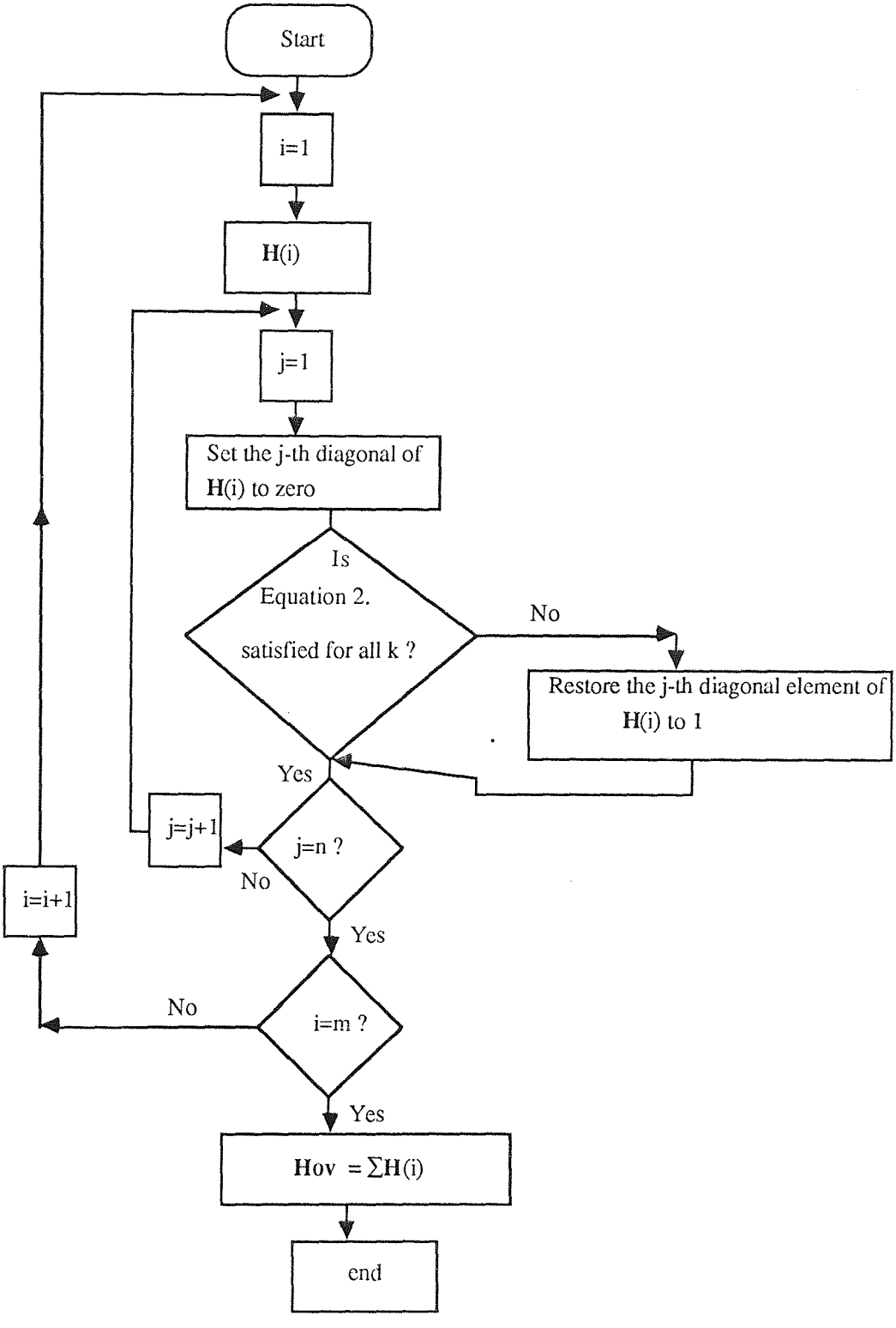

Figure 2.7 Flowchart for finding the minimum number of state variables to be measured for feedback (Takamatsu and Kawachi (129))

2.6.4 Applications to distillation column control.

Takamatsu et al. (130) applied the state feedback controller of Equation 2.42 designed using the geometric approach of Wonham and Morse (178) for load disturbance rejection to the dual composition control of the top and bottoms products composition of a simulation of nine plate binary distillation column. The studies were performed by computer simulation using a very simple nonlinear model of the column. They pointed out that the properties of the controller depends on the model structure and never affected by the kind and number of disturbances that affect the process. This means dependence on the structure of the A and B matrices of the model in Equation 2.38. They reported a case measuring only two state variables which were the second and ninth tray compositions, the controller completely rejects the effect of feed composition disturbance on the top and bottoms compositions. The effect of feed flow disturbances on the bottoms composition could not be completely rejected and this deficiency appeared as an offset in the bottoms composition. This deficiency was also observed in the studies of Shimizu and Matsubara (113) who used the state feedback decoupling controller (Equation 2.40 with $\mathbf{w} = \mathbf{0}$) on a 10 plate binary ethylene-ethane distillation column with pressure variation. This indicates the similarities in the characteristics of controller design based on the geometric approach and the state feedback decoupling and disturbance rejection controller. Shimizu and Matsubara have noted that the coefficients from the 3rd column to the n-1 th column of $\mathbb{K}$ in Equation 2.42 are equal to those of the same columns of $\mathbf{F}$ in Equation 2.40.

Takamatsu and Kawachi (129) applied their proposed method for finding the minimum number of state variables that must be measured for feedback to achieve complete decoupling control of a distillation column with the top and bottom products compositions as the controlled variables. They found that only five state variables need to be measured for the design of the decoupling controller. These variables were the first, second, third, n-1th and nth tray compositions, numbering from the top tray to the reboiler drum. They point out that this number, and the variables, does not depend on the number of trays on the column, rather it depends on the structure of the model.

The significance of this is that the cost of measuring may not necessarily increase for application on a column with more trays as long as the structure of the model is the same.

Takamatsu and Kawachi did not claim that their result, on the minimum of tray compositions required for their conventional binary distillation columns, applies to binary distillation columns in general. However, the number of tray composition measurements and their actual locations obtained by Shimizu and Matsubara (113) agreed with the result of the former. Shimizu and Matsubara found that 6 state variables were required to be measured for feed back. These were the 5 tray compositions and the column pressure.

A drawback of the decoupling and disturbance rejection control strategy is due to the assumption of a linear system. Distillation columns are nonlinear systems with the main factors causing the non-linearities being the curvature of the vapour-liquid equilibrium surface and the vapour and liquid enthalpy surfaces. The assumption of linearity would not be valid if the operating conditions of the column change significantly from the point of linearisation, particularly if it is highly nonlinear. Therefore, the achievable performance of the decoupling control system will be limited. These considerations are important for assessing the practicality of the control scheme on a real process.

Shimizu and Matsubara (114) emphasised that non-linearities are more pronounced in a column were a highly nonideal mixture is being distilled or the column is operated at elevated pressures closer to critical point. However, all the workers mentioned above have not used highly nonideal mixtures nor did any model their respective columns at elevated pressures in applying the decoupling control scheme. Shimizu and Matsubara (113, 114) simply argued that industrial columns distill near ideal mixtures and are operated well below their critical points. Takamatsu and Kawachi used a model which is very simplified with the only non linearity in the model due to a simple vapour liquid equilibrium relationship which was only slightly non linear.

It was noticed that Shimizu and Matsubara (113) and Takamatsu and Kawachi (129) did not examine the setpoint tracking capabilities of the decoupling and disturbance rejection control scheme. There have also been no reported experimental applications of the decoupling control scheme to distillation columns in the literature surveyed.

2.7 Derivative Decoupling Control

There is another approach to decoupling control called Derivative Decoupling Control. This was proposed by Liu (81). The approach is based on decoupling the *state derivatives* rather than the state variables themselves, as the disturbance rejection approach does. Derivative decoupling has been applied to practical systems by Palmenberg and Ward (103), Hutchinson and McAvoy (51), Cheng and Ward (52) and Jung and Lee (60). Hutchinson and McAvoy (51) highlighted some difficulties in obtaining the controller equations. Jung and Lee (60) extended the design method to deal with unmeasured load changes and to handle input constraints. They used a laboratory scale mixing tank in the investigations and the derivative decoupling control technique was reported to perform better than controllers designed by the Inverse Nyquist Array (INA) design method. The results obtained by all these workers mentioned above show that the Derivative Decoupling control strategy relies heavily on good process models so that, like most control systems, it has its limitations as regards sensitivity to model errors.

2.8 Time Delay Compensation

Effective and robust control of processes with significant time delays between the input and outputs response is usually difficult to achieve. Time delays, or dead-time, will reduce the maximum controller gain that can be used in a PID controlled system. Qualitatively, the control action must be slowed, by reducing the controller gain, for example, to maintain the stability and robustness of the closed loop system. A typical

example of where large dead-times frequently occur are in the composition control of distillation columns. Composition analysers are usually associated with large dead-times needed for analysis.

A way to improve the control under these circumstances is to incorporate the Smith dead time compensator (DTC) (172, 173) in the control scheme. The DTC attempts to directly cancel out the time delays so that control can be performed on the system as if there are no time delays present. Figure 2.8 expresses the DTC in block diagram form for feedback control. From this diagram the G_{tk} is the compensator which outputs $y^* - y^*_D$, where y^* is the simulation of the undelayed output while y^*_D is the simulation of the delayed output. This output is added to the process output, y, and the resulting value, y_{dtc} , is fed back to the controller, which may be of advanced or conventional type. G_{tk} is in essence the difference between two process models. If the models are exact then $y = y^*_D$ and exact time delay compensation will be achieved.

In theory any appropriate model formulation can be used, state variable or transfer function models (Ogunnaike and Ray (95)). Furthermore, the exact value of the time delay is required by the DTC. However, in real processes time delays may be varying or may not be known accurately and the quality of control provided by the DTC control scheme can be very sensitive. This is demonstrated in the article by Morari (150).

According to Palmor and Powers (102), investigations of DTC control schemes have shown that some special sensitivity and stability properties is induced by the DTC itself into the closed loop system. These properties exhibited by the DTC control schemes showed that it is inadequate to design the primary controller, G_{pc} in Figure 2.8, for the equivalent system which has no dead time simply because a DTC is incorporated.

2.8.1 Application to chemical engineering systems

Many simulated and pilot scale experimental applications have shown that incorporating a DTC into conventional control systems offers an improvement over

conventional control. Meyer et al. (90) reported the earliest practical application of the DTC.

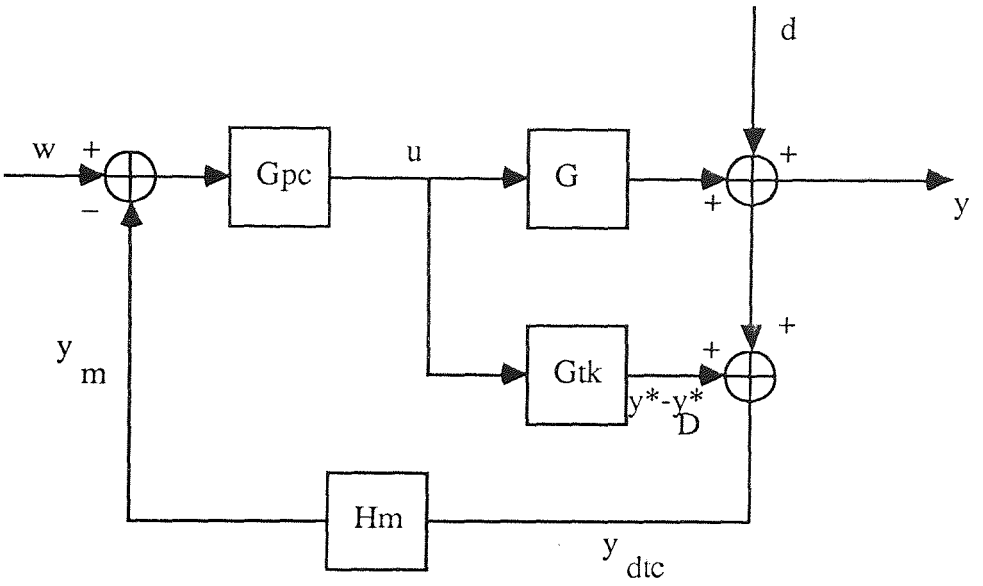

Gtk=Gp- Gp*

Gp process model without time delay , Gp* process model with time delay

y* output of Gp, y_D* output of Gp*

Figure 2.8 Dead Time compensation using Smith Predictor

They applied the DTC in the PI control of the top product composition of a pilot scale methanol-water binary distillation column with 8 bubble cap trays and 22.5cm in diameter. They reported that the performance of the PI controller with the DTC incorporated provided significant improvements in control than ordinary PI control both in simulated and experimental applications.

Extension of the DTC to multivariable systems were made by Ogunnaike and Ray (95). They also considered multivariable systems with multiple time-delays. Ogunnaike et al. (96) then implemented the multiple - delay DTC of Ogunnaike and Ray (95) combined with PI controllers to control a laboratory scale binary distillation facility. The top, bottom and sidestream compositions of the column were simultaneously controlled and significant improvements over conventional PI were reported in both simulated and laboratory experiments. A very high level of robustness

of the multiple delay DTC based control system in the face severe model uncertainty was observed. This indicated a promising future for time - delay compensation techniques.

Ogunnaike and Ray (98) have also addressed the problem of incomplete state feedback in a time delay compensated control schemes. They describe a method for estimating the necessary state variables for implementing a multivariable time-delay compensator. Jerome and Ray (58) present improved forms of the multivariable dead time compensation techniques like those of Ogunnaike and Ray (95). They generalised the approach thus extending the types of systems to which they can be applied.

Palmor and Powers (102) extended the DTC approach to predict the effects of measurable load disturbances on the controlled output. They achieve this by cancelling the time delay associated with the load disturbance response. Furthermore, they argued that compensation of all the dead-time may not always be the best strategy and subsequently introduced the idea of partial cancellation of the time delays. A design parameter, which indicates how much of the time delay is to be cancelled, is introduced into the DTC design. Their results show that partial cancellation can sometimes be beneficial. This partial cancellation technique could be valuable in digital process control schemes where fractional delays and varying time delays are common.

2.9 Adaptive Control

2.9.1 Introduction

Control systems that automatically adjust their controller parameters to compensate for changes in process conditions or the environment are called adaptive control systems. These control systems are of practical value to process control since processes are usually nonlinear and have time varying process parameters. During the last two decades adaptive control systems that are based on recursive identification of the process system have been receiving a great deal of attention. The reason for this is that the control systems are generally very easy to design, they are flexible and they are easily implemented on computers. The significant improvements in computer technology have made it possible to apply adaptive control cheaply and simply on real systems.

Adaptive control concepts are regarded by Seborg et al. (140) as having reached a mature state of development. This assertion is based on evidence of the many successful practical applications of the techniques to chemical engineering systems. Some of these applications were reviewed including a survey of applications in industry. Isermann (54) and Astrom (4) also give comprehensive reviews on the theory and applications of adaptive control.

According to Seborg et al. (140), adaptive control design techniques can be grouped into three main classes. These are

(1) design methods based on optimising quadratic cost functions, e.g. self tuning regulators (STR) by Astrom and Wittenmark (154) and self tuning controllers (STC) by Clarke and Gawthrop (156, 157),

(2) design methods based on stability theory such as model reference adaptive control (MRAC) (Landau (197), Sen de. la. (124)) and

(3) Pole-zero assignment techniques (Astrom and Wittenmark (9)).

Adaptive control methods which are based on state space representation of the process have also been developed (Hesketh (50) and Samson and Fuchs (120)). All these techniques are closely related; they differ only in the way the controller

parameters are adjusted (Astrom (4)). Figure 2.9 illustrates the general structure of adaptive control systems. Recently, Gawthrop (43) proposed some adaptive control designs which have PID controller structure and can, therefore, be used for automatic tuning of PID controllers.

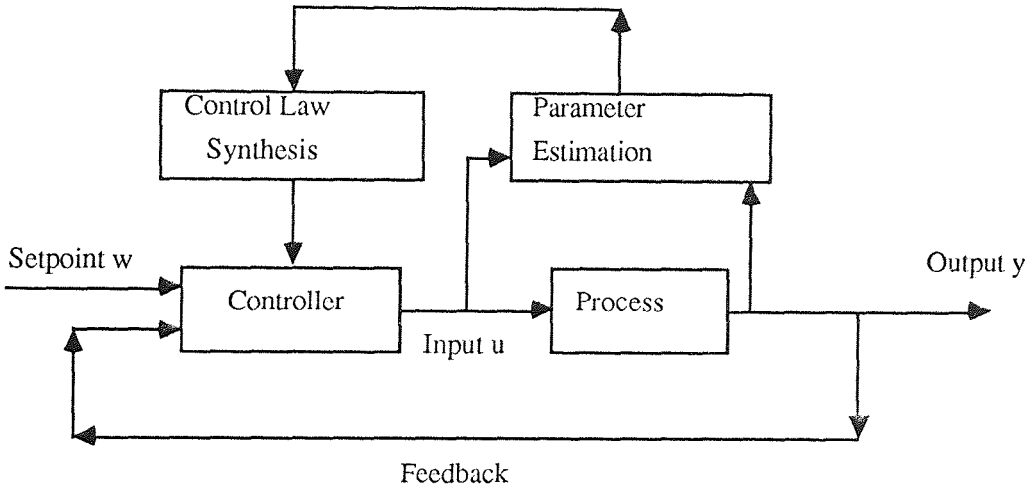

Figure 2.9 General structure of adaptive control systems (Seborg et al (140))

The basis of an adaptive control system is to estimate the parameters of an assumed process model on-line and then adjust the controller settings based on the current parameter estimates. This procedure is carried out continuously at regular time intervals. In this way the problem of model uncertainty is directly addressed. The recursive least squares estimation technique is a method that is commonly used for parameter estimation. Other methods such as the projection algorithm and instrumental variables algorithms are also used. These techniques are treated more fully in the book on adaptive filtering, prediction and control by Goodwin & Sin (39).

One advantage of using an adaptive control system is that the assumed process model only needs to be a local approximation, that is, the model is only required to give an adequate fit to the system within and around the sample interval. This means that the assumed model can be made relatively simple in terms of the number of

parameters that need to be regularly updated and lower order process model can be used to fit higher order processes. Some adaptive control designs can also be formulated in predictive form by formulating the parameter estimator to predict the future outputs of the system. For example, in a system with significant time delays the estimator could be made to predict the output over the time delay so that control can be based on this output prediction. The adaptive controller will then function as a time delay compensator as well. Therefore, in principle, the adaptive concept tackles directly (i) model uncertainty issues, such as non-linearities in the system and time varying process parameters, in control systems design and (ii) the problem of time delays; both of which limit the achievable performance of conventional constant parameter control systems such as the conventional PID control.

There are two main ways of organising the combination of the recursive parameter estimator and the control algorithm in an adaptive control system. They are the explicit, or indirect, and implicit, or direct, formulation (Seborg et al. (40). In the explicit formulation, the process model parameters are first estimated, then the controller parameters are explicitly solved using these estimates of the process parameters. However, the solution involves iterative calculations so that the numerical problems, such as illconditioning of the parameters, can arise. Isermann (54) pointed out that the explicit formulation is widely used because it allows for many estimator - controller combinations and the direct access to the process parameters at all times during operation.

In the implicit formulation, the controller parameters are estimated directly. This eliminates the extra calculations for the controller equations and, hence, computation time can be saved. The name implicit arises because the controller is based on estimates of an implicit process model (Astrom (4)). This formulation reduces the risk of numerical problems that could arise as in the explicit formulation. The formulation is more restrictive in terms of the number of estimator-controller combinations possible (Seborg et al. (140)). Evaluation of implicit formulations of adaptive control systems has also shown that, sometimes, the number of parameters that need to be estimated

may increase, compared to the explicit formulation, so that it may not always be the case that computation time can be saved (Isermann (54)). In this thesis, attention will be focussed on the implicit formulation.

A significant proportion of the publications on applications of adaptive control have been on the self-tuning approach based on optimising a quadratic cost function has been. The basis of these methods is the self-tuning regulator STR by Astrom and Wittenmark (154). This was later modified by Clarke and Gawthrop (156, 157) to the self-tuning controller (STC) which overcome some of the inadequacies of the STR. The STC also extends the range of process systems to which the self tuning approach can be applied. In the following, a summarised version of the synthesis of SISO STR and STC will be presented. More details can be found in the original articles of Astrom and Wittenmark (154) on the STR, Clarke and Gawthrop (156,157) on the STC, Seborg et al. (140) and Clarke (20) on both methods.

2.9.2 The Self Tuning Regulator

The usual assumption in the design of adaptive control systems is that the process is modelled by a linear difference equation:

$$\mathbf{A}(z^{-1})\, y(t) = \mathbf{B}(z^{-1})\, u(t-k) + \mathbf{C}(z^{-1})\xi(t) + d(t) \qquad 2.64$$

where $\mathbf{A}$, $\mathbf{B}$ and $\mathbf{C}$ are polynomials in the z domain,

$$\mathbf{A}(z^{-1}) = 1 + a_1 z^{-1} + a_2 z^{-2} + \ldots\ldots + a_n z^{-n}$$

$$\mathbf{B}(z^{-1}) = b_0 + b_1 z^{-1} + \ldots\ldots + b_m z^{-m}$$

$$\mathbf{C}(z^{-1}) = 1 + c_1 z^{-1} + c_2 z^{-2} + \ldots\ldots + c_n z^{-n}$$

considering single input single output (SISO) case. The y and u are the respective plant inputs and outputs. The z^{-1} is commonly referred to as the backward shift operator, so that $z^{-1}y(t) = y(t-1)$; it also represents z-transform. The n and m are integers which represent the orders of the $\mathbf{A}(z^{-1})$ and $\mathbf{B}(z^{-1})$ polynomials, so that they represent the order of the process given by Equation 2.64. The t is an integer which represents the number of sampling intervals, ΔT, rather than continuous time. The symbol k is an integer representing the process time delay t_d, so that k = 1+

$INT(t_d/\Delta T)$, where INT denotes integer. The k includes the inherent unity delay due to sampling, so that $k \geq 1$. The $\xi(t)$ represents the zero mean random noise disturbances. The d(t) represents offset due to non-zero mean disturbances, unmeasured load disturbances, local linearisation and inaccuracies in initial values (Clarke (20),Clarke et al. (21)). It is sometimes called the bias term. It is usually the case that the noise cannot be modelled by $\mathbf{C}(z^{-1})$ because real plants are characterised by the disturbances that represent d(t), mentioned above. Clarke (20) mentions that in the case were $\mathbf{C}(z^{-1})$ is unknown a noise shaping filter can be introduced.

The y and u can be *full valued data*, that is data as they are obtained. The corresponding adaptive controller is commonly referred to as a positional controller, by analogy with the positional form of the PID control algorithm.

The self-tuning regulator (STR) is a minimum variance controller based on the prediction of the system output, $y^*(t+k)$, given data up to time t, where k is the time delay of the process and the superscript * denotes prediction. The controller attempts to set this prediction to zero at each time interval. The objective of the controller is to minimise the following cost function:

$$J_1 = y^*(t+k)^2 \qquad 2.65$$

If the explicit formulation is used the following polynomial identity

$$\mathbf{C}(z^{-1}) = \mathbf{E}(z^{-1})\ \mathbf{A}(z^{-1}) + z^{-k}\mathbf{F}(z^{-1}) \qquad 2.66$$

is that which must be solved to obtain the controller parameters. The $\mathbf{E}(z^{-1})$ and $\mathbf{F}(z^{-1})$ are of the form

$$\mathbf{E}(z^{-1}) = 1 + e_1 z^{-1} + \ldots\ldots + e_{k-1} z^{-(k-1)}$$
$$\mathbf{F}(z^{-1}) = f_0 + f_1 z^{-1} + \ldots + f_{n-1} z^{-(n-1)} \qquad 2.67$$

These polynomials are obtained given $\mathbf{A}$, $\mathbf{C}$ and k.

According to Clarke (20), by writing Equation 2.64 at time t+k and multiplying by $\mathbf{E}(z^{-1})$ gives

$$\mathbf{E}(z^{-1})\mathbf{A}(z^{-1})y(t+k) = \mathbf{E}(z^{-1})\mathbf{B}(z^{-1})u(t) + \mathbf{E}(z^{-1})\xi(t) + \mathbf{E}(z^{-1})d(t) \qquad 2.68$$

Note that $y(t+k) = z^{+k}y(t)$ which implies y at k intervals in the future.

Using Equation 2.66 and defining $G(z^{-1}) = E(z^{-1})B(z^{-1})$ then Equation 2.68 becomes

$$C(z^{-1})\, z^{+k}\, y(t) - z^{+k}\, z^{-k} F(z^{-1}) y(t) = G(z^{-1})u(t) + E(z^{-1})\xi(t) + E(z^{-1})d(t)$$

which by rearranging becomes

$$C(z^{-1})\, y(t+k) = F(z^{-1})y(t) + G(z^{-1})u(t) + E(z^{-1})\xi\,(t) + E(z^{-1})d(t) \qquad 2.69$$

where

$$G(z^{-1}) = g_0 + g_1 z^{-1} + \ldots + g_{m+k-1} z^{-(m+k-1)}$$

If the noise is not modelled by a polynomial then $C(z^{-1}) = 1$ can be assumed.The predictor model can then be written as

$$y^*(t + k) = F\, y(t) + Gu(t) + d \qquad 2.70$$

where $d = E(1)d(0)$ by assuming d(t) is constant; the z^{-1} has been dropped for clarity. The prediction error ep(t+k) is given by $ep(t) = E(z^{-1})\xi\,(t+k)$. The control law that minimises Equation 2.6.5 is given by

$$Fy(t) + Gu(t) + d = 0 \qquad 2.71$$

which then gives

$$u(t) = -\,(Fy(t) + d)/G \qquad 2.72$$

The denominator $G(z^{-1})$ of the controller Equation 2.72 has as a factor the numerator of the process model which is $B(z^{-1})$ (see Equations 2.68); the STR controller poles therefore attempt to directly cancel out the process zeroes.

For the self tuning version of the control law, considering implicit formulation, a regression model is defined as

$$y^*(t) = F\, y(t - k) + Gu(t - k) + d \qquad 2.73$$

by writing the predictor model Equation 2.70 at t = t - k . The controller parameters F and G are arranged in the parameter vector.

$$\theta^T = [f_0, f_1, \ldots..; \; g_0, g_1, \ldots.; d] \qquad 2.74$$

with the data or measurement vector arranged as

$$\emptyset^T (t - k) = [y(t - k), y\,(t - k- 1)\ldots.; u(t - k), u(t-k-1), \ldots.;1] \qquad 2.75$$

The "1" in the vector Ø (t - k) is for the estimation of the offset level d. This approach is usually called the "one in the data vector " method. An alternative to this method was suggested by Morris et al. (86). The method is to use the integrated prediction error

$$mn(t) = mn(t-1) + \varpi ep(t) \qquad 2.76$$

where ϖ is a scaling factor that must be prespecified. The mn(t) replaces the 1 in vector Ø(t - k). This approach has been called "proxy of the residuals", as the prediction error is sometimes referred to as " the residuals ".

The vector θ contains the controller parameters which are estimated directly if implicit formulation is considered. Expressed more clearly, the predictor model of Equation 2.73 is given as

$$y^*(t+k) = [f_0y(t) + f_1y(t-1) + ...+ f_{n-1}y(t-n+1) + g_0u(t) + g_1u(t-1)+.....$$
$$.....+ g_{m+k-1}u(t-m-k+1) + d] \qquad 2.77$$

The control law is simply derived by setting the future prediction error to zero, that is

$$ep(t+k) = y(t+k) - y^*(t+k) = 0.$$

The minimum variance control law is then

$$u(t) = -1/g_0[f_0y(t) + f_1y(t-1) +...+ f_{n-1}y(t-n+1) + g_1u(t-1) +$$
$$...+ g_{m+k-1}u(t-m-k+1) + d] \qquad 2.78$$

At each time interval the new **F** and **G** parameters are updated into the controller equation, Equation 2.78, and then the control action u(t) is computed.

2.9.3 Reported deficiencies of the self tuning regulator

There STR has several diadvantages. These have been noted by many workers including Seborg et al. (140) and Clarke and Gawthrop (156,157). One is that the STR generates large control actions due to the minimum variance control. Secondly, since the STR controller poles attempts to cancel out the process zeroes, complete instability will result if the process is stable but exhibit non minimum phase behaviour. This is because the zeroes of the non minimum phase system which are outside the unit circle become unstable poles of the STR control law. According to Clarke (20), even if exact cancellation is achieved, the finite wordlength of the computer, or computer round-off,

will still induce instability into the system. Nonminimum phase behaviour greatly limits the performance of minimum variance adaptive control schemes, thus, various methods and adaptations of the standard method of adaptive control design methods have been developed (eg. Samson and Fuchs (120), Clarke (20) and Boland and Giblin (12)) to address the problem.

Difficulties will occur if the parameters are not identified accurately. Such problems will arise if sufficient excitation of the closed loop system is not achieved so that not all the parameters can be identified properly. Some parameter estimates may converge to wrong values, or be biased, and cause control problems. For example, the leading parameter of $\mathbf{G}$, g_0, which determines the STR controller gain (see Equation 2.75) may become biased; it may converge close to zero causing large control actions, or it may converge to very large values causing very sluggish closed loop response. The parameter may also assume the wrong sign so that control actions will be computed in the wrong direction which may cause an unstable system. For these reasons g_0 is usually fixed *a priori*. Trial and error approach is usually employed to obtain the best value of g_0. An example of where this is done is in the work of Dahlqvist (31). Finally, the STR does not explicitly address set point tracking.

2.9.4 The Self Tuning Controller

The generalised minimum variance (GMV) self-tuning controller (STC) by Clarke and Gawthrop (156, 157) is another approach based on optimising a quadratic cost function. This approach overcomes many of the limitations of the STR as well as extend the number of systems that the self tuning approach can be applied. The synthesis procedure of STC is similar to that of the STR and so only a summary is given here.

The STC of Clarke and Gawthrop (157) optimises a modified objective function:

$$J_2 = [[\, \mathbf{P}(z^{-1})\, y(t+k) - \mathbf{R}(z^{-1})\, w(t)]^2 + [\mathbf{Q}'(z^{-1})u(t)]^2] \qquad 2.79$$

The w(t) is the set point. The $\mathbf{P}(z^{-1})$ is called the output weighting polynomial, $\mathbf{R}(z^{-1})$ is called the setpoint filter polynomial and $\mathbf{Q}'(z^{-1})$ is the control weighting polynomial.

They all have the form $P(z^{-1}) = P_N(z^{-1}) / P_D(z^{-1})$, where the N and D denote the numerator and the denominator of the polynomial. The Q' penalises excessive control action, the R filters the setpoint to prevent excessive overshoot of the output after a setpoint change. The output weighting polynomial P equips the resulting controller with model following features as it acts like a reference model..

For the STC the identity of Equation 2.66 is now

$$C(z^{-1})P_N(z^{-1}) / P_D(z^{-1}) = E(z^{-1})\ A(z^{-1}) + z^{-k} F(z^{-1})/ P_D(z^{-1}) \qquad 2.80$$

Assuming the noise model is not identified (ie. $C(z^{-1}) = 1$), the corresponding predictor equation is given as:

$$Py^*(t + k) = (F / P_D)y'(t) + Gu(t) + d \qquad 2.81a$$

This becomes

$$Py^*(t + k) = Fy'(t) + Gu(t) + d \qquad 2.81b$$

where $y'(t) = y(t) / P_D$.

The optimal control law that minimises the Equation 2.79 w.r.t is given by

$$\partial J_2/\partial u = 0 = \psi(t+k)^* = P\ y^*(t + k) - R\ w(t) + Q\ u(t) \qquad 2.82$$

where $Q = Q'Q'(0)/G(0)$. This gives

$$u(t) = \left(R\ w(t) - P\ y^*(t + k)\right)/Q \qquad 2.83$$

The minimisation procedure is given fully in the articles by Clarke & Gawthrop (157). By substituting Equation 2.82 into Equation 2.81, the general predictive control law becomes

$$Fy'(t) + Gu(t) + d - (Rw(t) - Qu(t)) = 0 \qquad 2.84$$

which, by rearranging, becomes

$$u(t) = [\ G + Q]^{-1}\ [\ -F\ y'(t) + R\ w(t) - d\ ] \qquad 2.85$$

The closed loop equation may be obtained by substituting the above equation into Equation 2.64. This gives

$$y(t) = \frac{z^{-k}\ BR}{PB + QA}\ w(t) + \frac{G + Q}{PB + QA}\ \xi(t) \qquad 2.86$$

The characteristic equation is therefore

$$PB + QA = 0 \qquad 2.87$$

which shows that P and Q can be used to manipulate the poles of the closed loop system. Therefore, the STC can be applied to a nonminimum phase plant when the proper choices of P and Q are made. The structure and implementation of the positional STC is given schematically in Figures 2.10 and 2.11. Since the delay term z^{-k} does not appear in the characteristic equation the STC, therefore, provides time delay compensation (Morris et al. (85)). The STC becomes the STR when P = I, Q = 0 and w(t) = 0. When P = I and Q = 0 the STC becomes a minimum variance controller with set point tracking capabilities.

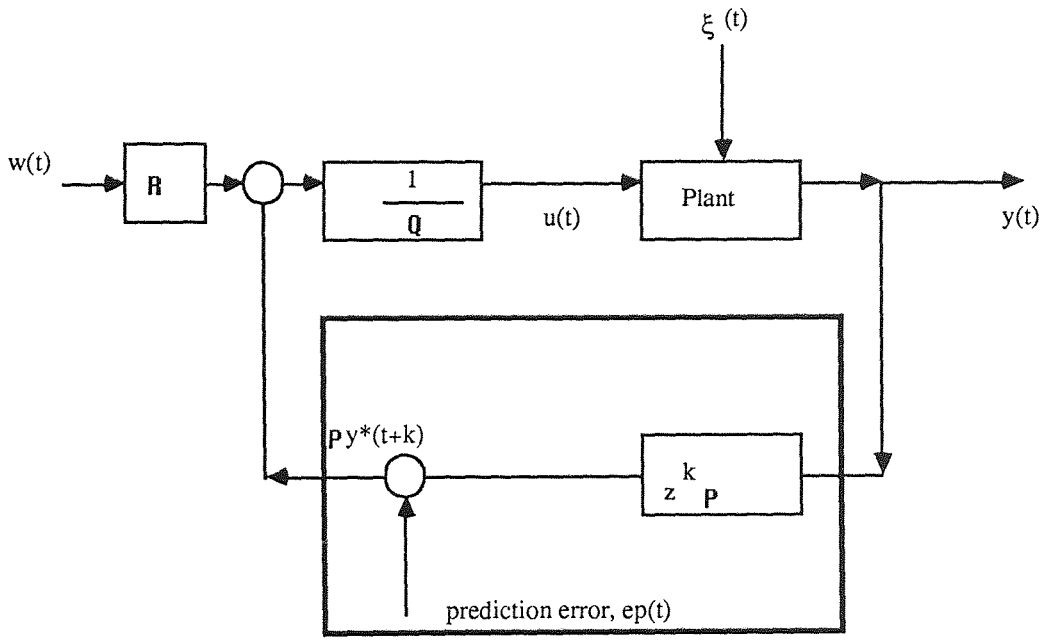

Figure 2.10 Structure of the positional self tuning controller (Clarke et al (21))

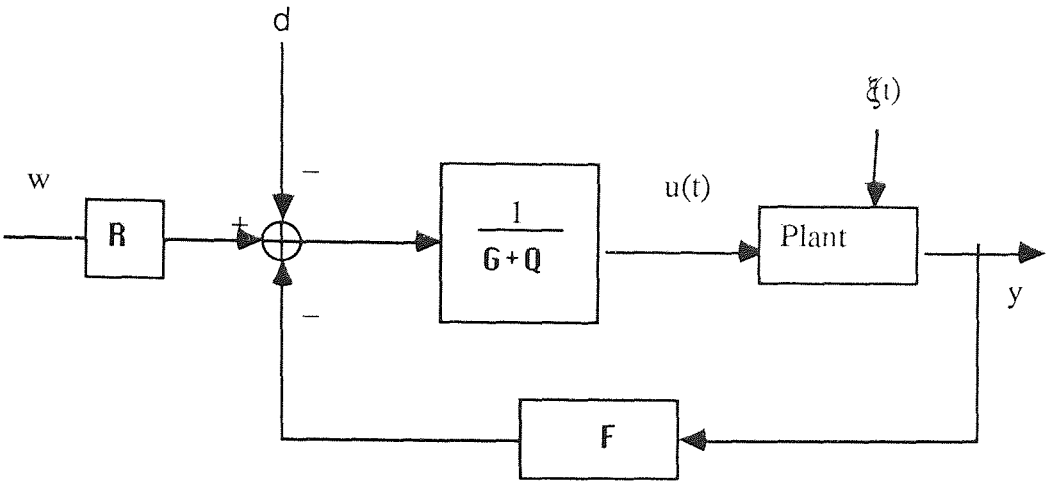

Figure 2.11 Implementation of a positional self tuning controller (Clarke et al (21))

The STR and the STC are in positional form as presented above, where full value data is used for parameter estimation and control calculations. The implication is that the initial values of the input and output data, y_0 and u_0, need to be accurately determined. In practice, this is not always possible as process systems are rarely ever at exact steady state. Offsets are therefore likely to occur in practice if the reference values are in error. Several ways for obtaining good estimates of the reference values have been suggested by Latawiec and Chyra (78), but these methods still do not guarantee that offsets will be eliminated completely.

The use of scalar control weighting $\mathbf{Q} = \lambda$ induces an offset commonly known as lamda offset. This offset arises because $\mathbf{Q}(1) \neq 0$. Lamda offset can be removed by choosing $\mathbf{Q}$ such that $\mathbf{Q}(1) = 0$. The simplest possibility is $\mathbf{Q} = \lambda\Delta_1$, where $\Delta_1 = 1\text{-}z^{-1}$, so that changes in the control u(t) - u(t-1) are penalised rather than absolute values. In this case the cost function Equation 2.79 becomes:

$$J_3 = [[\mathbf{P}\, y(t+k) - \mathbf{R}u(t)]^2 + [\mathbf{Q}\,(1- z^{-1})\, u(t)]^2] \qquad 2.88a$$

and the control law becomes

$$\partial J_3/\partial u = 0 = \mathbf{P}\, y^*(t+k) - \mathbf{R}\, w(t) + \mathbf{Q}\,(1- z^{-1})\, u(t) \qquad 2.88b$$

2.9.5 Selecting the design parameters for the self tuning controller

The performance of the STC, and all adaptive control schemes, depends on appropriate selection of the various model, controller and estimator parameters. Comprehensive reviews concerning the selection of these parameters are given in articles by Seborg et al. (140), Isermann (54) and Astrom (4, 21). These articles show that, with reasonable understanding of the process, the selection of only a few of the parameters is crucial. The crucial parameters are the sampling period and the time delay assumed in the process model.

1) *Model parameters*:

The four model parameters necessary are the model order represented by n and m, the sampling interval, ΔT and the integer k representing the time delay. The assumed model order is usually chosen to be 1st, 2nd or 3rd (n and m = 1, 2 or 3) since the model only needs to be a local approximation. Low order models fitted to higher order processes are usually good approximations provided sampling interval is reasonably long (Clarke (20)). In industrial applications, however, larger model orders may be needed resulting in larger number of parameters that need to be estimated.

Selecting ΔT can be done by standard methods used to select sampling intervals for applications of conventional control (Isermann (54)). In general, the robustness of the STC, and adaptive control systems in general, improves as t_S becomes larger. A small t_S can make the process model become non-minimum phase, while longer t_S can be used to avoid non-minimum phase zeroes, reject high frequencies disturbances and badly modelled plant modes, but sluggish response may result (Clarke (20)) .

The time delay k usually need to be accurately determined and must be exact multiples of ΔT. Kurz and Goedecke (69) have reported that the performance of adaptive control algorithms based on recursive parameter estimation are very sensitive to incorrect choice of the process time delay, more sensitive than the incorrect choice of the process model order. They report that if the time delay is not known exactly, or varies significantly with time, the control may be poor or instability may even result.

They consequently proposed that the time delay could be estimated on-line, if it varies significantly.

Another approach to self tuning control is called the extended horizon approach. Ydstie et al. (146) suggested this approach to deal with varying time delays as well as non minimum phase behaviour. In this method the controller does not attempt to drive the predicted output to the setpoint in one step, rather the controller is allowed more time, that is, the time horizon of the controller is extended. Ydstie et al. (146) point out that by doing this it is possible to look beyond the process time delay and periods of nonminimum phase behaviour. They applied the method to a pilot scale carbon dioxide absorber-desorber unit and reported that the effect of extending the horizon of the controller is to detune the controller. Other extensions exist where both the control and prediction horizon can be extended. An investigation of such extensions were carried out by Montague et al. (88) on a linear model of a distillation column. Their results showed that, when both the control and the prediction horizons become larger than the actual process time delay, improvements in controller performance are insignificant. Using a non-linear model of the column they reported that deterioration of performance resulted. They also pointed out that obtaining the best combination of control and prediction horizons can be a tedious task.

2) *Estimator parameters*

The parameter estimation step is a crucial step in all adaptive control schemes. The recursive least squares (RLS) in standard form is given as,

$$\theta(t) = \theta(t-1) + K(t)\,[y(t) - \emptyset(t-k)^T\theta(t-1)]$$

$$= \theta(t-1) + K(t)ep(t) \qquad 2.89$$

$$K(t) = (PP(t-1)\,\emptyset(t-k)/[1 + \emptyset^T(t-k)\,(PP(t-1)\,\emptyset(t-k)$$

$$2.90$$

$$PP(t) = PP(t-1) - \frac{PP(t-1)\emptyset(t-k)\emptyset(t-k)^T PP(t-1)}{1 + \emptyset(t-k)^T PP(t-1)\emptyset(t-k)}$$

$$= [I - K(t)\,\emptyset(t-k)]PP(t-1) \qquad 2.91$$

where t is the time, $\theta(t)$ is the vector of the parameter estimates, $\emptyset(t-k)$ is the data vector. The K(t) is the estimator gain, PP(t) is the covariance matrix, I is the identity

matrix and ep(t) is the output prediction error , or the residuals as it is sometimes called.

The estimator requires the specification of the initial covariance matrix, PP(0), and the initial parameter vector, $\theta(0)$. Choosing the initial parameter estimate $\theta(0)$, is usually not difficult particularly if the process response data is available *a priori*.. The common practice is to use a suitable conventional controller to initially `tune in` the $\theta(t)$ parameters. The adaptive controller is then switched on when, for example, the prediction error is small over several samples and the control actions of the self tuning controller are the same as those of the conventional controller. A large initial covariance matrix, PP(0), implies poor confidence in $\theta(0)$ and will produce rapid initial changes in $\theta(t)$ because the estimation gain K(t) depends directly on PP(t). A small PP(0) indicates good confidence and slow initial changes in $\theta(t)$.

In some situations it may become necessary to avoid updating the controller with new parameters, that is to "freeze" the controller parameters, if some or all the parameters drift or jump into undesirable space. Examples of where such preventative measures are necessary is when large disturbances enter the system yielding a large prediction errors. The parameter estimates may then fluctuate drastically for a few iterations and it is then important not to update the controller with bad or unrealistic parameter estimates Seborg et al (140). A common test used to prevent this is to specify the maximum allowable prediction error and freeze the controller parameters if this limit is exceeded. If a good knowledge of the parameters are known, an additional test is to specify the upper and lower bounds within which the controller parameters must lie.

3) *Controller parameters*

The weighting $\mathbf{P}(z^{-1})$ is a transfer function that can be specified to give a desired closed loop response to setpoint changes, while $\mathbf{Q}(z^{-1})$ is used to reduce excessive control activity and introduce integral action into the controller structure. With proper selection of $\mathbf{P}(z^{-1})$ and $\mathbf{Q}(z^{-i})$ an unstable process can be stabilised. The weighting, $\mathbf{R}(z^{-1})$, is a transfer function used to filter the set point; thus tailoring the set point

response without affecting load disturbance response. It is useful in situations where the output is not desired to follow sudden jumps in set point and can therefore in the reduce overshoots. Only $\mathbf{P}(z^{-1})$ affects the parameter estimates, as it appears in the predictor model (Equation 2.79). The order of $\mathbf{P}(z^{-1})$ has been suggested by Clarke and Gawthrop (157) to be chosen as at least of the order of the assumed process model, to avoid under performance of the controller.

To avoid steady state offsets the relationship $\mathbf{P}(1) = \mathbf{R}(1)$ must be satisfied. This can be verified by examination of the closed loop equation, Equation 2.81, putting $\mathbf{Q}(z^{-1}) = 0$ and $\xi(t) = 0$ in the equation.

Morris et al. (85) have reported that choosing $\mathbf{Q}(z^{-1})$ as the inverse of a conventional PID controller of the system yielded good results. This allows the system closed loop behaviour to be modified by a design of a controller using a conventional design method.

2.9.6 Operational problems of the recursive least squares scheme

It is the characteristic of the RLS, and most parameter estimation schemes, to loose sensitivity; that is the estimator gain becomes too small. This happens because the PP(t), and hence K(t), tend to zero as more data is processed so that corrections to the parameters in $\theta(t)$ become smaller and smaller. When this happens the parameter estimator will not be able to track slowly time varying parameters. To prevent this a weighting factor, υ ($0 < \upsilon \leq 1$), called the forgetting factor, can be introduced into Equation 2.91 to give

$$PP(t) = [I - K(t)\, \emptyset(t - k)]PP(t - 1)/\upsilon \qquad 2.92$$

Choosing υ to be less than 1 weighs new data more heavily. The effect is to prevent the covariance matrix PP(t) from becoming too small since it is scaled by a factor less than 1. This would maintain the sensitivity of the estimator so that process parameter variations could be tracked. However, if the data y and u are zero or do not change much, that is, the closed loop system is not excited, the PP(t) will begin to grow when υ is less than 1. The PP(t) can become too large and so make the estimator

too sensitive. This is called covariance windup. The consequence is that large and violent changes in the parameter estimates, or "bursting", would occur if small changes in the data enters the system and this may lead to instability of the closed loop system. This characteristic of adaptive control schemes is treated in Hsu and Costa (143), Ydstie et al. (146) and Goodwin & Sin (39).

To reduce the risk of covariance windup several variable forgetting factor algorithms have been suggested. These include those of Fortescue et al. (34), Wellstead and Sanoff (121), Ydstie et al. (146), Ydstie (151), Lozano-Leal (79) and Zarrop (139). In general, each variable forgetting factor algorithm reduces $\upsilon(t)$ when the prediction error increases. This has the effect of increasing the size of the covariance matrix and hence increases the speed of the adaptation. The forgetting factor converges to unity as prediction error becomes smaller. The variable forgetting algorithms do not entirely eliminate covariance windup, except that of Lozano-Leal which computes the forgetting factor to maintain a constant Tr(PP(t)), where Tr represents the trace. In doing this covariance windup is effectively eliminated. The success of the method depends, however, on the closed loop system being persistently excited to the appropriate degree.

The robustness of adaptive control systems is also an important issue. Anderson (7) has shown that even without the effect of covariance windup bursts can occur and lead to instability as a result of the parameters drifting due to lack of excitation, model mismatch, and computer round off errors. Rohrs et al. (108) have also shown that unmodelled disturbances and wrong model order could easily lead to instability of the adaptive controlled system, if sufficient excitation of the system is not ensured.

Several modifications have been proposed to improve robustness of the adaptive control system. These include an approach called "dead zone" where the adaptation of the parameters are stopped if the error is small, smaller than a user specified limit. Another method is to introduce a " leakage " term which introduces a linear drift term into the parameter estimator updating equation, Equation 2.90. Ydtsie (151) gives a combined form of the leakage and dead zone approach as

$$\theta(t) = \theta(t-1) + K(t)ep(t) + \alpha(\theta(t-1) - \theta^{*}(t)) \qquad 2.93$$

where α is the leakage term and $\theta^{*}(t) = \theta^{*}(t-1)$ if $K(t)\, ep(t) \leq \varepsilon$ and $\theta^{*}(t) = \theta(t-1)$ otherwise.The term ε is the deadzone specified by the user and the leakage α is usually chosen to be small. Ydstie (151) points out that this approach will not always work because model mismatch will not always manifest itself as a slow drift.

In the computation of PP(t) using Equation 2.91, computer roundoff can result in PP(t) loosing positive definiteness. This will cause the estimator calculations to become unstable and an unstable system could result. This will happen in fewer iterations on computers that use short wordlengths. Methods available which overcome this problem include using the square root filter (SQRTF) algorithm (Perterka (155)) or the UD factorisation method, given in Astrom and Wittenmark (206) and Ydstie (151)), to update the PP(t). A very clear presentation of the SQRTF algorithm for computer programming is presented in Kiovo (70)

There have been many modifications of the RLS method. For example, when the noise is to be modelled ($C(z^{-1}) \neq 1$), other techniques such as the extended recursive least squares (ERLS) technique must be used to estimate the parameters including the noise model parameters. The ERLS approach has been used by Chien et al. (24). The technique and its applications are treated fully by Lai and Wei (77). Fuchs (35), Sin and Goodwin (175) also present modified forms of the RLS.

This page has been left intentionally blank

This approach has been used successfully by some workers (McDermott et al. (38, 84)), but is considered undesirable (Absjorben (2), Kershenbaum and Fortescue (158)) because a significant increase the variance of the outputs will result. The actual level and proper frequency of the application of the signals may also be difficult to determine.

2.9.8 Adaptive algorithms that avoid the persistent excitation condition

Numerous work have been done to address the problem of parameter identifiability in adaptive control systems where sufficient excitation of the closed loop system is not obtained. These workers include Lozano-Leal and Goodwin (147), and Ossman and Kamen (94) who have suggested various adaptive control approaches that do not require persistent excitation for good parameter estimation.

The approach of Ossman and Kamen (94) will be focussed on in this thesis. The method assumes that the system parameters, θ, belongs to a known bounded interval $[\theta^{min}, \theta^{max}]$ and a reasonable assumption, or *a priori* information, of these bounds is available. The method also assumes that the plant is stabilisable for all possible values of the unknown system parameters. The RLS estimation scheme is then modified to force θ into the bounded interval, over several sampling intervals. The basic algorithm for a SISO system is given as follows. A vector $\mathbf{f}$ is defined as

$$\mathbf{f}(\theta(t-1)) = \begin{cases} \theta(t-1)-\theta^{max} & \text{when } \theta(t-1)>\theta^{max} \\ \theta(t-1)-\theta^{min} & \text{when } \theta(t-1)<\theta^{min} \\ 0 & \text{when } \theta(t-1) \text{ is inside the bound } [\theta^{min}, \theta^{max}] \end{cases} \qquad 2.94$$

The $\mathbf{f}$ is an np x 1 vector and np is the number of parameters. The parameter updating equation Equation 2.90 is then modified to

$$\theta(t) = \theta(t-1) + K(t)[y(t) - \emptyset(t-k)^T\theta(t-1)] - \alpha PP(t-1)\mathbf{f}(\theta(t-1)) \qquad 2.95$$

where α is a positive scalar chosen such that

$$\alpha\ PP(0) < 2I \qquad 2.96a$$

where PP(0) is a diagonal matrix with diagonal elements of equal values (aI, where a is any positive value, eg 100I). Note that if the diagonal elements are not the same then Equation 2.96 should in effect become

$$\alpha \max(PP_i(0)) < 2 \qquad 2.96b$$

where i denotes the i-th diagonal element.

Apart from the introduction of the correction term, another modification of the RLS algorithm was used by Ossman and Kamen. This modification is a data normalisation procedure which ensures that the covariance matrix, PP(t), converges to a positive semi-definite matrix with magnitude less than PP(0). The procedure is given as

$$\eta_{t-1} = \begin{cases} 1 \text{ when the determinant of } PP(t) > \varepsilon, \\ \text{where e is a small positive number} \\ \max(1, \| \emptyset(t-k) \|) \text{ otherwise} \end{cases}$$

where $\| x \| = [x^T x]^{(1/2)}$ and ε is chosen as any positive number. Ossman and Kamen suggested that ε should be chosen to be very small since they found that too large ε sometimes resulted in large transients in the system response. The η_{t-1} is introduced in the computation of PP(t) to give

$$PP(t) = PP(t-1) - \frac{PP(t-1)\emptyset(t-k)\emptyset(t-k)^T PP(t-1)}{\eta^2_{t-1} + \emptyset(t-k)^T PP(t-1)\emptyset(t-k)}$$

so that the term $K(t)[y(t) - \emptyset(t-k)^T\theta(t-1)]$ in Equation 2.89 becomes

$$\frac{PP(t-1)\emptyset(t-k)[y(t)-\emptyset(t-k)^T\theta(t-1)]}{\eta^2_{t-1} + \emptyset(t-k)^T PP(t-1)\emptyset(t-k)}$$

and Equation 2.95 becomes

$$\theta(t) = \theta(t-1) + \frac{PP(t-1)\emptyset(t-k)[y(t)-\emptyset(t-k)^T\theta(t-1)]}{\eta^2_{t-1} + \emptyset(t-k)^T PP(t-1)\emptyset(t-k)} - \alpha PP(t-1)\mathbf{f}(\theta(t-1)) \qquad 2.96c$$

The algorithm becomes the standard least squares with the correction term if η is always 1.

The properties of the estimation algorithm includes that the prediction error tends to 0 as t tends to infinity. The proof of the characteristics of the estimation algorithm is lengthy and is not presented here since it is the basics of the approach that is of main

concern. According to Ossman and Kamen, the modified RLS scheme they propose is not a projection algorithm which forces the estimates to converge to the "target " bounds $[\theta^{min}, \theta^{max}]$ every sampling instant, t. Instead, the "correction term" in Equation 2.95 only forces the estimates to converge to these bounds as t tends to infinity.

It clear that the "correction term" – $\alpha PP(t)\mathbf{f}(\theta\ (t - 1))$ can be incorporated into any suitable estimation algorithm. Also, implicit in the algorithm is the ability to compensate for parameter drifts from their true values, or more precisely, away from their admissible bounds. The algorithm is, however, quite different from the deadzone approach which avoids updating the parameters if the prediction error is small in order to avoid parameter drifts. The method is also not a form of the leakage approach since the leakage term does not have a "target" parameter bound that must be reached.

Ossman and Kamen (94) combined the method with a multivariable STR and applied it to a linear multivariable system. They reported that improved controller performance was achieved. They also conjectured that the approach could be applied in situations where the bounds of only some of the parameters are known. This implies that it may be possible to retain good controller performance while only correcting some of the parameters. This would be advantageous since it may sometimes be that only some key parameters need to be closely monitored. For example, the parameters that directly determine the controller gain may need to be monitored to prevent it from attaining wrong values.

A possible drawback of the approach as regards practical application is that, in practice, it may not be easy to obtain sufficient knowledge about the parameter bounds of the system especially for processes that are poorly understood. This problem will be more acute if the system is non linear. The literature also contains no practical application of the approach.

2.9.9 Incremental self tuning control algorithms

One property of the RLS scheme and, all parameter estimation schemes, is that if the noise affecting the data is not zero mean the parameter estimates determined will be of wrong mean values; that is, the parameter estimates will be biased. Positional forms of adaptive control algorithms use full value data for parameter estimation and control calculations. They, therefore, suffer from the fact that non-zero mean noise levels in the plant data would cause biased parameter estimates, and prediction offsets (Clarke et al.(21)). Clarke et al. showed that the performance of the "one in the data vector" and the "proxy of residuals" methods in estimating offset level d could be significantly degraded by non-zero mean data when a positional self tuning control algorithm is used.

The use of incremental data for parameter estimation and control calculations alleviates these problems. As stated by Clarke et al. (21), this is primarily because zero-mean data naturally result when incremental data is used for parameter estimation. The incremental approach is simple. It involves differencing the plant data with previous data prior to parameter estimation, and then following exactly the same procedure to obtain the corresponding control law. A parameter estimator which uses differenced data is called an incremental predictor and a self tuning controller based on an incremental predictor is, therefore, referred to as an incremental self-tuning controller.

The method proposed by Clark et al. (21) is the k - incremental controller where the parameter estimator uses data differenced by Δ_k. It is derived as follows. The predictor is obtained by shifting the positional predictor, Equation 2.81b, backward in time to give

$$P y^*(t) = F y'(t-k) + G u(t-k) + d \qquad 2.97$$

Subtracting Equation 2.97 from the Equation 2.81b gives

$$P(z^{-1})\Delta_k y^*(t+k) = F\Delta_k y'(t) + G\Delta_k u(t) \qquad 2.98$$

This is the k- incremental predictor. This can be re-arranged to give

$$P(z^{-1})y^*(t+k) = P(z^{-1})y^*(t) + F\Delta_k y'(t) + G\Delta_k u(t) \quad 2.99$$

The control law is the same as that used by the positional predictor in Equation 2.82, or Equation 2.88b if removal of lamda offset is required. Thus the controller output is computed as

$$\Delta_k u(t) = [\, G + Q]^{-1} \; [-P(z^{-1})y^*(t) - F\Delta_k\, y'(t) + R\; w(t)] \qquad 2.100$$

and $u(t) = u(t-k)+\Delta_k u(t)$.

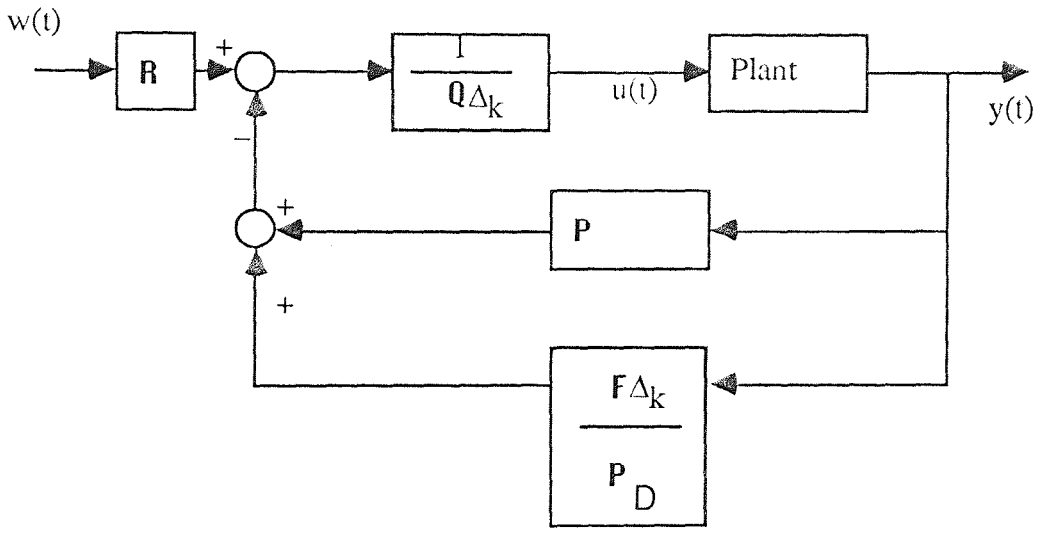

Figure 2.12 Implementation of a k-incremental control law (Clarke et al. (21))

Apart from reducing the risk of biased parameter estimates and prediction offsets, an incremental self tuning controller is equipped with integral action. This is unlike the positional counterpart where integral action must be pre-specified by the designer. Clarke et al. (21) showed that a k- incremental predictor implicitly estimates the offset level, d, and that changes in this offset level only lasts for k samples. The resulting incremental controller removes all possible offsets that may occur. Another feature of incremental controllers is that they do not require accurate knowledge of initial, or reference, values as required by positional forms. For the dual composition control of binary distillation column model and pilot plants, Tham et al. (131, 132) have reported that the use incremental control improves the decoupling properties of the multiple loop self tuning control system.

2.9.10 Deficiencies of incremental self tuning control algorithms

Despite all the advantages provided by incremental adaptive control algorithms, it has been reported many times in the literature that they deliver more vigorous and sensitive control actions than there positional counterparts. Such reports include those of Montague et al. (88), Kam et al. (67, 68), Tham et al. (131, 132) and Clarke et al. (21). Clarke et al. (21) observed that k-incremental self-tuning controllers are more sensitive than their positional counterparts to incorrect choice of the plant time delay when minimum variance control is required.

One source of sensitivity in incremental controllers is due to noise in the process data, if indeed noise is present in the data. It is the property of incremental predictors to amplify high frequency noise in the process data (Berger (11). This will make the closed loop response of a system under control by an incremental self tuning controller sensitive. To reduce the high frequency noise amplification in a system under control by an incremental self tuning controller, Berger (11) suggested passing the plant data through a moving average filter (MAF) prior to parameter estimation. The basic formulation of this filter is given as

$$F_{j,k}(\alpha) = 1 - \sum_{i=1}^{j} \frac{z^{1-i-k}}{j + \alpha} \qquad 2.101$$

where k is the time delay. Introducing the filter model into the appropriate predictor model for minimum variance control (Equation 2.69), for example, becomes

$$\mathbf{C}(z^{-1})\, F_{j,k} y(t+k) = \mathbf{F}(z^{-1}) F_{j,k} y(t) + \mathbf{G}(z^{-1}) F_{j,k} u(t) + \mathbf{E}(z^{-1}) F_{j,k} \xi(t) + \mathbf{E}(z^{-1}) F_{j,k} d(t) \qquad 2.102$$

According to Berger, α in Equation 2.101 is chosen as a small number and it is used when the noise model is identified to prevent the zeroes of $\mathbf{C}(z^{-1})F_{j,k}$ from lying on the unit circle (the $\mathbf{C}(z^{-1})F_{j,k}$ term is similar to $\mathbf{C}(z^{-1})\, y(t+k)$ in Equation 2.69, except that the filter term is introduced). If this is not done then problems of convergence of the parameter estimates and problems of stability of the closed loop system may occur.

Equation 2.102 implies that the plant data is differenced by the the average values of j previous values. The generality of the k-incremental controller is still retained due to the k in the filter formulation since $F_{j,k}(\alpha) = \Delta_k$ when $\alpha = 0$ and j=1.

According to Berger (11), if k = 1 and $\alpha = 0$, the effect of the filter on a signal composed of u and zero mean white noise e_t, the filtered output will be

$$w_t = e_t - \frac{\sum_{i=1}^{j} e_{t-j}}{j} \qquad 2.103$$

with variance

$$\sigma_w^2 = \sigma_e^2 (1 - 1/j) \qquad 2.104$$

where σ_e^2 is the variance of the noise input and σ_w^2 is the variance of the filtered data. The filter therefore reduces noise amplification as the filter depth j is increased. Thus, the sensitivity of the controlled system reduces. The filter depth j is chosen by the designer depending on the requirements of the system.

Berger showed that no benefits are obtained using the moving average filter when low frequency noise is affecting the system. No experimental application of this approach has been reported in the literature.

2.9.11 Stability and convergence of adaptive control algorithms.

Astrom (4) points out that the closed loop systems obtained in adaptive control are non linear and this makes their analysis difficult especially if random disturbances are affecting the system. The stability and convergence analysis of adaptive control systems are key problems to which much effort has been devoted to address. Astrom (4, 166) gives a review of efforts done in this area. He points out that to ensure stability of the adaptively controlled system, the data vector Ø must be bounded.

The performance of adaptive control systems in the presence of unknown disturbances is of great interest and several workers including Xianya and Evans (136) and Samson (122) have carried out investigations in this area. Samson studied the stability of adaptive control systems subject to bounded disturbances with unknown

statistics. His view is that the property of stability of the closed loop system should be established in order to be able to obtain good robustness of the control. He points out that in order to be able to perform a stability analysis on the system the parameter estimator should satisfy the following; (1) the parameter vector must be bounded, (2) the prediction error must be very small compared to the size of the data vector and (3) when the data vector becomes large the difference between two successive parameter estimates must become very small to allow the control of a time varying system. Samson pointed out that, in the deterministic case, these properties can be verified in most parameter estimation algorithms.

The analysis of convergence of adaptive control systems is dealt with in Anderson and Johnson (8). They showed that a persistent excitation condition is necessary for exponential convergence, which guarantees the robustness of the adaptive controller to model mismatch noise and other uncertainties. More details on the stability and convergence of adaptive control systems can be found in the articles mentioned above.

2.9.12 Extensions of self tuning control to multivariable systems

Extensions of the Self-Tuning Controller of Clarke and Gawthrop (156, 157) to multivariable systems were proposed by Kiovo (70), Morris et al. (86) and Chien et al. (24). Chien et al. (24) presented extensions to deal with multiple delay multivariable systems. Morris et al. (86), Montague et al. (88) and Tham et al. (131, 132) also considered multivariable algorithms with each loop sampled at different rates. These workers have pointed out that the computational requirements are much more involved, particularly for multiple sampling cases.

For a multivariable system the assumed model equation becomes

$$\mathbf{A}\,(z^{-1})\ \mathbf{y}\,(t) \;=\; z^{-kii}\,\mathbf{B}\,(z^{-1})\ \mathbf{u}\,(t) \;+\mathbf{C}\,(z^{-1})\,\xi(t) \;+\mathbf{d}(t) \qquad 2.105$$

The $\mathbf{A}(z^{-1})$, $\mathbf{B}(z^{-1})$ and $\mathbf{C}(z^{-1})$ are now polynomial matrices. The **u**, **y**, **d**, and ξ are all vectors. An important consideration that the designer is faced with in the design of a multivariable self tuning controller is the assumption of the structure of the

assumed process model, particularly regarding the $\mathbf{A}(z^{-1})$ polynomial matrix. The two choices are given by Tham et al. (131, 132) as

(i) the P-canonical form, where the $\mathbf{A}(z^{-1})$ is assumed to be diagonal, and

(ii) the V-canonical form, where $\mathbf{A}(z^{-1})$ is full.

They noted that the P-canonical form is usually preferred for simplicity. With this formulation the $\mathbf{A}(z^{-1})$, $\mathbf{B}(z^{-1})$ and $\mathbf{C}(z^{-1})$ matrices, for a 2 input 2 - output system, are defined as

$$\mathbf{A} = \text{diag}(\mathbf{A}_1, \mathbf{A}_2)$$

$$\mathbf{B} = \begin{bmatrix} \mathbf{B}_{11} & z^{k_{11}-k_{12}}\mathbf{B}_{12} \\ z^{k_{22}-k_{21}}\mathbf{B}_{21} & \mathbf{B}_{22} \end{bmatrix}$$

$$\mathbf{C} = \text{diag}(\mathbf{C}_1, \mathbf{C}_2)$$

Note that k_{ii} is the delay between y_i and u_i and k_{ij} is the delay between y_i to u_j; it is assumed that $k_{ij} > k_{ii} > 1$. Equation 2.105 can be decomposed into 2 multiple-input single output (MISO) subsystems, described by

$$\mathbf{A}_i y_i(t) = \mathbf{B}_{ii} u_i(t-k_{ii}) + \mathbf{B}_{ij} u_j(t-k_{ij}) + \mathbf{C}_i \xi_i(t) + \mathbf{d}_i(t) \qquad 2.106$$

The P-canonical form facilitates reduction of the multivariable system structure into sets of multiple input-single output (MISO) sub-systems. Each sub-system can then be treated independently. For each sub-system, the corresponding self tuning controller can be determined by following the synthesis procedure of the SISO STC controller. Then, strictly speaking, a multiple loop self tuning control system is obtained, with the capability of compensating for control loop interactions. The use of multiple sampling rates are also more readily accommodated.

The identity of Equation 2.66 becomes

$$\mathbf{CP} = \mathbf{E}_i \mathbf{A}_i + z^{-kii} \mathbf{F}_i \qquad 2.107$$

and $\mathbf{d} = \mathbf{E}(1)\mathbf{d}$. The corresponding self tuning controller design parameters are denoted as $\mathbf{P}(z^{-1})$, $\mathbf{Q}(z^{-1})$ and $\mathbf{R}(z^{-1})$ which are diagonal polynomial transfer function in the multivariable case. The k_{ii} - step ahead predictor for each loop becomes

$$\mathbf{P}_i y_i(t+k_{ii}) = \mathbf{F}_i y'_i(t) + \mathbf{G}_{ii} u_i(t) + \mathbf{G}_{ij} u_j(t + k_{ii} - k_{ij}) + \mathbf{d}_i \qquad 2.108a$$

and the corresponding control law is obtained as in the single loop case. Following the derivation of the STC in Section 2.94, the corresponding controller equation for each loop is

$$u_i(t) = [\, \mathbf{G}_{ii} + \mathbf{Q}_i]^{-1} \; [\, -\mathbf{F}_i\, y'_i(t) - \mathbf{G}_{ij} u_j(t + k_{ii} - k_{ij}) + \mathbf{R}\, w_i(t) - \mathbf{d}_i \,] \qquad 2.108b$$

Control loop interactions are accomodated via the $\mathbf{G}_{ij}$.

2.9.13 Chemical engineering applications of adaptive control

A large proportion of the published work on applications of adaptive control systems have been by simulation. Quite a few successful laboratory scale applications have been reported of which Seborg et al. (140) gives a fairly detailed review. Clarke and Gawthrop (22) demonstrated the flexibility and ease of applying of STC on a portable microprocessor. Dexter (27) described the development of a STC on a single chip microcomputer. He demonstrated the viability of a simple STC algorithm suitable for low cost control applications in consumer products. Sharaf and Hogg (123) assessed various types of process identification methods to the optimal control of a laboratory scale turbogenerator. The identification methods they used include the recursive least squares, the extended recursive least squares and the recursive instrumental variable.

Examples of experimental applications of adaptive control for the dual composition control of distillation systems are by Badre et al. (14), Morris et al. (85, 86) who used the STC of Clarke and Gawthrop (156, 157), and Martin-Sanchez and Shah (89) who used the model reference approach. McDermott et al. (34, 84) applied the pole placement approach to control a fixed bed auto thermal reactor.

Some industrial applications have also been reported by Seborg et al. (140), Keyser and Cauwenberge (65) and by Dumont (176). Keyser and Cauwenberge (65) successfully implemented a self-tuning multiple step predictor on an industrial blast furnace to guide the operator in selecting control inputs. Very good and trouble free

performance of the predictor over a period of months was reported. Dumont (190) applied an STR to control the motor load of a chip refiner in an industrial thermomechanical pulp production unit. The application was successful despite the slow drifts and occasional sign changes of the incremental gain of the motor load.

Chien et al. (23) proposed an extension to the STC for decoupling control of MIMO systems. The method is based on a novel way to choose the control weighting matrix, **Q**. Qualitatively, the **Q** is chosen to be a full matrix rather than a diagonal. Tade et al. (133) also developed an adaptive approach to decoupling control. The method allows for the specification of the closed loop behaviour of the system in form of a reference model and uses a linear difference model to represent the system. Non linear versions of adaptive control techniques have also been developed (Agarwal and Seborg (3))

Tionoven (63) developed an algorithm which automatically adjusts the control weighting, **Q**, when the STC is in operation. They justified there work on the basis that it may sometimes be difficult to find the proper weightings *a priori*. They addressed the case of regulatory control only and point out that the method does not necessarily give good performance on a non minimum phase system.

Many applications of adaptive control systems, by both simulations and experiments, have been to distillation processes. These include the investigations of Morris et al. (86), Chien et al. (24), Badre et al. (14), Montague et al. (88) and Tham et al. (131, 132), Martin-Sanchez and Shah (89) and Dahlqvist (31). This reflects the importance of distillation as a key process in the chemical industry. As distillation possesses many of the characteristics that limit the performance of conventional control system, adaptive control is perceived as one approach that can solve the major control problems in this field.

2.9.14 Application of adaptive control in the chemical industry

Dumont (176) made a comprehensive survey of the use of adaptive control in the pulp and paper, chemical and petrochemical industries. He found that adaptive control

has had limited use in industry, contrary to what was predicted by proponents of adaptive control particularly in the early 1980s. His report reveals that industrial practitioners agree that adaptive control is useful and there are some control loops where there is the need for it, but they find adaptive control still too complicated to use.

To illustrate some of the reasons for this view in industry, the survey gives several examples in industry where adaptive control has been applied, and some cases where projects on application of adaptive control have been terminated. Major difficulties encountered in applying adaptive control systems to industrial processes were usually due to problems of model identification, reliability and robustness of the algorithms. The number of parameters that need to be estimated is usually quite large for industrial systems, so that it becomes difficult to identify them all. Reports of some failures due to this problem were given. The survey also revealed that commissioning and tuning of adaptive control systems can take up long periods of time, sometimes weeks or even months.

In conclusion, Dumont (176) emphasized the need for close liaison between universities and industry regarding the needs and application of adaptive control. He pointed out that key issues such as the robustness and convergence of adaptive control algorithms need to be addressed for their applications in industry to be progressed.

2.10 Estimator aided control of chemical plant

In practice several factors will dictate the number and the types of measurements that will be made on a chemical plant. Control may dictate a different priority: Control may require measurements which present severe practical difficulty, or even impossibility. Measurements vital for control may be corrupted by noise in the measuring instruments; faulty instruments may also induce inaccuracies in the measurements; the measurements may be available at infrequent times because of long analysis times, or the difficulty or high cost of measurement. Only some easily measurable variables, or secondary variables, that relate, in some way, to the variables needed for control may be available. In these circumstances a method must be devised in order to infer accurate values of the variables needed for control from these secondary measurements to enable the design of an effective control system.

Distillation column control is a typical example were such problems frequently arise as has been discussed in Chapter 1. Composition analysers are usually very expensive, have significant time delay due to analysis time and can be very unreliable. More usually, only easily measurable tray temperatures are available. In this event the composition control scheme must be developed to operate without the missing composition measurements. Since for a binary mixture the temperature on a plate is usually a good indicator of the composition on that plate and the temperature of a tray near an end of the column is also a good indicator of the product composition at that end, the tray temperature can either be controlled instead or be used to infer the product composition.

A combination of a mathematical model of the process and the noisy, inaccurate or secondary measurements could be employed to provide the "best" estimate of the controlled variable. This is the basis of an "estimator aided" control scheme. The performance of the estimator will strongly depend on the adequacy of the mathematical model and how well the available measurements indicate the controlled variable whose estimate is required. Several workers (Daie (26), Luyben and Shah (110), Yu and

Luyben (137), Hamilton et al. (49) and Dahlqvist (162)) have used control schemes based on this approach.

Estimators of these types can be broadly classified into two types. These are static and dynamic estimators; static estimators employ steady state models and dynamic estimators employ dynamic models. The estimation can be done sequentially or non-sequentially (Daie (26)). Sequential estimation techniques basically means that the estimates of state variables of the process are generated at each sampling instant. This is commonly referred to as recursive filtering and an example of such a technique is the Kalman filtering technique (Kalman (163), Bozic (145)). The non-sequential approach to estimation is based on a series of measurements over a period of time to estimate the desired variables (Daie (26)).

Luyben and Shah (110) applied an estimator based PI control system to control the products of a 24 tray 20.3cm diameter binary distillation column distilling a mixture of water and methanol. A tray by tray non-linear steady-state model of the column was used to back-calculate product compositions. Only four tray temperatures and two flowrates were needed as measured variables for the estimator-based scheme. The resulting product composition estimates were then used as the controlled variables. Simulated and experimental results showed that the estimator based control scheme performed better than conventional control. It was also noted that there is a predictive feed-forward control action implicit in estimator based control schemes.

Extensions of the approach of Luyben and Shah to multicomponent distillation system were developed by Yu and Luyben (137). In their work, however, the singular value decomposition (SVD) technique was employed to select the proper location of tray temperature measurements, as mentioned earlier in this chapter. The performance of an estimator based PI control scheme was tested on four different multicomponent distillation processes by computer simulation. The results showed the estimator based schemes gave better performance than direct PI control. Yu and Luyben, however, point out that a disadvantage of the static estimator they employed is that the dynamic behaviour of the output of the estimator may not match the actual dynamic responses of

the process outputs. This is expected since the estimator employs a steady state model rather than a dynamic model.

The other workers, Hamilton et al. (49), Dahlqvist (162) and Daie (26), all used the Kalman filter technique in their estimator based control schemes. Comprehensive treatments of the theory of Kalman filtering can be found in the books by Astrom (166) and by Kalman (163). Also the theses of Payne (99), Daie (26) and Shaffii (115) give reasonably comprehensive reviews of the theory, applications and advances that have been made concerning Kalman filtering and its applications in process control. These reviews form the basis of the summarised treatment to follow.

The Kalman filter is a sequential estimation technique which employs a linear dynamic model of a process to generate the true process variables from noisy measurements at each sampling instant. The technique can be used to estimate process variables and parameters from secondary process measurements. Both Dahlqvist (162) and Daie (26) have employed the technique to estimate product compositions of distillation column from tray temperature measurements. A short presentation of the basic theory of the Kalman filtering approach will be given first.

2.10.1 The Kalman Filter algorithm

The fundamental idea of the Kalman filter is to determine the optimal estimates of the state variables of a given process from a knowledge of outputs and inputs (controls, disturbances etc.) and a mathematical model of the process. The basic assumption is that the process is (a) modelled by first order linear differential equations, (b) excited by additive zero-mean "white gaussian" noise and (c) such that some measurements are available, corrupted by experimental errors. The measurements must be combinations of the state variables.

"Whiteness" of the noise implies that the noise level is not correlated in time, meaning that all the values of the noise are mutually independent. "Gaussianess" is related to the noise amplitude. It implies that at any single point in time the probability density of the noise amplitude takes on a normal bell-shaped curve, the Gaussian

probability density function. Daie (26) noted that the assumption of "white gaussian" noise makes the mathematics of performing Kalman filtering more tractable.

The derivation of the Kalman filter and the characteristics have been extensively dealt with by several workers including Payne (99) and Daie (26). Therefore, only a brief treatment will be presented here.

The process is assumed to be described by linear time invariant state variable model as

$$\mathbf{dx}(t)/dt = A\mathbf{x}(t) + B\mathbf{u}(t) + \mathbf{w}(t) \qquad 2.109$$

$$\mathbf{y}(t) = M\mathbf{x}(t) + \mathbf{v}(t) \qquad 2.110$$

where $\mathbf{w}(t)$ is n x 1 vector of random system disturbances and $\mathbf{v}(t)$ is the nm x 1 vector of random measurement disturbances represented by a zero mean white Gaussian noise process. Therefore, $\mathbf{E}[\mathbf{v}(t)] = 0$ and $\mathbf{E}[\mathbf{w}(t)] = 0$, where $\mathbf{E}$ is the mathematical expectation operator. The matrix A is the n x n system matrix, B is the n x m input driving matrix and M is the nm x n measurement matrix. The vector $\mathbf{x}(t)$ is the n x 1 vector of the true state variables and $\mathbf{u}(t)$ is the m x 1 vector of the inputs. The n, m and nm are the number of states variables, inputs and measurements, respectively.

The solution of equation is given (see Daie (26), Shaffii (115) and Astrom and Wittenmark (206)) by

$$\mathbf{x}(t) = \Phi(t,t_k)\mathbf{x}(t_k) + \int \Phi(t,\tau)B\mathbf{u}(\tau)d\tau + \mathbf{w}(t_k) \qquad 2.111$$

The $\Phi(t,t_k)$ is an n x n matrix called the transition matrix and is given by

$$\frac{d\Phi(t,t_k)}{dt} = A\,\Phi(t,t_k) \qquad 2.112$$

$$\Phi(t,to) = \exp(A\,\Delta T) \qquad 2.113$$

where $\Delta T = t - t_k$. The initial value of $\Phi(t,t_k)$ at $t = t_0$ is

$$\Phi(t,t_0) = \Phi(t_0, t_0) = I \qquad 2.114$$

where I is the identity matrix. The state at the next sampling interval t_{k+1} is thus given by

$$\mathbf{x}(t_{k+1}) = \exp(A\,(t_{k+1}-t_k))\,\mathbf{x}(t_k) + \int_{t_k}^{t_{k+1}} \exp(A\,(t_{k+1}-\tau))B\mathbf{u}(\tau)d\tau + \mathbf{w}(t_{k+1}) \qquad 2.115$$

which gives

$$x(t_{k+1}) = \exp(A\,(t_{k+1}-t_k))\,x(t_k) + \int_{t_k}^{t_{k+1}} \exp(A\,(t_{k+1}-\tau))d\tau B u(t_k) + w(t_{k+1}) \qquad 2.116$$

as B is time invariant.

Dropping the t, the system becomes as

$$x(k+1) = \Phi(k+1, k)x(k) + \Gamma(k)u(k) + w(t_{k+1}) \qquad 2.117$$

$$y(k+1) = M(k+1)x(k+1) + v(k+1) \qquad 2.118$$

These equations are valid only at the sampling instant k .

Using the simple Euler method is used for the discretisation gives

$$\Phi = (I + A\,\Delta T) \qquad 2.119$$

$$\Gamma(k) = B\Delta T \qquad 2.120$$

$$M(k+1) = M \qquad 2.121$$

as M is time invariant, where ΔT is $t_k - t_{k-1}$ interval.

The Kalman filtering problem is to determine the estimate x^(k+1, k +1) of the state so as to optimise the following quadratic cost function given (Shaffii (115)) by

$$J_k = 1/2 \left([x(k,k) - x^(k,k)]^T \underline{P}^{-1}(k,k)[x(k,k) - x^(k,k)] \right)$$
$$+ 1/2 \sum_{j=0}^{j=k-1} \left([y(j+1) - M(j+1)\,x^(j+1, j)]^T\, R^{-1}(j+1)\, [y(j+1) - M(j+1)\,x^(j+1, j)]\right) \qquad 2.122$$

where the superscript -1 and T denotes matrix inversion and transpose, respectively. The x (k, j) is the estimate of the states obtained at time k given a set of observations through to time j. The optimisation yields the following matrix recursion relations (Daie (26)).

Prediction step

$$x^*(k+1,k) = \Phi(k+1, k)x^*(k, k) + \Gamma u(k) \qquad 2.123$$

$$\underline{P}(k+1, k) = \Phi(k+1, k)\,\underline{P}(k, k)\,\Phi^T(k+1, k) + \underline{Q} \qquad 2.124$$

Estimation step

$$\underline{K}(k+1) = \underline{P}(k+1, k)M^T(k+1)[M(k+1)\,\underline{P}(k+1, k)$$
$$M^T(k+1) + \underline{R}]^{-1} \qquad 2.125$$

$$\mathbf{x}^{\wedge}(k+1,k+1) = \mathbf{x}^{*}(k+1, k) + \underline{K}(k+1)\,[\mathbf{y}(k+1) - M(k+1)\mathbf{x}^{*}(k+1, k)] \quad 2.126$$

$$\underline{P}(k+1, k+1) = [I - \underline{K}(k+1)M(k+1)]\,\underline{P}(k+1, k) \quad 2.127$$

or

$$\underline{P}(k+1,k) = [I - \underline{K}(k+1)M(k+1)]\,\underline{P}(k+1,k)\,[I - \underline{K}(k+1)M(k+1)]^{T} + K(k+1)R(k+1)\,K(k+1)^{T} \quad 2.128$$

$\mathbf{x}^{*}$ and $\mathbf{x}^{\wedge}$ are, respectively, the prediction and the estimate if the state $\mathbf{x}$

$\underline{Q}(k)$ is the n x n system noise covariance matrix, $\mathbf{E}\,[w(k)\,w(k)^{T}]$

$\underline{R}(k)$ is the m x m measurement noise covariance matrix, $\mathbf{E}\,[v(k)\,v(k)^{T}]$

$\underline{P}(k,k)$ is the n x n covariance matrix of the error in $\mathbf{x}^{*}(k, k)$

$\underline{K}(k+1)$ is the n x nm filter gain matrix

The term $\mathbf{y}(k+1) - M(k+1)\mathbf{x}^{*}(k+1,k)$ in Equation 2.126 represents the difference between the measurements and the predicted measurements, that is, the prediction error or measurement residuals, as in the recursive least squares method.

Payne (99) pointed out that the discrete time form of the Kalman filtering procedure is preferred because it is composed of matrix recursion relations which makes the technique easily implementable on a computer. He also regards the Kalman filter as an optimal recursive data processing algorithm since all previous data are not required to be kept in storage and reprocessed every time new process measurements are taken. This is vital for the practicality of the filter implementation on digital computer as memory requirements are kept to a minimum.

In applying the filter to generate the state of the system the issue of observability becomes important. Provided the system remains controllable and observable the estimate of $\mathbf{x}^{\wedge}(k+1,k+1)$ and the filter algorithm will be stable for all k. The condition for observability is that a matrix L_{od} given (Shaffii(115) by

$$L_{od} = (\Phi^{T}(1,0)M^{T}(0),\ \Phi^{T}(1,0)M^{T}(1),\ldots\ldots\ldots\ldots,\ \Phi^{T}(k,0)M^{T}(k)) \quad 2.129$$

has the rank n, where n is the number of states to be estimated. Thus, L_{od} grows with k. If the system becomes unobservable the best way to combat it is by increasing the number of measurements supplied to the filter.

The noise covariance matrices, $\underline{Q}(k)$ and $\underline{R}(k)$, are positive semi-definite matrices and they are usually assumed to be constant for simplicity. To initialise the filter $\underline{Q}$, $\underline{R}$ and an estimate of the initial values of the state vector, $\mathbf{x}^*(0,0)$, are required. The initial error covariance matrix, $\underline{P}(0,0)$, is also required and is given by

$$\underline{P}(0,0) = \mathbf{E}\,[(\mathbf{x}\,(0,0) - \mathbf{x}_{me}\,(o))(\,\mathbf{x}(0,0) - \mathbf{x}_{me}\,(0))^T] \qquad 2.130$$

where $\mathbf{x}_{me}(0)$ is the mean of the actual initial state $\mathbf{x}(0)$ and is given as

$$\mathbf{E}[\mathbf{x}(0)] = \mathbf{x}_{me}(0) \qquad 2.131$$

and $\underline{P}(0,0)$ is a positive definite matrix.

To compute $\underline{P}(k,k)$ in the filter algorithm, Equation 2.124 is preferred because it is better conditioned numerically and will retain positive definiteness and symmetry of $\underline{P}(k,k)$ (Payne (99)). Equation 2.119 represents the integration of the state vector over the sample interval. This can be done by integrating the filter process model with the advantage of removing inaccuracies that could be incurred in in the computation of the transition matrix, particularly in the case of nonlinear systems.

The $\underline{P}(k,k)$ represents how uncertainties in the filter estimates propagate with time. It is the measure of the spread of the distribution of the estimates of the states, $\mathbf{x}^*(k,k)$, about the true state $\mathbf{x}(k,k)$; this true state is unknown, except in simulation. Loosely speaking, the square roots of the diagonal elements of $\underline{P}(k,k)$ represent the errors of the corresponding estimates of $\mathbf{x}^*(k,k)$ from their true values is $\mathbf{x}(k,k)$.

In practice, the noise spectra of the system and measurements are usually not readily available. This means that $\underline{Q}$ and $\underline{R}$ cannot be obtained directly and must, therefore, be assumed. However, $\underline{Q}$ may be used to represent uncertainty in the filter process model. A large $\underline{Q}$ implies the process model is highly uncertain. From Equations 2.120 and 2.121 it can be deduced that a large $\underline{Q}$ will result in a large filter gain so that the filter will rely more on the measurements, $\mathbf{y}(k)$. This large gain will be maintained because the computed error covariance matrix, $\underline{P}(k,k)$, is prevented from

becoming too small. This will reduced the risk of filter instability that may occur due to large filter model uncertainties. The R matrix can also be used in a similar way. A large R implies small filter gain and vice versa.

The P(0,0) and $\mathbf{x}^*(0,0)$ affect the initial response of the filter . As explained in Daie (26), the larger the error in $\mathbf{x}^*(0,0)$ the longer the filter takes to converge because until the system becomes observable the filter relies on the initial estimate, $\mathbf{x}^*(0,0)$. Chosing a large P(0,0), the filter gain will initially be large. This also increases the time the filter will reach steady state as a high gain filter would rely more on noisy measurement residuals.

Thus, compared to the static estimation techniques used in the works previously reviewed the Kalman filter is more easily "tuned" using P, Q and R matrices.

2.10.2 Application to non-linear systems - The Extended Kalman Filter

The Kalman filter is in terms of a linear model. It is, therefore, only applicable to linear systems. To apply the technique to nonlinear systems, which is common to many chemical processes, the system and measurement models must be linearised about a known and suitable reference trajectory. The Taylor series expansion is a convenient method of linearisation and is therefore commonly used. This is the basis of the Extended Kalman filter. This technique has been used by Daie(26), Payne(99) and Shaffii (115). Their theses therefore provide details about the characteristics of extended Kalman filters which form the basis of this review.

The development of an extended Kalman filter is as follows. The following model describes a general non-linear system:

$$\frac{d\mathbf{x}}{dt} = \mathbf{f}(\mathbf{x}, \mathbf{u}) + w(t) \qquad 2.132$$

$$\mathbf{y}(t) = \mathbf{h}(\mathbf{x}) + v(t) \qquad 2.133$$

The linearised transition matrix becomes

$$\Phi(k+1,k) = I + \partial\frac{\mathbf{f}(\mathbf{x}(k), \mathbf{u}(k))}{\partial \mathbf{x}(k)} \Delta T$$

$$= I + \mathbf{J}\,\Delta T \qquad 2.134$$

and the linearised measurement matrix

$$M(k+1) = \frac{\partial h(x\ k)}{\partial x} \qquad 2.135$$

where **J** is the Jacobian matrix. The linearisation is done around **x**(k). The second and higher order terms of the Taylor series expansion are usually neglected from the linearisation procedure. Rather than use actual states the state deviations, $\delta x = x^*(k+1) - x\hat{}(k)$, $\delta y = y(k+1) - y\hat{}(k)$, are processed through the filter algorithm presented. However, Daie (26) has shown that it is possible to use the actual states as opposed to deviations if the measurement relationship is linear or very mildly nonlinear.

In an extended Kalman filtering application the frequency of linearisation of the process model as the filter operates will depend on the sample time and on the severity of nonlinearity in the system. Typically, the values of the latest estimates at sampling instant k are chosen as the reference trajectory for re-linearisation since they are the "best" values that will be available at that time (Shaffii (115)). The implication is that linearisation may have to be done during every interval to obtain new transition and measurement matrices, Φ and $\underline{M}$, with significant increase in computational overheads, particularly if the order of the process model and number of measurements are large.

It is reported in the theses of Payne (99), Daie (26) and Shaffii (115) that in the extended Kalman filter approach the estimates may no longer be optimal. Observability may also be lost since now the Φ and $\underline{M}$ both vary. This is because the system is assumed to be linear within the sampling interval, ΔT, so that if the sampling interval is not small enough there is then the risk of violating the linearity assumption. This will give rise to bias effects and divergence of the estimates and will, therefore, affect the stability of the filter algorithm. Unmeasured disturbances will also cause biased estimates (Morari and Fung (91)). It is possible to estimate the biases in the estimates and then use it to correct the estimates produced by the filter. One such approach was presented by Friedland and Grabousky (141), which can also detect sudden changes in biases. To combat the problems of biased estimates due to violation of non linearity, the sampling time can be made smaller and higher order terms in the Taylor series expansion can be retained. In doing this the problems may not be completely solved. If

the filter cycle time is already a large fraction of the sample time then adding higher order terms in the Taylor series would require more storage space, increase the computational load and, thus, the filter cycle time. This may require an increase in the sampling interval, or a more powerful computer.

2.10.3 Application of Kalman Filtering to process control

Compared to applications in the space and electronics industry the Kalman filter has had much less practical application to chemical engineering systems (Shaffii (115)). The applications to chemical engineering systems that have been reported in the literature show promise of increased future applications. Hamilton et al. (49) reported that significant improvements in control of a pilot scale double effect evaporator was achieved when an extended Kalman filter was inserted into the multiple PI control loops. A stationary form of the filter algorithm, that is, a constant gain filter, was used. In the work of Payne (99), an extended Kalman filter was implemented in open loop on a large double effect evaporator. His work highlighted the many difficulties that can be encountered during on-line implementation of the filter algorithm. These problems included long filter cycle time due to computational requirements of the filter, and the assumptions required to be made in the development of the filter to enable operation within the limits imposed by the equipment used.

Daie (26) developed an estimator aided feedforward (EAFF) control algorithm based on an extended Kalman filter for a pilot scale binary distillation process. He designed the extended Kalman filter for the estimation of the tray compositions of the distillation column from tray temperature measurements and combined the filter with two PI controllers to control the top and bottom tray compositions of the column. Implicit in the design of the EAFF control scheme is the ability of the filter to predict the future effects of load disturbances on the outputs so that feedforward compensation could be achieved without the need for separately designing feed forward compensators. Hence, the name estimator aided feedforward (EAFF) control.

Daie demonstrated by simulation that the EAFF scheme performed better than the ordinary PI controllers in the face of large load disturbances and a large time lag due to the large liquid holdups in the reboiler. What was significant in the results of Daie is that with very tightly tuned PI controllers, which resulted in severe oscillatory closed loop response of the outputs, the EAFF completely eliminated the output oscillations. Furthermore, the EAFF was found to perform quite well even when very long sampling intervals, relative to the speed of response of the system, were used. The significance of these results is that by introducing the filter in the multiple PI control loops tighter control could be achieved than when the PI controllers were used directly. The extended Kalman filter not only acted as a composition analyser, it also improved the robustness of the closed loop system as oscillatory response is removed.

Shaffii (115) tried to extend the work of Daie by attempting to implement the extended Kalman filter on a distillation process. He used a linked Honeywell H316 minicomputer and Motorola M6800 microcomputer for data acquisition. Several problems were encountered and these prevented on-line application of the EAFF scheme. The extended Kalman filter required relatively large intersample computational load so that the minimum sampling interval achievable was too long in relation to the response time of the distillation system. The bulk of the filter cycle time was found to be taken up by program overlay, which was necessary within every interval due to computer memory limitations, the integration of the state at the prediction step using the nonlinear model of the column, and the computation of the error covariance and transition matrices, $\underline{P}(k,k)$ and $\Phi(k+1,k)$. Consequently, Shaffii proposed the simplification of the filter algorithm in order to enable on-line application of the EAFF scheme. He suggested the use of a constant state transition matrix, constant gain and reduction of the filter order .

The approach to implementing adaptive control can also been applied to indirect control of the controlled variable. Guilandoust et al. (41) have presented two adaptive estimators for estimating the bottom product composition of a binary distillation column which is subject to long time delays. The estimators use a secondary output,

tray temperature, to produce estimates of the controlled output (product composition), and where derived using different approaches. One approach assumes the plant is model in state variable form and the other uses input - output model, both of discrete formulation. Guilandoust et al. found that the two approaches resulted in estimators with similar structure, after some valid simplifying assumptions were made. The estimators made it possible to perform control at a faster rate than the rate the product composition measurements were available.

The estimators are simple to design and require moderate computing effort when compared with estimators such as those based on Kalman filtering. A disadvantage in one of the approaches, the one based on input-output model, is that the number of parameters to be estimated increase as the time delay increase so that the tuning in period of the estimator may be long. Guilandoust et al. claim that for a delay of up to 6 sampling intervals the tuning period increases only slightly; these were from simulation exercises which were unreported. They demonstrated that the estimators can be combined with adaptive or non-adaptive feedback control algorithm. The estimators were found to be insensitive to the selection of the secondary variables and can cope well with time varying behaviour of the process.

2.11 Chapter Conclusion

This chapter has given a review on some recently developed methods that are useful in the design, analysis and applications of control systems to process systems. A review of some advanced control design methods was carried out together with their applications with chemical engineering systems.

CHAPTER THREE

Restatement of The Problem

3.1 Introduction

In the introductory chapter the primary objective of this research work was described. It is to apply three advanced control methods to a pilot scale binary distillation column using a microcomputer for direct digital control. A detailed description of the actual issues that have been addressed in this work are given in this chapter.

3.2 The approach to the research

As discussed in Chapter 1, there is evidence in the literature that there has been a wide gap between advanced control theory and its application in the chemical and petrochemical industries. There are a wide variety of advanced controller design methods which have had limited applications on practical chemical engineering systems. Computer simulations have been frequently used to demonstrate the advantages of advanced control methods over conventional methods. This has provided the evidence for the benefits of the application of advanced design methods on chemical processes. Therefore, at the outset the aim of this research work was not to develop new control algorithms, but rather, to select some design methods already available in the literature and attempt to evaluate their performances on a pilot scale distillation column.

The advanced controller design methods that were selected for investigation in this work are (1) the Disturbance Rejection and Decoupling Control approach based on the work of Falb and Wolovich (179) (2) the Estimator Aided Feedforward (EAFF) control scheme of Daie (26) and (3) the Self Tuning Controller design method of Clarke and Gawthrop (157). These have been treated in detail in the previous chapter. These methods result in control policies that are very different and they addressed different control problems. The Disturbance Rejection and Decoupling Control design method addresses the problem of interaction in the multivariable controller design, the EAFF

operates in situations measurements of the controlled variables are not available, and the self-tuning controller adapt the controller parameters to compensate for changes in process conditions or the environment. The methods were chosen to cover a reasonably broad class of advanced controller design methods. The PI, given in Appendix A.2.2.1, was used as the reference which the performance of the methods were assessed

The existence of the mathematical proofs that underlie the selected design methods has also been discussed. An understanding of the philosophies behind the approaches and the synthesis of the control policies has also been given. From the point of view of Doyle & Morari (213) and Morari (150), a control engineer in industry requires controller synthesis procedures rather than extended analysis of the control schemes; the existence of mathematical proofs of the various control schemes is more important than the detail.

The importance of distillation columns in the chemical industry and their characteristics which make them good examples for illustrating advanced control schemes, were given in the introductory chapter. It was mentioned that they possess process control problems that are typical of those frequently encountered on chemical plant. The goal in this work is to compare the performances of the selected control schemes on the distillation column, particularly as regards the stability and robustness of their respective closed loop systems, since these are basic requirements of any control scheme. To achieve this goal feasibility studies were necessary, and this was performed by computer simulation. This required reliable process models to enable meaningful simulations to be carried out. Thus, after the building and instrumentation of the distillation column, the first major task was to seek a model that described the dynamic behaviour of the column. The model was required to be good enough so that the decision to proceed with on-line application of any of the control schemes could be based on the performance of the control scheme on the model.

In summary, the general approach taken to achieve the objectives of this work is as follows;

1) Formulate the mathematical model of the column

2) Check the model with experimental data.

3) For each controller design method;

a) Design the controller

b) Test controller by computer simulation using the model

c) Decide if the controller is viable for on line application

d) Formulate the real-time version of the control policy

e) Apply the control scheme to the column .

f) Compare the performance with that of conventional PI control

3.3 The issues addressed

A number of issues where considered worthwhile to investigate after the review of the literature was carried out. These are discussed in this section.

3.3.1 The Decoupling and Disturbance Rejection Control scheme

The Disturbance Rejection and Decoupling Control design method is a typical example of the multivariable control design methods that have been developed by workers in other fields of engineering than chemical engineering. The applications of the approach by Takamatsu & Kawachi (129) and Shimizu & Matsubara (113, 114) to chemical engineering systems such as distillation columns were reviewed in Section 2.6.4. These workers focussed on the disturbance rejection capability of the control scheme and did not examine feedforward compensation and the setpoint tracking capabilities of the control scheme. In this work attention is focussed on the setpoint tracking ability of the controller, since servo control properties of any control scheme are of importance as any controller which cannot track setpoint changes lacks necessary flexibility. To recap on Section 2.6.2 , the decoupling control scheme is given as

$$\mathbf{u} = \mathbf{F}\mathbf{x} + \mathbf{G}\mathbf{w} \qquad 3.1$$

for the system described in state variable form

$$\mathbf{dx/dt} = \mathbf{Ax}+\mathbf{Bu}+\mathbf{Dzd} \qquad 3.2$$

$$\mathbf{y} = \mathbf{Cx} \qquad 3.3$$

where **x**, **y**, **u**, **w**, and **zd** are the state, output, control input, setpoint and load disturbance vectors. The A, B, D and C are the state, input , disturbance and output matrices. The **F** and **G** are the controller matrices.

From the articles of Takamatsu & Kawachi (129), Shimizu & Matsubara (113, 114) it could easily be presumed that the value of $\mathbf{K}^* = I$ is a suitable choice in the relationship

$$\mathbf{G} = (B^*)^{-1}\mathbf{K}^* \qquad 3.4$$

given in Chapter 2, Equation 2.49. In fact, Takamatsu and Kawachi (129) did not introduce this $\mathbf{K}^*$ term into the above relationship, implicitly assuming $\mathbf{K}^* = I$. This is probably because they did not examine setpoint tracking, but their presentation suggests that the choice of $\mathbf{K}^*$ is not crucial to the controller performance. For load disturbance rejection only, the precompensator, **G**, will not have any effect on the disturbance rejection capabilities, since if the setpoint is constant the output from the compensator will be zero. Shimizu and Matsubara (113) also assumed $\mathbf{K}^* = I$ to compute the precompensator, but did not study the setpoint tracking case. There are no guidelines available from these authors for choosing $\mathbf{K}^*$.

A problem addressed in this work is to examine the importance if $\mathbf{K}^*$ to setpoint tracking, and to establish how to choose its diagonal elements. In order to do this, the setpoint tracking properties of the decoupling control scheme have been investigated.

3.3.2 The Kalman Filtering studies

Section 2.10 dealt with the EAFF control scheme developed by Daie (26) for the dual composition control of a distillation column. They can also be applied to SISO or MIMO systems where only measurements of secondary variables are available for control, or where the measurements of the controlled variables are subject to very long time delays and the control is required to be done at a faster sampling rate. Attempts by Shaffii (115) to apply the method on-line were unsuccessful. The major obstacle to real time application was the excessive computational load of the filter. He consequently proposed the simplification of the extended Kalman filter that functions as the estimator in the EAFF.

In this work a simplification of the filter is aimed at reducing the computational load and execution times of the filter algorithm to acceptable levels so as enable real time application of the EAFF scheme. A linear model of the column is used as the filter model, as opposed to a comprehensive non-linear model of the column as used by Daie (26) and Shaffii (115). The filter algorithm must perform satisfactorily for on-line application to be feasible. Criteria such as stability of the estimates produced and the stability of the filter itself must be satisfied for the real time application of the EAFF to be feasible. Such evaluations are best done by simulation and by off-line analysis using real process data. In this work, off-line analysis with experimental data were used to evaluate the performance of the filter.

3.3.3 The Self Tuning Controller design method

The literature review discussed and highlighted that there is interest in the robustness of control systems to model errors such as input uncertainties, instrument failure, constraints in the manipulated variable and errors in model parameters. These impose limitations on the performance of any control scheme. Many investigators have written that the robustness of self tuning control algorithms is good, but reports of on-line operation of these control systems under severe conditions of uncertainties are limited in the literature. Thus, investigations in this work were aimed at demonstrating the operation of self tuning controllers under such environment by suitable experiment.

The Parameter Correction (PC) method

As discussed in Section 2.9.8, Ossman and Kamen (94) suggested a method to provide good parameter estimates of the adaptively controlled system in the absence of persistent excitation. The method forces the parameter estimates into their admissible ranges that are specified by the user. The implication is therefore that the proper ranges of all the system parameters need to be known *a priori*. .

However, Ossman and Kamen suggested the method could be applicable in situations where only the bounds of some of the parameters are known, but they noted that, in such cases, the stability of the system cannot be guaranteed for all the possible

system parameters. The implication of this is that it may be possible to apply the method to force only some of the parameters to their correct ranges and still retain good robust controller performance. If this can be achieved, the advantage would be significant to cases where the estimates of some key parameters are bad and cause poor controller performance. In this work was, this possibility has been investigated.

3.4 Chapter Conclusion

This chapter has given, in more detail, the formulation of the goals of this work. The major part of the remainder of this thesis describes the various work done in achieving these goals. In the next chapter the pilot plant distillation column and interfacing with the microcomputer is described.

CHAPTER FOUR

The pilot plant distillation column and the interface to the System96 microcomputer

4.1 Introduction

The experimental equipment used in this work is a pilot plant distillation column. This column has been interfaced to a real time multitasking microcomputer called System96 for the purpose of data acquisition and process control studies. The interface box is a separate unit called the Monolog and it houses the analog to digital, signal conditioning and digital to analog converter modules. The distillation column, its instrumentation and the computer are described in this chapter.

4.2 The pilot scale distillation column

The original distillation column was donated to the Department of Chemical Engineering at the University of Aston by IBM UK Limited. It has been used in a number of research projects including Daie (26) and Shaffii (115). A schematic diagram of the arrangement used by these two workers is given in Figure 4.1.

The column is a 3 inch general purpose glass column with 10 sieve plates of which the enriching section has 6 trays and the the stripping section has 4 trays. The characteristic dimensions of a tray are shown on Table 4.1, and a schematic diagram of it is shown on Figure 4.2. Each tray has a thermocouple well into which a thermocouple can be placed in order to measure the temperature of the vapour above the liquid held on the tray. Two cylindrical feed tanks each with a capacity of 30 litres are situated at a height above the feed entry point into the column and two product tanks are available for the top and bottoms products of the column.

Figure 4.1 Schematic diagram of the distillation column arrangement used by Daie (26) and Shaffii (115)

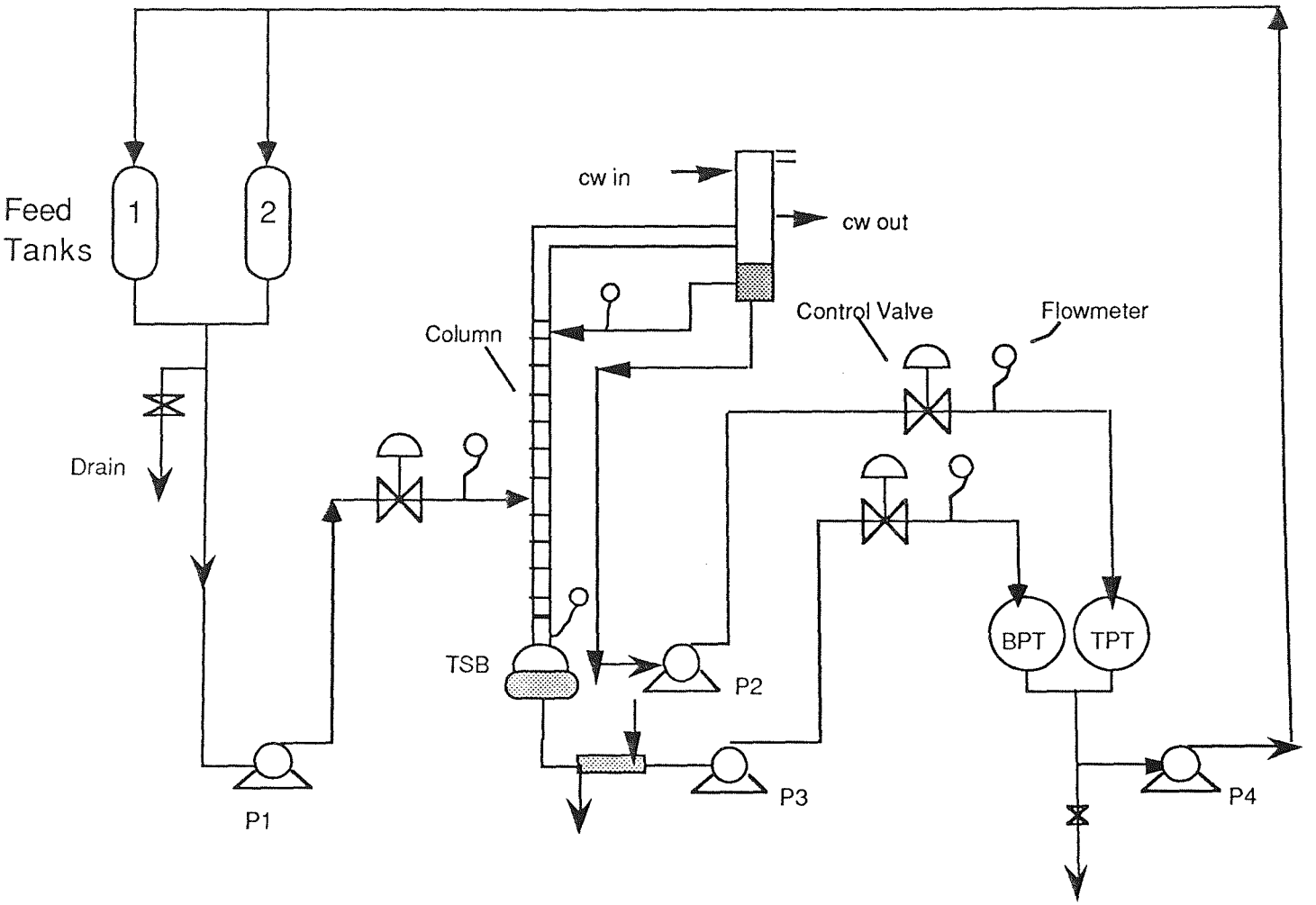

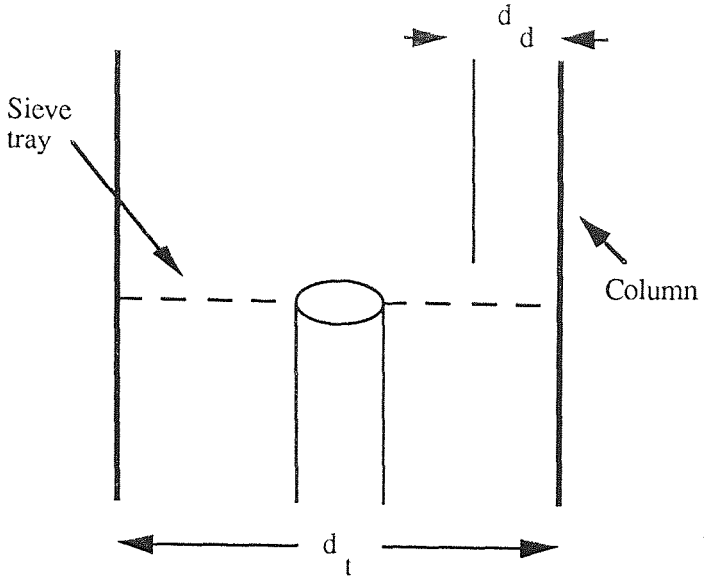

d_t is the tray diameter, d_d is the downcome diameter

Figure 4.2 Schematic diagram of a sieve tray of the column

Table 4.1 Dimensions of a Tray, in metres (m)

Diameter of tray, d_t	0.0762
Diameter of Downcomer, d_d	0.0105
Tray thickness	0.0002
Diameter of perforations	0.00011
Number of perforations per tray	145 holes per tray
Weir height	0.0003
Tray spacing	0.08

Four 60W Stuart Turner centrifugal pumps are available for delivery of the feed into the column, top and bottom products into the product tanks, delivery of the reflux back to the column and the recycle of the product tanks back to the feed storage tanks to enable continuous operation of the column. A 3 inch standard condenser is arranged to condense the vapour from the top of the column into a 3 inch glass reflux drum connected directly below it. This condenser-reflux drum arrangement is connected to the top of the column by a 3 inch glass column called the vapour line. A heat exchanger is available to cool down the bottoms product before it passes to the delivery pump and the corresponding control valve.

4.2.1 The operational problems of the original distillation column arrangement and the modifications made in the design

The original arrangement of the column, as schematically shown in Figure 4.1, had many operational problems which meant that it was difficult to obtain useful results. These problems and their sources were discussed by Daie (26) and are summarised below.

The reboiler arrangement consisted of a large spherical tank mounted on a 2.4 KW double circuit isomantle heater as shown in Figure 4.3.

During operation of the column, the liquid holdup in this reboiler drum was usually about 10 litres which was much larger than the total liquid holdup on all the trays. This meant that large quantities of liquid were held inside the column during operation. The heater was also underpowered. Even at maximum setting this reboiler arrangement could barely produce vapour boilup rate was quite low. It was therefore difficult to perform reasonable dynamic and control studies on the column. The large reboiler liquid holdup swamped the variations in the vapour temperatures on the trays, particularly those in the stripping section, to changes in heat input.

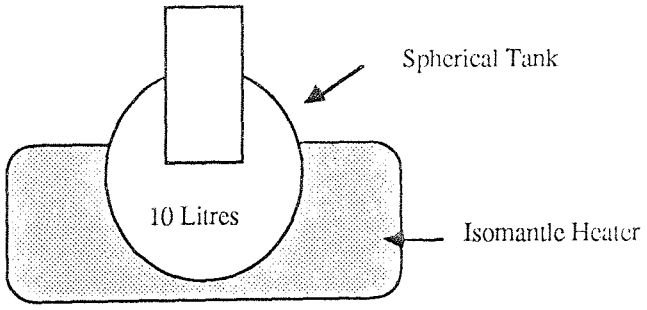

Figure 4.3 The reboiler drum on the isomantle heater

The piping around the column was made of 1/2 inch stainless steel pipes of 16 gauge (SWG). This made transportation lags around the column significant as the column required flow rates of about the range of 1 to 15 litres per hour for operation. Accurate and reproducible flow measurements were difficult as orifice plate type flowmeters were used; errors as large as 3.0 l/hr could occur. The flow control valves suffered from electrical and mechanical faults. Furthermore, tray temperature measurements

were not very accurate. Daie could only obtain them to the accuracy of 0.1°C, and even then lengthy calibrations and modifications of the temperature measurement device were necessary .

The vapour line was 2 metres long and was unlagged. This long vapour line, the large reboiler liquid holdup and the underpowered heater, caused very little vapour to be condensed in the reflux drum. The range of flow of reflux that could be used for control was therefore limited. Gravity flow of reflux was also used and this added difficulties in reflux flow measurement and control implementation.

The consequence of all these was that no experimental studies on the control of the distillation column could be done by both Daie (26) and Shaffii (115). The few open loop feed flow step response tests that were managed by Daie were just adequate to be used for dynamic model verifications.

Since it was the objective of this research work to apply advanced control schemes to the distillation column it became necessary to improve on its design and instrumentation. The following modifications were made;

1. New digital to pneumatic flow control valves were purchased to replace the old ones
2. The vapour line from the top to the condenser was reduced to 1 m in length and it was lagged in order to reduce the extra reflux condensing in the vapour line
3. The reflux is pumped back into the column rather than allowing gravity flow. The distillate line is also connected to the reflux line
4. Where appropriate, 1/4 inch 16 gauge stainless steel pipes were used for the piping system around the column
5. Nickel- Chromium & Aluminium thermocouples with accuracy of up to 0.01 °C were used for temperature measurement
6. Low cost turbine flowmeters were used for liquid flow measurement
7. A new reboiler arrangement, a thermosyphon type arrangement, which uses a firerod catridge heater for heating the liquid in the reboiler drum, was designed by Fuller (182). The nominal holdup of the reboiler drum during operation of

the column is about 1.5 litres. A diagram of the reboiler is shown in Figure 4.4. and Table 4.2 gives the dimensions of the parts. A diagram of the heater is shown in Figure 4.5.

A diagram of the new distillation column arrangement is shown in Figure 4.6 and Table 4.3 gives the column dimensions. Plate 1 shows the actual column.

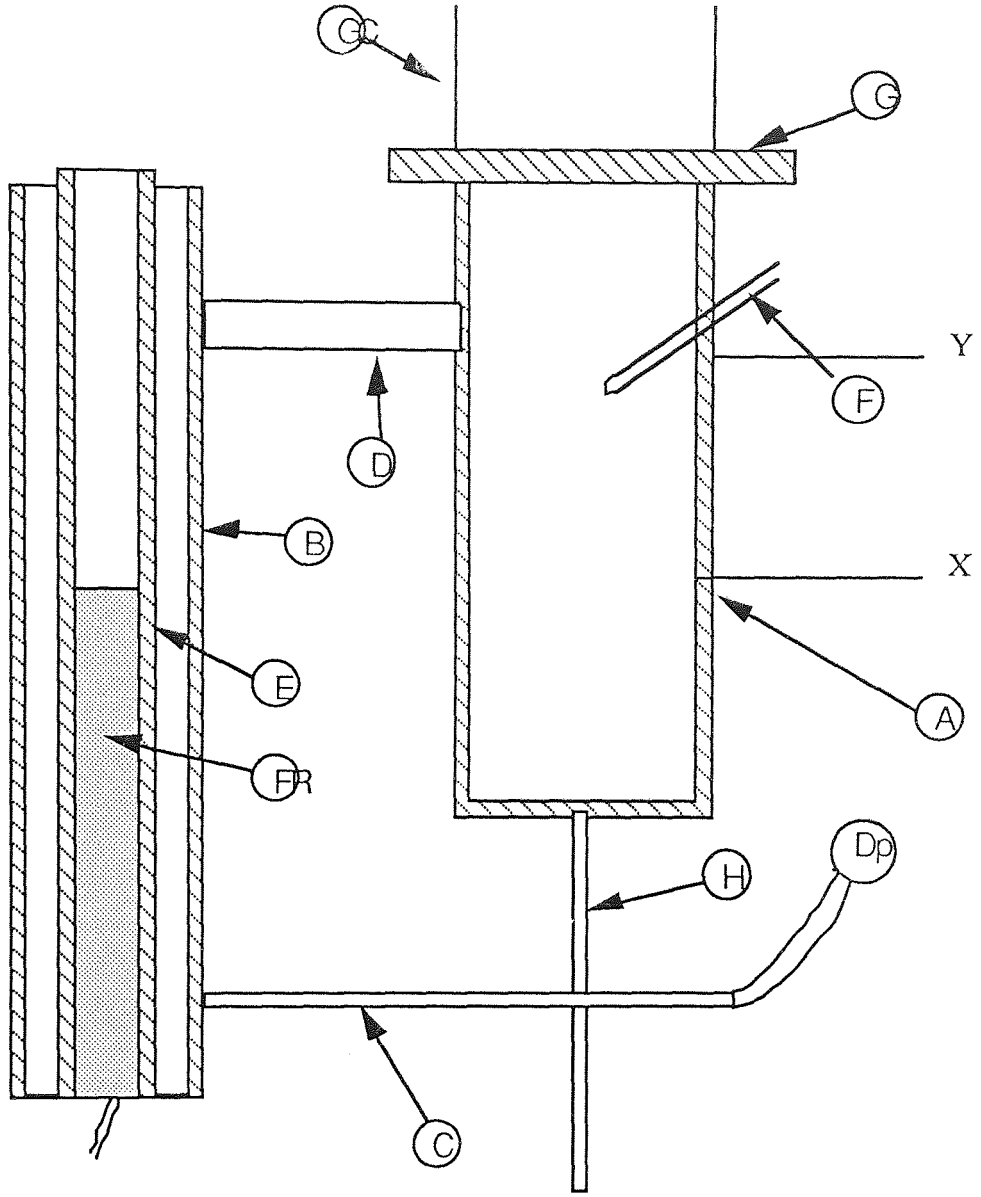

Figure 4.4 The thermosyphon reboiler arrangement

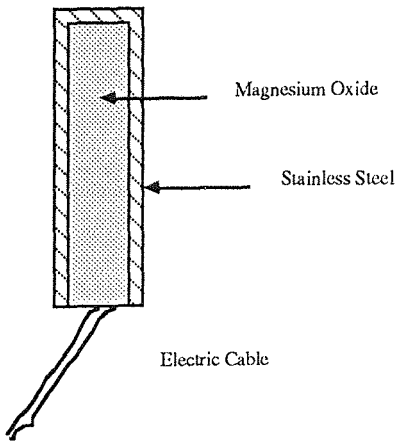

Figure 4.5 The firerod catridge heater

Table 4.2 Dimensions of the thermosyphon reboiler parts

Material of construction is stainless steel

Part
A 380 mm long pipe 31/4 " OD 10 SWG
B 440 mm long pipe 11/8 " (** 2") OD 16 SWG
C 185 mm long pipe 1/4" (** 3/8 ") OD 16 SWG
D 150 mm long pipe 1/2" OD 16SWG
E 460 mm ling pipe 3/4 " (**5/8 ") OD 16 SWG
F 100mm long pipe 1/4" OD 16 SWG plugged at one end (thermocouple well)
G Flange 1/4 " thick plate 190 mm diameter
H 75mm long pipe 3/8 " OD 16SWG
Dp Differential pressure transducer
FR Firerod heater
GC Bottom end of Column
** Denotes the dimensions of the reboiler that was eventually used in this work

Table 4.3 Column Dimensions

	Dimensions in metres, m
Column diameter (OD)	0.0762
Length of Enriching section	0.65
Length of Stripping section	0.55
Diameter of reflux drum	0.0762
Diameter of reboiler drum	0.0762
Length of vapour line	1.0
Number of trays in the enriching section	6 trays
Number of trays in the stripping section	4 trays
Product tank capacities	50 litres

Figure 4.6 Schematic diagram of distillation column used in this work

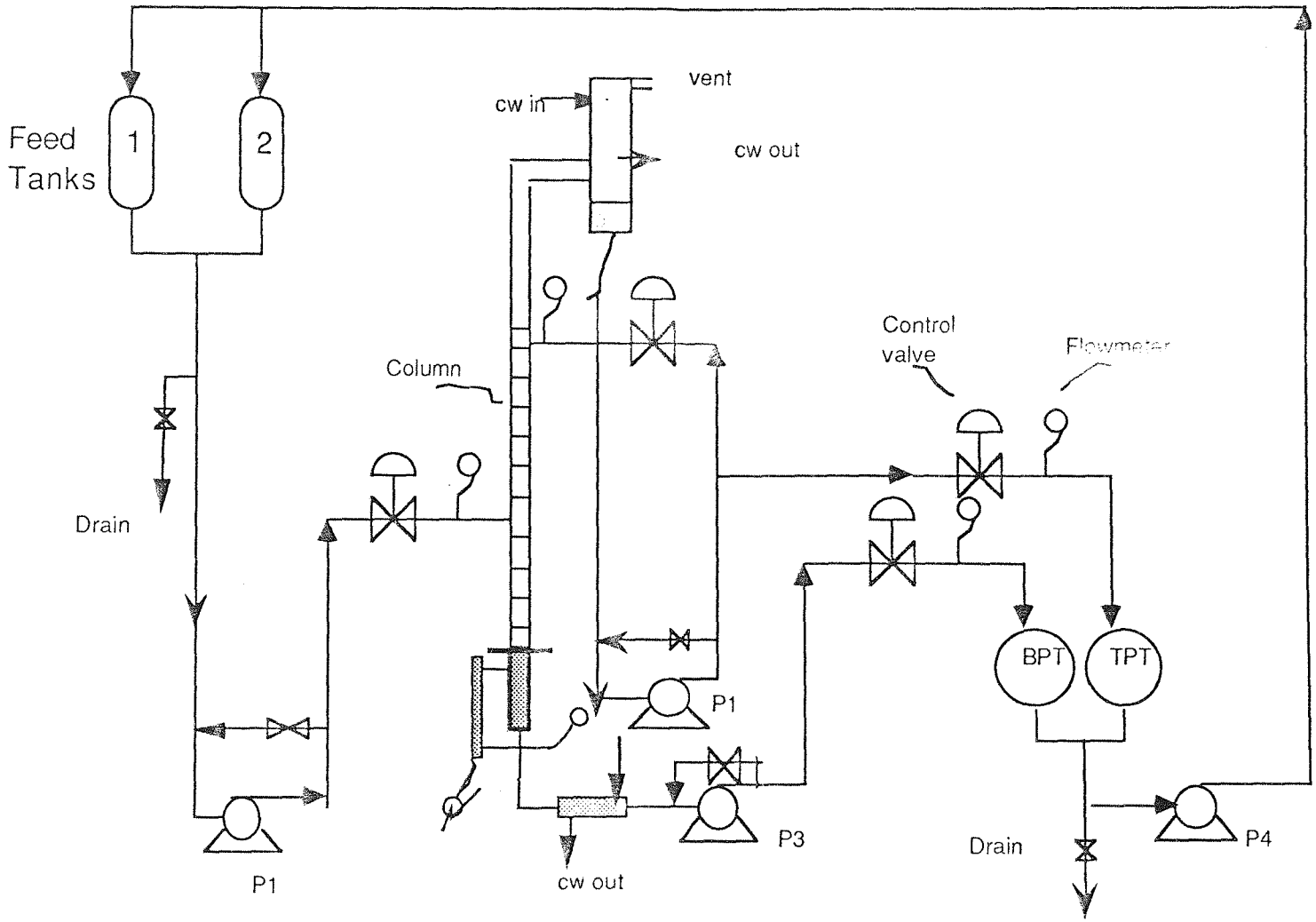

4.3 Instrumentation of the column

4.3.1 Flow measurement

The feed, reflux, distillate and bottoms flowrates required for the operation of the column range from 1 to 15 l/hr. For accurate and precise measurement of these low flowrates special turbine flowmeters were required.The cost of measuring all the flows with such flowmeters was considerable.The turbine flowmeters that were used were of simple design and much cheaper. They were supplied by RS Components Ltd. The body and the rotor of the flowmeter are made of acetal rubber. The rotor of the meter is fitted with 3 stainless shaft ceramic magnets. The metering principle is velocity counting. The output of the flowmeter is electrical pulses of which the frequency is linear to flowrate.

For compatibility with the data acquisition hardware, or more precisely, the analog to digital (A/D) converter, the output frequency is converted to voltage in the range 0-5 volts by a frequency to voltage converter. The accessories for this converter were also supplied by RS Components and was assembled in the departmental workshop. Figure 4.7 shows a simplified schematic diagram of the flowmeter.

The manufacturers specified that the reproductivity of of the flowmeter is about ±1% of the maximum flow which was specified as 100 l/hr. This meant that the flowmeters were always operating at the lower end of the flow range were the precision is very low, hence, high uncertainties in the flow measurements were more likely. Furthermore, the flowmeters are appropriate for monitoring mild and noncorrosive liquids such as water. The liquid mixture used in the column is a binary mixture of trichloroethylene and tetrachloroethylene. The suppliers of the flowmeters provided a chart showing the effects of various chemicals on the acetal rubber that the flowmeters are made from. The chart showed that this material has limited resistance to trichloroethylene. For a 1mm thick piece of acetal rubber completely immersed in the liquid for 30 days at temperatures of 20-60 °C, trichlorethylene increased the weight by 9% and reduced the tensile strength by 30%. Thus, during preliminary experiments the flowmeters were found to have a short operating life sometimes as short as eight 1 hr

experiments. The operating life of a flowmeter was even shorter when it was used to monitor the reflux, bottoms and distillate flows, since these streams were warm.

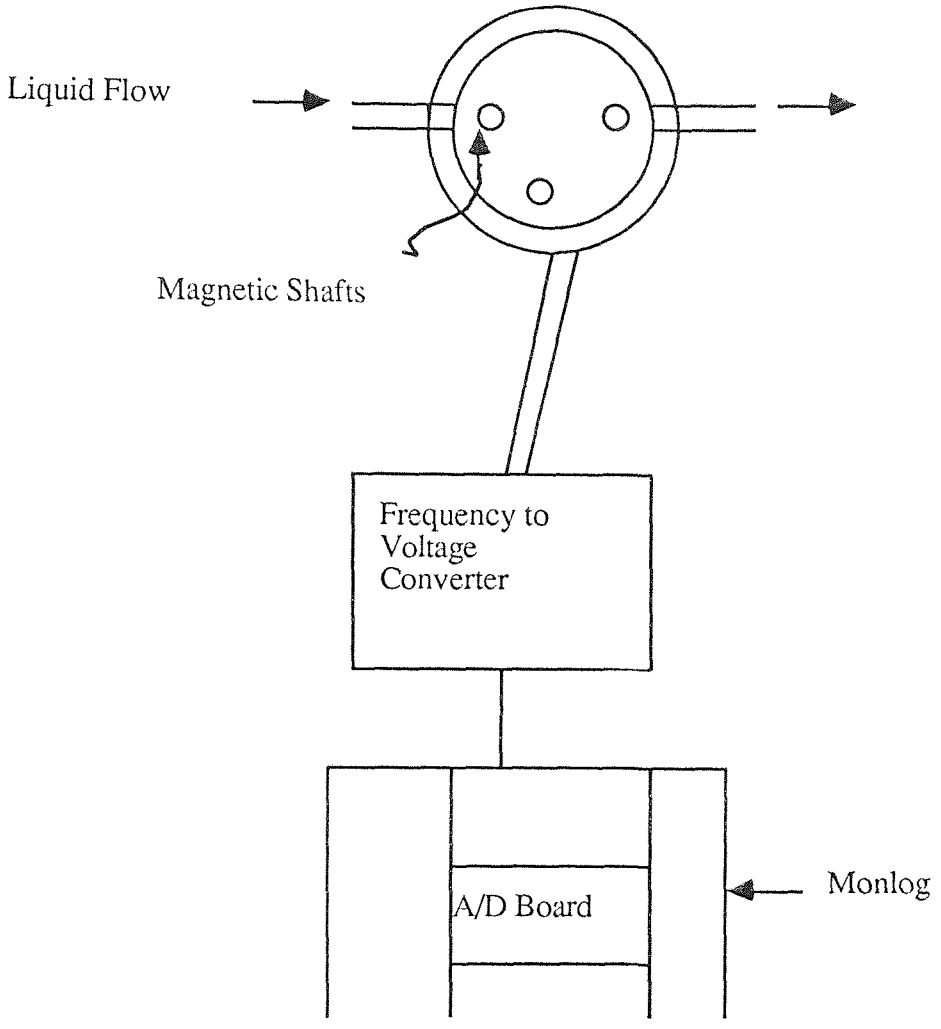

Figure 4.7 Schematic of the turbine flowmeter used on the Column

The small internal area of the meter meant that liquid flow through it was easily blocked by small dirt that entered the piping system around the column.

4.3.2 The control valves

The new control valves for automatic control of flowrates are miniature air-operated valves supplied by Platon Flowbits Limited. The valves are suitable for automatic control of liquids, gases and steam in 1/4" and 1/2" pipes. Each control valve has an associated unit which is a digital to pneumatic converter as shown on Plate 2. These converters accept 8 or 10 bit binary numbers to produce a proportional output in

pressure ranges of up to 120 psi (8 bar). The low pressure version of the converters using a range of 15 psi (1 bar) was used in this work.

The converters are actually current to pneumatic converters with the current range of 4 - 20 mA. It was thus necessary to construct digital to current converters for each, to enable the direct manipulation of the valves by the computer. These digital to current converters are 8 bit converters as the data line from the interface box to the digital to current converters is an 8 bit parallel line which is called the versatile interface adapter (VIA). A schematic of the interface from computer to control valve is depicted in Figure 4.8.

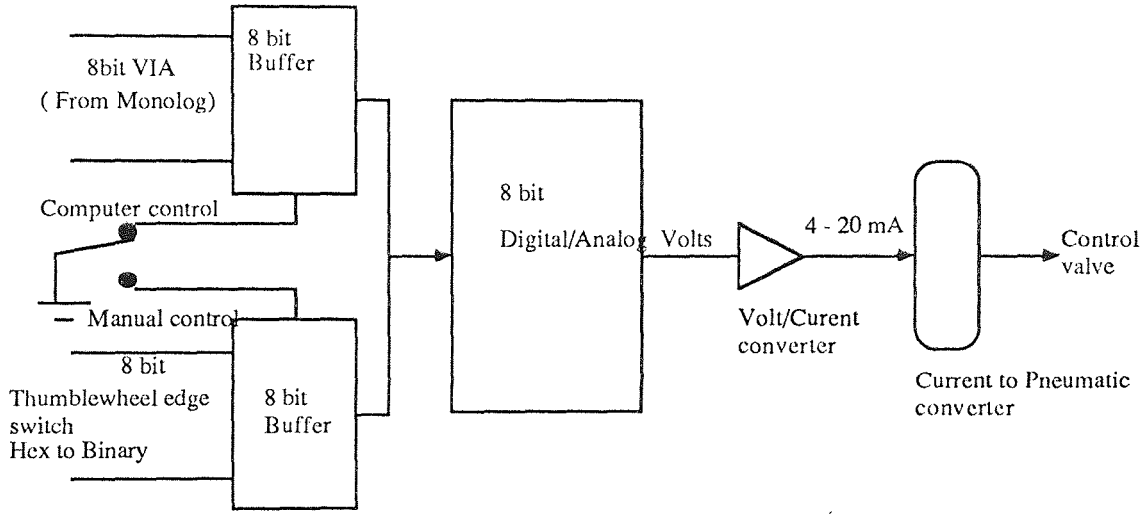

Figure 4.8 Circuit description of the interface between the control valve and the computer

The valves can be manipulated by sending a digital signal, integer number in the range 0 - 255, from the computer to the digital to current converter which converts the signal to a current in the range 4-20mA. This current is converted to pressure signal in the range of 3-15 psig to adjust the valve stem position accordingly. The valves can also be operated manually by depressing a switch for each valve on the panel shown on Plate 3.

The valves require an air supply of 20 psig to operate satisfactorily. The departmental compressed air supply is at a much higher pressure so that a pressure regulator is installed to reduced the pressure to 20 psig for the operation of the valves.

Each of the centrifugal pumps could deliver in excess of 140 l/hr of liquid across nominal heads of 2 to 3 meters. As the required flowrates for column operation are much lower than this, by-passes had to be made around each pump as shown schematically in Figure 4.6. This was done in order to prevent buildup of pressure in the upstream side of the valve and to reduced mechanical strain on the pump.

4.3.3 Valve calibration results

Benchmark calibration of the control valves on installation the experimental column was performed. The calibrations were done in two ways; 1) by the bucket and stop-watch method were the time required to deliver 2 litres of liquid was measured, and 2) by the turbine flow meters. The by-passes of the respective pumps where made fully open during calibrations. The calibrations were done with water at room temperature and the with 50/50 % w/w trichloroethylene/ tetrachloroethylene (T/T) mixture. The results could then be correlated with fractional opening of the valve using the least squares fit method given in Adby and Dempster (167). However, standard programs that correlate data were available on the graphical package used to draw the graphs.

Figures 4.9a to 4.9f shows typical plots of flow with fractional valve openings for each control valve.

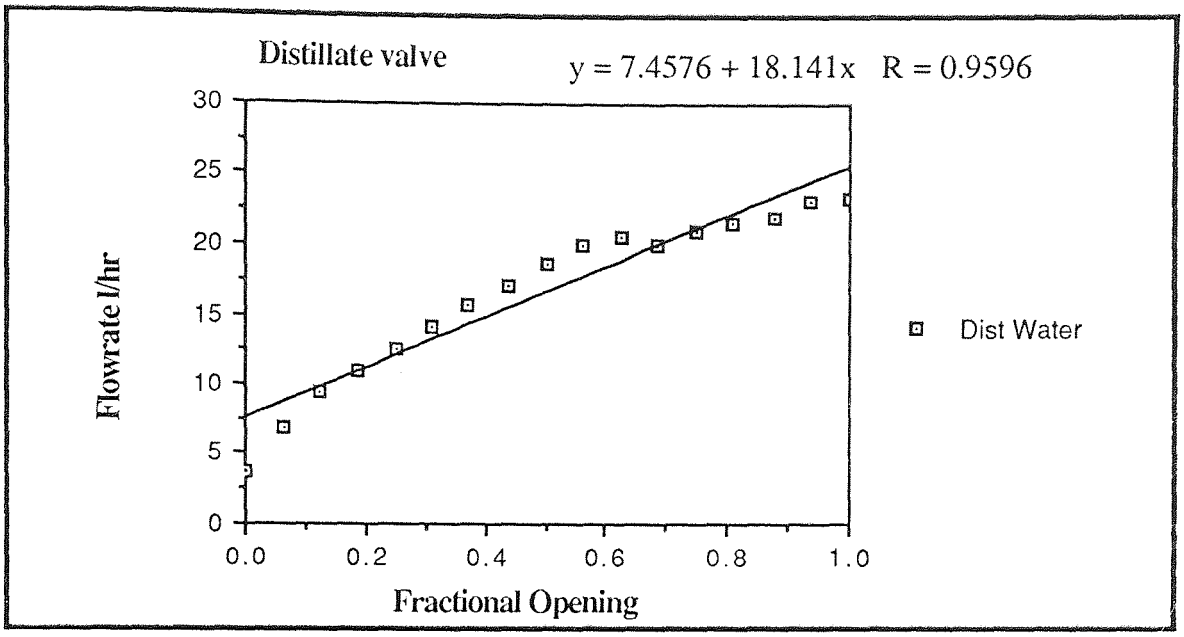

(a) Water at room temperature, flowmeter readings

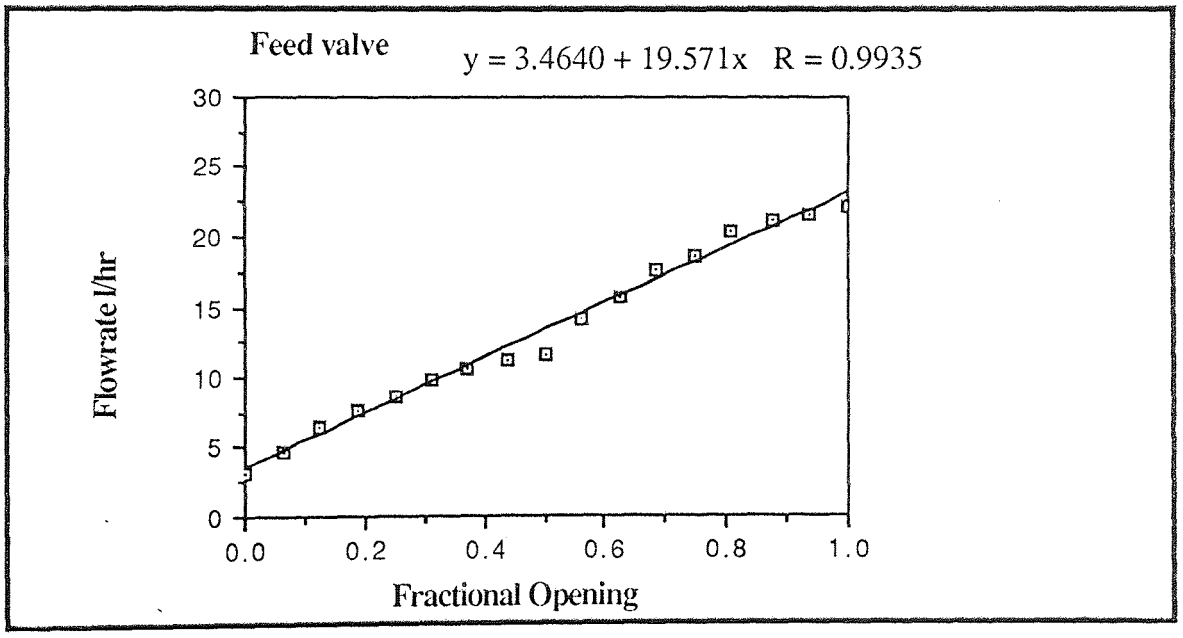

(b) Water at room temperature, flowmeter readings

(R= correlation coefficient, x= fractional opening)

Figure 4.9 a) and b) Control valve characteristics

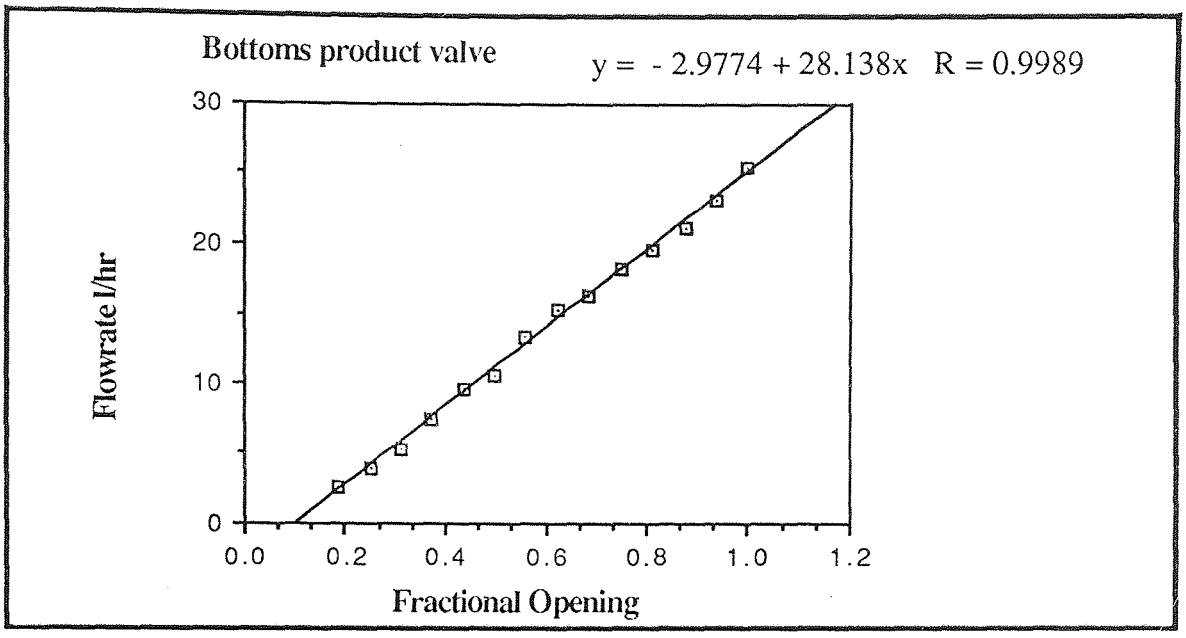

(c) Water at room temperature, flowmeter readings

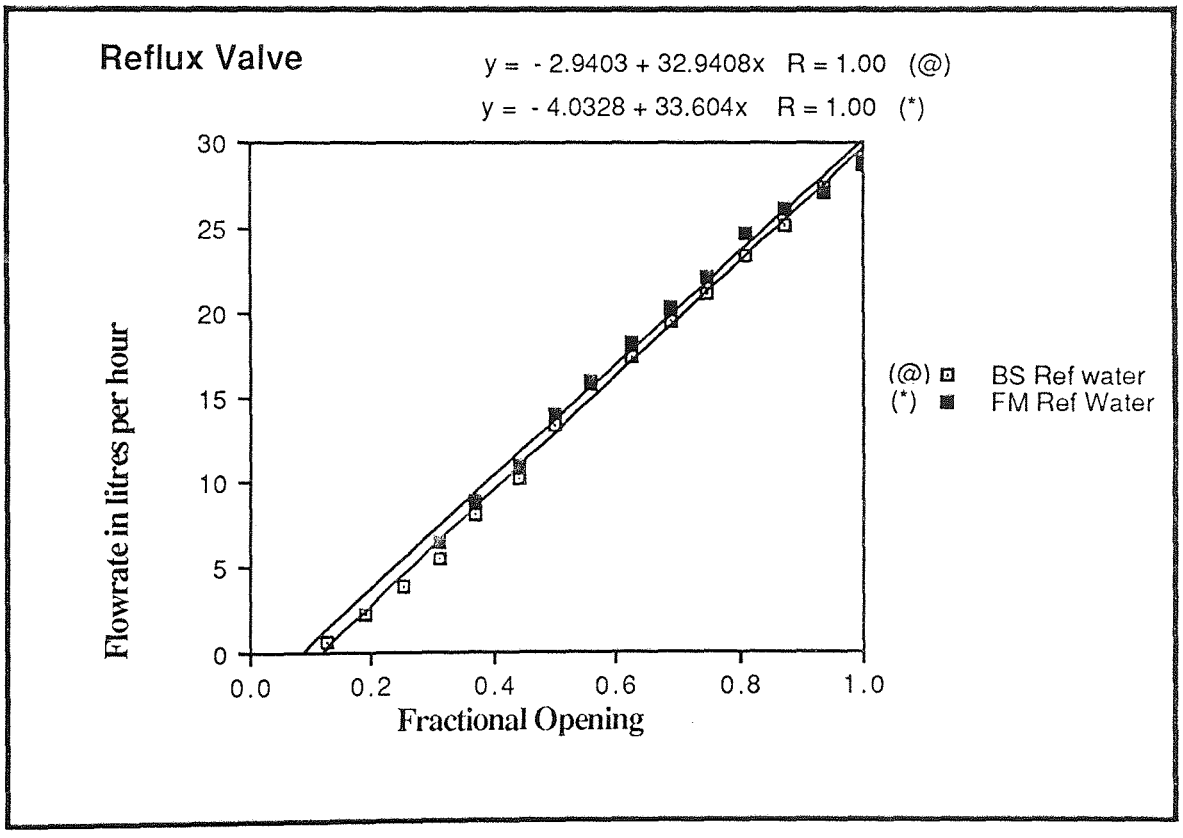

(d) Water at room temperature, BS- Bucket and Stop watch method,

FM - flowmeter readings (R= correlation coefficient, x= fractional opening)

Figure 4.9 c) and d) Control valve characteristics (Continued)

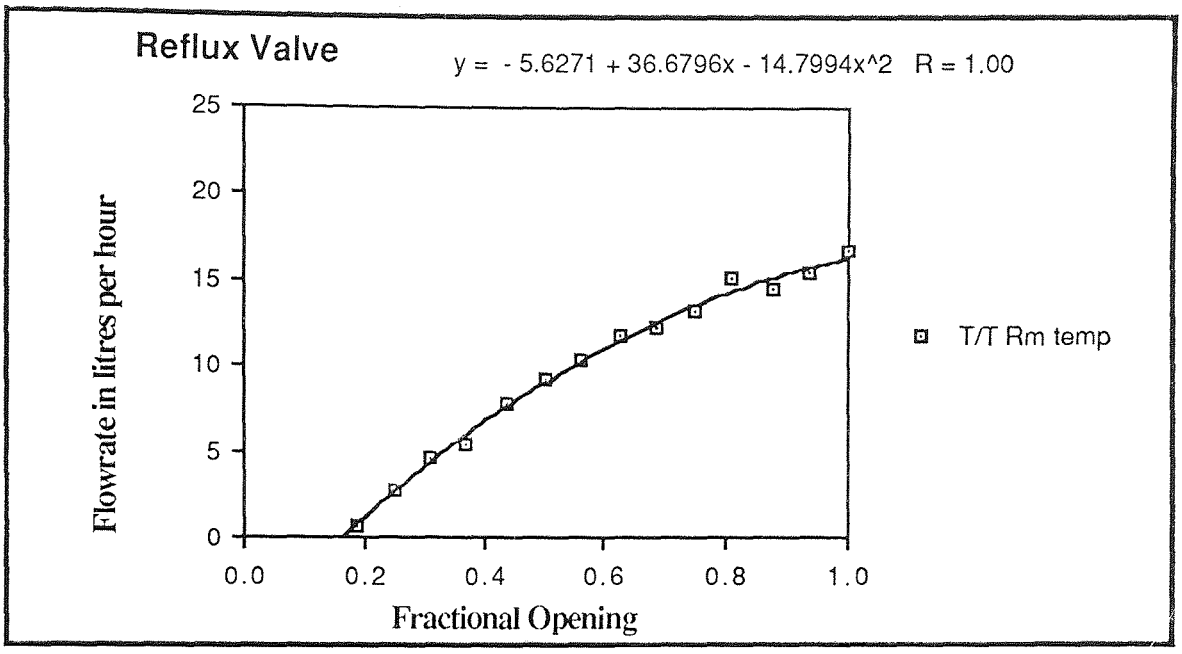

(e) Trichloroethylene and Tetrachloroethylene (T/T) at room temperature

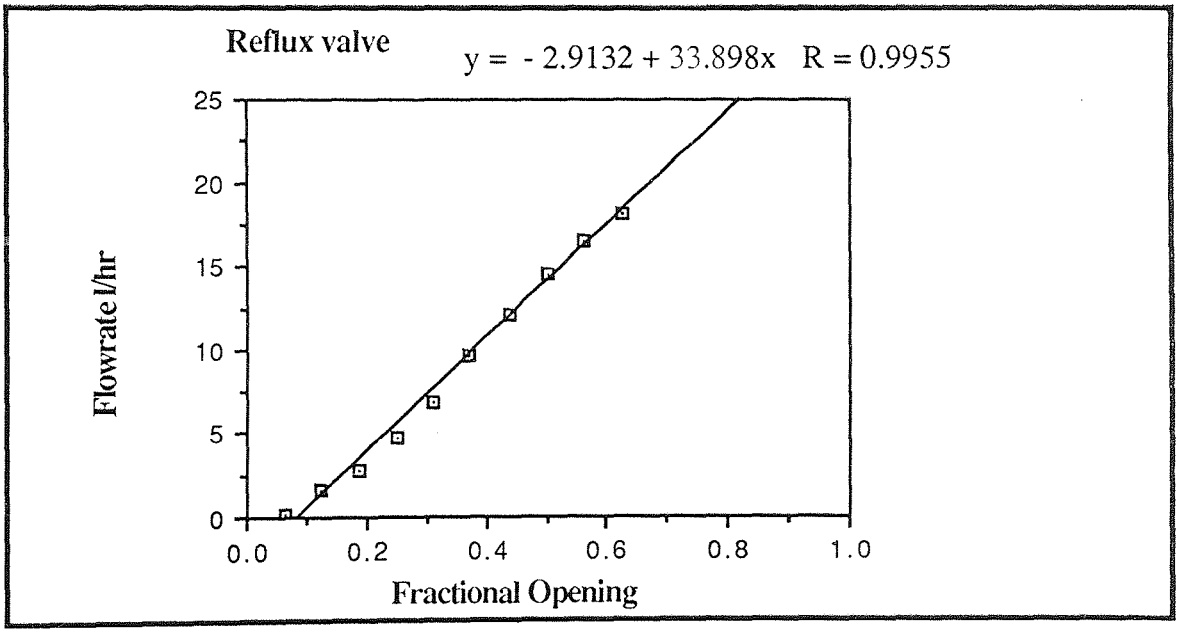

(f) Trichloroethylene and Tetrachloroethylene at about 50 °C

(R= correlation coefficient, x= fractional opening)

Figure 4.9 e) and f) Control valve characteristics

4.3 4 The thermosyphon reboiler arrangements and operation of the heater

A stainless steel thermosyphon reboiler arrangement which uses a 1/2 inch diameter 8 inches long 2.0 KW firerod heater was designed by Fuller (182). The schematic is on Figure 4. 4. The firerod heater (Figure 4.5) is located inside the tube E of the heated arm B. The liquid that is heated up is in the annular space between E and B. The vapour rises and exits through the pipe D into the column. The liquid level must be maintained above X to ensure the heated portion of tube E is always immersed in liquid. The liquid level must also be maintained below Y to prevent blockage the entry of vapour into the column. During column operation, the nominal liquid holdup capacity is about 1.5 litres, and only the maximum of about 0.5 litres of this holdup is heated up in the annular space in the heated arm.

Special electrical accessories such as a transformer, a solid state switch and a digital control timer were needed to operate the firerod heater manually and by computer signals. The heater operates in cycles with periods of **Th** seconds; where **Th** is 4 seconds. At full value of computer signal, which is 255, the voltage supply to the heater will be on for the full **Th** seconds. It instantaneously switches off and on to start another period of length **Th** ; this operation is carried out by the digital control timer and the solid state switch. The voltage supply to the heater is on for a period of time which is proportional to the computer signal (integer signal 0 - 255). A schematic of the operation is depicted below for computer signal 128.

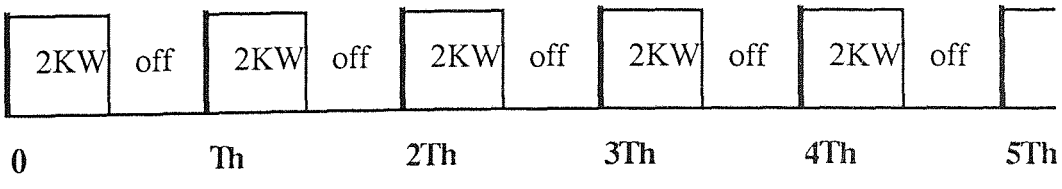

Figure 4.10 Diagram representing how the heater works

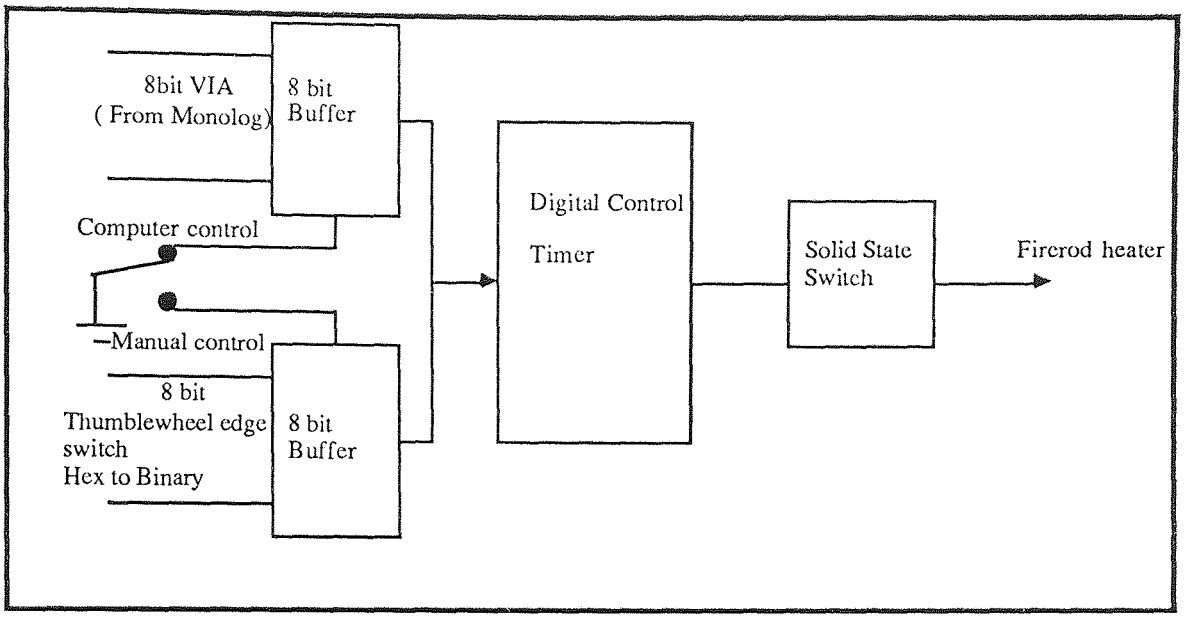

Figure 4.11 Circuit description of the interface of a control valve to the computer

The new reboiler arrangement significantly changed the dynamic behaviour of the column, particularly to heat input changes, compared to the old arrangement shown in Figure 4.2 . As the heated liquid is only a small proportion of the total liquid holdup and the vapour enters directly into the column, the effects of changes in heat input on the tray temperatures were much greater and felt more quickly .

The thermosyphon reboiler arrangement still posed some problems. The first problem encountered was with the original design made by Fuller (182). It was found that the heated arm of the reboiler, B, was easily starved of liquid because the pipe C, see Figure 4.4, was of small inside diameter (1/4 inch OD 16 SWG). In fact, heater "burn out" resulted and when this happened the heater becomes grossly underpowered or completely loses power. This made it necessary to replace C with a pipe of 3/8 inch OD 16SWG pipe to ensure B is never starved of liquid.

Secondly, the firerod heater required a tight fit with the tube E to reduce the risk of burn outs. This tight fit could not be guaranteed due to expansion and contraction resulting from cooling and heating of the annular tube E and the heater body itself. In fact, on the first occasion after a burnt out occurred, the heater had to be forced out of the tube E to allow a new one to be inserted. It was then decided to replace the heated arm of the reboiler with a new one of the same design but different dimensions. The modified design has E with 5/8 inch OD 16SWG pipe and B of 2 inch OD 16 SWG

pipe. With all these minor modifications the operation of the reboiler became more reliable.

With the reboiler arrangement installed, the actual heat supplied to the liquid in the reboiler was required, since for control and model verification purposes reasonably accurate knowledge of the actual heat into the column is needed. It became necessary to calibrate the heat input with the computer signal on installation, similar to the calibrations of flowrate with fractional valve opening. The method of calibration used was to measure the time taken for a known mass of the liquid (pure trichloroethylene or tetrachloroethylene) in the heated arm of the reboiler to reach boiling point from a known initial temperature. A thermocouple located in the well denoted F on Figure 4. gave the temperature of the vapour coming out of the heated arm. These were logged by the computer and stored in floppy disks. There where several disadvantages to this method. In the first place the shortest sampling interval that could be used was 10 seconds, as the data logging program required 6 seconds to retrieve data and the other 4 seconds was allowed for purposes of data logging. This meant that errors of up to 10 seconds could be in the measured time, particularly since it was necessary to wait for at least one sample interval to ensure the vapour temperature is reasonably constant. Since the amount of liquid heated up is small, boiling was usually reached within two sampling periods such that an error of even one second in the measurement time is significant. A typical example for Trichloroethylene (MVC) is shown in Table 4.4

It was decided to assume that the heat input is proportional to the computer signal and thus linear to the fraction of the period **Th** that the heater is on. The validity of the linearity assumption was checked in the model of the distillation column. This assumption of linearity is a very rough approximation for many reasons including the following; (1) the expansion contraction of the heater body, (2) cooling of the heater during the off-periods, (3) the fact of the tight fit between the heater body and the inside of the annulus it is placed and (4) heat losses and heat transfer from the heater into the tube. Thus, means should be sought for better calibration of the heater.

Table 4.4 Results of heater calibrations.

Integer signal 0 - 255	Mass of Liquid (g) (MVC) (±%5)	Temperature rise (±1)	Sample intervals (10 seconds per sample)
64	304	66	5
128	304	65	3
192	304	66	2
255	304	64	2

4.3.5 Temperature measurement

Nickel-Chromium Aluminium thermocouples were used for temperature measurement. They were supplied by RS Components Ltd. No calibrations were necessary as they can be connected directly to the signal conditioners that precede the A/D converters and provide the measurements in the units required by the user. Accuracy of 0.01 °C were obtained in the temperature measurements.

4.3.6 Liquid level measurement

Two air differential pressure transducers were used to monitor the liquid level in the reboiler and reflux drums. The transducer measures the pressure difference between two points on the vertically mounted drums. This pressure difference is proportional to the liquid level in the drum. Each output of the transducer is a voltage which is further converted by the A/D converter for compatibility with the computer. The relationship between the voltage reading and the level is linear. The range of voltage readings is 0-5 volts for 0-20 inches of water (gauge pressure). This is equivalent to 0-13.3 inches of T/T mixture assuming relative density of 1.5.

4.4 The System96 microcomputer

The computer used in this work for real-time process control studies is a System96 Level II microcomputer from Measurement Systems Limited. It is a 6809 8 bit microprocessor based computer with dual disk drives, and it operates at the speed of 2 Mhz. The System96 supports a real-time multitasking operating system called OS9. OS9 is modeled after the UNIX operating system of Bell Laboratories. At present the the computer has the random access memory (RAM) capacity of 256K expandable in units of 128K. The disks drives use double sided double density 5 1/2 inch floppy disks with memory capacity of 720K.

Since OS9 is multitasking, several programs, or tasks, can be run concurrently, but the memory requirements of each task has a limit of 64K. One important feature of OS9 is that software, both user written and system software, is re-entrant and position independent. This means that only one copy of all the necessary modules needs to be in the computer memory at one time, although there may be more than one user, or program, accessing any of the modules. This reduces the overall memory requirements of software.

The central processing unit (CPU) of the computer is interrupted by a hardware real time clock which generates interrupts at regular intervals of about 10 per second; this time unit is called a tick. At the occurrence of a tick of the real time clock, the OS9 can suspend the execution of a program and start the execution of another. Programs can be assigned priority and the time slice that a program gets depends on its assigned relative priority to other processes and events occurring in the system. The processes can be classified into three categories :

a) Active processes are those which have useful useful work to do and each is allocated CPU time (time slice)

b) Waiting processes are suspended pending the occurrence of some event

c) Sleeping processes are suspended by a self request for specific time interval.

Waiting and sleeping processes are not allocated CPU time until they are activated by some signal or event.

The command interpreter of the computer is called the Shell. The Shell is not part of OS9, but is the interface between the user and the "kernel" of the computer. The Shell has optional facilities to modify program execution. These facilities include input and output redirection, sequential and concurrent execution and "pipes". Pipes are connections between two programs. The standard output of one is the connected to the standard input of the other, rather than to files or input/output devices. These "pipes" can be used to transfer data from process to process in one direction only. This is from the source, which sends the data, to the sink which receives the data. The transfer of data is synchronised so that the output of the source never gets ahead of the input of the sink. This can result in delays, for example, if source does not send data as fast as the sink requires the data for its operations. When delay of 20 seconds or more occur then programming error corresponding to no input data results.

4.4.1 The Unified Input / Output system of the System96

The unified input/output (I/O) system means that all devices (visual display unit, printer, disk drives etc.) connected to System96 are regarded as files, so that hardware dependencies are eliminated using software routines. The structural organisation of I/O related systems on the System96 is shown schematically on Figure 4.12.

The input output manager (IOMAN) module provides the first level of service for the I/O system calls by routing data on I/O paths from processes to or from the appropriate managers or device drivers such as the asynchronous interface adapter (ACIA), parallel interface adapter (PIA) and the disk driver.

The function of a file manager is to process data stream to or from device drivers for similar class of device. The two file managers in the system are the random block file manager (RBFMAN) and the sequential character file manager (SCFMAN) and both are re-entrant program modules. The RBFMAN operates random access block structured devices such as the disk system. The SCFMAN operates single character oriented devices such as the visual display unit and printers.

The device driver modules (PIA, ACIA, Disk Drivers, SLAVE) are subroutine packages that perform basic low-level input and output data transfer to or from a

specific type of device hardware controller. The modules are re-entrant. The device descriptor modules (D0, D1, T1, T2, /M0) are small non-executable modules which provide information that associates a specific I/O device with its logical name, hardware controller addresses, device driver name, file managers and initialisation parameters. An example of a device descriptor module is given in Appendix A7.

The unified I/O structure of System96 offers several advantages :

1) Programs run correctly regardless of the I/O device used when the program is executed

2) Inputs and outputs can be redirected to alternate files and devices at run time.

3) The same system calls used for physical I/O functions can be used for interprocess communications.

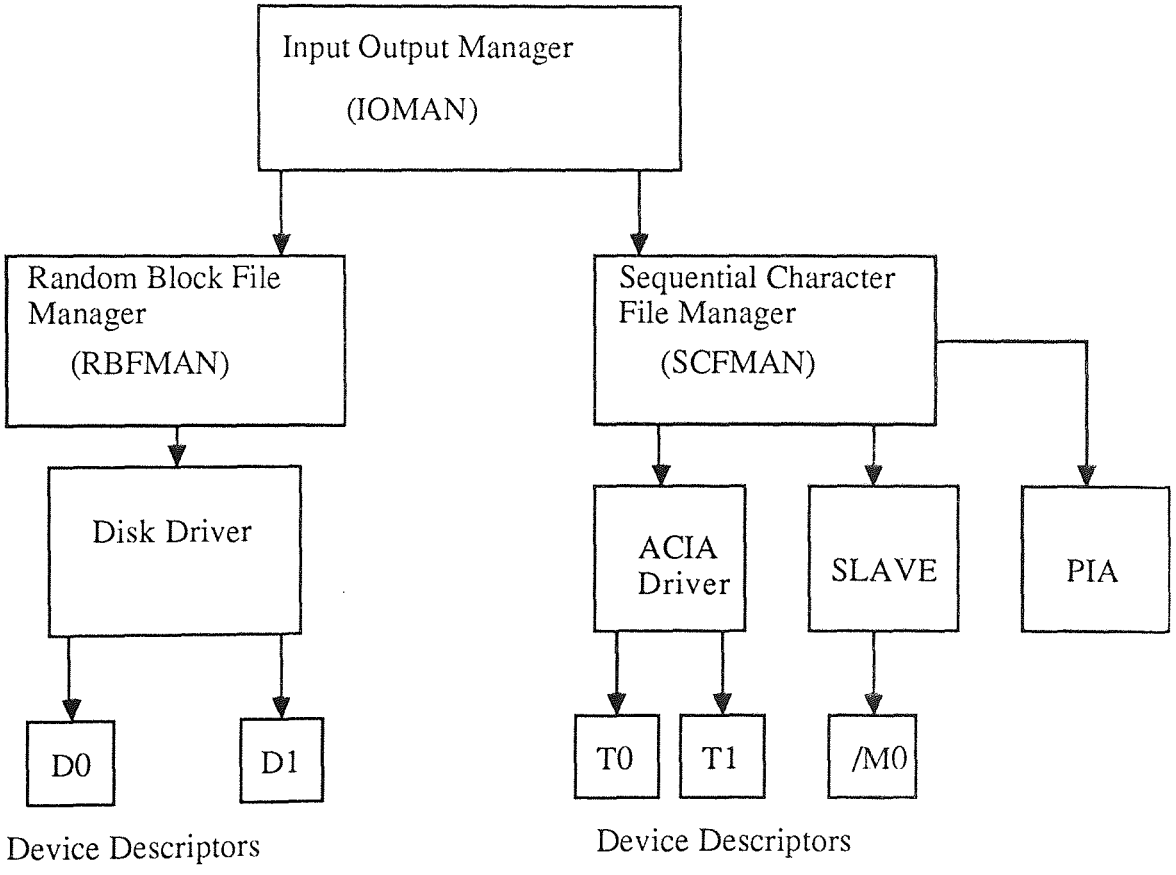

Figure 4.12 Structural organisation of Input / Output related modules of the System96

4.4.2 The Basic09 programming language

The System96 supports a high level programming language called Basic09 which is claimed by the the manual (29) to have strong resemblance to Pascal. Important features of Basic09 include;

1. Procedure, or subroutine, calls by names and parameters. The subroutines can have local variables.
2. Optional line numbers
3. Data types include bytes, integers, real, boolean, strings as well as complex data types which are combinations of the former types
4. One, two and three dimensional arrays
5. Control structures such as If.. then..Else; For...Next; Repeat...Until; Loop...Endloop; Do..Until;
6. The "Pack" command produces shorter and more efficient programs
7. Access to the any capability of OS9 using the Shell command
8. Programs written in assembler language can be accessed from any Basic09 program
9. Recursive programs can be executed; that is a program can repeatedly call itself
10. Error trapping is efficient

Unlike the original Basic, Basic09 does not have the facility for specifying global variables. Unlike Fortran77, Basic09 does not have the facility of common blocks system of variables. Also array sizes of arguments must be explicitly specified and cannot be changed during execution. For fuller details about the System96 and Basic09 consult the user manual (29).

The Plot10 graphics package (28) has been converted to Basic09 from Fortran IV in the Department of Chemical Engineering at the University of Aston in Birmingham.

4.5 The interface of the Distillation Column and the System96

To acquire real process data and control the column by computer control, a data acquisition unit called a Monolog was installed to interface the column and the System96. The Monolog provides the host computer, System 96, with analogue and

digital input/output facilities. The Monolog is a separate processing unit as shown on Plate 3. It houses the Analog to digital (A/D) converters, Digital to Analog (D/A) converters, signal conditioners, and digital input/output cards. It is driven entirely by the host computer and can be remotely located from both the host computer and the distillation column. The host computer sends commands to the Monolog to set or read analog or digital signals. The communication is conducted in decimal ASCII characters which can be processed by any general purpose computer.

More than one Monolog can be connected to the System96. This facilitates the use of System96 for hierarchical and supervisory control of several processes remotely located from each other and from the System 96.

At present, the Monolog unit consists of the following;

1. One 1010E A/D converter card which can handle up to 256 input channels with 12 or 16 bit resolution;
2. Two 1020E signal conditioning cards, each with a capability of handling 8 input channels with the aid of in-built multiplexers. More A/D channels can be used by adding extra signal conditioning cards.
3. One RM1000E single board computer (SBC) card which has a 16K programmable read only memory (PROM) in which the Monolog program resides. The board also has a 2K read/write memory (RAM), one 8 bit digital input port and one 8 bit digital output port
4. One digital input /output board, which is a general purpose input/output card called RM5223 General Purpose Interface (GPIF) parallel interface board. This card has prefixed addresses so that it can be configured as either an input or output card according to the user requirements. Upto 15 digital input/output ports can be supported by adding extra GPIF boards.
5. One RS232 interface board called RM5451 board, through which the Monolog is connected to the System96. This board is software initialised and the standard baud rate fixed as 300 characters per second in the PROM of the SBC

The Monolog is connected to the control valves and the heater of the column by a 8 bit parallel interface, VIA, from the GPIF board through the respective logic unit cards

that activate the control valves and the heater. These cards are housed inside the panel next to the column as shown in Plate 3, and a schematic diagram of the cards have been given in Figures 4.8 and 4.11 for the valves and heater respectively. Switches to manually activate the valves and the heater are placed on this panel as well.

In this work, the Monolog box was located on this panel which was two floors down from the host computer. It was necessary to locate the Monolog unit closer to the column since the connection of the column and the Monolog is a parallel line (VIA). Data transfer through parallel lines becomes less efficient as the distance the data has to travel increase. This is less of a problem in serial interfaces so that the System96 was located remotely from the column.

The functions that can be executed by Monolog include a) read and report analog channels once or continuously, b) halt the reading of analog channels, c) read digital port, d) set digital port and analog port, e) set data format and f) set up alarm reporting. These functions are initiated by commands in the software package in System96. If all 256 analog channels are in use, they are scanned sequentially from 1 to 256, or from 32 to 256 and then from 1 to 31

A variety of sensors can be connected to the signal conditioning cards and the readings converted into engineering units, depending on the choice of the user, and reported to the host computer. The engineering units that can be obtained include temperature in degrees centigrade, dc voltage, resistance in micro-ohms, strain gauge full bridge in micro strain and dc current in microamps. Thermocouples can be connected directly to the signal conditioners and several types including Ni-CrAL and platinum resistance thermocouples can be used. Fuller details on the functions of the Monolog are given in Appendix A1.2.

4.5.1 The Data Acquisition Software

The acquisition of data and the implementation of control action is done with the aid of software provided by the suppliers of the System96 and Monolog. This software package is resident in System96. The package consists of a user interface routine called

Master, a device driver called **Slave** and an OS9 format device descriptor table called **/M0**. The **Slave** and **/MO** have been introduced in Section 4.41 and in Figure 4.12.

The **Slave** routine handles the physical link into the Monolog and all the line protocols necessary to perform functions such as (1) opening and closing physical link to the Monolog, send commands to set up the Monolog and receive data from the Monolog. The device descriptor table **/MO** corresponds to the RS232 port on the System96 to which the Monolog is connected. The programs are re-entrant and position independent which means they can be used by more than one Monolog operating independently. Each Monolog must have its own RS232 port on the System96.

The **Master** program is the link between the user and the Monolog. The user can retrieve process data and send control actions to the column by specifying the appropriate functions as parameters to the **Master** program. The user is notified of any errors that occur during communication with the experimental column as well as give details of the status of the Monolog, so that **Master** is also the primary means by which the user can interact with the Monolog itself. Fuller details on the various functions of the Monolog as well as how to use the **Master** are provided in Appendix A1.2

Since **Master** was designed to form the sole means of communication of the System96 with the "outside world" program developments for on-line application of control were required to be done only in Basic09. The user written programs centre around the **Master** program.

Separate Master calls are needed to acquire data which have different engineering units. Therefore, it is convenient to group like channels to nearby channel numbers; that is, those analog channels with the same engineering units should be grouped together to minimise the number of calls to Master, since the channels are scanned in one direction only, as mentioned earlier. At present, 16 analog input channels are in use as given in Table 4.5, so that only two signal conditioners are housed in the Monolog box. The channels 1 to 8 are used for temperature measurements; channels 9 to 16 are configured

for voltage readings. Therefore, only two separate calls of Master were needed each time process data was required.

The digital outputs are sent to the control valves and the firerod heater through two GPIF boards each configured as output boards. Two output ports on the GPIF were used for sending these signals. Port 7 carries a signal that is used to select the instrument to be activated, as given in Table 5.5. Port 6 carries the digital signal corresponding to the control signal. An example subprogram that performs this function is **Valve-Out**, and a listing is given in Appendix A7.

4.5.2 Program timing for real-time applications

During real-time experiments measurements and control actions are acquired at discrete times. A mechanism that ensure that these actions are done at the correct times must be built into the data acquisition software. This is achieved using the real-time clock of the computer. For the Monolog, it is specified in the user manual the the delay between readings can be set by the user. This refers, however, to the delay between each analog to digital conversion cycle and the maximum delay possible is much less than one second. This means that measurement and control time intervals of 10 to 30 seconds (required for the monitoring and control of the column) cannot be set in the **Master** program. The Delay function in Basic09 can fulfil this requirement by temporarily suspending the System96 program execution. However, in this work the function of a timer is achieved in a different way without the use of the Delay function. Two small Basic09 routines were written. One is called Real-time, which has the function of getting the "real time" from the real time clock. The other routine is called Delta-t, which continuously compares the time of the previous sampling interval with the present one until the time difference is exactly the specified sampling interval. The measurements are then taken and control action is effected. Any sampling interval greater than 1 second can be selected. These two programs are in Appendix A7 and there computational overheads are very small.

4.6 Process operation

During preliminary operation of the column it was found that the delivery of the distillate and the bottoms rate were inconsistent. This, combined with the very small distillate and bottoms offtake rates, which were between 0 - 4 litres per hour, meant that reliable flow measurements could not be obtained. In the case of the bottoms, considerable back pressure was always present and this caused the inconsistencies. All these were major obstacles to the effective control of the reboiler and reflux drum liquid level. As a consequence some compromise had to be reached. The distillate flow control valve was usually set to an opening to deliver approximately 3 - 4 l/hr of distillate flow. This meant that the reflux level was allowed to vary according to the amount of vapour condensed in, and liquid removed as reflux from, the reflux drum. The level could vary between 1 and 30cm in the reflux drum before liquid can overflow back on to the column. The control of the liquid level in the reboiler drum is more important since, as explained earlier, the liquid level must be kept between level X and Level Y as shown on Figure 4.3. It was decided to employ two position control for reboiler level control between a range of 8cm, with 6 cm safe range above level X.

A significant number of experiments were done to gain experience of the operation of the column, particularly as many improvisations were made. The inconsistencies in the distillate and bottoms flows and the problems of reflux flowmeter failures made the reproduction of experiments difficult; this was one motivating factor in developing a good mathematical model of the column. The duration of experiments were limited to the maximum of 1 hour, as experience showed that this prolongs the operating life of the firerod heater and reduces strain on the pumps.

4.7 Chapter conclusion

This chapter has described the experimental equipment and its interfacing with the distillation column. Some operational problems of the column have been discussed. The next step is the modelling of the column and testing with experimental data.

Table 4.5 Typical set of measurements taken during on-line applications

Analog Inputs	
Channel number	Measurement
1	Reflux temperature Tlr
2	Top tray temperature T_1
3	Second tray temperature T_2
4	Feed temperature Tf
5	Feed tray temperature T_7
6	Ninth tray temperature T_9
7	Bottom tray temperature T_{10}
8	Reboiler drum temperature T_b (F in figure 4.3)
9	Not used (millivolts)
10	Reflux drum level pressure transducer (millivolts)
11	Reboiler drum level pressure transducer (millivolts)
12	Bottoms flow turbine flow meter (millivolts)
13	Feed flow turbine flow meter (millivolts)
14	Distillate flow turbine flow meter (millivolts)
15	Reflux flow turbine flow meter (millivolts)
13	Not used (millivolts)
Digital Outputs	
Output Port Number = 6	
Unit Number	Equipment
(Sent through Port 7)	
1	Bottoms product control valve
2	Distillate product control valve
3	Feed flow control valve
4	Reflux flow control valve
5	Firerod heater

This page is left intentionally blank

Key to Plate 1

A	Feed tank
B	Cooling water tank
C	Column with lagging
D	Thermosyphon reboiler drum
DA	Heated arm of reboiler
E	Condenser
F	Bottom product tank
G	Top product tank
H	A Pressure transduscer
I	A control valve (bottom product)
J	Feed entry point
K	Switches to manually control the heater and control valves

Plate 1 The pilot plant distillation column

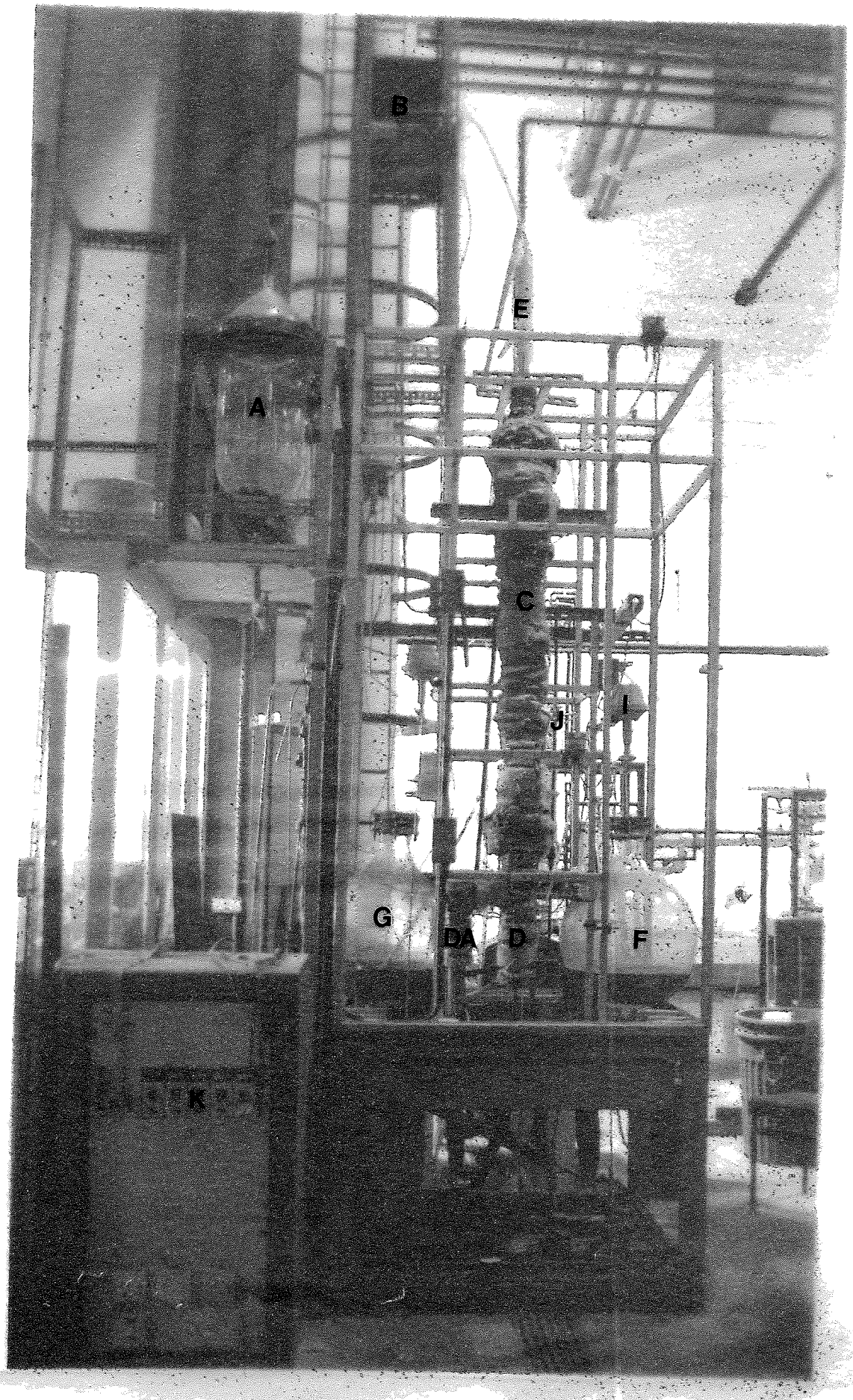

Plate 1 The pilot plant distillation column

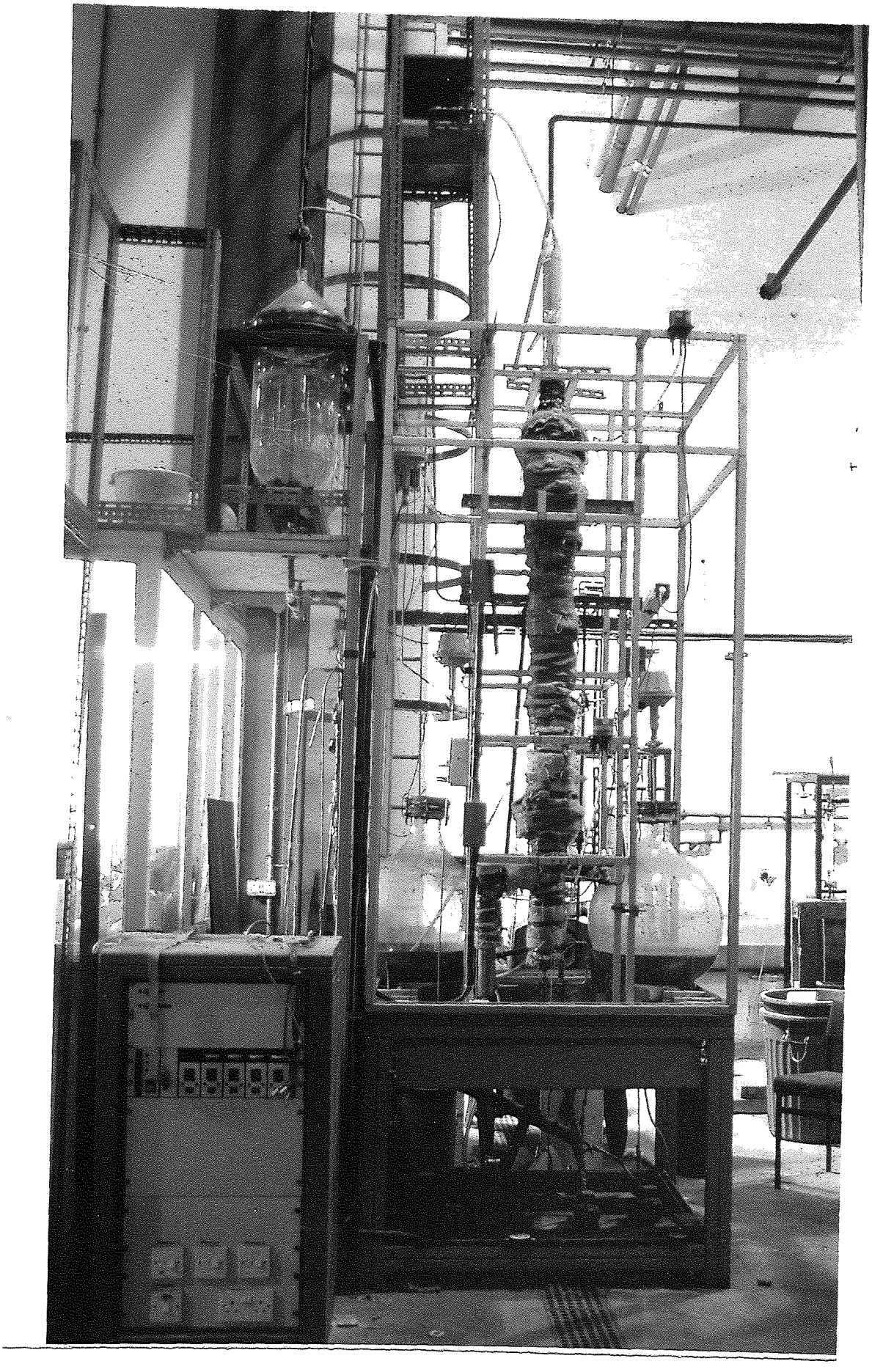

Key to Plate 2

A	A control valve
B	digital to pneumatic converter
C	Feed entry point
D	The Monolog interface box
E	Panel containing switches for manual control of valves
F	VDU screen

Plate 2 The control valves

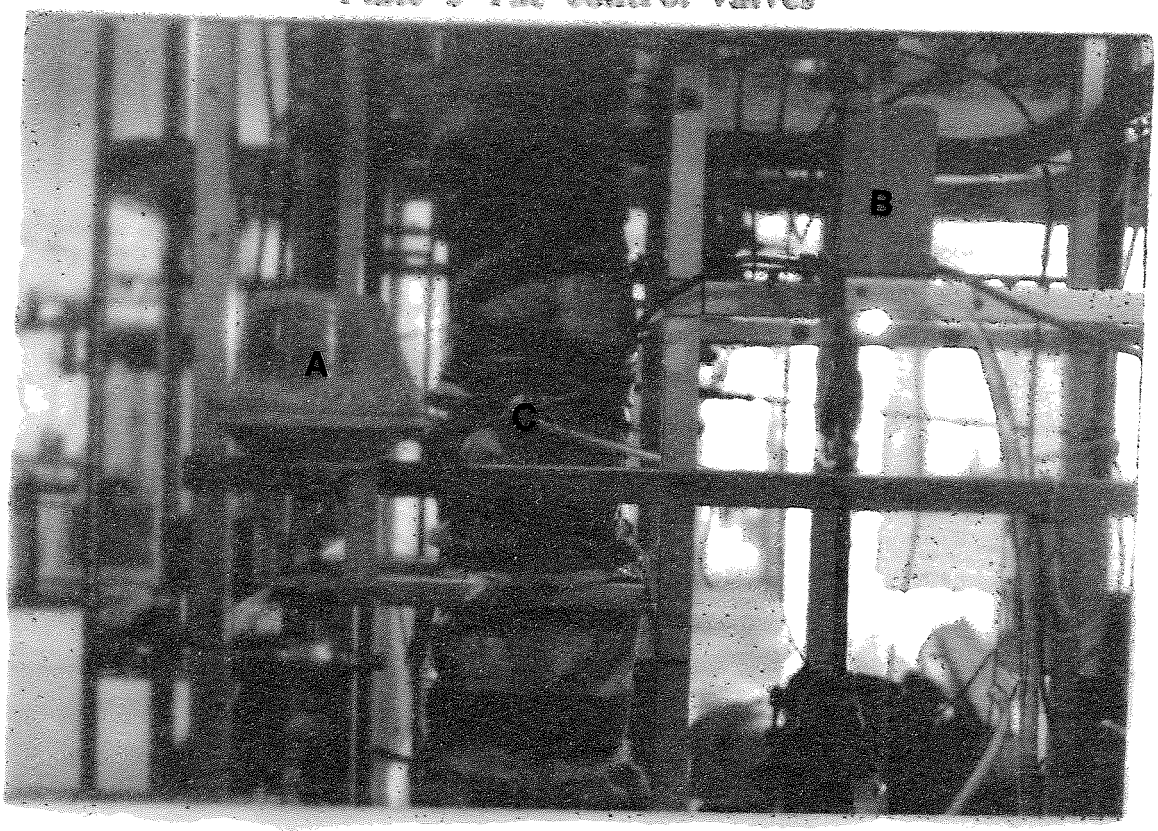

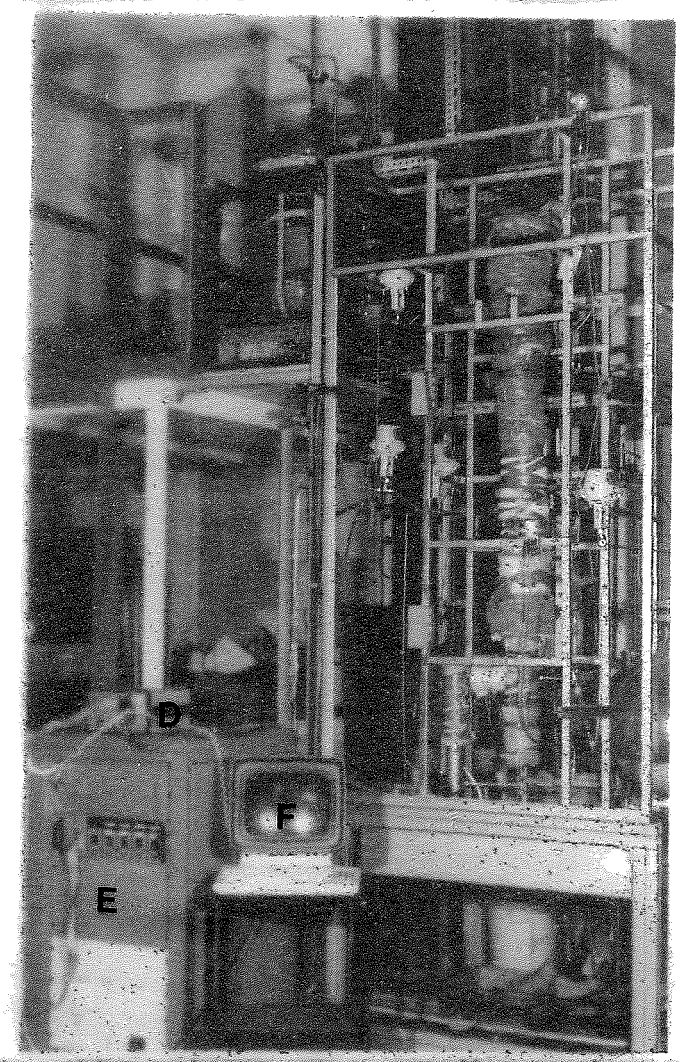

The column on a smaller scale

Plate 2 The control valves

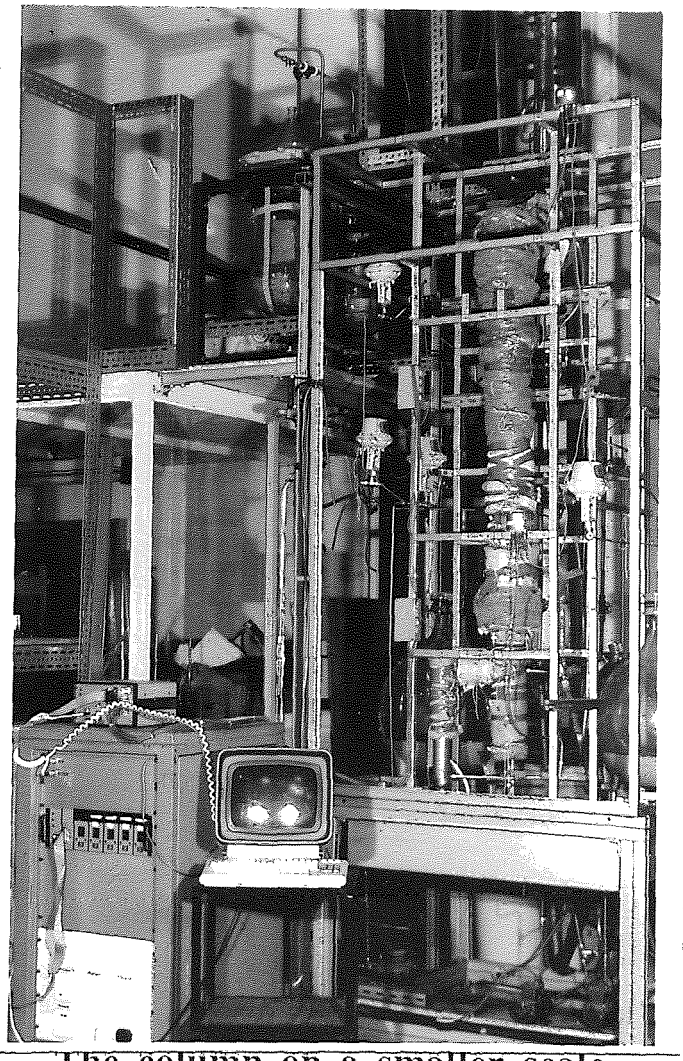

The column on a smaller scale

Key to Plate 3

A	Monolog interface box
B	VDU screen (in pilot plant)
C	switches to manually control heater and control valves
D	VDU screen (on the first floor)
E	The System96 microcomputer
F	Printer

Plate 3 The control panel

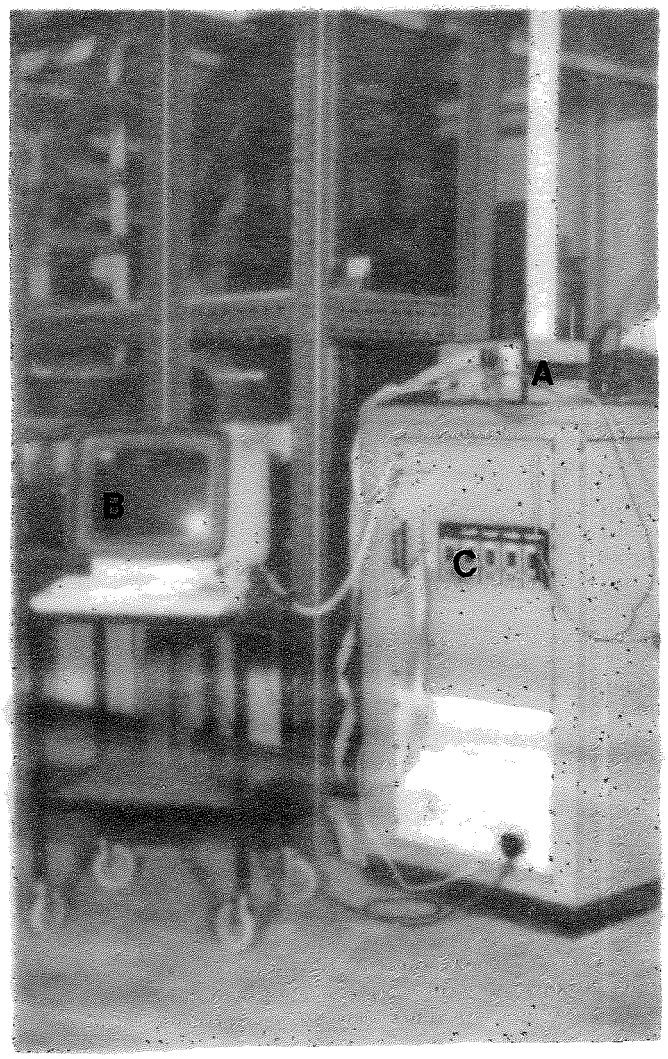

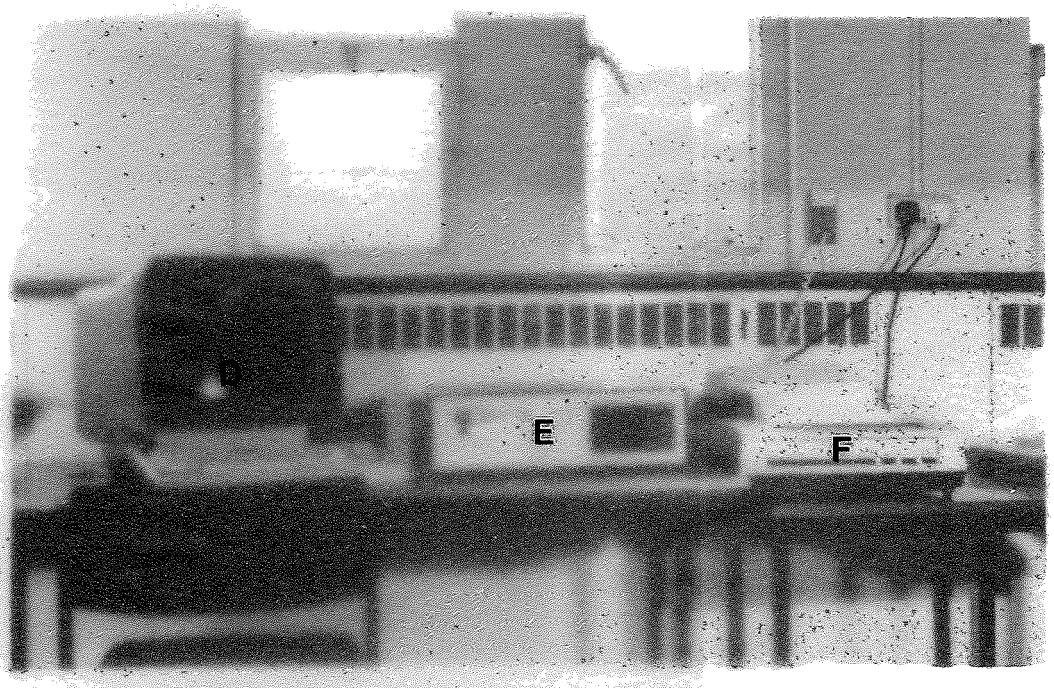

Plate 3 The control panel

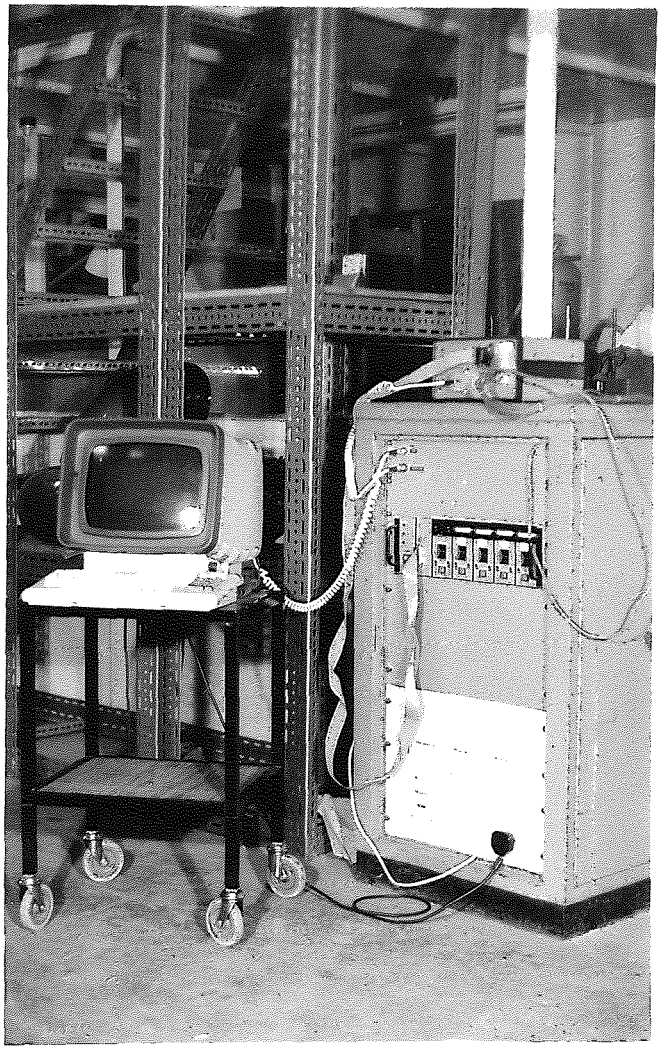

The System96 Microcomputer

CHAPTER FIVE

Mathematical modelling of the distillation column and model verification

5.1 Introduction

Mathematical modelling of the process to be controlled is important to the design and analysis of the control systems. Many subsequent decisions can be based on results derived from mathematical models of the system such as the type of control system to use and modifications that may need to be made on the system design. Control systems design implies work with dynamic systems and the first major task will be to build a mathematical model that approximates the dynamic behaviour of the system. The degree to which the model behaviour represents the real system will depend strongly on the validity of the assumptions made in deriving the model. The experience and judgement in constructing the model are therefore important to adequately describe the dynamics of the system. The intended use of the model will influence the required complexity and the assumptions made in deriving it. For instance, a model that is required for the design of a conventional feedback control system is may not need to be as complicated as a model that is required for system optimisation, where optimum operating points of the system are required, and the detail testing of the performance of various control systems. For each model a suitable solution method must be found.

For control system design and analysis and the simulation of fairly complex processes like distillation, a good mathematical model is necessary that will be valid over a wide range of operating conditions of the process. Given a suitable solution method such a model can then be used to study the dynamic characteristics for various load disturbances at various operating points by computer simulation. Different control configurations and alternative control systems can be analysed for all the possible setpoint demands and load disturbances that could possibly affect the real system. It is thus possible to greatly reduce the number of pilot plant experiments

necessary to verify the operation of the full scale plant. Potentially, a significant reduction of commissioning costs can be obtained. This makes the time and money spent on mathematical modelling worthwhile.

Chemical systems are generally quite difficult to model adequately, because in operations several complex phenomena are taking place simultaneously and the process parameters can change significantly. Also many chemical processes such as chemical reactions are not well understood. Therefore there are usually significant errors between a model and the process it represents. Examples of typical phenomena common to chemical systems are heat and mass transfer, chemical reactions, mass transport, density changes and phase changes. Mathematical and empirical relationships describing these phenomena are not always available and, if available, they are sometimes associated with error.

5.1.1 Modelling of tray distillation columns

The steady state and dynamic modelling of a tray distillation process involves the description of mass and energy transfers occurring on an individual tray and stepping this up from a single tray to a column with a number of similar trays. Typically the equations describe mass and energy balances, equilibrium relationships, efficiency of separation and component summation; this is possible case for packed columns and absorption columns as well. A comprehensive steady state model of a typical distillation column model comprises of nonlinear algebraic equations (AE's) while a comprehensive dynamic model comprises of nonlinear differential and algebraic equations (DAE's); this is the case for all separation processes as well (Holland and Liapis (48)). In the dynamic case, the common approach is to use lumped differential equations in order to avoid having to solve partial differential equations. The usual assumptions made in deriving the model relate to the tray hydraulics, vapour hold up dynamics, equilibrium relationships and efficiency. These assumptions would depend mainly on the particular column, its size, the mixture to be distilled and the intended application of the model. Sufficient computing power must be available to perform the calculations.

In present times sufficient knowledge about the physical nature of distillation is available to enable the development of adequate mathematical models of the process (Daie (26)). Many workers have successfully developed dynamic models for conventional tray distillation columns which are in reasonably good agreement with the actual columns they describe. Such studies include Gunn et al. (36), Stathaki et al. (112), Cairns and Furzer (135), Kumar et al. (61) and Kisakurek (62). Numerous work on the steady state and dynamic modelling for studying steady state and dynamic behaviour of distillation systems have also been carried out. These include the works of Kinoshita et al. (45,46) and Takamatsu and Kinoshita (128) on steady state modelling; and Rosenbrock (106), Brierly (16), Yue and Billing (138), Schuil and Bool (127), Ranzi et al. (107), Furzer (32), Ohmura et al. (93) and Wahl and Harriot (134) on dynamic modelling.

In the dynamic modelling of process systems, selecting an appropriate solution procedure to solve the DAEs is important. This is particularly true if non-linearities are pronounced and if the differential equations contain time constants which differ by orders of magnitude; that is, the differential equations are stiff. Stiff differential equations frequently arise in dynamic models of distillation columns since in most tray distillation columns the dynamic response of the liquid composition on a tray is usually much slower than the dynamic responses of the vapour holdups, liquid holdups and the pressure inside the column. The implication of this is that the integration interval must be chosen based on the differential equation with the smallest time constant. Stability and convergence problems are likely to arise during solution of the equations if the integration interval and solution method are not carefully selected. Solution methods such as the Gears method (Gallun and Holland (37), Holland and Liapis (48)), are available which deal with stiff differential equations and where the integration interval can be adjusted automatically. Ogbonda (181) gives a comprehensive review of such solution procedures. Sensitivity analysis of the DAEs and AEs (Leis and Kramer (120)) of the system can be carried out to aid in the selection of the solution procedure.

The detailed dynamic modelling of distillation columns generally results in a large set of DAEs. Large sets of equations can be difficult to handle and require significant computing power for their solution. Model order reduction techniques can be useful in alleviating such problems in that they can reduce the number of equations of the model to more manageable forms. An example of such techniques is the model order reduction procedure proposed by Cho and Joseph (17, 18, 19). They have shown that it is possible to reduce the number of DAEs that describe a distillation column by a factor of 4 and still retain reasonable accuracy .

The recent advances made in computer technology have made available computers with high computing power and large memory storage capabilities at reasonable low costs. The computing power required to solve large sets of equations is no longer a major limitation to developing comprehensive models. In recent times some general purpose dynamic simulation software packages for solving DAE's and AE's have been developed. Examples of such packages are ACES (Kocak (183)) and DASP (Ogbonda (181)). Shacham (125) presents a variety of software that is available for solving nonlinear algebraic equations of the types which arise in models of chemical engineering systems. As regards DASP, the package is resident and operational on an IBM PC AT.

5.1.2 Modelling requirements for this work

To evaluate different controller designs for a particular objective it is advantageous for the evaluations for all the different controllers be done under the same set of disturbances, load and setpoint changes. It is usually not possible to reproduce operating conditions exactly and consistently on the real systems as, for example, the surroundings temperatures and the nature of disturbances may change. Simulations are thus very useful in this respect as operating conditions can be reproduced exactly. Thus given a suitable model the screening of the controller designs can be performed.

In this work, the need for a model which can be used as a substitute of the actual distillation column became more important as the operational problems on the column began to emerge. These problems were reported in Chapter 4 to make obtaining

steady state operating conditions consistently so that evaluations as those mention in the previous paragraph could be carried out on the experimental column.

For the purpose of this research work, three types of models have been derived for the experimental binary distillation column described in the previous chapter. They are:

(i) a non-linear steady state model

(ii) a non-linear dynamic model, and

(iii) a linearised state variable dynamic model.

The models (i) and (ii) are based on mass and energy transfer, vapour liquid equilibrium and component summation relationships which result in AEs and in DAEs in the dynamic case. The linearised state variable model is obtained by linearising of the non-linear dynamic model about a steady state.

The non-linear dynamic model was required for studying of the dynamic behaviour of the column and to perform detailed assessment of the performance of control schemes prior to experimental applications. The primary requirement of this dynamic model was therefore to adequately predict the direction and magnitude of the responses of the variables of the column to input changes. The steady state model was required to aid the selection of operating points and to provide good initial values for the dynamic model. The linearised state variable dynamic model was required for off-line Kalman filtering exercises and the design of multivariable control schemes based on the state variable description of the column.

5.2 The steady state model

As mentioned earlier a steady state model was required to provide good initial values for the dynamic model and aid the selection of operating points. In binary distillation column simulation, short cut methods such as the McCabe and Theile method (Coulson et al. (189) and Treybal (53)) can give approximate initial values which can be used to initialise the dynamic model. The dynamic simulator is then allowed to reach steady state, thus refining the approximate values and give a steady state operating point. This approach was used successfully by Daie (26). It is a crude

method, but it avoids developing a good steady state model. It may be difficult to find good initial estimates for highly non linear distillation systems and multicomponent distillation systems, so that developing a steady state model cannot be avoided.

In order to avoid using a dynamic model to refine approximate initial values, a steady state model which is more accurate than the McCabe and Theile method was needed. The literature was searched to find a suitable algorithm for distillation systems which will require moderate programming requirements, easy to understand and use.

A suitable method is the steady state simulation procedure proposed by Kinoshita et al. (45) for multicomponent distillation problems processing non-ideal or chemically reactive solutions. The method is based on the use of the Newton-Raphson iterative procedure in the main calculation loop and the specification of a unique set of functions to be zeroed. Global material and energy balance equations are employed to solve for the internal liquid and vapour flowrates and the liquid mole fractions on the trays are chosen as the independent variables.

Kinoshita et al. carried out case studies which showed that the stability properties of the algorithm were high and showed a high speed of convergence. They also showed that wild initial estimates of the liquid mole fraction could be tolerated. This is considered a good feature by Takamatsu and Kinoshita (128) because good initial estimates are usually difficult to find for steady state simulation of multicomponent distillation systems processing a non ideal mixture. Kinoshita et al. showed that the heat balances around the column can be readily incorporated into the algorithm; the simulation could be performed with or without incorporating heat balances. They also showed that regardless of incorporation heat balances, non ideality and chemical reactions, the independent variables are always liquid mole fractions.

The algorithm has been used successfully to solve a wide variety of systems. Kinoshita et al. (46) applied the method to simulate multicomponent distillation columns with three phases and with partially immiscible liquids. Takamatsu and Kawachi (128)) extended the algorithm to cases were the specifications of Murphree vapour efficiencies are taken into account. They confirmed that introducing tray

efficiencies, the algorithm still retained the high convergence rate and stability using the liquid mole fractions as the independent variables.

In this research work, the algorithm referred to above was employed for the steady state simulation of the distillation column. Although the algorithm was developed to solve multicomponent system, the algorithm could be formulated to solve a binary system. This was done in this work. The following assumptions were made in the derivation of the model;

(i) total condenser

(ii) no heat of mixing; that liquid and vapour have the same temperature;

(iii) the reboiler is considered as an equilibrium stage.

(iv) the trays are assumed to be 90% efficient in separation

(v) the liquid on the trays and in the reboiler and reflux drums are well mixed.

(vi) no entrainment of liquid by the vapour leaving a tray;

(vii) column is adiabatic .

(viii) no pressure drop across the column

The steady state equations formulated for the binary distillation are given below. Figure 5.1 shows a schematic diagram of the column as used for the steady state modelling. Figures 5.2a to 5.2c show the balances on the trays, the reflux and reboiler drums respectively.

The assumption of 90% efficiency on all trays was arrived at on the basis of the simulation results of Daie (26). Daie wrote a package for predicting Murphree vapour efficiencies of the trays based on the well established A.I.C.H.E methods for predicting efficiencies of columns. The method used by Daie required the prediction of a wide spectrum of the physical properties of the liquid system such as the critical properties and the vapour and liquid diffusivity. The resulting computer program greatly increased the computational load of the dynamic simulation package as program size was of the order of the dynamic simulator program as well. It was found that the efficiencies were reasonably time invariant, so that they were computed at some predetermined steps much longer than the integration interval. The simulation results of Daie showed that the efficiencies of the trays in the column range from 99%

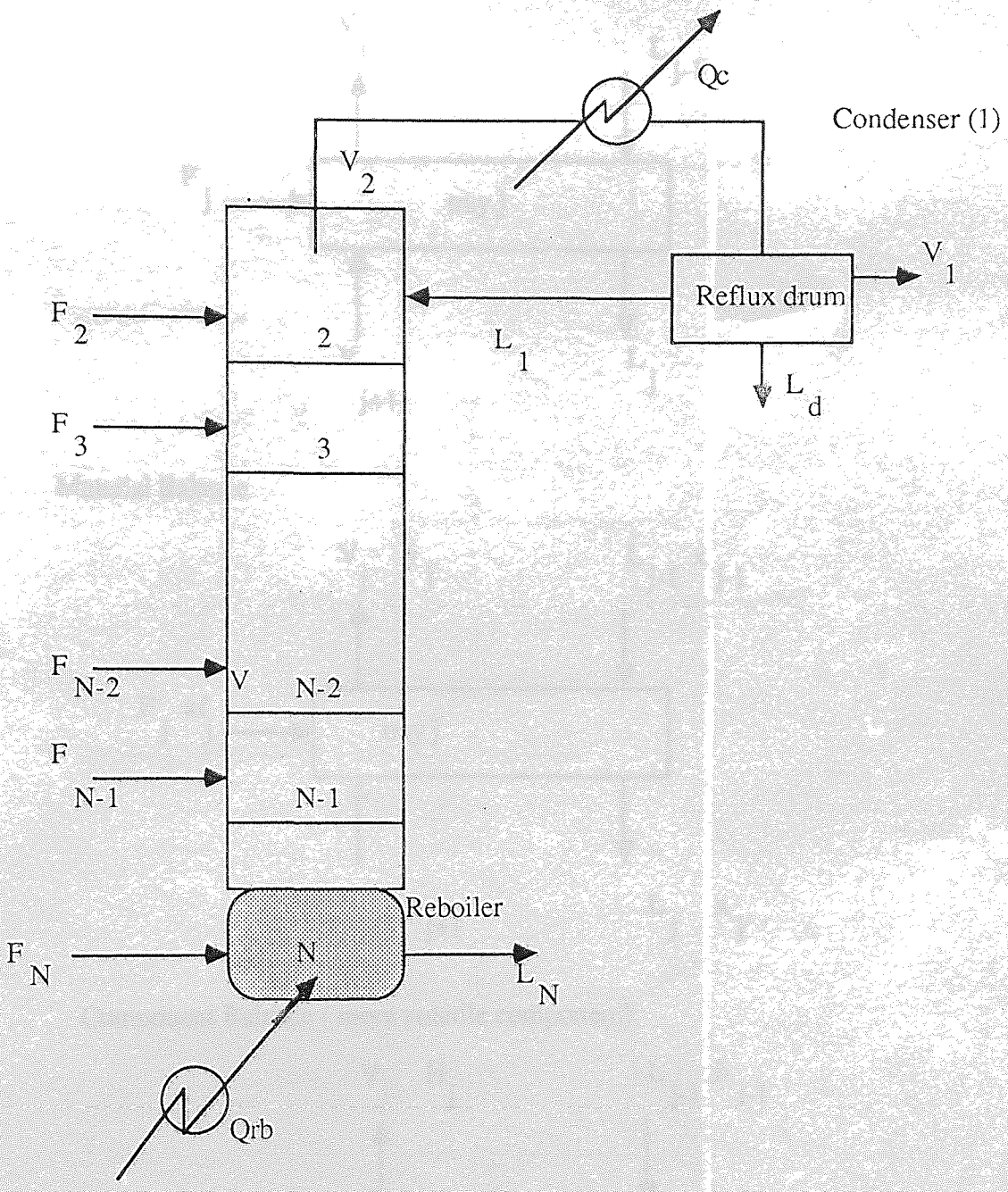

Figure 5.1 Schematic diagram of column for the steady state modelling

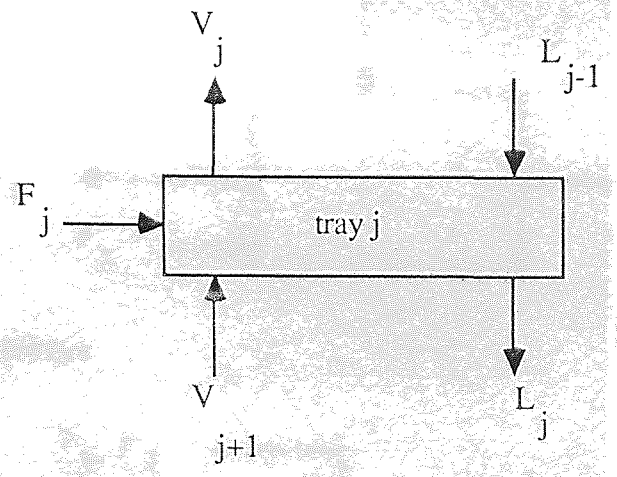

Material Balance

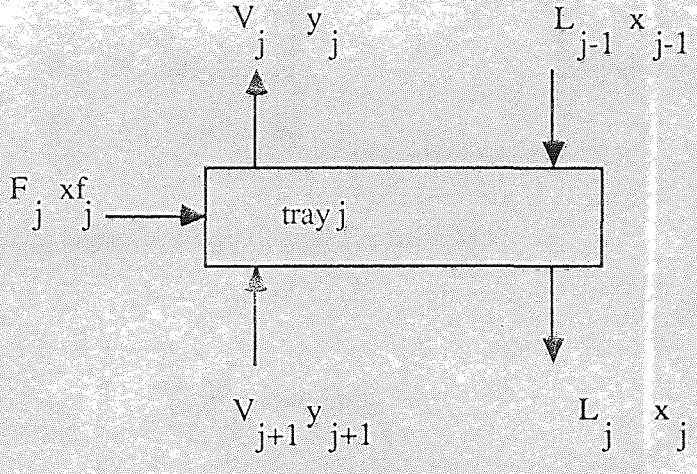

Component Balance (more volatile component)

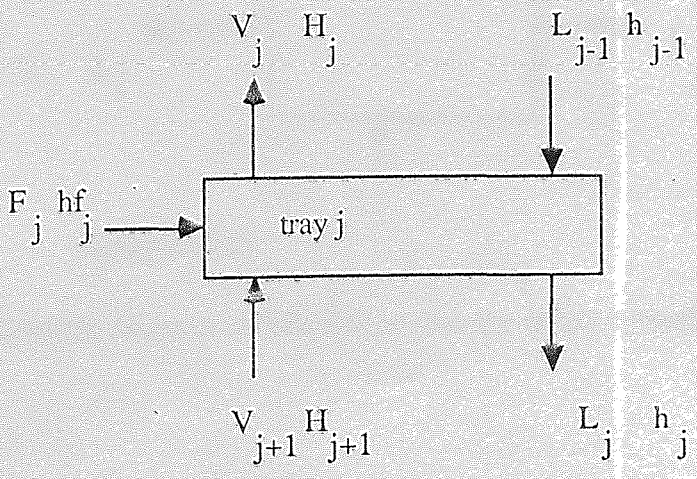

Energy Balance

Figure 5.2 a Schematic diagram of balances around a tray

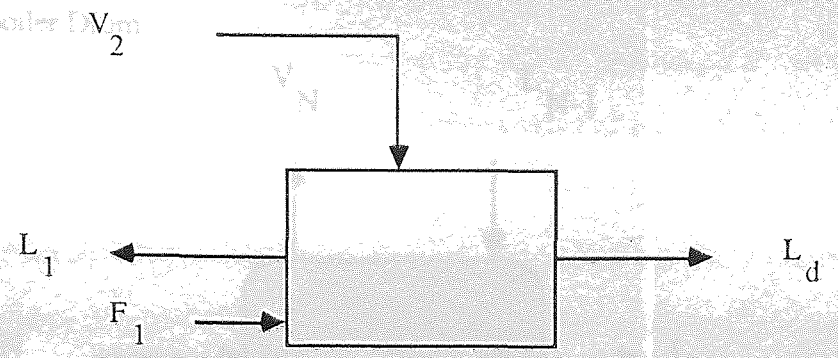

Material Balance

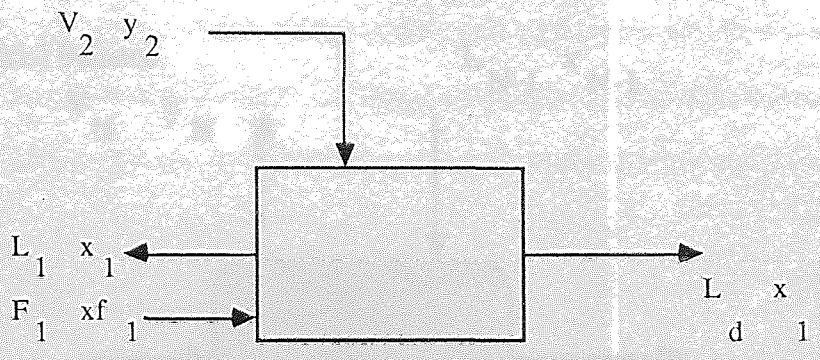

Component Balance (More Volatile Component)

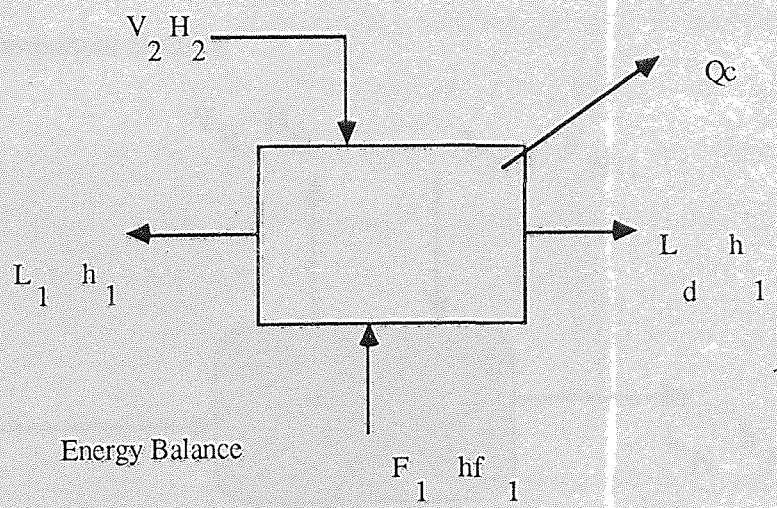

Energy Balance

Figure 5.2b Schematic diagram of balances around the reflux + condenser

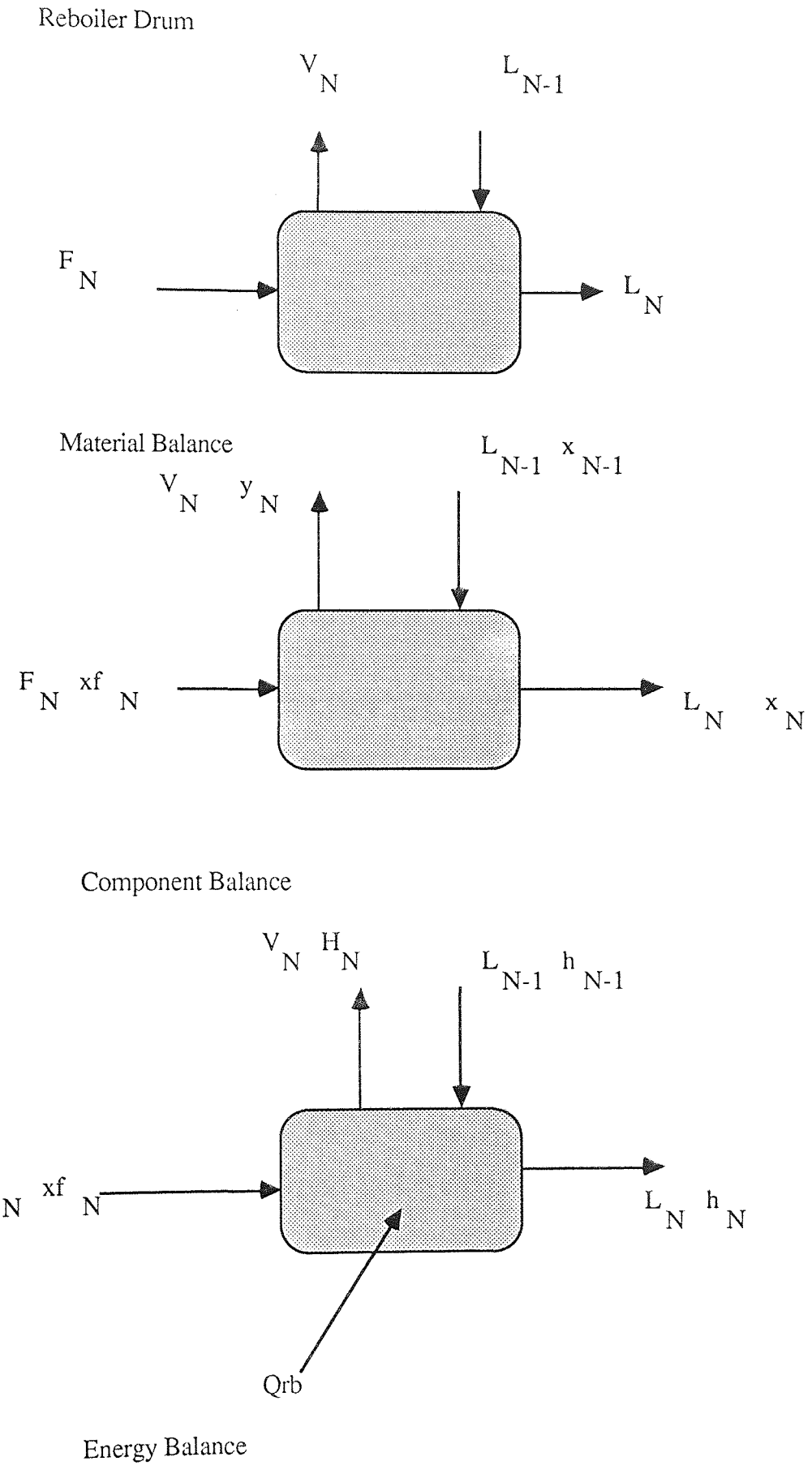

Figure 5.2c Schematic diagram of balances around the reboiler

from the top to 88% at the bottom. The assumption of 90% efficiency for all the trays was chosen as an estimate within this range. Better values of tray efficiencies can be obtained from pilot plant tests.

Recently, Fletcher (64) presented a numerical method for incorporating the efficiency model of Standart (92) into the rigorous calculation of distillation column. The approach is applicable to both binary and multicomponent distillation calculations. The calculations involve the solution of extra equations representing fictitious ideal flows, compositions, temperatures and enthalpies which are used in the definition of the efficiency. Fletcher performed calculation using experimental data at total reflux and presented results which show good fit with experimental data.

5.2.1. The steady state model equations

The distillation column has 10 trays with the tray 7 as the feed tray. In the following L and V denotes the vapour and liquid flowrates inside the column. The symbols j denotes the tray where the stages are numbered from the condenser, j = 1, to the reboiler, j = 12. The symbol i denotes component and N denotes the total number of stages is12. the number of components nc = 2 number of trays nt is 10 and for the feed tray j = 8. The symbol F denotes feed flow and the symbol **x** and **y** are Nx1 vectors containing the liquid and vapour mole fractions of the more volatile component on each stage. Therefore, the vector **x**, is given as

$$\mathbf{x} = (x_d, x_1, x_2, x_3, x_4, x_5, x_6, x_7, x_8, x_9, x_{10}, x_b)^T.$$

Since nc=2 the model can thus be presented in terms of the more volatile component (mvc) only; the composition of the less volatile component (lvc) is obtained by difference. Table 5.1 shows the necessary physical property and equilibrium data for trichloroethylene and tetrachloroethylene needed for the model development

Group 1

Component balances

Condenser, j = 1

$$V_2 y_2 + (L_1 + L_d)x_1 = 0 \qquad 5.1$$

Trays j = 2 to N-1

$$L_{j-1}x_{j-1} + V_{j+1}y_{j+1} + F_j xf_j - L_j x_j - V_j y_j = 0 \qquad 5.2$$

Reboiler j = N = 12

$$L_{N-1}x_{N-1} + F_{N-1}xf_{N-1} - L_N x_N - V_N y_N = 0 \qquad 5.3$$

where F_j is feed entry to tray j.

Group 2

Vapour compositions

$$y^*_j = K_j x_j \text{ for } j = 2 \text{ to } N \qquad 5.4$$

where y^*_j is the vapour composition in equilibrium with x_j, and K denotes the equilibrium relationship . The equilibrium relationship is defined by

$$y^*_j = g_j P^0(T_j)x_j / P_T \qquad 5.5$$

where P_T is the column pressure, Tj is the temperature on tray j, $P^0(T_j)$ is the saturation vapour pressure of the mvc in tray j and g_j is the activity coefficient if mvc on tray j

$$y_j = y^*_j, \; j = 1 \qquad 5.6$$

$$y_j = emv_j y^*_j + (1- emv_j)y_{j+1}, \; j = 2 \text{ to } N-1 \qquad 5.7$$

$$y_N = y^*_N \qquad 5.8$$

where emv_j is the Murphree vapour efficiency on tray j given by

$$emv_j = (y_j - y_{j+1})/(y^*_j - y_{j+1})$$

Group 3

Global material and heat balances material

The overall material balance is

$$L_j + V_2 - L_1 = V_{j+1} + \Sigma F_k \qquad 5.9$$

The overall heat balance is

$$L_j h_j + V_2 H_2 - L_1 h_1 = V_{j+1}H_{j+1} + \Sigma F_k hf_k$$

The subscript k in F_k denotes the feed entry to stage k The summation ΣF_k represents the sum of the feed entries into trays k = 2 to j.

Eliminating V_{j+1} and using $V_2 = L_1 + V_1 + L_d$ gives

$$L_j = (L_1 h_1 - (L_1 + V_1 + L_d)H_2 + (V_1 + L_d)H_{j+1} - H_{j+1}\Sigma F_k + \Sigma F_k hf_k)/(h_j - H_{j+1})$$

for j = 2 to N-1. 5.10

Note that $V_1 = 0$ since a total condenser is assumed.

H_j is the enthalpy of vapour stream leaving tray j

h_j is the enthalpy of liquid stream leaving tray j

hf_j is the enthalpy of feed stream entering tray j

The enthalpy symbols are

$$h_j = (\Sigma h_i x_i)_j$$

$$H_j = (\Sigma H_i y_i)_j$$

$$H_i = h_i + \lambda_j$$

$$h_i = \int Cp_i \, dT = a_i \Delta T + b_i \Delta T^2/2 + c_i \Delta T^3/3$$

where h_i is the liquid enthalpy of component i, H_i is the vapour enthalpy of component i, Cp_i is the heat capacity of the of component i, and x_i and y_i are the liquid and vapour compositions of component i and $\Delta T = T - T_0$; T_0 is the reference temperature chosen as 25°C

Group 4

The functions to be zeroed are

$$f_j = x_j - X_j \qquad 5.11$$

where X_j are given as

$$X_j = V_2 y_2/(L_1 + L_d) \quad j = 1 \qquad 5.12$$

$$X_j = (F_j x f_j + L_{j-1} X_{j-1} + V_{j+1} y_{j+1} - V_j y_j)/L_j \quad j = 2 \text{ to } N-1 \qquad 5.13$$

$$X_j = (L_{N-1} X_{N-1} - V_N y_N)/L_N \quad j = N \qquad 5.14$$

Table 5.1 Properties of Trichloroetyhlene and Tetrachloroethylene

Heat Capacity	Trichloro-	Tetrachloro-
Constants	ethylene	ethylene
a	0.9935	1.042
b	0.00611	0.005129
c	3.676×10^{-6}	3.433×10^{-6}
$Cp = a + b\Delta T + c\Delta T^2$, $\Delta T = T - T_0$, where T_0 is the reference		
temperature at (eg. room temperature (19 °C - 25 °C)). Cp is in J/gramme		
Density		
grammes / cm^3	1.466	1.6475
Molecular weight		
grammes	131.4	165.85
Vapour Liquid Equilibrium		
Antoine Constants		
*C*1	7.4266	8.08374
*C*2	1549.3	2128.93
*C*3	254.082	288.34
Van Laar Constants		
A = 0.0042		
B = -0.0004		

5.2.2 The solution procedure for the steady state model

After supplying the model with initial composition profile of the mvc, reflux ratio, distillate or bottoms flow, feed flow, feed composition, feed temperature, the steps followed to solve the equations of the steady state model are given below.

Step 1) Compute the compositions for the less volatile component (lvc) on each tray by difference.

$$x_{j,lvc} = 1 - x_j \qquad 5.15$$

Step 2) Determine the **y***s by the bubble point method. This involves solving a non-linear equilibrium relationship Equation 5.5 for T_j for each tray, except for the reflux stream if the reflux is assumed to enter the column as a cold liquid. The solution is an iterative procedure requiring a guess value for T_j, Newton Raphson iterative procedure was used in this work

Step 3) Obtain the actual vapour compositions y_j using the Group 2 equations, Equations 5.6 to 5.8, which reperesent Murphree vapour tray efficiency

Step 4) Calculate the vapour and liquid enthalpies and then calculate V_j and L_j using the Group 3 equations, Equations 5.9 and 5.10 alternately.

Step 5) Using the Group 4 equations, Equation 5.12 to 5.14, compute new liquid mole fractions, **X**

Step 6) After normalising the vector **X** in the following way

$$X_{i,j} = \frac{X_{i,j}}{\sum_{i=1}^{nc} X_{i,j}}$$

Xi,j /the functions to be zeroed, f_j for j = 1 to N in Equation 5.11, are computed using Equation 5.12 to Equation 5.13.

Step 7) The Jacobian matrix **J** is numerically evaluated as

$$J_{i,j} = \partial f_i / \partial x_j \qquad 5.16$$

where $J_{i,j}$ is the element in row i column j of **J**. The symbol ∂ denotes a small perturbation.The Gaussian elimination with maximal pivoting algorithm given in Burden et. al. (56) was used to solve $- J\, \delta x^r = f^r$ for δx^r.

Step 8) The new values of x_j are then calculated as

$$x_j^{r+1} = x_j^r + \delta x_j^r \qquad 5.17$$

where r is the iteration step and δx^r is given as

$$\delta x^r = - J^{-1} f^r \qquad 5.18$$

Step 9) Before updating the new x_j^r the absolute values of δx_j^r are checked to see if they are not too large. This is is done by checking if $\|\delta x_j^r\|$ exceed ρx_j^r where ρ is a damping factor chosen as $0 < \rho < 1$. The x_j^{r+1} are then updated as

$$x_j^{r+1} = x_j^r + \text{SIGN}\,(\rho x_j^r,\ \delta x_j^r) \qquad 5.19$$

where SIGN (a, b) is a number whose absolute values is a and sign is the same as that of b.

Step 10) Check if the x_j^{r+1}'s violate the limits 0 and 1 and reset as

$x_j = 0.0001$ if $x_j < 0$ or

$x_j = 0.9999$ if $x_j > 1.0$

Step 11) Go to Step 12 if convergence criteria

$$Jcv = \| f \|_1 / N < \varepsilon \qquad 5.20$$

where ε is a tolerance chosen appropriately, otherwise return to Step 2).

Step 12) Calculate reboiler and condenser heat duty and stop procedure.

In this work a simple procedure was used to select the damping factor ρ in Step 9 to avoid specifying a damping factor for each state variable. At each iteration step, r, the element with the largest magnitude in the vector, δx_j^r was obtained. Denoting this value as ζ, the ρ was chosen as follows;

$\rho = 0.1$, if $\zeta > 0.3$

$\rho = 0.3$, if $0.2 < \zeta < 0.3$

$\rho = 0.5$, if $0.1 < \zeta < 0.2$ 5.21

otherwise $\rho = 1.0$. Then

$$x_j^{r+1} = x_j^r + \rho\, \delta x_j^r$$

5.3 The nonlinear dynamic model - the column simulator

The dynamic model is also based on non-linear mass and energy balances and equilibrium relationships. The tray by tray concept of modelling was employed and the equations were grouped in a cause and effect sequence to ensure stability of the solution. The phrase "cause and effect sequence" means that the information flow in the mathematical model is made to coincide with material flow in the distillation column to the best of the ability of the modeller. For example, the vapour leaving each tray should be calculated from the reboiler upwards and the liquid flow leaving each tray should be calculated from the top to the bottom tray; these are the directions of travel inside the column.

The following assumptions are made in the development of the dynamic model to avoid stiff differential equations and to have a model that is not too complex and which requires only moderate computational time. A set of DAE's were generated by the modelling exercise .

The assumptions made for the steady state model stated in Section 5.2 were used. The additional assumptions for the dynamic model are:

(i) the liquid hold up on each tray is constant and the vapour holdup on each tray is negligible compared to the liquid holdup.

(i) the heat dynamics are very fast compared to the composition dynamics.

(iii) the feed tray is modelled like all other trays above and below it, with additional terms such as the feed entering the column.

(iv) the thermosyphon reboiler arrangement is modelled as a simple well mixed tank

(v) all the heat supplied to the reboiler vapourises liquid in the reboiler.

Assumptions (i) and (ii) meant that the mass and energy balance equations reduce to algebraic equations from which the liquid and vapour rates were calculated. Under these assumptions the only significant dynamics in the model are due to the dynamics of the component balances of the liquid on each tray. This effectively avoids stiff differential equations because the composition time constants are of the same order (1

- 3 seconds). The holdups on each tray were approximated by the Francis wier formula given in Treybal (53).

5.3.1 The dynamic model equations

The dynamic model of the distillation column is schematically shown in Figure 5.1. However, unlike the steady state model, local energy and mass balances around each tray and the reboiler and reflux drums were employed. These are represented schematically in Figures 5.2a to 5.2c. For the dynamic model, $F_j = 0$ for all j except the feed tray which is j = 8 numbering from the reflux drum to the reboiler. The model equations are given by the following.

Model of a tray, j = 2 to N-1

$$dMj/dt = 0 = L_{j-1} + V_{j+1} - L_j - V_j + F_j \qquad 5.22$$

$$Mjdxj/dt = L_{j-1}x_{j-1} + V_{j+1}y_{j+1} - L_jx_j - V_jy_j + F_jxf_f \qquad 5.23$$

$$Mjhj/dt = 0 = L_{j-1}h_{j-1} + V_{j+1}h_{j+1} - L_jh_j - V_jH_j + F_jhf_j \qquad 5.24$$

$$y^*_j = g_j P^0(T_j)x_j / P_T \qquad 5.25$$

$$y_j = emv_j y^*_j + (1- emv_j)y_{j+1} \qquad 5.26$$

where g is the activity coefficient and $P^0(Tj)$ is the saturation vapour pressure of the more volatile component, and P_T is the column pressure.

From the energy balance equation , Equation 5.22, the vapour leaving a tray can be computed as

$$V_j = (L_{j-1}h_{j-1} + V_{j+1}h_{j+1} - L_jh_j + F_jhf_j) / H_j \qquad 5.27$$

From the mass balance equation, Equation 5.22, the liquid leaving a tray can be computed as

$$L_j = L_{j-1} + V_{j+1} - V_j + F_j \qquad 5.28$$

Model of the reflux drum, j = 1

$$dM_j/dt = V_{j+1} - L_j - L_d \qquad 5.29$$

$$M_jdx_j/dt + x_jdM_j/dt = V_{j+1}y_{j+1} - Ljx_j - L_dx_j \qquad 5.30$$

so that

$$M_j dx_j/dt = - x_j dM_1/dt + V_{j+1}y_{j+1} - L_1 x_d - L_d x_d \quad 5.31$$

Since a total condenser is used then, $y_1 = y_2$, $x_1 = x_d$, and $M_1 = M_d$.

$$y_j = y^*_j = g_j P^0(T_j)x_j /P_T \quad 5.32$$

Model of the reboiler drum j = N = 12

$$dM_N/dt = L_{N-1} - L_N - V_N \quad 5.33$$

$$M_N dx_N/dt + x_N dM_N/dt = L_{N-1}x_{N-1} - L_N x_N - V_N y_N \quad 5.34$$

so that

$$M_N dx_N/dt = - x_N dM_N/dt + L_{N-1}x_{N-1} - L_N x_N - V_N y_N \quad 5.35$$

$$M_N hj/dt = 0 = L_{N-1}h_{N-1} - L_N h_N - V_N H_N + Qrb \quad 5.36$$

where $M_N = M_b$

From Equation 5.36, the vapour leaving the reboiler drum is obtained as

$$V_N = L_{N-1}h_{N-1} - L_N h_N + Qrb \quad 5.37$$

$$y_N = emv_N y^*_N \quad 5.38$$

$$y^*_N = g P^0(T_N)x_N /P_T \quad 5.39$$

where Qrb is the reboiler heat input

P_T column pressure

M_j hold up of liquid on tray j

The prediction of the vapour liquid equilibrium in both the steady state and dynamic models was done using the Antoine relationship for the saturation vapour pressure and the Van Laar equation for the activity coefficients. The Antoine relationship is given as

$$Log_{10}P_i^0(T) = C1_i - C2_i/(C3_i - T) \quad 5.40$$

where T is the temperature in degrees centigrade and the subscript i denotes the component i. The activity coefficients, g_i, are predicted from the Van Laar relationship given as

$$Log_{10}g_1 = (2B-A)x_2^2 + 2(B-A)x_2^3 \quad 5.41$$

$$\text{Log}_{10} g_2 = (2B\text{-}A)x_1^{\,2} + 2(B\text{-}A)x_2^{\,3} \qquad 5.42$$

where the subscript i in g and x denote the component i.The *C1,C2* and *C3, A and B* are constant parameters given in Table 5.1. These values were obtained from Daie (26). Figures 5.3a and 5.3b shows a comparison of the prediction of Equation 5.40 using column pressure at 760 mmHg with published experimental data of Bachman et al. (180).

5.3.2 Solution procedure for dynamic simulation

An outline of the sequence of solution is given below:

Step 1) Obtain initial values of feed flow, reflux flow, reboiler heat input, feed composition, feed temperature, reflux temperature, liquid and vapour flows entering and leaving each stage from the results of the steady state model. The column pressure was assumed to be at 760 mm Hg.

Step 2) Ensure the tray compositions are in the limit 0 and 1 and take appropriate corrective action if they are not. This was done by setting

$x_j = 0.0001$ if $x_j < 0$ or

$x_j = 0.9999$ if $x_j > 1.0$

Step 3) Perform bubble point calculations to obtain T_j and y^*_j for all trays and then obtain actual vapour composition y_j using the Murphree tray efficiencies specified from the reboiler to the condenser.

Step 4) Calculate the enthalpies of the liquid and vapour streams leaving each tray, and the enthalpies of the feed and reflux streams.

Step 5) Compute the vapour rates leaving each tray from the reboiler to the top tray.

Step 6) Compute the liquid rates from the top to the bottom tray.

Step 7) Compute the differential, dx_j/dt for all the trays in including reboiler and reflux drums and dMj/dt for both drums only

Step 8) Integrate the differential equations by the simple Euler integration method.

Step 9) Return to Step 2) and continue until specified time duration is reached.

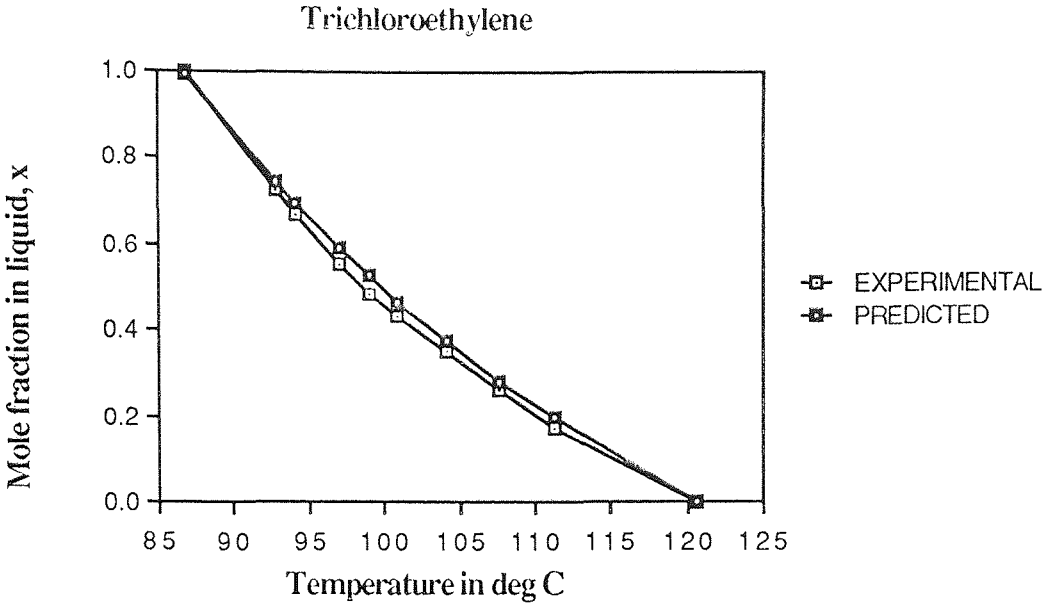

a)

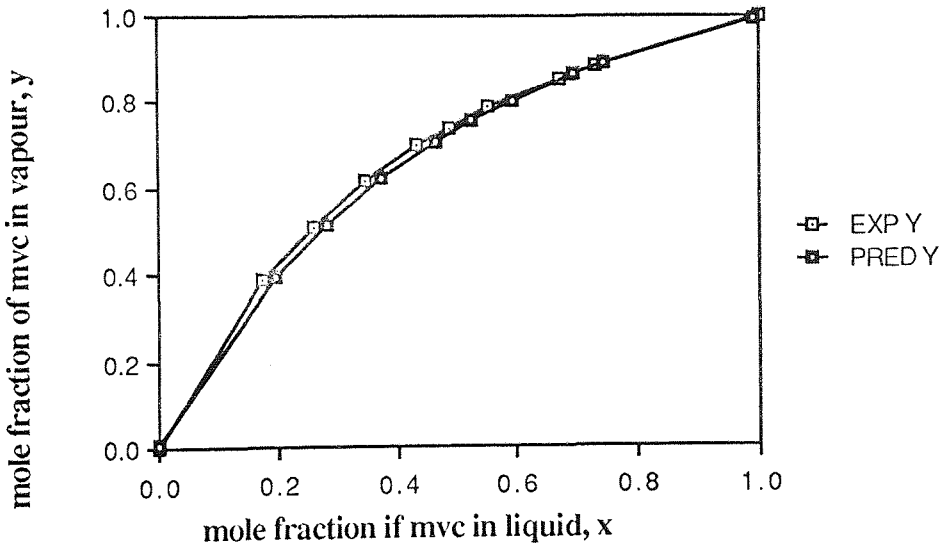

b)

Figure 5.3 Comparison of predicted vapour liquid equilibrium with published experimental data of Bachman et al (180)

Appendix A5.2 explains the functions of the computer programs that perform the dynamic simulation. The actual model equations of the column are in the module **Dynmodel**. For flexibility and computational efficiency the integration of the differential equations is done outside the **Dynmodel** in the main calling program,and the main program handles data output at the specified interval. Control action, when required, is also performed in the main calling program.

The bubble point temperature calculations were done using the temperatures of the previous integration step as the starting guess temperature for the present step. This improved on the computational efficiency of the solution as the number of bubble point iteration steps required to solve for T_j was significantly reduced. A similar approach was used in the steady state model by using temperatures of the previous iteration step as the guess temperatures.

5.4 The linear state variable model

The linearised state variable model is represented as

$$dx/dt = Ax + Bu + Dzd \qquad 5.43$$

where A is the system state matrix (n x n), B is the input driving matrix (n x m), and D is the disturbance matrix (n x nd). The **u** and **zd** are the input and disturbance vectors (m x 1) and (nd x 1), respectively and **x** is the state vector (n x 1). The n, m and nd are the number of states, inputs and disturbances respectively. State variable models of a process are useful in the design of state variable feed back control systems for the process.

For the column the vectors **u** and **zd** are

$$\mathbf{u} = [\Delta Lr, \Delta Qrb]^T \qquad 5.44$$

$$\mathbf{zd} = [\Delta F, \Delta xf]^T \qquad 5.45$$

where Δ represent deviation from steady state. The Lr, Qrb, F and xf are the reflux flow, reboiler heat input, feed flow and feed composition, respectively. Their respective units, as used to derive the linearised state variable model, are l/hr, KW, l/hr, mass fraction and °C, respectively. The vector **x** contains the tray compositions of the more volatile component

$$\mathbf{x} = (\Delta x_d, \Delta x_1, \Delta x_2, \Delta x_3, \Delta x_4, \Delta x_5, \Delta x_6, \Delta x_7, \Delta x_8, \Delta x_9, \Delta x_{10}, \Delta x_b)^T \qquad 5.46$$

To obtain the state variable model of the column, the vapour and liquid flow rates leaving the trays were calculated by solving the mass and energy balance equations for all the trays simultaneously using the Newton-Raphson procedure. This method is more accurate than the Steps 5) and 6) in the previous section, but required more computer memory for program storage and the extra calculations required since it involves an iterative procedure. The approach was therefore used for linearising the dynamic model to obtain linear state variable models of the column.

The A, B, and D matrices of the model were obtained by linearising the non-linear equations of the column simulator about a steady state. This was done numerically by perturbing the variables of the column. Tables 5.2b and 5.2b. contain two sets of A, B and D matrices obtained at different operating points. Those on Table 5.2a

correspond to the state variable model at high top product purity of 96.5% mvc which will be called model LM1. The matrices in Table 5.2b was obtained when the column was at lower top product purity of 86% mvc and it will be called model LM2. The state matrices are essentially tridiagonal as the other entries are relatively small as shown in Table 5.2c. These small entries were eliminated when the models were used for simulations and design of controllers based on state variable description of the column

Table 5.2a Linearised state variable model LM1

A

-0.1195	0.0393	0.0000	0.0000	0.0000	0.0000	0.0000	0.0000	0.0000	0.0000	0.0000	0.0000
5.8717	-9.1433	2.9931	0.0000	0.0000	0.0000	0.0000	0.0000	0.0000	0.0000	0.0000	0.0000
0.0000	6.5078	-9.7826	3.6109	0.0000	0.0000	0.0000	0.0000	0.0000	0.0000	0.0000	0.0000
0.0000	0.0000	6.4969	-10.1417	4.3077	0.0000	0.0000	0.0000	0.0000	0.0000	0.0000	0.0000
0.0000	0.0000	0.0000	6.4553	-10.8023	5.4197	0.0000	0.0000	0.0000	0.0000	0.0000	0.0000
0.0000	0.0000	0.0024	0.0000	6.4169	-11.9408	6.8967	0.0000	0.0000	0.0000	0.0000	0.0000
0.0000	0.0000	0.0000	0.0003	0.0000	6.4023	-13.4965	8.3748	0.0000	0.0000	0.0000	0.0000
0.0000	0.0000	0.0000	0.0000	0.0000	0.0000	5.7254	-19.4654	8.8343	0.0000	0.0000	0.0003
0.0000	0.0000	0.0000	0.0000	0.0000	0.0000	0.0000	11.7103	-20.8274	11.3931	0.0000	0.0000
0.0000	0.0000	0.0000	0.0000	0.0000	0.0000	0.0020	0.0022	11.5833	-23.3442	14.7516	0.0000
0.0000	0.0000	0.0000	0.0000	0.0000	0.0000	0.0000	0.0000	0.0000	11.4777	-26.7498	14.4325
0.0000	0.0000	0.0000	0.0000	0.0000	0.0000	0.0000	0.0000	0.0000	0.0000	0.1791	-0.3003

B

-1.212 E -7	-3.471 E-10
0.000748	-0.00000172
0.001529	-0.00000345
0.002692	-0.00000609
0.004059	-0.00000917
0.004845	-0.00001113
0.004406	-0.00001048
0.002572	-0.00000973
0.001885	-0.00001276
0.001972	-0.00001372
0.002178	-0.00001124
0.0000047	-0.000000089

D

0.000000	0.0
0.000000	0.0
0.000000	0.0
0.000000	0.0
0.000000	0.0
0.000000	0.0
0.000000	0.0
0.0002622	6.0858
0.001334	0.0
0.001384	0.0
0.001125	0.0
0.0000094	0.0

Table 5.2b Linearised state variable model LM2

A

-0.1247	0.047	0.0000	0.0000	0.0000	0.0000	0.0000	0.0000	0.0000	0.0000	0.0000	0.0000
5.5422	-9.2974	4.0186	0.0000	0.0000	0.0000	0.0000	0.0000	0.0000	0.0000	0.0000	0.0000
0.0000	6.1700	-10.654	5.6626	0.0000	0.0000	0.0000	0.0000	0.0000	0.0000	0.0000	0.0000
0.0000	0.0000	6.2367	-12.0977	7.3298	0.0000	0.0000	0.0000	0.0000	0.0000	0.0000	0.0000
0.0000	0.0000	0.0000	6.2661	-13.8578	8.8088	0.0000	0.0000	0.0000	0.0000	0.0000	0.0000
0.0000	0.0000	0.0024	0.0000	6.3097	-15.4256	9.7902	0.0000	0.0000	0.0000	0.0000	0.0000
0.0000	0.0000	0.0000	0.0003	0.0000	6.3292	-16.4148	10.2870	0.0000	0.0000	0.0000	0.0000
0.0000	0.0000	0.0000	0.0000	0.0000	0.0000	5.6291	-21.0371	11.2850	0.0000	0.0000	0.0003
0.0000	0.0000	0.0000	0.0000	0.0000	0.0000	0.0000	11.5247	-23.2216	14.4463	0.0000	0.0000
0.0000	0.0000	0.0000	0.0000	0.0000	0.0000	0.0020	0.0022	11.4351	-26.3319	17.7526	0.0000
0.0000	0.0000	0.0000	0.0000	0.0000	0.0000	0.0000	0.0000	0.0000	11.3371	-29.5507	16.0096
0.0000	0.0000	0.0000	0.0000	0.0000	0.0000	0.0000	0.0000	0.0000	0.0000	0.1760	-0.3173

B

-1.47 E -7	-4.06 E -10
0.003143	-0.00000686
0.004805	-0.00001049
0.005384	-0.00001174
0.004544	-0.00000987
0.002944	-0.00000667
0.001652	-0.00000366
0.000279	-0.00001146
0.001974	-0.00001291
0.001687	-0.00001054
0.001264	-0.00000701
0.0000018	-0.000000048

D

0.000000	0.0
0.000000	0.0
0.000000	0.0
0.000000	0.0
0.000000	0.0
0.000000	0.0
0.000000	0.0
0.002727	6.0712
0.001401	0.0
0.001196	0.0
0.0007619	0.0
0.0000053	0.0

Table 5.2c State matrix coefficients for the state variable model LM2 with errors

-0.1247	0.047	0.0063	0.0008	0.0001	0.0000	0.0000	0.0000	0.0000	-0.0000	0.0000	0.0000
5.5422	-9.2974	4.0186	0.0034	0.0004	-0.000	-0.0001	-0.0001	-0.0002	-0.0004	-0.0007	0.0000
-0.0096	6.1700	-10.654	5.6626	0.0214	-0.0001	-0.0002	-0.0002	-0.0002	-0.0005	-0.0009	0.0000
-0.0057	-0.0062	6.2367	-12.0977	7.3298	0.0345	0.0003	-0.0004	0.0006	0.0012	0.0002	0.0000
-0.0031	-0.0051	0.0053	6.2661	-13.8578	8.8088	0.0370	0.0015	0.0023	0.0040	0.0084	0.0001
-0.0073	-0.0034	0.0024	-0.0004	6.3097	-15.4256	9.7902	0.0467	0.0026	-0.0045	-0.0009	0.0000
-0.0014	-0.0182	0.0018	0.0003	0.0002	6.3292	-16.4148	10.2870	0.0522	0.0006	0.00015	0.0000
-0.0043	-0.0086	0.0003	-0.0004	-0.0007	-0.0009	5.6291	-21.0371	11.2850	-.0062	-0.0061	0.0003
-0.0029	-0.0308	0.0027	0.0003	0.0000	-0.0001	0.0000	11.5247	-23.2216	14.4463	-0.0064	0.0000
-0.0016	-0.0252	0.0032	0.0014	0.00143	-0.0002	0.0020	0.0022	11.4351	-26.3319	17.7526	0.0031
-0.0023	-0.0175	0.0013	-0.0001	-0.0004	-0.0006	0.0007	-0.0007	-0.0012	11.3371	-29.5507	16.0096
-0.0002	-0.0001	0.0000	0.0000	0.000	0.0000	0.0000	0.0000	0.0000	0.0000	0.1760	-0.3173

Table 5.2d Operating conditions of the column simulator at point of linearistion

Linearised state variable model LM1

xf=0.4 mass fraction, Lr = 165 g/min (6.6 l/hr) , F = 200 g/min, reflux ratio = 2.2, 56778.0 j.min (0.9463 KW), xd = 0.987 mass fraction, xb = 0.0502 mass fraction, efficien trays = 90%

Linearised state variable model LM2

Operating condition obtained by driving the column simulator to a steady state with top tray composition control 0.85 mass fraction. xf = 0.4 mass fraction, Lr = 157 g/min (6.6 l/hr) , F = 200 g/min, Qrb = 56778.0 joules/min (0.9463 KW), xd = 0.942 mass fraction, xb = 0.025 mass fraction, efficiency of trays = 90%

5.5 Steady state simulations

5.5.1 Results and Discussions

In all the steady state simulations the same initial composition estimates were used. These initial values were obtained from rough calculations using the McCabe and Thiele procedure. Table 5.3 gives details of the simulation experiment performed as well as the initial composition profile used to initialise the steady state algorithm and the final solutions. Figure 5.4a shows the trajectory of the convergence criteria, Jcv, for ε chosen as $9. \times 10^{-4}$.

Some other simulations were performed to examine the effects of tray efficiencies less than 100% and the frequency of computing the jacobian on the convergence properties of the algorithm. In these simulations, the following were specified; F = 165 g/min, Lr = 188 g/min, $Lr/L_d = 2.2$, xf = 0.47 mass fraction, feed temperature, Tf = 25 °C, $\varepsilon = 1. \times 10^{-5}$ and reflux temperature, Tlr = 55°C. Figure 5.4b shows that the rate of convergence is significantly affected by the efficiency values assumed.

Reducing the plate efficiencies from 100% to 90% efficiency slightly affected the convergence of the steady state model. The convergence rate using 90% efficiency of each plate improved slightly after 6 iterations. Reducing the frequency at which the jacobian is computed from every iteration to every 4 iterations degraded convergence of the steady state model. There was a "delay" in when the rapid convergence to the solution began.

The results of the simulation procedure verified that the simulation procedure is satisfactory to simulate the binary distillation system at steady state. The next stage was to explore the accuracy of the converged solution, relative to the dynamic model. This is treated in the next section.

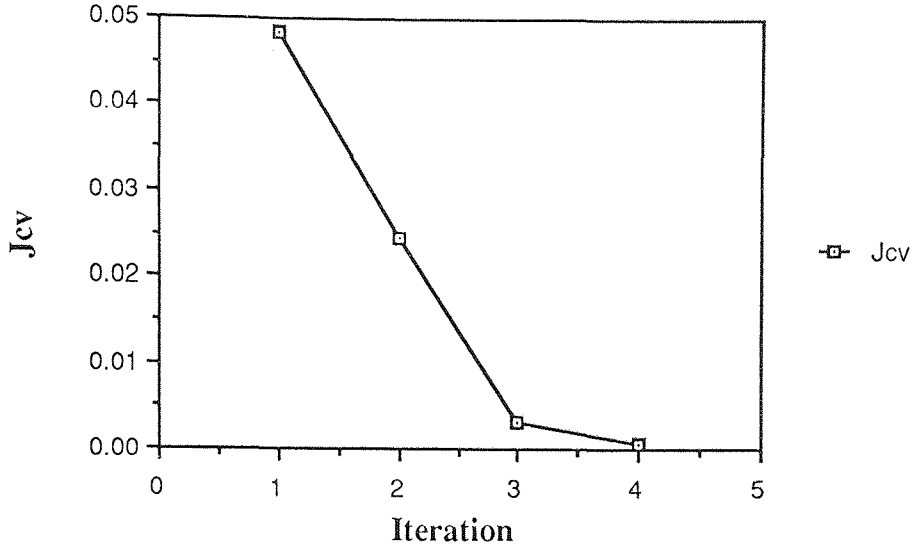

a) Corresponding result used to initialise dynamic model

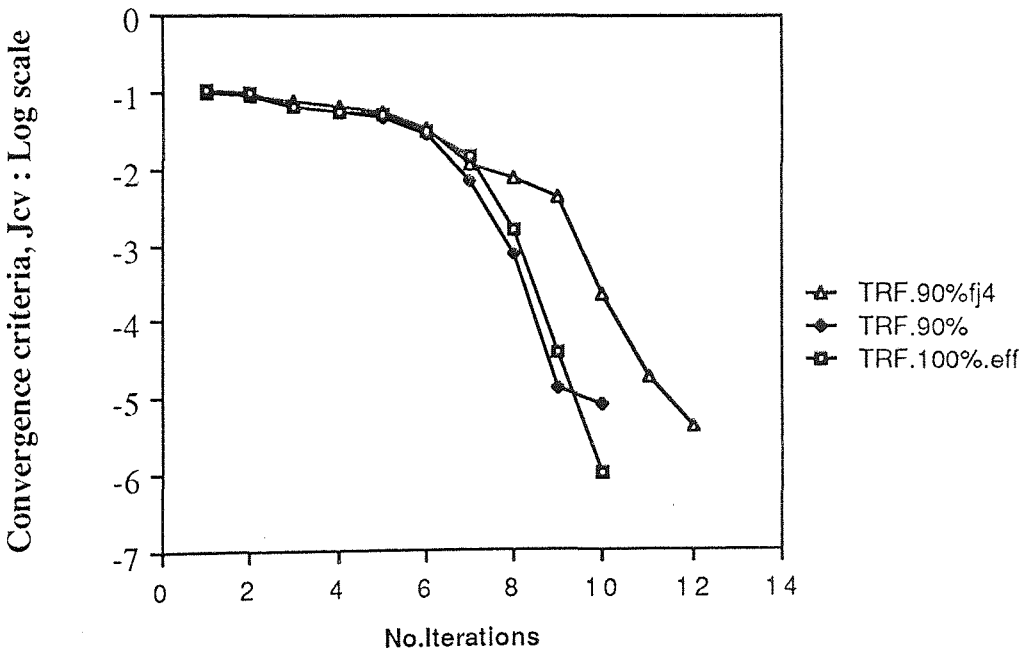

b) Effect of frequency (f_J) of jacobian computation and efficiency on convergence of the steady state model

Figure 5.4 Convergence criteria trajectories of the steady state simulations

5.6 Dynamic simulation

In this research work the single step Euler method was used to integrate the differential equations of the column simulator and adequate results were obtained. The integration step size of 0.025 minute gave adequate results. The running times of the column simulator on the System96 is also very high. With the integration interval of 0.025 minutes, the ratio of computer time to process time is about 5.5 to 1. This means 5.5 minutes of computer time is required to simulate 1 minute of process time. On the IBM PC AT this ratio significantly reduces to 0.5 to 1 for integration interval of 0.025. This gave an idea of the speed of the System96 computer compared with that of the IBM PC AT.

5.6.1 Results and Discussions

For the simulated step response studies, the feed and the reflux streams were assumed to enter the column as saturated liquids at their bubble points. The reboiler and reflux drum levels were controlled by conventional PI method. The distillate rate was used to regulate the reflux drum liquid level and the bottoms offtake rate was used to regulate the reboiler liquid level. The same settings were used for both level controllers; the proportional gain used was 30 (g/min)/cm and integral time of 3.0 minutes.

The column simulator was initialised with the results of the steady state model of which Table 5.3 correspond. The sampling interval used was 0.5 minutes. The tray temperatures moved to new points as shown in Figure 5.6 which compares the original temperature profile of the column with the new or "refined" profile. Figure 5.5 shows the corresponding response for the top and bottom tray temperatures. These graphs demonstrate that the refinement of the initial values was not very much, indicating the accuracy of the steady state predictions, relative to the dynamic model. The shift of the steady state profile of the column can be mainly attributed to a difference in the assumptions in the dynamic and steady state model. This is the assumption of 100%

Table 5.3 Details of a steady state simulation

Tray	Initial	Final	
	Composition	Composition	Temperature
Reflux	0.90	0.967289	87.26
1	0.7594	0.921198	88.08
2	0.7394	0.848688	89.44
3	0.7067	0.745829	91.55
4	0.6563	0.621191	94.44
5	0.5861	0.498221	97.82
6	0.50	0.398310	101.01
7	0.413	0.333808	103.35
8	0.349	0.257999	106.43
9	0.2615	0.178680	110.11
10	0.168	0.109078	113.79
Reboiler	0.09	0.059627	116.71

F = 200g/min (8 l/hr), Lr = 165g/min (6.6 l/hr), Lr/L_d = 2.2, xf = 0.4 mass fraction, Feed and reflux enter column as saturated liquids, efficiency 90%, jacobian **J** computed every 4 iterations, ε = 0.0009, Number of iterations to reach convergence = 4

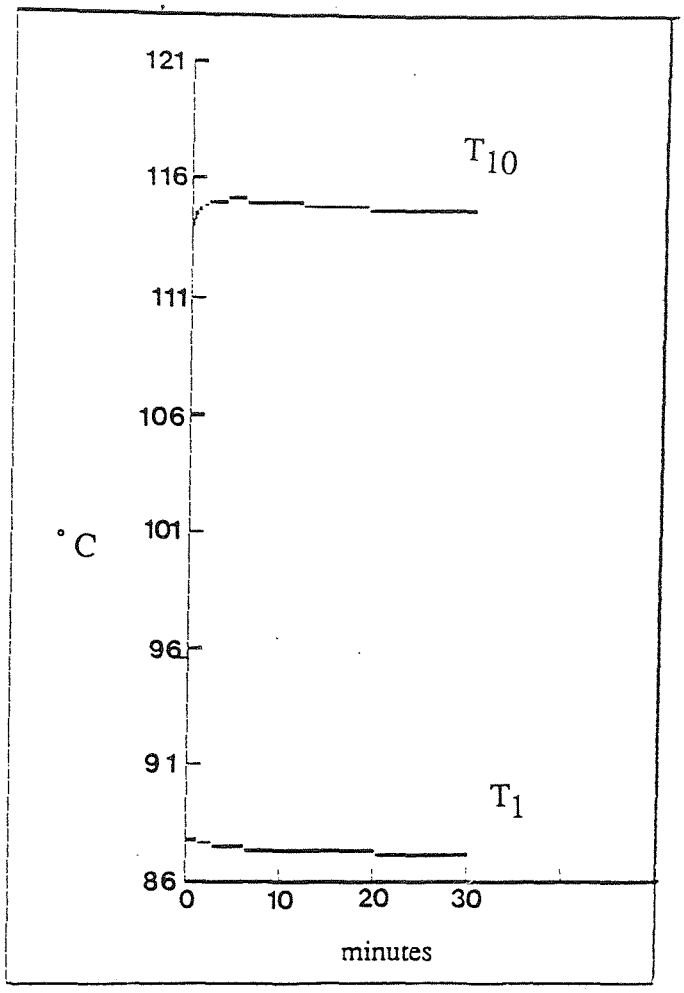

Figure 5.5 Refinement of the initial steady state: Top tray and bottom tray temperatures

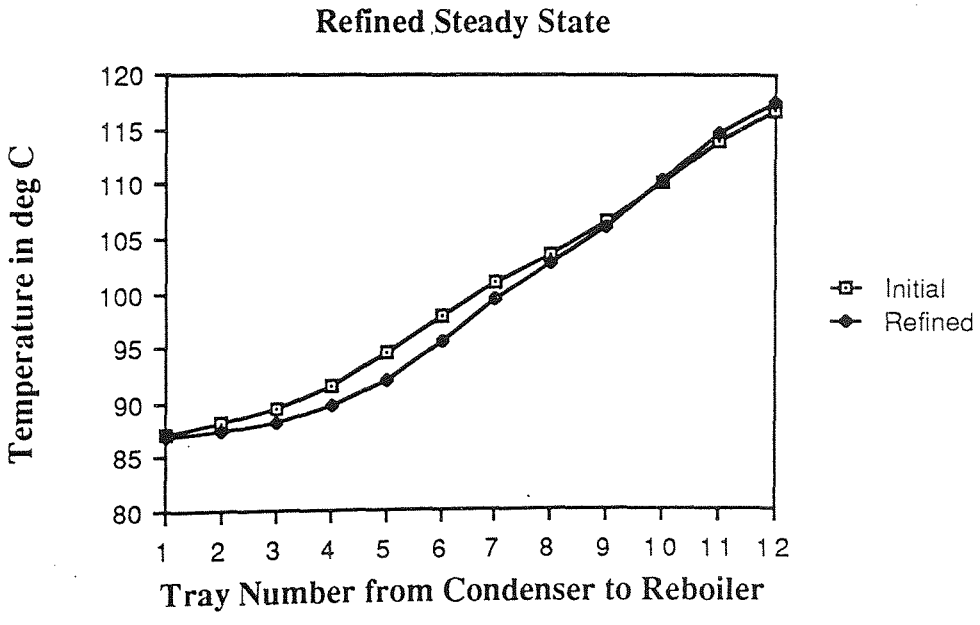

Figure 5.6 Refinement of steady state: Shift of the temperature profile of the column

efficiency in the reboiler in the steady state model and 90% in the dynamic model. The "refined" steady state values were used as initial values for the column simulator.

A series of step response tests were carried out by introducing 15 % step increases and step decreases in the feed flow, feed composition, reflux flow and reboiler heat input denoted F, xf, Lr and Qrb, respectively. Each input has significant effects on all the tray temperatures. The dynamic behaviour of the tray temperatures of the distillation column is dominated by first order responses for all the step input changes, except the response of T_1 to the step increase in Lr. Figures 5.7a and 5.7b show this for the top and bottom tray temperatures, T_1 and T_{10}, for step inputs in Qrb, Lr and F.

Table 5.4 shows the steady state gains and approximate time constants relating each input to the outputs T_1 and T_{10} for the +15% and -15% step changes in the inputs. The significant differences in the steady state gains and the time constants for positive and negative step changes in the inputs indicate the non-linearities in the distillation column. This behaviour is more pronounced for the (Lr, T_1), (Qrb, T_1) and (xf, T_1) combinations. The results indicate the assymetric behaviour of the column (Coppus et al. (25), Stathaki et al. (112)).

The implications of this pronounced non-linear behaviour of the column has been discussed in Chapter 2 Section 2.2.6. The significant non linear behaviour of the column indicates a high degree of illconditioning of the distillation system and sensitivity to model errors under closed loop control. This is because the initial steady state is reasonably close to the maximum of 100% purity; 97%w/w top product quality as indicated on Table 5.3. High purity columns are difficult to control because they can be very sensitive to model errors (Skogestad and Morari (153)).

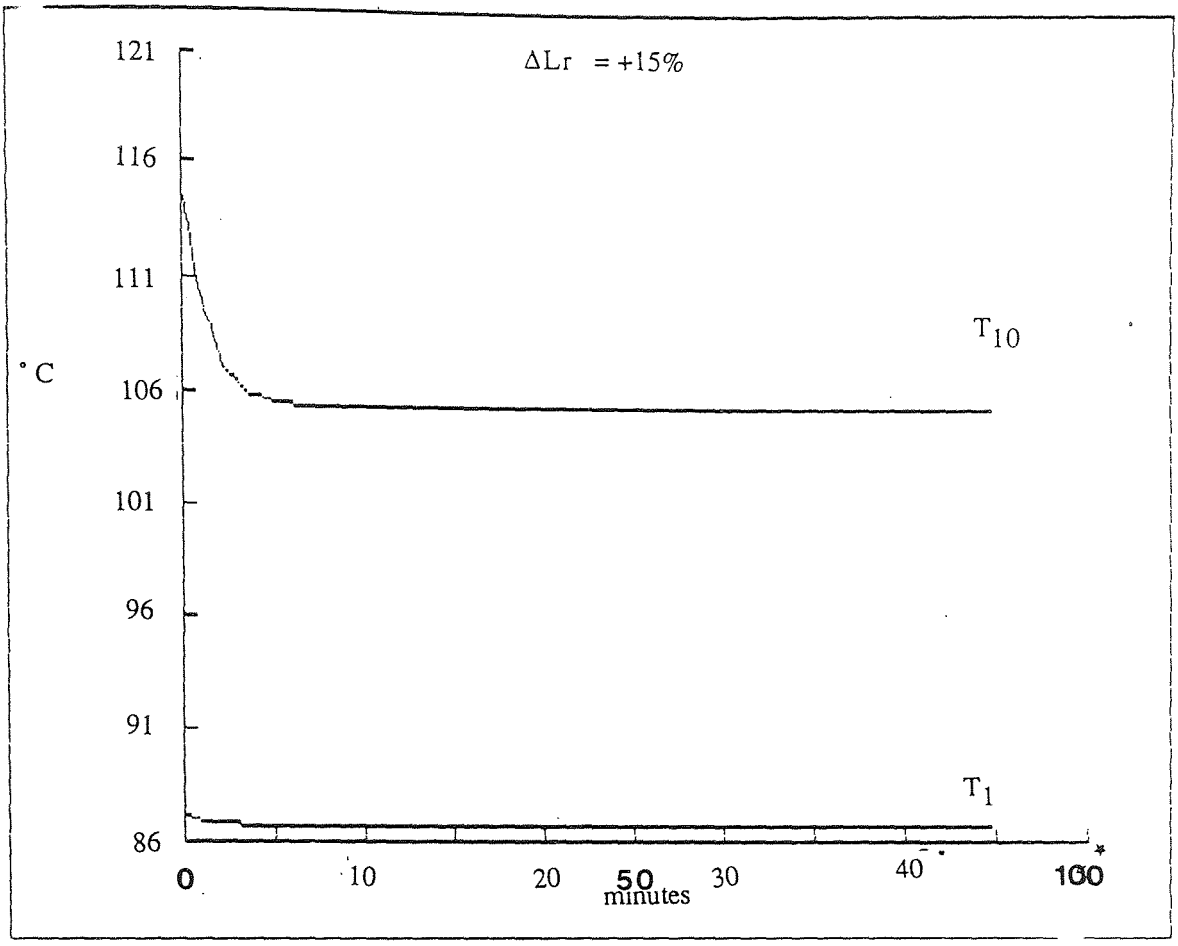

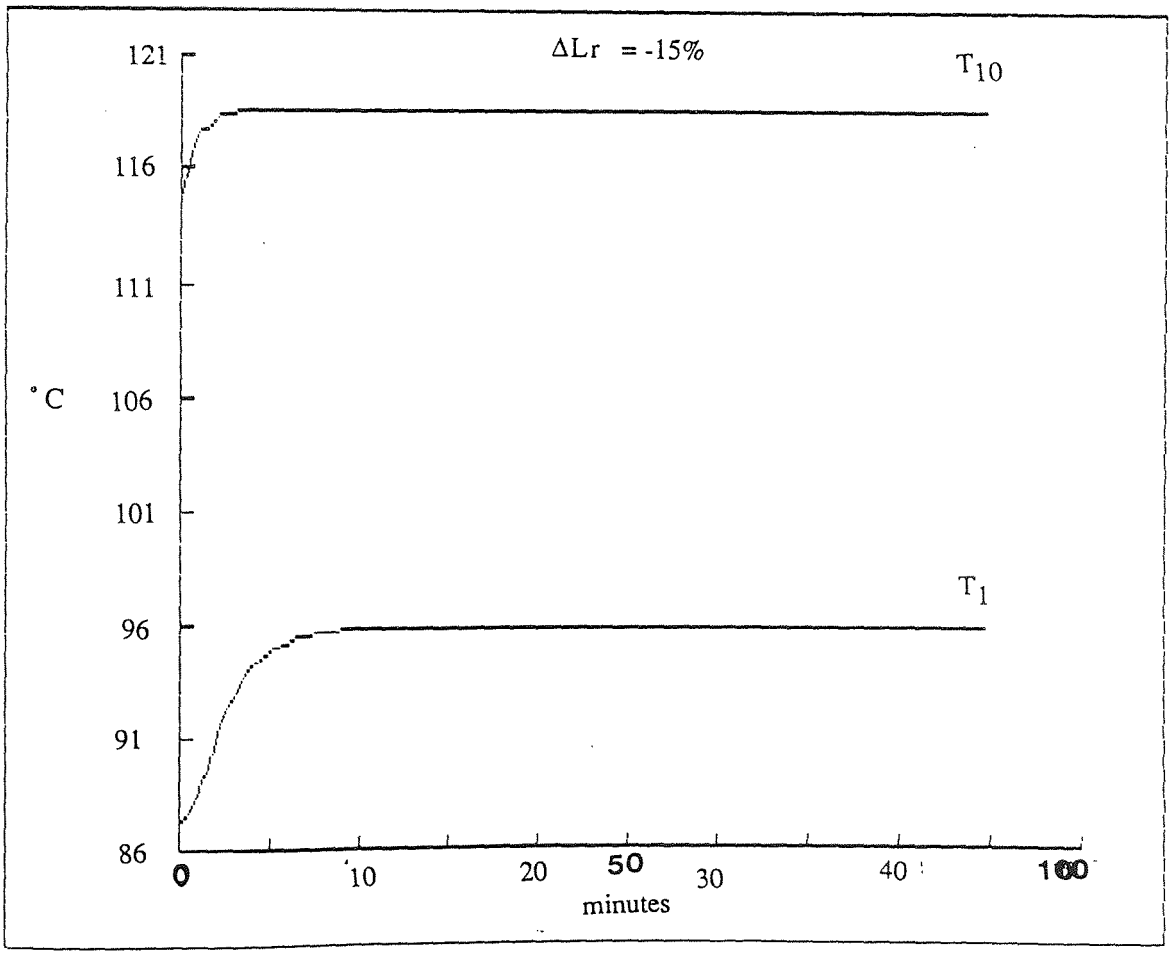

Figure 5.7a Simulated open loop responses of the column simulator :
Responses of top and bottom tray temperatures to reflux flow changes

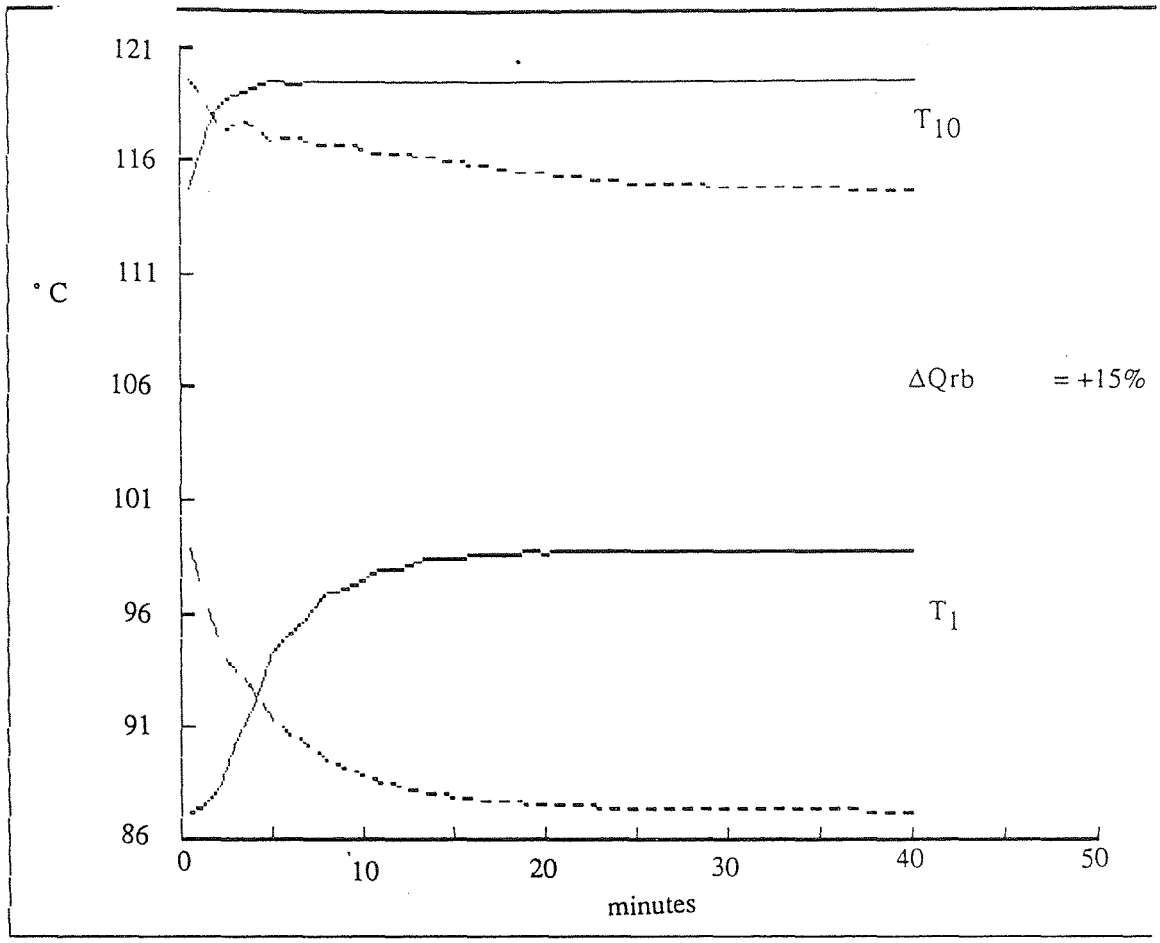

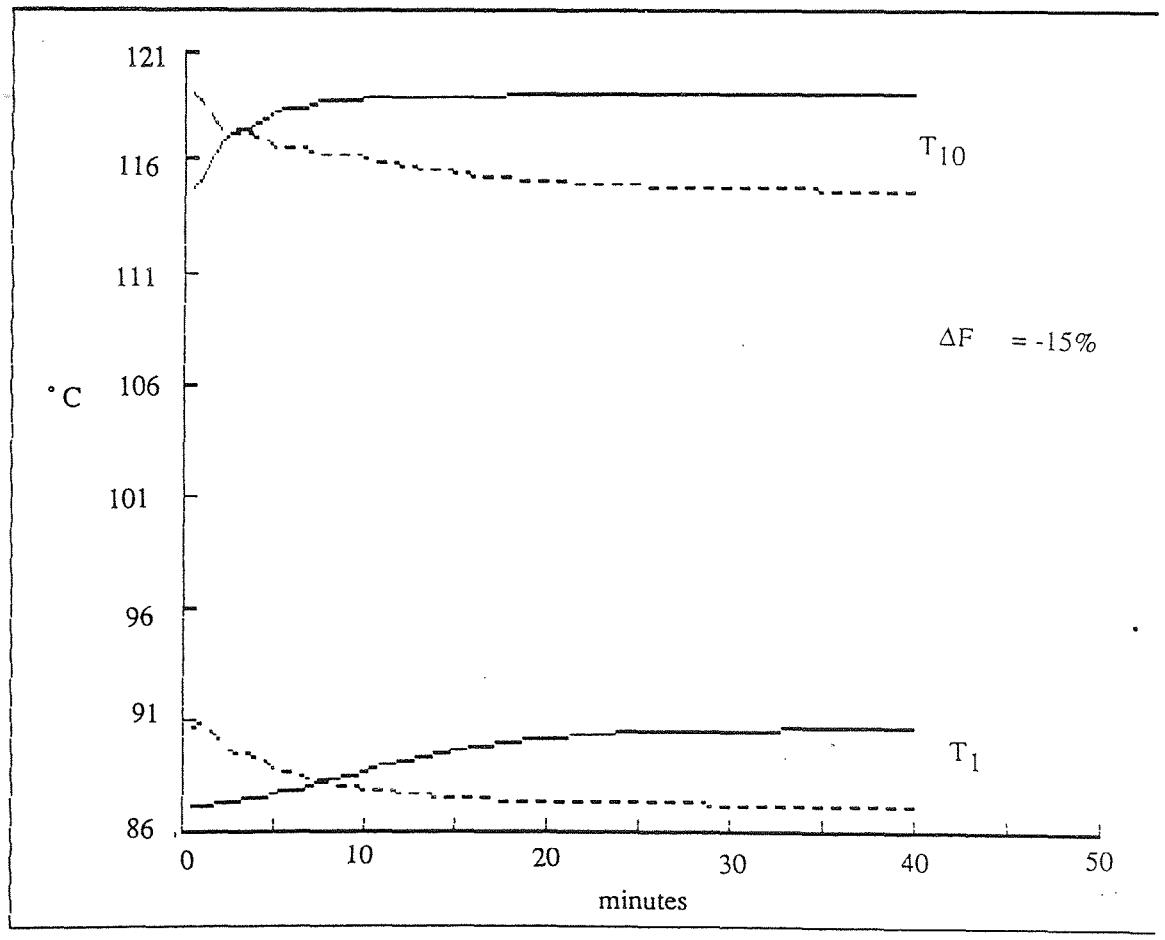

Figure 5.7b Simulated open loop responses of the column simulator : Responses of top and bottom tray temperatures to reboiler heat input and feed flow changes

Table 5.4 Open loop gains and time constants of the column simulator

Step Change	Top Tray Temperature (T_1)		Bottom Tray Temperature (T_{10})	
15%	Kp	τ	Kp	τ
↑ Lr	-0.5	1.92	-9.53	2.96
↓Lr	-8.67	5.59	-3.89	1.43
↑ Qrb	81.01	4.59	33.99	1.02
↓Qrb	3.56	1.18	80.77	2.17
↑ F	-0.16	3.30	-3.71	2.28
↓F	-2.86	16.17	-3.53	2.26
↑ xf	-5.29	4.36	-91.97	4.57
↓xf	-49.92	14.9	-59.1	3.13

Kp = Gain, τ = time constant in minutes

*** For the units of the gains Lr and F are in l/hr, Qrb in KW, xf in mass fraction T_1 and T10 in °C The arrows indicate the direction of the step change: The reboiler and reflux drum holdups were $\mathbf{M}_b$ = 2472.0g $\mathbf{M}_d$ = 2211.0 g, $\mathbf{M}_j$ = 28.0g in enriching section j = 1 to 6, **M**j = 32.0 g in stripping section j = 7 to 10, where j denotes trays from top tray to bottom tray.

5.7 Open loop experiments on the pilot plant distillation column

Experiments were performed on the pilot scale distillation column to study its dynamic behaviour to step changes in the inputs. The start up procedure for the experimental column is outlined in Appendix A1. After the column has reached steady state, step changes in the feed flow, reflux flow and reboiler heat input (Qrb) were made. The computer program **Log-new** described in Appendix A1.1.3 was used for the data logging, data conversion and storage of information on the floppy disk. The sampling interval of 0.5 minutes was used. The tray temperature measurements taken were T_1, T_2, T_7, T_9,T_{10}, T_b. These are the vapour temperatures above the liquid on the top, second, feed, ninth, bottom trays and the reboiler drums, respectively.

5.7.1 Results and Discussion

Figure 5.8 and Figure 5.9 show the results of two step response experiments. The feed composition for these two runs are 41% trichloroethylene and 47% trichloroethylene, respectively. The figures show drifts in the feed flow and the oscillatory behaviour of reflux flow. The oscillations were more severe at low flow rates where the fixed reflux valve opening was small. One reason for this oscillatory behaviour was pressure variations in the upstream side of the reflux valve due to the pump operation. Feed flow measurements were usually not oscillatory because gravity flow was employed to deliver feed into the column; the drifts occurred due to the variations in the liquid head in the feed tank .

Figure 5.9 represents a result of the experimental open loop step response. The responses of the tray temperatures to changes in F, Lr and Qrb can be assumed to be approximately first order. The response of the top two tray temperatures, T_1 and T_2, to feed flow change were delayed by about three sample intervals (1.5 minutes). This was because the effects of a change in feed flow first have first to travel down the column to the reboiler and then back up the column. The reboiler holdup is significantly larger than tray holdups and this introduced significant lag in the responses of the trays temperatures in the enriching section to feed flow changes. By contrast, the effect of reflux flow change and reboiler heat input is felt on all the trays

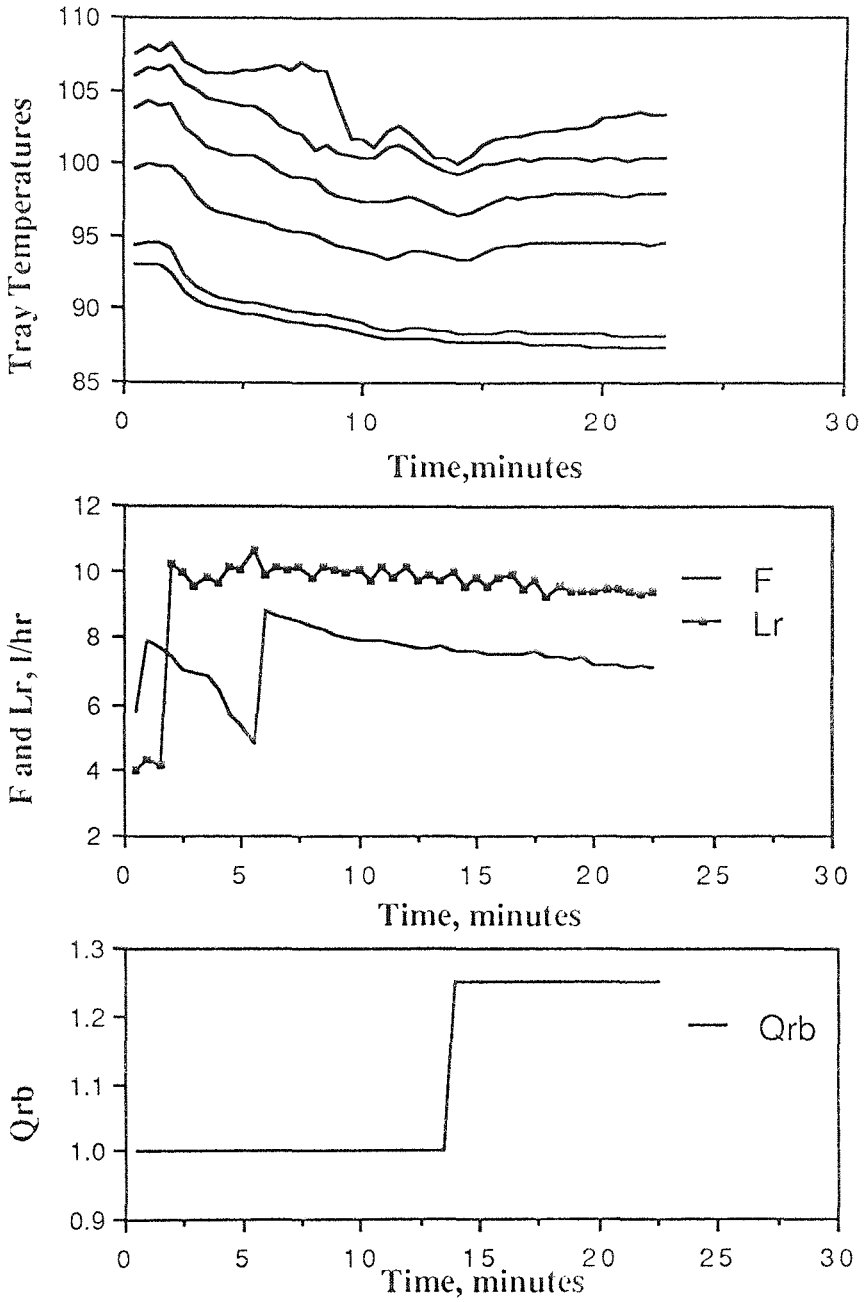

Figure 5.8 Open Loop Experiment No 1.

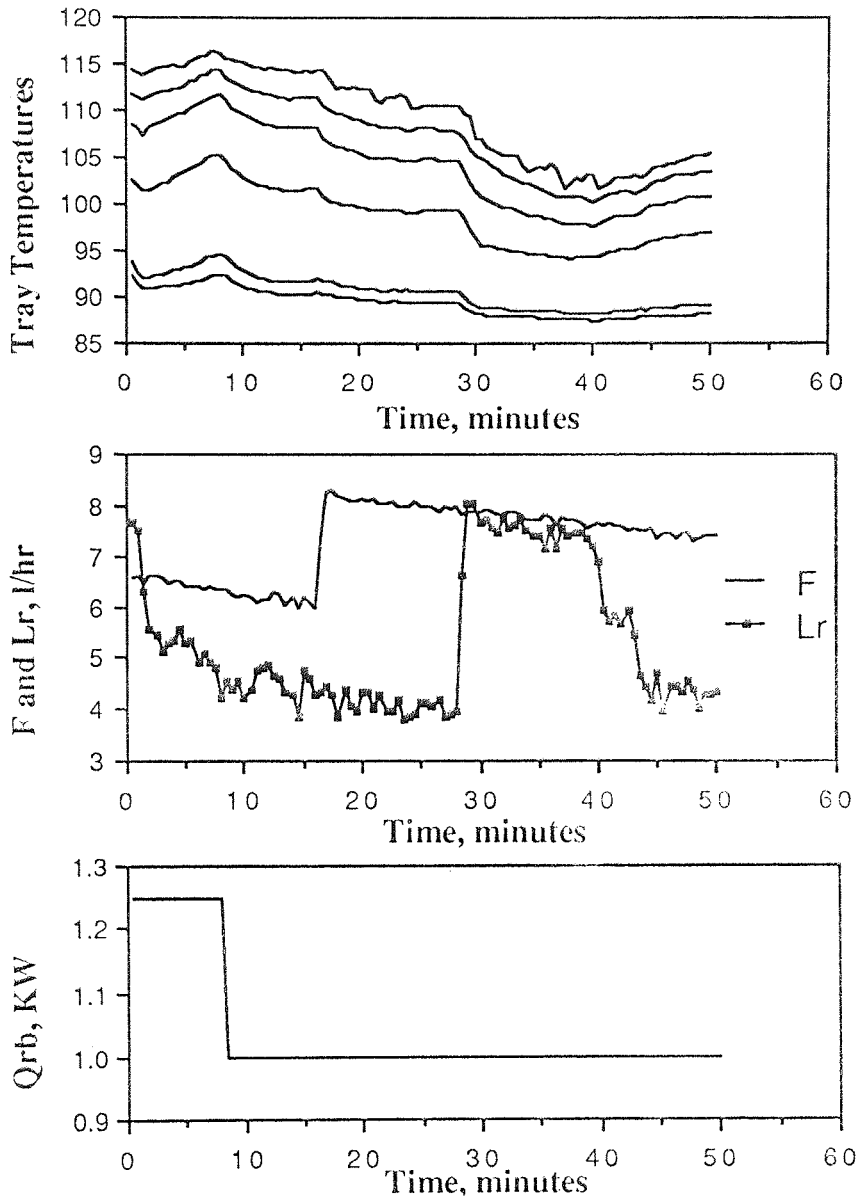

Figure 5.9 Open Loop Experiment No 2

within a sampling interval. The responses of the tray temperatures to reboiler heat input change were close to first order response.

As mentioned in Chapter 4, the operational problems of the column prevented effective PI control of the reboiler drum and reflux drum liquid level. This made it necessary to allow the reflux drum level to vary by withdrawing constant distillate flow, and using two position control to control the reboiler drum liquid level. Figures 5.10 show the trajectories of the drum levels during the open loop experiment represented by Figure 5.9.

Figure 5.9 shows the response of the temperature of the vapour above the liquid in the reboiler drum, T_b, was affected by effects other than the dominant responses to the input changes. The T_{10} did not exhibit oscillatory response since the corresponding tray, tray 10, is two tray spacings from the vapour entry point so that the disturbances causing the oscillations in T_b are dampened out by the liquid holdup on the tray.

5.8 Model verifications

5.8.1 The column simulator vs the pilot plant

The response of the column simulator to step changes in the feed flow reflux flow and reboiler heat input was examined using experimental data. As composition analysers were not installed on the column, model-plant comparisons could be conveniently done only by comparing tray temperatures. This experiment will compare the actual distillation column response to throughput changes with the model prediction. The model should then predict the columns response to feed composition changes with comparable accuracy.

To test the validity of the column simulator, the procedure given below was followed:

(1) Real plant measurements from the open loop experiments were obtained and stored in a floppy disk.

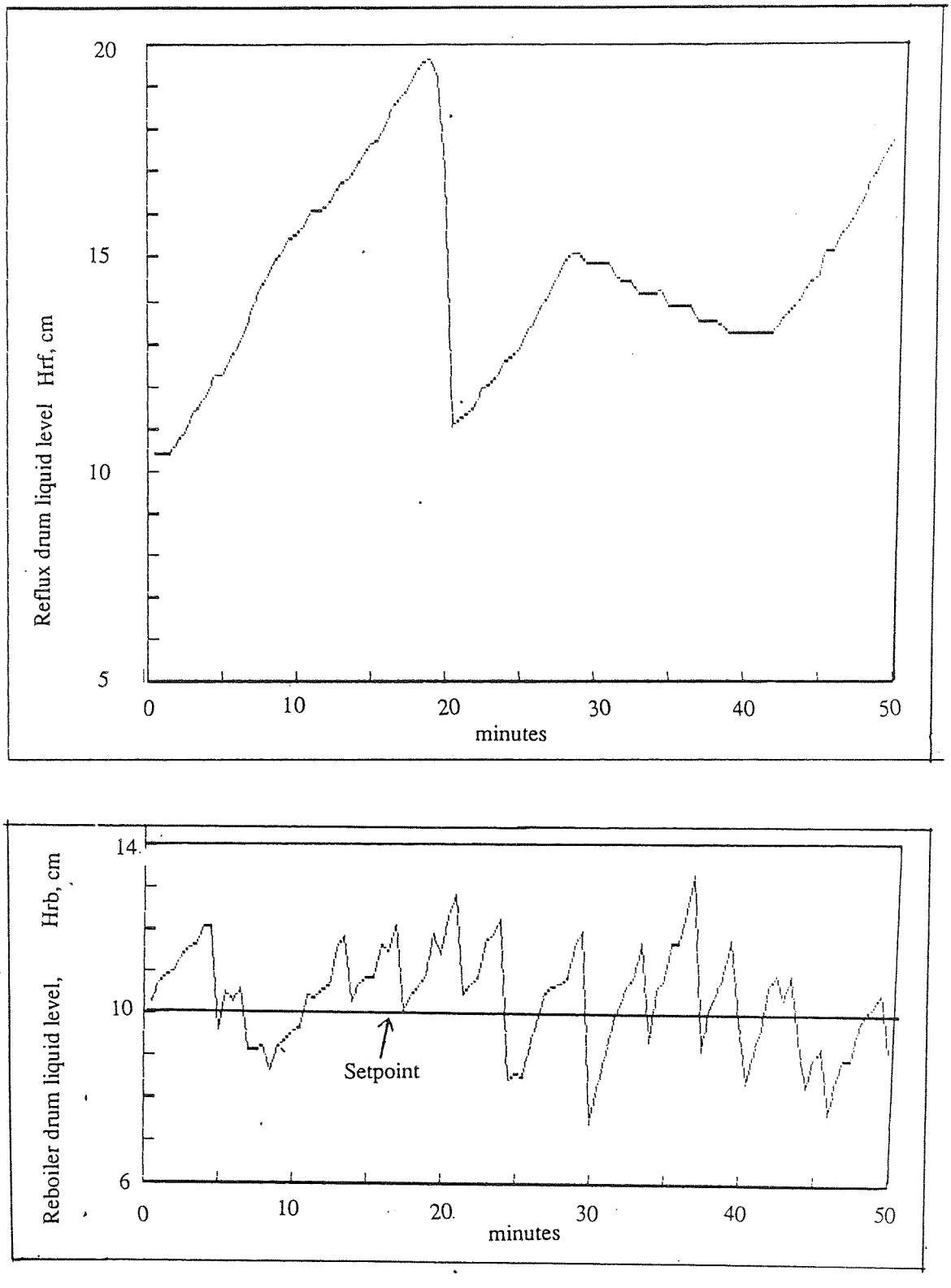

Figure 5.10 Trajectories of the liquid levels in the reboiler and reflux drums : Reboiler liquid level under two position control

(2) Initial values of feed flow reflux flow, reboiler heat input, feed composition, feed temperature and the reflux temperature were supplied to the column simulator and the simulator then allowed to reach steady state.

(3) The simulator was then used to simulate the plant using, at every sampling interval, the measured values of the inputs, F, Lr, and Qrb, which were fed as inputs to the column simulator.

The following adjustments were made to obtain consistent data. The feed temperature was at measured room temperature which was usually between 19 °C and 22 °C. The reflux temperature was assumed to be constant at 55 °C in the column simulator and the column pressure was assumed to be 760 mmHg. The reboiler holdup in the model was assumed to be 0.5 litres to be of the order of the amount of liquid heated up in the heater arm of the thermosyphon reboiler; the reflux drum holdup was also assumed to be 0.5 litres. During the model verifications, the reflux and reboiler drum levels could be controlled by PI controllers or assumed constant (perfect level control). In the latter approach, the distillate and bottoms product rates are calculated by total mass balance around the column at every sampling interval. The mass balance option was used in the verification exercises. Since the holdups in the reflux and reboiler drums were considerably larger than that of a tray the assumption of perfect level in the control simulator is not unrealistic, although there were practical problems with this on the plant.

5.8.2 Results and Discussion

Exercise Number One

In this exercise the data obtained from the experimental open loop response test shown in Figure 5.8 was used. Figure 5.11 show the predicted tray temperature responses compared with actual experimental data. Figure 5.12 shows the predicted initial and final steady state tray temperatures compared with experimental data. The initial steady state predictions of the first and second tray temperatures were reasonably close to experimental data, but were worse in the stripping section. However, the final steady state predictions in the stripping section were better. This

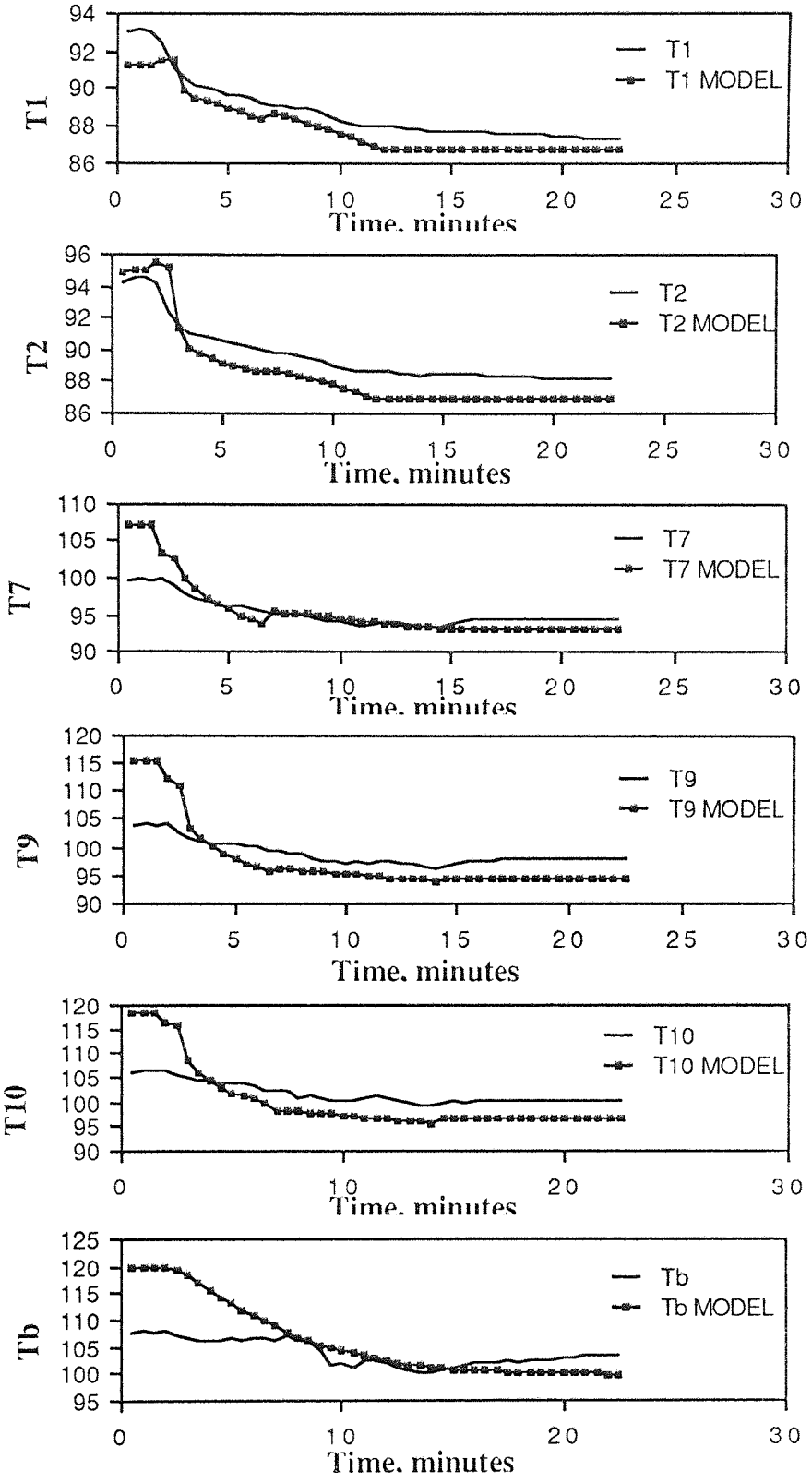

Figure 5.11 Model Verification No 1.

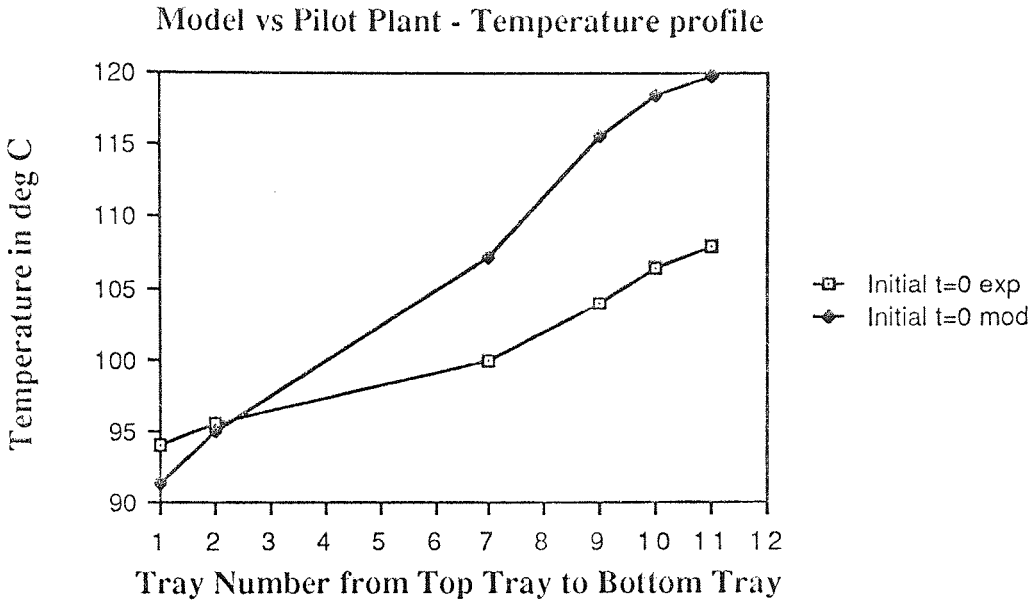

(a) Initial steady state temperature profile

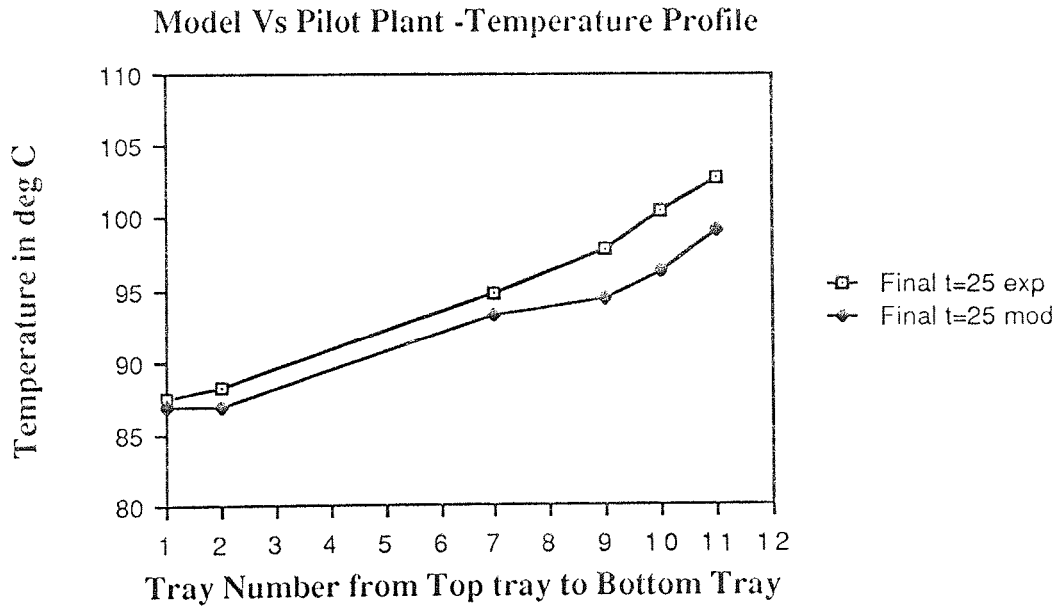

(b) Final steady state temperature profile

Figure 5.12 Steady state temperature profiles of the column, Model vs Column

means that, for the initial operating condition, the column simulator does not satisfactorily represent the steady state at stripping section of the column. This demonstrated that uncertainties in the column simulator varies significantly with operating conditions and varies at different locations along the length of the column.

Figures 5.11 shows that the column simulator responded to the data supplied to it at every sampling interval. For example, the kick in each of the predicted tray temperatures was in response to the kick in the feed flow at about t = 5 minutes. The graphs also demonstrated that the column simulator exaggerates the dynamic response of the actual column as the gains are much larger in the column simulator.

Exercise Number Two

In this exercise the results of the experimental open loop response test shown in Figure 5.9 was used. Figure 5.13 show the predicted tray temperature responses compared with the experimental responses. The column simulator predictions to the large changes in the feed flow, reflux flow and reboiler heat input were in the same directions as the actual column responses. There were also large errors in the initial steady state predictions.

The column simulator also exaggerated the response of the column, particularly the response to the large step increase in the reflux flow at about t = 27 minutes. The column simulator predicted a smooth profile of T_b since the thermosyphon reboiler arrangement on the actual column was modelled as a simple mixing tank in which only vapourisation of liquid was only taking place.

The exaggeration of the actual column response as regards the speed of response and the larger gains can be attributed to two main assumptions made in the model during the model verification exercises. The first is the assumption of adiabatic condition in the column which is not strictly true since heat losses were present. The second is the assumption that the reboiler holdup is 0.5 litres which is very small compared with the 1.5 litres holdup in the actual column.

The assumption which may have contributed significantly to the errors in the steady state predictions is the uncertainty in the reboiler heat input to the column. This

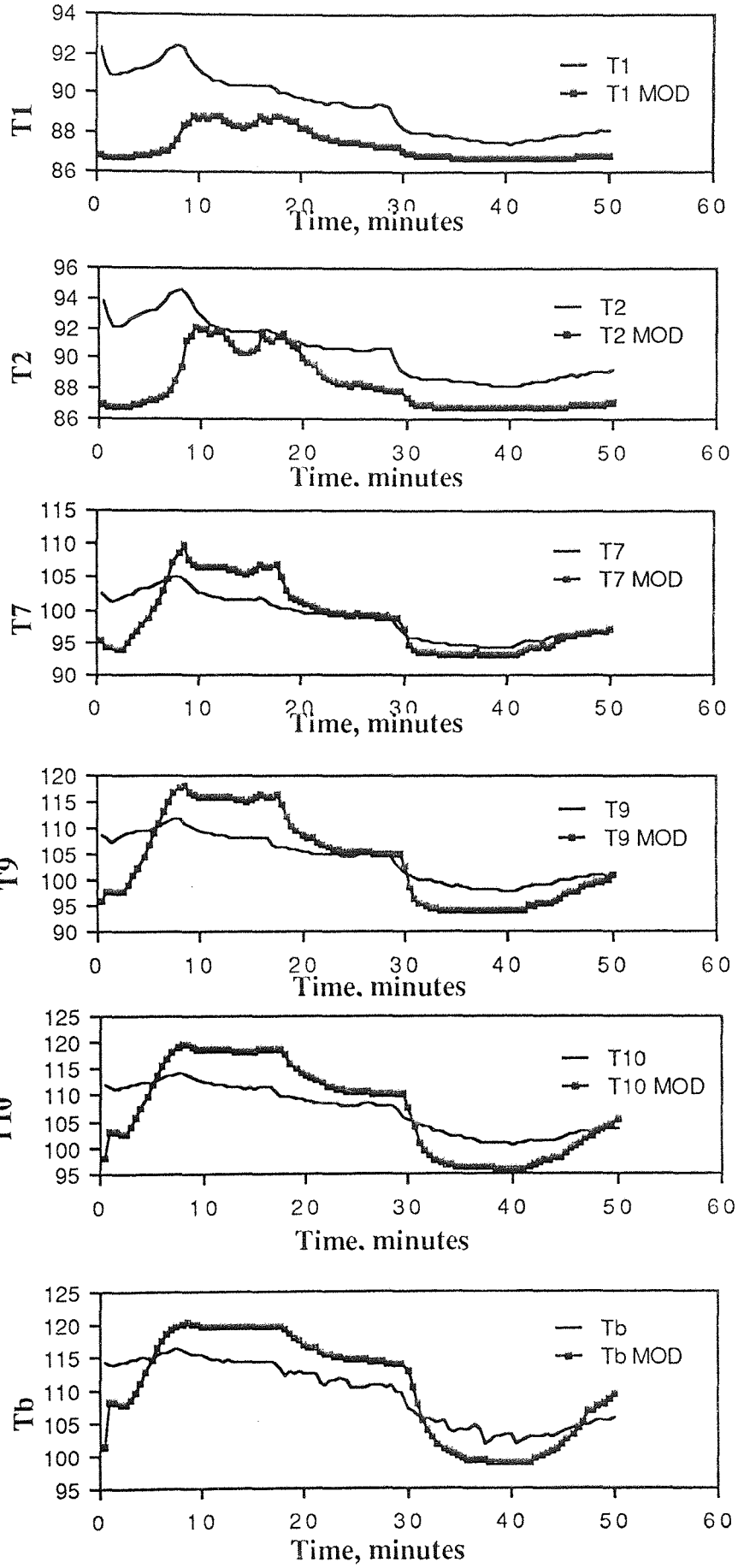

Figure 5.13 Model Verification No 2.

was assumed to be linear with the digital signal from the computer. This was a rough approximation which was made due to difficulty in accurately calibrating the heat input with computer signal when the reboiler was installed. The responses of the column simulator to heat input changes adequately describes the dynamic behaviour of the column and this demonstrated that the assumption is reasonable.

There is also a useful information that can be drawn from the model verification results. It concerns the uncertainties in the reflux flow and feed flow measurements that were supplied to the column simulator. Two results provide the information. They are

1) the kick in each of the tray temperatures in the column simulator due to the kick in the feed flow in Figure 5.11 and
2) the responses of the top tray and second tray temperatures to the reflux flow between t = 10 minutes and t = 20 minutes as shown in Figure 5.13.

The absence of these responses in the actual column suggested that either the model is insensitive to the input changes at that particular operating condition or that the variations in the measured values of the feed flow and reflux flow are due to imprecise measurements. In view of the responses of the column at other operating conditions it is unlikely that the case would be insensitivity to changes in input. The practical problems on the column, discussed earlier and in the previous chapter, suggested that the discrepancies between the model and the column in the regions mentioned above were primarily due to imprecise measurements of the reflux flow and the feed flow. The model was, in a sense, useful to detect faults in the operation of an instrument which in the cases under discussion are the flowmeters.

5.8.3 The linearised model vs the column simulator

Figure 5.14a shows the responses of the top and bottom tray compositions of the linear model compared with that of the column simulator for 15% step decrease in reflux flow. Although the direction of the responses are the same, the graph indicate clearly that the linearised state variable model is only valid in a very small range around the steady state linearisation point. This is more apparent in the response to the top tray composition as the responses of the bottom tray compositions of both models agree quite well. For a 15% step decrease in feed flow, both the top tray and the bottom tray compositions of the state variable model are relatively insensitive to the feed flow changes compared with the responses of the column simulator. This is shown in Figure 5.14b. These results in Figure 5.14a and 5.14b implies that the class of control systems that are designed using the state variable models will be put to severe test.

Before going into the discussion on the usefulness or limitation of the column simulator and the linearised state variable models some simple steady state analysis performed on the column simulator will be dealt with.

5.9 Steady state analysis using relative gain array and condition number

The discussions in Chapter 2 Sections 2.2, focussed on how to compute the steady state relative gains and the condition number of a system and the useful information that can be drawn from them regarding the likely problems that could be encountered in multivariable or multiple loop control of the variables of the system. In the case of the distillation column under study in this work the likely problems in the multiple loop are multivariable control of top and bottom tray temperatures of the column is addressed.

Using the relationships in Equations 2.2 and 2.21 in Chapter 2, the relative gain array and condition number of the column were computed. The steady gain matrices used were those obtained from the step response data obtained from the column simulator for the control configuration

Figure 5.14a Column simulator vs the state variable model : Responses of the top and bottom tray compositions to step change in reflux rate.

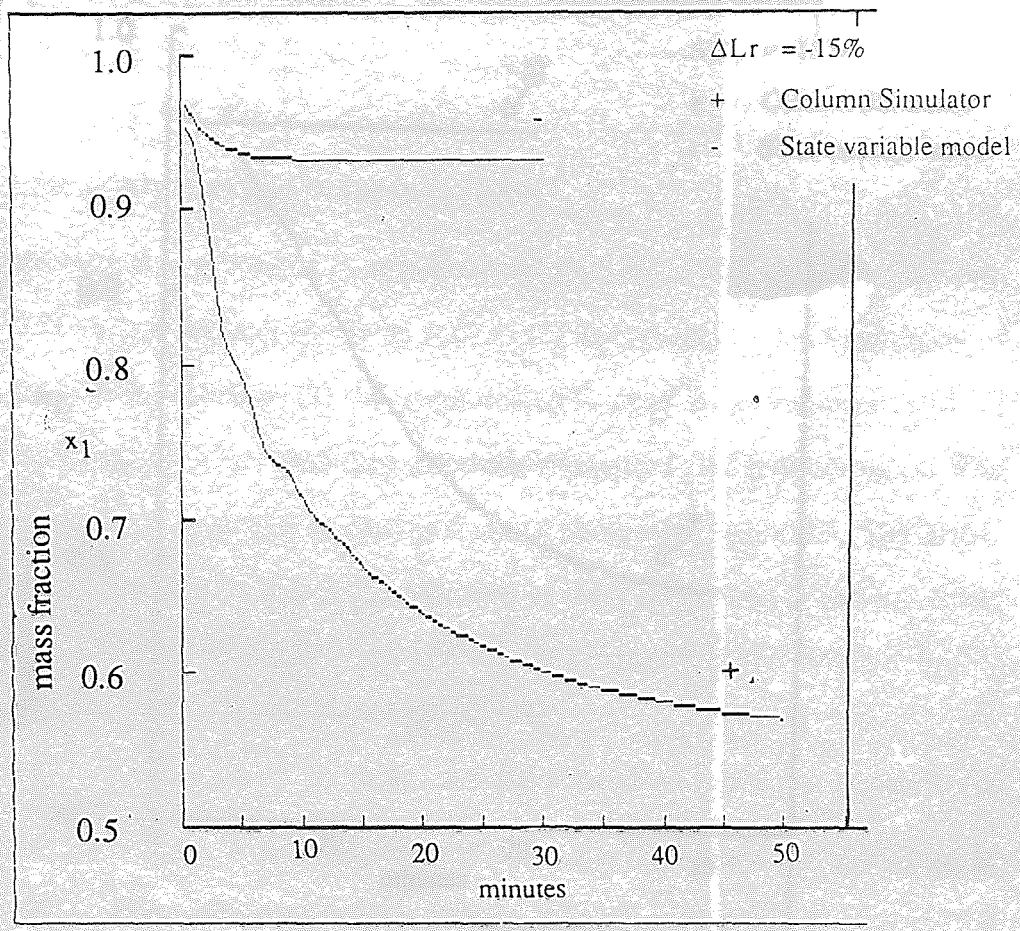

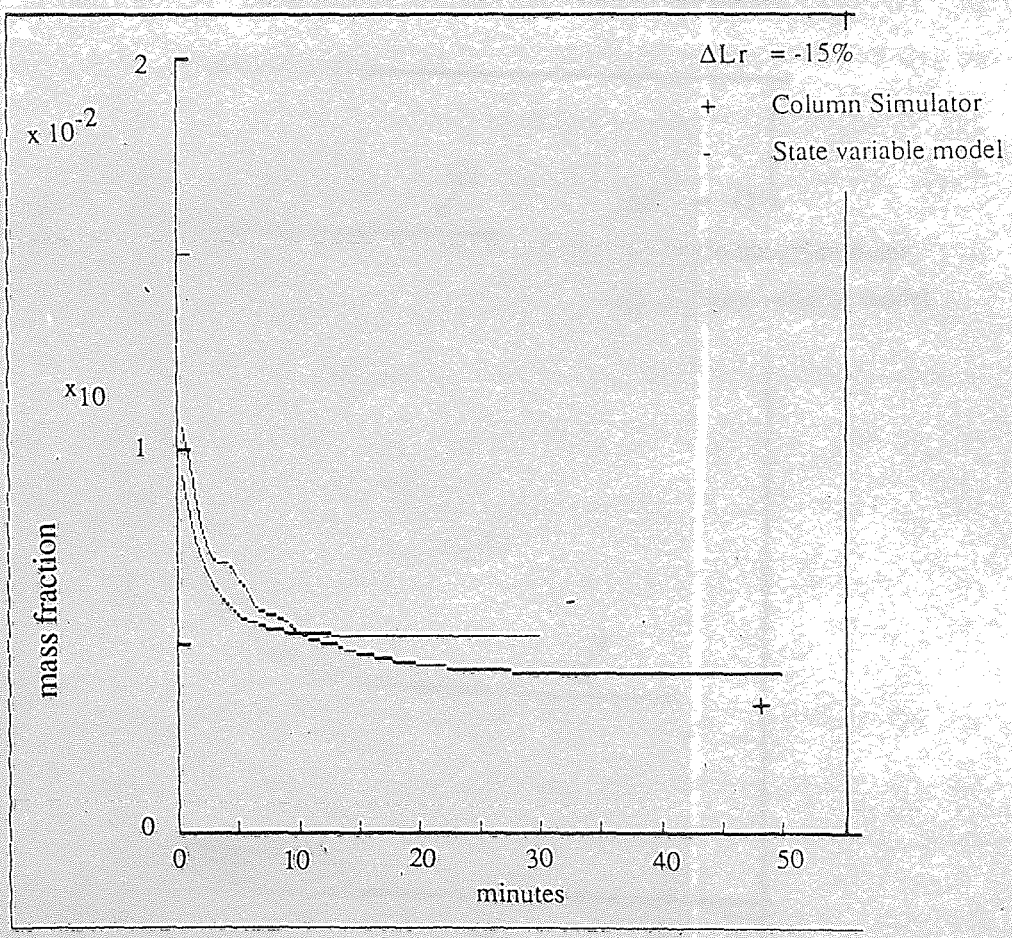

Figure 5.14b Column simulator vs state variable model : Responses of the top and bottom tray compositions to step change in feed flow rate.

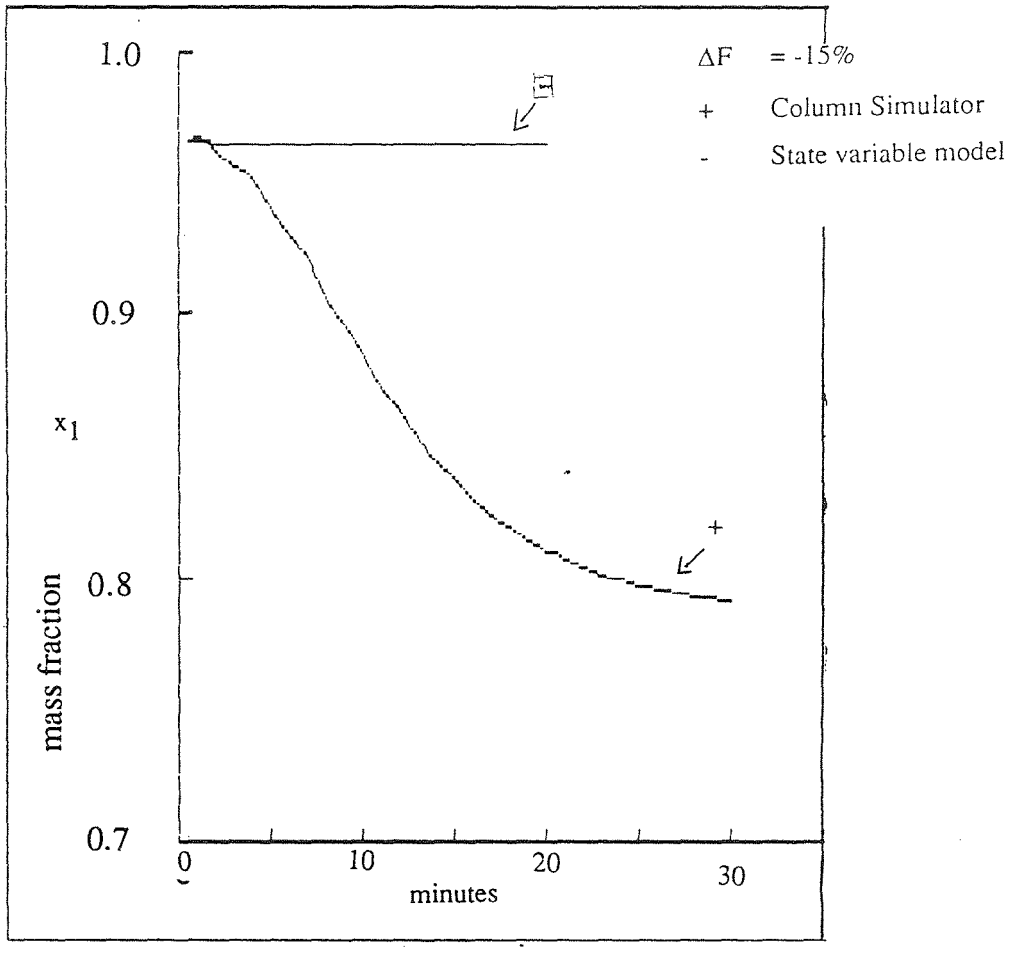

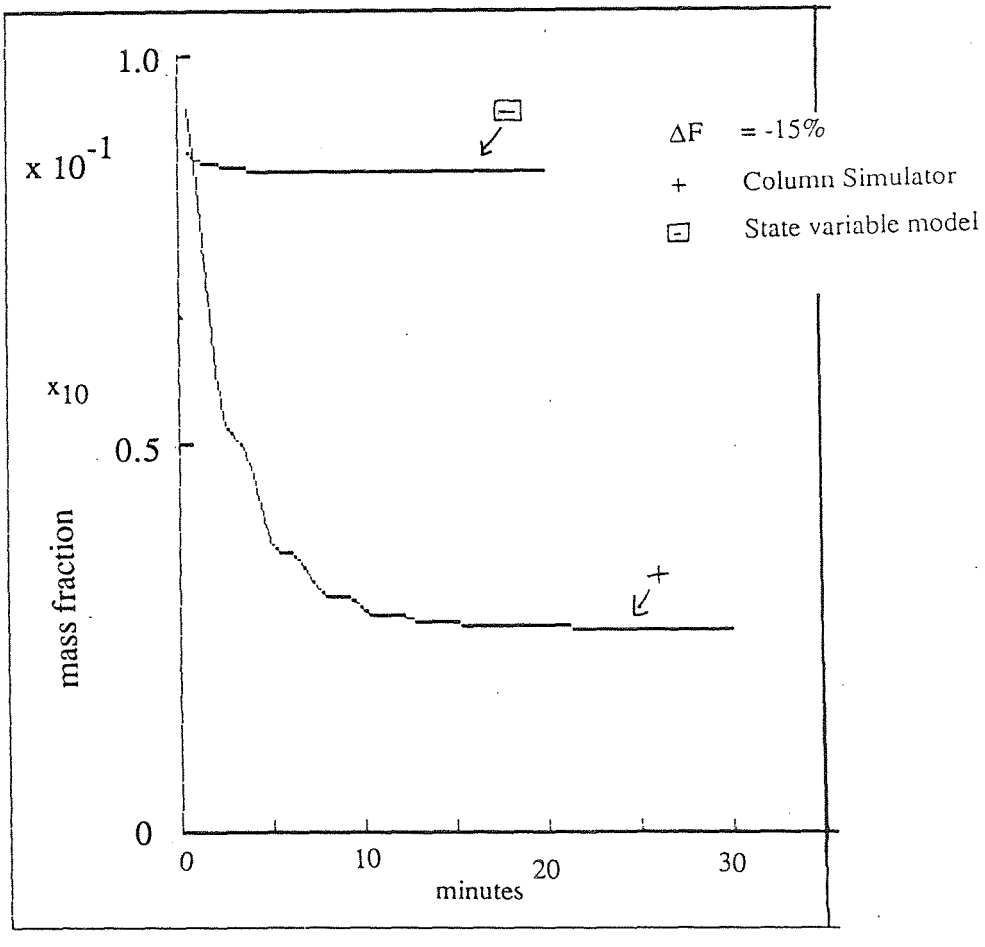

$$\mathbf{y} = Gp(0)\mathbf{u}$$

In this relationship $\mathbf{y} = (T_1, T_{10})^T$, $\mathbf{u} = (Lr, Qrb)^T$ and Gp(0) is given as

$$Gp(0) = \begin{bmatrix} g_{11} & g_{12} \\ g_{21} & g_{22} \end{bmatrix}$$

where g_{ij} is the steady state gain between $\mathbf{y}_i$ and $\mathbf{u}_j$

Simulated data was preferred to experimental data since the experimental step responses will include secondary effects such as (1) disturbances form the control of the liquid level in the reboiler, (2) the uncontrolled level in the reflux drum and (3) uncertainties in the reflux and feed flow measurements and in the reboiler input. The steady state gains are arranged in matrix form as shown on Table 5.5. The arrow beside each gain element indicates the direction of the step change in the input that resulted in the corresponding gain. The relative gain, π_{11}, condition number $\gamma_m(G)$ and the size of the $\| \Lambda \|_1$ are also shown on the table.

The $\| \Lambda \|_1$ and γ_m (G) are small for the gain matrices whose elements were obtained from step changes in Lr and Qrb in the same directions. As discussed in Chapter 2, this small $\| \Lambda \|_1$ and γ_m (G) suggest that the distillation system is well conditioned and the closed loop response of the distillation column will not be sensitive to model errors when using a multiple loop or a multivariable control system to control T_1 and T_{10} simultaneously. The $\|\Lambda\|_1$ and $\gamma_m(G)$ are, however, much larger for the other gain matrices with the input changes in opposite directions. The large $\|\Lambda\|_1$ show the strength of steady state interactions. Together with the large $\gamma_m(G)$, indicate that closed loop sensitivity problems may arise during multivariable or multiple loop control of T_1 and T_{10}. Furthermore, the large $\|\Lambda\|_1$ and $\gamma_m(G)$ predict that introducing decoupling in the simultaneous control of T_1 and T_{10} can make the system very sensitive to model errors (Skogestad and Morari (153, 119) and Morari (150)).

The values of the RGA elements for all the gain matrices differ so widely that it is difficult to draw any conclusions on the appropriate control loop pairing for the simultaneous control of T_1 and T_{10} using single loop controllers. In general, what the results predict is that sensitivity and interaction problems should be expected

particularly if control over a wide operating range is desired. In regulatory control over wide operating range is equivalent to controlling the column subject to large variations in the feedflow and feed composition entering the column. Multiple loop SISO controllers should thus be conservatively tuned when they are to be applied to control T_1 and T_{10}, simultaneously.

Table 5.5 The Relative Gain Array and the Condition Number of the column simulator

Plant matrix (Gp)	π_{11}	$\|\Lambda\|_1$	γ(Gp)
-8.67↓ 3.56↓ -3.88↓ 80.77↓	1.02	2.08	3.90
-0.5↑ 81.01↑ -9.53↑ 33.99↑	-0.0225	2.09	3.925
-8.67↓ 81.01↑ -3.88↓ 33.99↑	15.41	59.64	119.27
-0.5↑ 3.56↓ -9.53↑ 80.77↓	6.24	22.96	45.89

*** The arrows indicate the direction of the step change

y=Gp(0)**u**, **y**=(T_1,T_{10}), **u** = (Lr,Qrb), Gp(0) indicates the steady state gain matrix

*** For the units of the gains Lr and F are in l/hr, Qrb in KW, xf in mass fraction T_1 and T10 in °C

5.9.1 Selecting the manipulated and controlled variables of the distillation column

There a many options available to control the products of a distillation column. Numerous workers such as Skogestad and Morari (153), Desphande (168) and Shinskey (167, 142) have discussed the various methods that are used to control the products of distillation columns. In this work, interest is in the control of the products of a conventional binary distillation system which is the main theme of the work of Skogestad and Morari (153).

The schemes of distillation column product control are generally classified into material balance schemes and energy balance schemes (Desphande (168)). In a material balance scheme, a product rate (distillate or bottom product rate) is used to control the product composition in the case of single product composition control. For example, the distillate rate to control the distillate product composition or the bottoms product rate to control the bottoms product composition. In the dual composition control only one product rate can be the manipulated input as material balance around the column has to be satisfied. In energy balance schemes the reflux ratio and the vapour boilup from the reboiler are the manipulated inputs. Other options include using the ratio of the reflux and the distillate flow and the ratio of the vapour boilup and the bottoms offtake rates as manipulated inputs. Skogestad and Morari dealt with this in their work on the dual composition control of a binary distillation column. Some of his observations and suggestions have been discussed in Section 2.2.9.

Since composition analysers were not fitted on the distillation column used in this work, the top and bottom tray temperatures, T_1 and T_{10}, were selected as the controlled variables to indirectly control the product compositions.

The T_1 was chosen to indirectly control the top product composition since T_1 bears a direct relationship to the top product and because it is the closest to the top end of the column. The closer the temperature measurement location is to the top the smaller the error between the liquid composition on the top tray and the top product composition (Desphande (168)). For the control of the top product composition by

feedback manipulation of the reflux rate, moving the location of the measurement tray down the column decreases the critical frequency and the maximum controller gain that can be used because of the increasing number of hydraulic lags (Beaverstock and Hariot (10)). It is therefore better to choose the control plate as close to the top as possible. For similar reasons, the T_{10} was chosen to control the bottoms product composition. The T_{10} was preferred to the vapour temperature above the reboiler liquid level, T_b, because the former was not subject to oscillatory responses due to effects such as the two position control of the reboiler liquid level as shown in Figures 5.9a and 5.10.

For the control of T_1 only, the reflux flow, Lr, was the manipulated input. For the simultaneous control of T_1 and T_{10}, the Lr was paired with T_1 and reboiler heat input, Qrb, was paired with T_{10}. This configuration is equivalent to the dual composition control of the distillation column using the LV configuration, where L is the reflux which controls the top product and V is the vapour boilup controls the bottoms product composition. As discussed in Section 2.2.9, Skogestad and Morari (153) have demonstrated that the LV configuration provides fast initial response to setpoint and load disturbance changes.

5.10 General Discussions and Conclusions

The question to be addressed at this stage is whether the two models, the column simulator and the linearised state variable models, will be of any use in the design, analysis and the final screening of control systems that can be applied to the distillation column.

As regards the column simulator, the dynamic response of the actual column to step changes in the inputs was predicted adequately by the column simulator although many simplifying assumptions were made in building the model. However, the model verification results demonstrated that the column simulator exaggerates the speed of response and the gains of the actual column. This is considered useful from the perspective of controller design since if a controller performs well on the column simulator the controller should be expected to provide good control on the actual

column. A simple reason can be given. The proportional gain of a PI controller is proportional to the inverse of the process gain, as can be seen in the Cohen and Coon controller tuning equations in Appendix A2.2.1. Thus, it would be advantageous to use the larger gains of the column simulator to design PI controllers for the actual column as this would result in a PI controller that is not too tight (Table 5.6 shows corresponding PID controller settings using gains and time constants from Table 5.4). This means robustness is achieved to a certain degree.

Considering the conditions under which the controller will be operating, if adverse conditions are handled satisfactorily on the column simulator which exaggerates the responses of the column, the controller will be expected to handle similar adverse condition on the actual column which is slower and has smaller gains.

From these points of view, it is considered advantageous to use the column simulator as a substitute to the actual distillation column in the analysis and the screening of control systems for the column.

As regards the linearised state variable model, the comparison of its response with that of the column simulator indicated that the linearised model is only valid within a small region which the linearisation was done. The linear model severely underestimates the gains and the speed of responses of the column simulator and the actual column as well judging from the comparisons of the column simulator and the actual columns responses. Thus, as mentioned earlier in the chapter, controller designs that a based on using the state variable models directly would be put to severe test when they are applied on the column simulator and on the actual column. Since the linearised model underestimates the gains of the simulator it may result in controller design that are tight. If such a controller then performs satisfactorily on the simulator and then on the column, the benefits of the controller, particularly in terms of robustness, would be demonstrated.

The sources of errors in the predictions of the column simulator are numerous. Firstly, the assumption of only latent heat changes in the reboiler is not strictly true since not all the liquid content is heated up and some heat losses are present because some parts of the surface of the reboiler drum are exposed. This invalidates the

Table 5.6 Controller settings for PI and PID controller using the Cohen and Coon controller setting equations for setpoint tracking in Stephanopoulos (116).

Control loop		K	τ_p	Kp	τ_i	τ_d	Notes
Lr - T_1	↑	-0.5	1.92	-10.74	1.113	0.173	PID
				-7.07	1.08		PI
	↓	-8.67	5.59	-1.746	1.18	0.170	PID
				-1.17	1.403		PI
Qrb - T_{10}		81.01	4.59	0.154	1.18	0.178	PID
				0.10	1.45		PI
		3.56	1.18	1.05	1.03	0.169	PID
				0.605	0.895		PI

Sampling interval used in the calculations is 0.5 minutes

τ_p and τ_i are in minutes

assumption of adiabatic condition in the column. Furthermore, the whole reboiler is modelled as a simple mixing tank ignoring the more complex phenomena taking place in the thermosyphon reboiler arrangement.

Other sources of errors in the predictions of the column simulator were:

(1) uncertainties in the reflux and reboiler flow measurements.

(2) unknown extra reflux due to vapour line above the top of the column, which was observed to be significant.

(3) variations in the reflux temperature which is assumed to be constant in the model.

(4) errors of ± 2% w/w in determination of the feed composition.

(5) the assumption of constant pressure throughout the column. During the experimental investigations, it was observed that the pressure at the bottom end of the column was usually about 10 - 15 mm Hg greater than at the top end during operation of the column.

(6) the assumption of 90% efficiency, on the basis of the simulation results of Daie (26). Incorporating the approach for efficiency calculations developed by Fletcher (64) could be investigated in the search for better results.

5.11 Chapter Conclusion

This chapter has dealt with the steady state and dynamic modelling of the distillation column which were carried out in preparation for the design analysis and final screening of control systems for distillation system. The usefulness and possible limitations of the column simulator and the linearised state variable models as regards the analyses that they were required for were addressed in this chapter. The next stage was using these models for the intended analyses.

This page is left intentionally blank

CHAPTER SIX

Application of the Decoupling and Disturbance Rejection control to the linear and non-linear models of the binary distillation column

6.1 Introduction

The discussions in Chapter 4 dealt with the construction and instrumentation of the pilot scale distillation column on which control studies were carried out. Chapter 5 dealt with the development of models for the distillation column which were used for the design and analysis of the control systems for the distillation column. The two dynamic models of the column, the column simulator and the linear state variable model of the column, were those used for analyses. Chapter 3 gives details of the issues to be addressed on the controller designs selected for investigation in this work and this chapter focuses on one of these applications.

This chapter discusses modelling the behaviour of the decoupling and disturbance rejection control using the distillation column models. The linearised state variable models were used for the design of the control scheme. The column was modelled using either the linear models or the column simulator to assess the feasibility of on-line application of the control scheme. The results will demonstrate the limitations and usefulness of the approach in the design and applications of a control system based on state variable feedback approach. The setpoint tracking capabilities of the controller are also assessed.

The disturbance rejection and decoupling controller is a controller with proportional action only. Therefore it is not equipped with the ability to remove offsets which may be caused by unmeasurable input disturbances or model errors, as the controller has no integral action. adding integral mode to the controller would equip it with the capability of removing offset from steady state. The addition of integral mode, and derivative mode as well, into the control scheme is discussed in this chapter.

6.2 Synthesis of the Decoupling and Disturbance Rejection control scheme.

The synthesis procedure of the decoupling and disturbance rejection control policy have been presented in Section 2.6.2. It is presented here again for clarity.

The control law is

$$\mathbf{u} = \mathbf{F}\mathbf{x} + \mathbf{G}\mathbf{w} \qquad 6.1$$

for the distillation system, assumed for the purpose of controller design to be described by the linearised state variable model;

$$d\mathbf{x}/dt = A\mathbf{x} + B\mathbf{u} + D\mathbf{zd} \qquad 6.2$$

$$\mathbf{y} = C\mathbf{x} \qquad 6.3$$

The A is the n x n system matrix, B is the n x m input driving matrix, D is the n x nd disturbance matrix, C is m x n the output matrix, **y** is the m x 1 vector of the outputs to be controlled, **w** is the m x 1 vector of the setpoints, **u** is the m x 1 input vector of the controls, **zd** is the nd x 1 disturbance vector and **x** is the n x 1 vector of the state variables. The **F** is the m x n constant state feedback gain matrix and **G** is the m x m precompensator gain matrix sometimes referred to as the prefilter (Preuss (208)). The state feedback gain matrix, **F**, is designed to effect load disturbance rejection from the outputs, **y**, in the presence of unmeasured load disturbances, **zd**. The precompensator, **G**, equips the controller with the capability to track the setpoint, **w**.

By substituting Equation 6.1 into Equation 6.2 and then using Equation 6.3, and setting **zd** = **0**, the closed loop equation relating **y** to **w** can be obtained, in Laplace domain, as

$$\mathbf{y}(s) = C\,(sI - (A + BF))^{-1}BG\mathbf{w}(s) \qquad 6.4$$

where s denotes the Laplace transform operator. Similarly, the closed loop equation relating the **y** to **zd** is

$$\mathbf{y}(s) = C(sI-(A+BF))^{-1}D\mathbf{zd}(s) \qquad 6.5$$

For the distillation column used in this work nd = 2, m = 2 and n = 12 and the reboiler and reflux drum compositions are the controlled outputs. The state vector **x** contains

$$\mathbf{x}=(\Delta x_d, \Delta x_1, \Delta x_2, \Delta x_3, \Delta x_4, \Delta x_5, \Delta x_6, \Delta x_7, \Delta x_8, \Delta x_9, \Delta x_{10}, \Delta x_b)^T$$

The symbols x_d and x_b are the top and bottoms compositions, respectively, and Δ represents deviation from steady state. The subscript i in x_i represent the tray composition on tray i. The **u**, **zd**, and **y** are

$$\mathbf{u} = (\Delta Lr, \Delta Qrb)^T$$

$$\mathbf{zd} = (\Delta F, \Delta xf)^T$$

$$\mathbf{y} = (\Delta x_d, \Delta x_b)^T$$

The units of Lr, Qrb,F,and the compositions are in grammes per minute (g/min), joules per minute (j/min), g/min and mass fraction, respectively.

The control law in Equation 6.1 is obtained in the following sequence;

1) Determine the decoupling index d_i is

$$d_i = \min (j : C_i A^j B \neq 0 , j = 0,1,2,...,n-1)$$
$$= n - 1 \text{ (if } C_i A^j B = 0 \text{ for all j)} \qquad 6.6$$

2) Compute A* and B* as follows:

$$A^* = \begin{bmatrix} C_1 A^{d_1+1} \\ C_2 A^{d_2+1} \\ . \\ . \\ C_m A^{d_m+1} \end{bmatrix} \qquad 6.7$$

$$B^* = \begin{bmatrix} C_1 A^{d_1} B \\ C_2 A^{d_2} B \\ . \\ . \\ C_m A^{d_m} B \end{bmatrix} \qquad 6.8$$

where C_i is row i-th of the matrix C.

3) If B* is non singular then compute the controller matrices **F** and **G** as

$$\mathbf{F} = \left(\sum_{k=0}^{k=\partial} \mathbf{M}_k C A^k - A^* \right). \qquad 6.9$$

$$\mathbf{G} = (B^*)^{-1} \mathbf{K}^* \qquad 6.10$$

where $\partial = \max_i(d_i)$

$$\mathbf{M}_k = \text{diag}\ (\varsigma^{(1)}_k, \varsigma^{(2)}_k, \ldots\ldots, \varsigma^{(m)}_k)$$

$$\varsigma^{(i)}_k = 0 \text{ for } k > d_i$$

$$\mathbf{K}^* = \text{diag}(k_1^*, k_2^*, \ldots, k_m^*)$$

In the case studied here the poles have the units minute^{-1}. The diagonal matrix $\mathbf{K}^*$ was set as the identity matrix, I, when computing $\mathbf{G}$ for reasons that will be explained later.

4) Compute the feedforward compensator, $\mathbf{T_f}$, as

$$\mathbf{T_f} = -(\mathbf{B}^T\mathbf{B})^{-1}\mathbf{B}^T\mathbf{D} \qquad 6.11$$

for the feedforward controller

$$\mathbf{u} = \mathbf{T_f} \times \mathbf{zd} \qquad 6.12a$$

The feedforward compensation can also be combined with state feedback control to give

$$\mathbf{u} = \mathbf{F}.\mathbf{x} + \mathbf{T_f}.\mathbf{zd} \qquad 6.12b$$

5) Use the procedure of Takamatsu and Kawachi (129) to find the minimum number of state variables to be fedback for complete decoupling. This involves choosing a matrix $\mathbf{H}$ so as to satisfy

$$C_i A^k (I - \mathbf{H}) = 0, \quad i = 1 \text{ to } m, \quad k = 0 \text{ to } d_i+1 \qquad 6.13$$

for each output i. The diagonal elements of $\mathbf{H}$ which have the value 1 correspond to the state variables that must be measured. The flowchart for this procedure has been given in Figure 2.7. Figures 2.5 and 2.6 show the block diagrams for the closed loop systems with and without $\mathbf{H}$.

The synthesis procedure given above was written in Basic09 on the System96 microcomputer. The functions of the key program modules are presented in Appendix A3.1. Two linearised state variable models representing different steady state regions of the column simulator are used in the studies. The coefficients of the A, B and D matrices for these two steady states have been presented in Tables 5.2a and 5.2b. In this chapter, the linearised model derived at the region of high top product purity will be referred to as model LM1; the model derived at the region of lower top product purity will be referred to as model LM2.

6.3 Controller design.

The design of the decoupling and disturbance rejection control scheme requires the following to be specified;

a) the closed loop poles, which must be negative for closed loop stability to be achieved, to give the desired closed loop responses of the outputs

b) the diagonal elements of **K***, if setpoint tracking is considered.

Only the tridiagonal elements of the system matrix, A, were used in the models LM1 and LM2. The elements off the tridiagonal were considered as errors incurred due to the linearisation procedure and were made equal to zero when computing the controller matrices.

For the controlled variables chosen as the top and bottoms products, x_d and x_b, the following results were obtained from the controller synthesis procedure;

a) The decoupling index $d_i = 0$ for both outputs, i = 1 to m . The number of poles that can be arbitrarily assigned is

$$m + \sum_{i=1}^{i=m} d_i \qquad 6.14$$

which is equal to m. This implies that only two closed loop poles need to be assigned in the controller design. Thus,

$$\mathbf{M}_k = \mathbf{M}_0 = \mathrm{diag}(\varsigma^{(1)}{}_0, \varsigma^{(2)}{}_0) \qquad 6.15$$

which implies that one close loop pole is assigned for each output. According to Shimizu and Matsubara (113), the transfer function matrix between **y** and **w** is ,

$$\mathbf{G}(s) = \mathrm{diag}(k_1^*/(s-\varsigma^{(1)}{}_0), k_1^*/(s-\varsigma^{(2)}{}_0)) \qquad 6.16$$

This means that the closed loop response of each output, y_i, is required to be first order with time constant equal to the negative reciprocal of $\varsigma^{(i)}{}_0$.

b) A minimum number of four state variables should be fedback to achieve complete decoupling control. These variables are x_d, x_1, x_{10} and x_b. This result is not consistent with those of Takamatsu and Kawachi (129) who found that a minimum of 5 state variables, the 1st, 2nd,3rd, n-1th and the nth, were required to accomplish complete decoupling control of a binary distillation column with the top and bottom products as the controlled variables. The reason

for this is that the structure of the input matrix, B, of the linear state variable model of the column simulator is different from the structure of the model of Takamatsu et al. (130). The B_{11} and B_{12} elements of the model of the simulator are non-zero, but very small compared to the other elements in the corresponding rows. This is due to the way in which the column simulator was linearised (Section 5.4). The same elements in the model of Takamatsu et al. are zero, as they consider this to be the case for the usual binary distillation column. The non-zero B_{11} affected the decoupling index, d_1, which would have been 1 if $B_{11} = 0$.

The feedback gain matrix, **F**, and the precompensator matrix, **G**, were computed for different pole assignments $\mathbf{M}_0$ = diag(0.0, 0.0), $\mathbf{M}_0$ = diag(-0.3, -0.3), $\mathbf{M}_0$ = diag(-0.8, -0.8). As discussed in Chapter 2 Section 2.6.2, the assignment $\mathbf{M}_0$ = diag(0.0,0.0) implies an integrator decoupled system is desired. Table 6.1 show the **F** and **G** matrices for the above pole assignments. The **F** is a 2 x 12 matrix and the **G** is a 2 x 2 matrix. The **K*** = I was always assumed when calculating **G**. This was done to make it convenient to manipulate the diagonal elements of **K*** just prior to an application, should it be necessary. It is important to note that, from here on, the reference to the **F** matrix includes the multiplication of the **H** matrix which holds the information on the number of state variables that must be fed back.

Table 6.1 shows that only the elements of the first and the last columns of **F**, $\mathbf{F}_1$ and $\mathbf{F}_{12}$, are affected by the pole assignments, where $\mathbf{F}_i$ denotes column i of **F**. This is because $\mathbf{F}_2$ and $\mathbf{F}_{11}$ are uniquely determined but the $\mathbf{F}_1$ and $\mathbf{F}_{12}$ are used for pole assignment. This can be verified by examination of Equation 6.9 which will show that the poles $\mathbf{M}_0 = \text{diag}(\varsigma^{(1)}{}_0, \varsigma^{(2)}{}_0)$, will affect only $\mathbf{F}_1$ and $\mathbf{F}_{12}$. All the elements of, **F**, $\mathbf{F}_i$ for i = 3 to 10, have zero elements. Even if these elements were nonzero they will effectively become zero by **FH** because their corresponding state variables are not measured.

The entries of **F** and **G** are large in magnitude, indicating a very sensitive control system would result. The reason for these entries having large magnitudes is because the entries in the first and last rows of B, B_1 and B_{12}, and the diagonal entries $A_{1,1}$

and $A_{12,12}$ in the system matrix A are much smaller in magnitude compared to the other entries in the respective matrices. This is an indication of illconditioning of the distillation system and is due to the much larger holdups of the reflux and reboiler drums compared with the tray holdups. The consequence is a small B* and, hence, large **F** and **G** coefficients.

Table 6.1 Controller Matrices for Model LM2: Top and bottoms product compositions as the controlled variables

$$A^* = \begin{bmatrix} -0.1247 & 4.776 \times 10^{-2} & 0 & 0 & 0 & 0 & 0 & 0 & 0 & 0 & 0 & 0 \\ 0 & 0 & 0 & 0 & 0 & 0 & 0 & 0 & 0 & 0 & 0.176 & -0.3173 \end{bmatrix}$$

$$B^* = \begin{bmatrix} -1.4709 \times 10^{-7} & 4.0677 \times 10^{-10} \\ 4.7970 \times 10^{-6} & -4.8247 \times 10^{-8} \end{bmatrix}$$

$$\mathbf{G} = \begin{bmatrix} -5330252674.12 & 44962.49 \\ -5302526764.0 & -16255786.7 \end{bmatrix} \text{ for } \mathbf{K}^* = \mathbf{I}$$

$$\mathbf{F} = \begin{bmatrix} -665167.25 & 254722.70 & 0\,0\,0\,0\,0\,0\,0\,0 & -7915.84 & 14266.65 \\ -66136579.20 & 25326695.4 & 0\,0\,0\,0\,0\,0\,0\,0 & 2861901.06 & -5157981.35 \end{bmatrix}$$

for $\mathbf{M}_0 = \text{diag}(0.0)$

$$\mathbf{F} = \begin{bmatrix} 934734.28 & -254722.70 & 0\,0\,0\,0\,0\,0\,0\,0 & -7915.84 & 777.907 \\ 92939222.9 & 25326695.4 & 0\,0\,0\,0\,0\,0\,0\,0 & 2861901.06 & -281245.33 \end{bmatrix}$$

for $\mathbf{M}_0 = \text{diag}(-0.3,-0.3)$

$$\mathbf{F} = \begin{bmatrix} 3601236.84 & -254722.70 & 0\,0\,0\,0\,0\,0\,0\,0 & -7915.84 & 21703.34 \\ 358065560.0 & 25326695.4 & 0\,0\,0\,0\,0\,0\,0\,0 & 2861901.06 & 7846648.03 \end{bmatrix}$$

for $\mathbf{M}_0 = \text{diag}(-0.8,-0.8)$

6.4 Implementation of the control scheme to the linear model

Implementation on the linear model represent preliminary tests which were done to examine how the decoupling and disturbance rejection control scheme works. The simple Euler integration method was used to integrate the linear differential equations with the integration interval chosen as 0.02 minutes. Substituting Equation 6.1 into Equation 6.2 gives

$$dx/dt = (A + BF)x + BGw + Dzd \qquad 6.17$$

which represents the controlled system to be solved. The control interval of 0.25 minutes was used in all the simulations. Unless otherwise stated, model LM2 is referred to in the simulations reported here.

6.4.1 Load disturbance rejection

For load disturbance rejection only, the control law is $\mathbf{u} = \mathbf{Fx}$ since $\mathbf{w}$ will be equal to $\mathbf{0}$; $\mathbf{G}$ is not required to effect disturbance rejection. The first problem that arose was to select the $\mathbf{F}$ matrix from Table 6.1 that gives the best control; this implies the best pole assignment to give the best control.

Figure 6.1 shows the results for the case with $\mathbf{M}_0$ = diag(0.0,0.0) and $\mathbf{M}_0$ = diag(-.3, -.3) for 25% increase in the feed flowrate. The closed loop responses of the outputs for this case are clearly unsatisfactory. The manipulated inputs saturated at their lower constraints immediately after simulation commenced, and resided at these limits for a long period. They exhibited sharp bursts until they eventually moved to their upper constraints in one step. The outputs showed sudden changes in their directions which corresponded to the sudden movement of the inputs from their lower constraints to their upper constraints. For $\mathbf{M}_0$ = diag(-.3,-.3) the closed loop responses improved, but only slightly. The main difference is that the manipulated inputs did not show any intermittent bursts after they had saturated.

Several simulations where performed using smaller load disturbances and with different pole assignments. Unsatisfactory control was always delivered; the manipulated inputs always saturated. The reason for this behaviour was the large

magnitudes of the coefficients of the F matrices which subsequently produced very sensitive controlled system. This demonstrated the extent of illconditioning of the distillation system.

In the search for better and more useful results, it was decided to use the top and bottom tray compositions, x_1 and x_{10}, as the controlled variables. Another set of **F** and **G** matrices were computed for this case. Table 6.2 shows the corresponding **F** matrices, and the **G** matrix for $\mathbf{K}^* = \mathbf{I}$ for the pole assignments $\mathbf{M}_0$ = diag(0.0, 0.0), $\mathbf{M}_0$ = diag(-0.8, -0.8), $\mathbf{M}_0$ = diag(-5, -5), $\mathbf{M}_0$ = diag(-0.8, -5.0), $\mathbf{M}_0$ = diag(-5.0, -10). The results of the synthesis procedure showed that only two poles need to be assigned, as was the case when the x_d and x_b were the controlled variables. However, the number of state variable that must be fedback increased to 6 state variables. The state variables are x_d, x_1, x_2, x_9, x_{10}, and x_b. Table 6.2 also show that only the entries of the second and the eleventh columns of **F**, $\mathbf{F}_2$ and $\mathbf{F}_{11}$, were affected by the pole assignments. Furthermore, the entries of **F** and **G** are much smaller in magnitude compared with those obtained when x_d and x_b were the controlled variables as shown on Table 6.1. A less sensitive control system was thus given simply by choosing the control location as the trays at the ends of the column.

In the previous chapter, the top tray and the bottom tray were chosen as the location where temperature measurements are to be located for the dual composition control of the pilot plant distillation column. The results of the synthesis procedure of the decoupling and disturbance rejection control scheme supports this choice of the measurement location. This is because a less sensitive controller resulted when the top tray and the bottom tray compositions were selected as the controlled variables instead of the top and bottoms products. The disadvantage, however, is that the number of state variables that must be fedback has increased. Thus, from the point of view of reducing the cost of measuring, it is better to choose the controlled variables as the top and bottoms products while it is better to choose the top and bottom tray compositions as the controlled variables to obtain a less sensitive closed loop system. Therefore, not only has the synthesis procedure provided the controller matrices, the results it

produced provided useful information as regards sensitivity of the closed loop system and cost of performing decoupling and disturbance rejection control.

The results of the synthesis procedure were sensitive to the errors in the system matrix, A. When the entries that are not on the tridiagonal were retained, the result obtained suggested that all the 12 state variables must be fedback. A set of corresponding **F** and **G** matrices for $\mathbf{M}_0$ = diag (-0.8,-0.8) are shown in Table 6.4. This control structure is not practical since to measure all the tray compositions for feedback means that composition analysers must be located on each tray. This would

Table 6.2 Controller matrices for model LM2, with the top tray and bottom tray compositions are the controlled variables

$$A^* = \begin{bmatrix} 5.542 & -9.297 & 4.018 & 0 & 0 & 0 & 0 & 0 & 0 & 0 & 0 & 0 \\ 0 & 0 & 0 & 0 & 0 & 0 & 0 & 0 & 0 & 11.34 & -29.551 & 16.009 \end{bmatrix}$$

$$B^* = \begin{bmatrix} 3.143 \times 10^{-3} & -6.862 \times 10^{-6} \\ 1.265 \times 10^{-3} & -7.010 \times 10^{-6} \end{bmatrix}$$

$$G = \begin{bmatrix} 524.92 & -513.90 \\ 94719.14 & -235390.82 \end{bmatrix}$$

for $\mathbf{K}^*=I$

$$F = \begin{bmatrix} -2902.24 & 4880.41 & -2109.48 & 0 & 0 & 0 & 0 & 0 & 5826.22 & -15186.23 & 8227.39 \\ -524956.1 & 880642.91 & -380643.8 & 0 & 0 & 0 & 0 & 0 & 2668668.83 & -6955971.92 & 3768511.69 \end{bmatrix}$$

for M_0 = diag(0,0)

$$F = \begin{bmatrix} -2902.24 & 4460.48 & -2109.48 & 0 & 0 & 0 & 0 & 0 & 5826.22 & -14775.11 & 8227.39 \\ -524956.1 & 804867.6 & -380643.8 & 0 & 0 & 0 & 0 & 0 & 2668668.83 & -6767659.25 & 3768511.69 \end{bmatrix}$$

for M_0 = diag(-0.8,-0.8);

$$F = \begin{bmatrix} -2902.24 & 2255.806 & -2109.48 & 0 & 0 & 0 & 0 & 0 & 5826.22 & -12616.72 & 8227.39 \\ -524956.1 & 407047.21 & -380643.8 & 0 & 0 & 0 & 0 & 0 & 2668668.83 & -5779017.79 & 3768511.69 \end{bmatrix}$$

for M_0 = diag(-5.0,-5.0);

$$F = \begin{bmatrix} -2902.24 & 4460.48 & -2109.48 & 0 & 0 & 0 & 0 & 0 & 5826.22 & -12616.72 & 8227.39 \\ -524956.1 & 804867.81 & -380643.8 & 0 & 0 & 0 & 0 & 0 & 2668668.83 & -5779017.79 & 3768511.69 \end{bmatrix}$$

for M_0=diag(-0.8,-5.0);

$$F = \begin{bmatrix} -2902.24 & 2255.806 & -2109.48 & 0 & 0 & 0 & 0 & 0 & 5826.22 & -10047.2 & 8227.39 \\ -524956.1 & 407047.21 & -380643.8 & 0 & 0 & 0 & 0 & 0 & 2668668.83 & -4602063.67 & 3768511.69 \end{bmatrix}$$

for M_0=diag(-5.0,-10);

Table 6.3 Feed forward compensator for model LM2

$$T_f = \begin{bmatrix} 0.447 & 683.405 \\ 199.316 & 268207.056 \end{bmatrix}$$

Table 6.4 Controller Matrices for Model LM2: Effect of the errors in the state matrix on the coefficients of the controller.

$$G = \begin{bmatrix} 524.92 & -513.90 \\ 94719.14 & -235390.82 \end{bmatrix}$$

for $K^*=I$

$$F = \begin{bmatrix} -2924.401 & 4451.46 & 2108.81 & 54.7 & -0.4489 & -0.2687 & -0.300 & -0.300 & -0.46628 & 5852.46 & -14774.71 & 8273.83 \\ 531902.24 & 800737.17 & -380340.26 & -9893.45 & -144.43 & -132.182 & -152.245 & -160.49 & -244.78 & 2668712.82 & -6767586.02 & 3776891.28 \end{bmatrix}$$

for $M_0 = \text{diag}(-0.8,-0.8)$

be very expensive to do in practice. The result highlights that the combination of computer roundoff and small errors in the model used for controller design can significantly affect the results produced.

Simulations were carried out to assess the capabilities of the disturbance rejection controller in the presence of

1) for 25% increase in the feed flow rate

2) for 25% increase in the feed composition and

3) non-linearities,which is a type of model error commonly encountered in the design of control systems for processes.

The latter was done to assess how well the control scheme can tolerated non-linearities; that is how robust the controller is to non-linearities. The test was carried out by applying a controller designed using a linearised model at one steady state to control a linearised model derived at another steady state; by applying a controller designed using model LM1 on model LM2, for example. Feedforward compensation using Equation 6.12a and combined disturbance rejection and feedforward compensation, were both examined. The combined feedback and feedforward control law is Equation 6.12b.

Limits were placed on the control actions in order to represent reality. The limits were

$$1.0 \leq Lr \leq 16 \text{ l/hr}$$

$$0.3 \leq Qrb \leq 1.5 \text{ KW} \qquad 6.18$$

The observations that were made are outlined in the following.

1) Specifying the poles as M_0 = diag(0.0,0.0) required an integrator decoupled closed loop system and this resulted in poor controller performance as shown in Figure 6.2 for 25% increase in the feed flow rate. The manipulated inputs saturated at their lower constraints and resided at their limits throughout the time duration of the simulation. The response of the top tray composition showed an initial rise in response to the load disturbance. The attempt by the controller to return it back to the desired value resulted in the sharp change in the direction of

the output and subsequently settling at a steady state well below the desired value. The offset of the bottom tray composition was also significant. This demonstrated that specifying an integrator decoupled closed loop system is not a good choice, as it resulted in an undesirable closed loop response.

2) Feed flow disturbance resulted in offset in the bottom tray composition. This offset reduced as the magnitude of the poles increased. Figure 6.3 shows this for the cases with $\mathbf{M}_0$ = diag(-0.8,-0.8) and $\mathbf{M}_0$ = diag(-5,-5) specified. With the faster desired closed loop response ($\mathbf{M}_0$ = diag(-5,-5)) the quality of control improved because the rise of the top and bottom tray compositions were arrested more quickly, thus, reducing effect of feed flow on both outputs and the final offset in the bottom tray composition. These improvements were achieved with much less control effort as the manipulated variables only moved slightly from there original values compared to when $\mathbf{M}_0$ = diag(-0.8,-0.8) was specified. The feedforward compensator alone (Equation 6.12a), with the $\mathbf{T}_f$ shown on Table 6.3, could not completely remove the effects of the feed flow disturbance on both outputs as shown in Figure 6.4. The combination of feedback and feedforward control, using Equation 6.12b, resulted in poorer quality of control compared with state feedback control alone and feedforward compensation only. The closed loop system lost resilience as regards removal of the disturbance effects from the top tray composition. This is shown in Figure 6.5 in comparison with control without feedforward compensation. It can be seen that a considerable offset is in the steady state value of the top tray composition and there is still significant offset in the bottom tray composition.

3) The effect of feed composition disturbance on the top and bottom tray compositions were completely removed by the disturbance rejection controller as no offsets appeared in the final steady states of both outputs. Figure 6.6 compares the responses for $\mathbf{M}_0$ = diag(-.8,-.8) and $\mathbf{M}_0$ = diag(-5,-5). As was the case for feed flow disturbance rejection, as the poles become larger in

magnitude the maximum peak deviations of the outputs reduced, the final values of the control inputs were found more quickly and, thus, the system reached steady state more quickly. Feedforward compensator (Equation 6.12a) alone resulted in offsets in both outputs as shown in Figure 6.7, as was the case when the system was subjected to feedflow disturbance (Figure 6.4). The closed loop system behaved very badly, however, when the combined feedback and feedforward compensation (Equation 6.12b) was used to reject the effect of the feed composition disturbance on the outputs. This is shown in Figure 6.8 for $\mathbf{M}_0$ = diag(-0.8,-0.8) in comparison with state feedback control control alone. The manipulated variables saturated at their lower limits and remained there throughout the duration of the simulation and, thus, the offsets in the final values of the outputs were significant. This deterioration in control was worse than when feedforward compensation was included with state feedback to remove feed flow disturbance effects on the outputs (Figure 6.5).

4) To assess the effect of non-linearities on the control properties of the disturbance rejection controller and how well it can tolerate non-linearities, the controller designed using model LM2 was applied on model LM1 and the performance compared with that of a controller designed using model LM1 applied on model LM1. Table 6.5 contains the $\mathbf{F}$ and $\mathbf{G}$ matrices for $\mathbf{M}_0$ = diag(-0.8, 0.8) for model LM1. Comparing these with those on Table 6.2 for model LM2 with the same $\mathbf{M}_0$, the differences in magnitude between the entries of corresponding entries are quite significant, indicating that the disturbance rejection control scheme would be very sensitive to non-linearities in the distillation column. The result shown in Figure 6.9 confirmed this. The effect of non-linearities was to deteriorate the resilience of the closed loop system, causing offsets. However, instability did not result, indicating some degree of robustness. A better assessment of the robustness of the control scheme to non-linearities is to use the nonlinear column model. This is will be discused later in the chapter.

These sets of results show that an integrator decoupled system should be avoided for good stable control to be achieved. The complete rejection of the feed composition disturbance from both the top and bottom tray compositions, and the offset that appears in the case of feed flow disturbance rejection are consistent with the published result of Shimizu and Matsubara (113).

As stated Shimizu and Matsubara (113) and in Shah (207), using feedforward compensator $\mathbf{T_f}$ alone would not completely remove the effects of disturbances from the outputs if the number of manipulated inputs is less than the number state variables, that is if $m < n$. The results discussed above confirmed this as offsets occurred in both outputs when the feedforward compensation was used alone (Figures 6.4 and 6.7). The results also showed that there was degradation in the control when the feedforward compensator was combined with state variable feedback for both feed flow and feed composition disturbance rejection.

The results show that as the magnitude of the poles is increased the effects of the feed flow disturbances on the outputs are minimised and control effort required also reduced. It is therefore advantageous to maximise the closed loop poles in order to minimise the offset caused by feed flow disturbance, rather than trying to eliminate the offset completely by introducing the feedforward compensator $\mathbf{T_f}$.

A deficiency of the disturbance rejection controller observed from the simulations using feedforward compensation and introducing non-linearity, is that the control inputs tended to saturate very quickly and reside at the limits for most of the time. This easy saturation of the control inputs is also a serious disadvantage as the inputs were useless for control when they saturated.

Table 6.5 Controller matrices for model LM1

$$\mathbf{F} = \begin{bmatrix} -14185.80 & 21057.07 & -7231.27 & 000000 & 4260.34 & -9632.16 & 5357.14 \\ -2748845.08 & 3907347.49 & -1401746.27 & 000000 & 1847009.27 & -4175878.42 & 2322508.17 \end{bmatrix}$$

for $M_0 = \text{diag}(-0.8,-0.8)$

$$\mathbf{G} = \begin{bmatrix} 2515.95 & -371.18 \\ 463220.82 & -160921.40 \end{bmatrix}$$

for $\mathbf{K}^*=\mathbf{I}$

6.4.2 The setpoint tracking problem

As was mentioned in Chapters 2 and 3, previous workers (Shimizu and Matsubara (113, 114) and Takamatsu and Kawachi (129)) who applied the decoupling control approach to distillation systems did not examine the setpoint tracking problem and the gave no guidance on how to choose the proper $\mathbf{K}^*$. The investigations discussed here were aimed at answering the following questions;

1) How important is the choice of $\mathbf{K}^*$ to setpoint tracking capabilities of the controller?

2) How should the proper values of $\mathbf{K}^*$ be chosen ?

For setpoint tracking the control law is Equation 6.1

$$\mathbf{u} = \mathbf{F}\mathbf{x} + \mathbf{G}\mathbf{w}$$

The $\mathbf{w}$ is the vector of the setpoints $\mathbf{w} = (\Delta x_{1s}, \Delta x_{10s})^T$ where the subscript s denotes setpoint. As mentioned earlier, the $\mathbf{G}$ matrices were computed using $\mathbf{K}^* = \mathbf{I}$ to allow the manipulation of $\mathbf{K}^*$ to be done conveniently when the controller is commissioned.

Figure 6.10 shows the results for the case when $\mathbf{M}_0$ = diag(-0.8,-0.8) for different values of $\mathbf{K}^*$. The responses of both outputs followed their specified closed loop responses, which is a first order response with time constant of 1.25 minutes (1/0.8). The responses were also completely decoupled from each other, as desired.

One important observation that can be made from the graph is that offsets in the final values of the outputs occurred when $\mathbf{K}^*$ was not chosen as diag(+0.8,+0.8), that is, when $\mathbf{K}^* \neq -\mathbf{M}_0$. Figure 6.11 showed that specifying $\mathbf{M}_0$ = diag(-5,-5) the closed loop response is faster than when $\mathbf{M}_0$ = diag(-0.8,-0.8). Again offsets occurred when $\mathbf{K}^*$ was not chosen as diag(+5,+5). The elements $\mathbf{K}^*$ had to be changed form $\mathbf{K}^* = 0.8\mathbf{I}$ to $\mathbf{K}^* = 5.0\mathbf{I}$ in order to have zero offset.

Many similar simulations were performed with different pole assignments in the controller designs. The results consistently showed that for setpoint tracking $\mathbf{K}^* = -\mathbf{M}_0$ must be selected to avoid offsets in the final values of the outputs. Figures 6.12

and 6.13 show this for $\mathbf{M}_0$= diag(-0.8,-5.0), $\mathbf{K}^*$ = diag(0.8,5.0) and for $\mathbf{M}_0$= diag(-5.0,-10.0), $\mathbf{K}^*$ = diag (5,10), respectively.

The results discussed above gave a conclusive answer to the first question. These are that the choice of $\mathbf{K}^*$ is important to set point tracking, it depends on the closed loop poles and must be chosen as the magnitude of the poles. The second question concerning how to chose $\mathbf{K}^*$ needs justification and this is given later.

6.4.3 Effect of non-linearities on setpoint tracking

The condition that $\mathbf{K}^*$ must be chosen as $-\mathbf{M}_0$ to avoid offsets did not hold in presence of non-linearities in the distillation system. Figure 6.14 shows this clearly for the case using $\mathbf{M}_0$= diag(-0.8,-0.8) with the decoupling controller designed using model LM1 applied to control model LM2. As in the case for load disturbance rejection, the non-linearity degraded control significantly. The manipulated variables saturated at their their upper constraints within a short time after the simulation commenced.

This result showed that the decoupling control scheme is not very tolerant of non-linearities, that is, the performance of the control system is very sensitive to non-linearities. The implication is that new $\mathbf{F}$ and $\mathbf{G}$ matrices must be computed as the operation conditions change. This is a tedious task to perform as it implies recomputing the A, B and D matrices at the required times during operation of the column.

6.4.4 Comparison with conventional multiple loop PI control

The performance of the decoupling and disturbance rejection control scheme and multiple single loop PI controllers were compared. The Cohen and Coon (203) method was used to assist the determination of the PI controller settings. The settings are :

K_c = 800 (grammes/minutes)/mass fraction

τ_i = 3.0 minutes

for the Lr - x_1 loop,

Kc = -15,0000 (joules/minutes)/mass fraction

τ_i = 1.2 minutes

for the Qrb - x_{10} loop.

Figure 6.15 compares the closed loop responses for M_0 = diag(-5, -5) and the multiple PI controllers for +25% feed flow disturbance. Under the multiple loop PI controllers the system had not reached steady state even after 30 minutes and the control loop interactions were significant. By contrast, the disturbance rejection control scheme returned the outputs to steady state in much shorter time. Similar results were obtained for simultaneous load (25% increase in the feed composition) and setpoint changes. These is shown in Figures 6.16.

In conclusion, for the distillation system described by linearised state variable model, the decoupling and disturbance rejection control scheme is superior to multiple loop PI control in the following ways;

(a) It achieves complete decoupling of the responses of the outputs from each other

(b) It returns the outputs to their desired values in much shorter time, hence, increases the rate of recovery of the products of the distillation column.

The only advantage of using the PI controllers is that any offsets would eventually be eliminated by the integral actions in the controllers. The decoupling and disturbance rejection control scheme is not equipped with integral action and cannot, therefore, eliminate offsets.

6.4.5 Choosing K* for setpoint tracking

In Section 6.4.3 it was shown that for setpoint tracking if $\mathbf{K}^* \neq -\mathbf{M}_0$ then offsets will occur. This could be explained from a simple analysis given as follows. For the case where $d_i = 0$ for all i, from Equation 6.15, the transfer function between y_i and w_i is $k^*_i / (s-\varsigma^{(i)}_0)$. Using the final value theorem, the corresponding steady state gain is

$$- k^*_i / \varsigma^{(i)}_0 . \qquad 6.19$$

For $y_i = w_i$ at steady state, k^*_i must be chosen so that this gain has the value 1, which means that

$$k^*_i = - \varsigma^{(i)}_0 \qquad 6.20$$

This was verified by the results of the simulations in Figures 6.10 to 6.13.

If two poles are assigned for each output, that is $d_i = 1$, the transfer function between y_i and w_i will be $k^*_i / (s-\varsigma^{(i)}_0)(s-\varsigma^{(i)}_1)$. The steady state gain would then be

$$k^*_i / (\varsigma^{(i)}_0 \varsigma^{(i)}_1) \qquad 6.21$$

From this it could be presumed that k^*_i must be chosen as the absolute value of the product $(\varsigma^{(i)}_0 \varsigma^{(i)}_1)$. The further implication of this, is that, for the general case, $d_i > 1$, each k^*_i is the absolute value of the product of the poles assigned for that output i, with the poles nonzero. That is,

$$k^*_i = \prod_{j=0}^{j=d_i} (-1)^j \zeta^{(i)} \qquad 6.22$$

An alternative approach to finding the solution to the problem of selecting $\mathbf{K}^*$ can be given from the laplace transform relationship of $\mathbf{y}$ and $\mathbf{w}$ given by Equation 6.4. For zero offset in $\mathbf{y}$ to a step change in $\mathbf{w}$, the steady state gain between $\mathbf{y}$ and $\mathbf{w}$ should be 1. Since

$$\mathbf{G} = (B^*)^{-1}\mathbf{K}^*,$$

it then follows from Equation 6.4 that $\mathbf{K}^*$ should be selected such that

$$C (- (A+BF))^{-1} B (B^*)^{-1} \mathbf{K}^* = I \qquad 6.23$$

The $\mathbf{K}^*$ must be diagonal, to satisfy Equation 6.10.

The proof that $\mathbf{K}^* = -\mathbf{M}_0$ for $d_i = 0$ for i = 1 to m is given in the following.

Proof

For $d_i = 0$ for i = 1 to m

$$A^* = CA \qquad 6.24$$

$$B^* = CB \qquad 6.25$$

$$\mathbf{F} = B^{*-1}(\mathbf{M}_0 C - A^*) \qquad 6.26$$

Rearranging Equation 6.23 and substituting Equation 6.26 gives

$$BB^{*-1}\mathbf{K}^* = -(A + BB^{*-1}(\mathbf{M}_0 C - A^*))C^{-1} \qquad 6.27$$

which gives

$$BB^{*-1}\mathbf{K}^* = -A C^{-1} - BB^{*-1}\mathbf{M}_0 C C^{-1} + BB^{*-1}A^* C^{-1} \qquad 6.28$$

Substituting Equations 6.24 and 6.25 into the last term in the RHS of Equation 6.28 gives

$$BB^{*-1}\mathbf{K}^* = -A C^{-1} - BB^{*-1}\mathbf{M}_0 C C^{-1} + BB^{-1}C^{-1}CAC^{-1} \qquad 6.29$$

$$BB^{*-1}\mathbf{K}^* = -BB^{*-1}\mathbf{M}_0 \qquad 6.30$$

Hence

$$\mathbf{K}^* = -\mathbf{M}_0 \qquad 6.31$$

QED

The numerical solution of Equation 6.23 for $\mathbf{K}^*$ also confirmed that $\mathbf{K}^* = -\mathbf{M}_0$. For $\mathbf{M}_0$ = diag (-0.8,-0.8), $\mathbf{K}^*$ was obtained as

$$\mathbf{K}^* = \begin{bmatrix} 0.79999998 & -3.08 \times 10^{-8} \\ -9.65 \times 10^{-10} & 0.79999998 \end{bmatrix}$$

which is essentially $\mathbf{K}^*$ = diag(0.8, 0.8) as the small of diagonal elements can be attributed to roundoff errors from the floating point calculations. Similarly, for $\mathbf{M}_0$ = diag(-5, -5) the $\mathbf{K}^*$ was obtained as

$$\mathbf{K}^* = \begin{bmatrix} 5.0 & -2.55 \times 10^{-8} \\ -9.65 \times 10^{-9} & 4.99999999 \end{bmatrix}$$

From the above it is clear the an integrator decoupled system, $\mathbf{M}_0$ = diag(0.0,0.0), will not be suitable for set point tracking even if it results in good load disturbance rejection. This is because if $\mathbf{K}^* = 0$ no setpoint tracking can be achieved as the output from the precompensator $\mathbf{G}$ will be zero since $\mathbf{G} = 0$. In view of the

closed loop behaviour of an integrator decoupled system in Figure 6.1 and 6.2, an integrator decoupled system is thus not a satisfactory choice for this system for both setpoint tracking and load disturbance rejection.

The results of Equation 6.23 do not provide the answer for choosing **K*** for the general case, $d_i > 0$, nor does it refute Equations 6.22. To do this requires a system where $d_i > 0$ for at least one output i. Such a system is the model of a binary distillation system studied by Shimizu and Matsubara (113) and the use of the model in this work is discussed in the next section. However, before continuing, the solution of Equation 6.23 for **K*** for the case $d_i = 1$ will be given to demonstrate that the relationship for **K*** is more complex.

Solving **K*** for $d_i = 1$ for i = 1 to m gives the following

For $d_i = 1$ for i = 1 to m

$$A^* = CA^2$$

$$B^* = CAB$$

$$\mathbf{F} = B^{*-1} (M_0C + M_1CA - A^*) \qquad 6.32$$

Equation 6.29 thus becomes

$$BB^{*-1}\mathbf{K}^* = -A C^{-1} - BB^{*-1}M_0CC^{-1} - BB^{*-1}M_1CAC^{-1} + BB^{-1}A^{-1}C^{-1}CA^2C^{-1}$$

This results in

$$\mathbf{K}^* = -M_0 - M_1CAC^{-1} \qquad 6.33$$

For the general case it can be determined that

$$\mathbf{K}^* = -M_0 - (\Sigma M_iCA^iC^{-1}) \qquad \text{for i = 1 to } d_i \qquad 6.34$$

This indicates that choosing **K*** gets more complicated as the decoupling index increase from 0.

6.4.6 Application on the linear model of Shimizu and Matsubara (113)

The linear state variable model of the binary distillation system used by Shimizu and Matsubara (113) is shown on Table 6.6. The model represents a ten stage binary distillation system distilling a mixture of ethylene and ethane, and the column pressure, p, is also a state variable. The feed composition, xf, and the feed flow, F,

are the load disturbances. The controlled variables are the top and bottoms product compositions and the column pressure using reflux, Lr, condenser cooling water temperature, Tc, and the steam temperature, Th. The A, B and D matrices of the system have the dimensions 11 x 11, 11 x 3, and 11 x 2, respectively. The corresponding **zd**, **y**, and **w** are $(\Delta F, \Delta xf)^T$, $(\Delta x_d, \Delta x_b, \Delta p)^T$ and $(\Delta x_{ds}, \Delta x_{bs}, \Delta p_s)^T$, respectively, where the s denotes setpoint. The state vector **x** is

$$\mathbf{x} = (\Delta x_d, \Delta x_1, \Delta x_2, \Delta x_3, \Delta x_4, \Delta x_5, \Delta x_6, \Delta x_7, \Delta x_8, \Delta x_b, \Delta p)^T \qquad 6.35$$

and the control input **u** is

$$\mathbf{u} = (\Delta Lr, \Delta Tc, \Delta Th)^T \qquad 6.36$$

The compositions are in mole fractions, p is in bar, F and Lr are in Kg-mol/hr, Th and Tc are in degrees Kelvin. The synthesis procedure programmed on the System96 was used to compute the control scheme for this model. The following results were obtained.

1)The decoupling indices are $d_1 = 1$, $d_2 = 0$ and $d_3 = 0$ meaning that 4 poles need to be assigned, two poles for Δx_d response and one pole each for Δx_b and Δcp responses.

2)The minimum number of state variables to measure for feedback are 6, and they are the first, second, third, ninth and tenth stage compositions and the column pressure.

These agreed with the results published in Shimizu and Matsubara (113).

3) Using the pole assignments $\mathbf{M}_0$ = diag(-56, -9, -10) and $\mathbf{M}_1$ = diag(-15, 0, 0), as was specified by Shimizu and Matsubara, the corresponding **F** and **G** controller matrices for $\mathbf{K}^* = \mathbf{I}$ obtained are shown on Table 6.7. For comparison the published values obtained by Shimizu and Matsubara are also given. The coefficients agree well with the published data and the discrepancies are due to computer roundoff on the System96.

This distillation system is a good example on which to test validity of Equation 6.22 as more than one pole for one output i = 1 can be assigned, since $d_1 = 1$. Setpoint tracking case was considered, with

$$\mathbf{w} = (0.05, -0.05, 0.1)^T \qquad 6.37$$

The integration interval of 0.0001 hr and control interval of 0.001 hr were used. The results of simulations for setpoint tracking are discussed in the following.

Specifying $\mathbf{K}^*$ = diag(840, 9, 10) according to Equation 6.22, it is shown in Figure 6.17 that only Δx_b and Δp moved to their new setpoints with no offsets in their final values, while the final value of Δx_d had a large offset. This shows the decoupling nature of the control scheme since "bad" performance of one "control loop" did not propagate in the system and deteriorate control of the other outputs. If limits were imposed on the control inputs, which will be the case in practice, the large reflux flow input would have saturated and caused offsets in the other output variables.

The result shown in Figure 6.17 demonstrated that for a controlled output with more than one closed loop pole assigned for its desired response, $\mathbf{K}^*$ must not be chosen according to Equation 6.22. Using $\mathbf{K}^* = \mathbf{I}$, the outputs in no way moved to there new setpoints, as is superimposed in Figure 6.17.

However, solving Equation 6.23 numerically for $\mathbf{K}^*$, gave

$$\mathbf{K}^* = \text{diag}(56.00001, 8.99992, 9.9998) \qquad 6.38$$

which corresponds to $\mathbf{M}_0$. Figure 6.18 shows the corresponding closed loop response for this $\mathbf{K}^*$. Clearly, all the outputs moved to their setpoints and no steady state offsets resulted. This result contradicts Equation 6.33 as it indicates that the second term in the equation, $-\mathbf{M}_1\mathbf{C}\mathbf{A}\mathbf{C}^{-1}$, does not affect the choice of $\mathbf{K}^*$. The implication is that this term is zero, which is only true when $\mathbf{M}_1 = 0$. The further implication is that the $\mathbf{K}^*$ must be chosen as $-\mathbf{M}_0$ for the general case with $d_i \geq 0$.

Table 6.6 Distillation column model of Shimizu and Matsubara (113). Coefficients of Matrices

$$A = \begin{bmatrix}
-13.50 & 15.421 & 0.0 & 0.0 & 0.0 & 0.0 & 0.0 & 0.0 & 0.0 & 0.0 & -0.289 \\
33.750 & -87.094 & 54.673 & 0.0 & 0.0 & 0.0 & 0.0 & 0.0 & 0.0 & 0.0 & -10.016 \\
0.0 & 33.750 & -88.423 & 55.724 & 0.0 & 0.0 & 0.0 & 0.0 & 0.0 & 0.0 & -8.042 \\
0.0 & 0.0 & 33.750 & -89.474 & 56.520 & 0.0 & 0.0 & 0.0 & 0.0 & 0.0 & -6.162 \\
0.0 & 0.0 & 0.0 & 22.50 & -78.179 & 38.106 & 0.0 & 0.0 & 0.0 & 0.0 & -3.335 \\
0.0 & 0.0 & 0.0 & 0.0 & 40.499 & -78.606 & 38.654 & 0.0 & 0.0 & 0.0 & -4.319 \\
0.0 & 0.0 & 0.0 & 0.0 & 0.0 & 40.499 & -79.153 & 39.336 & 0.0 & 0.0 & -5.439 \\
0.0 & 0.0 & 0.0 & 0.0 & 0.0 & 0.0 & 40.499 & -79.835 & 40.153 & 0.0 & -6.614 \\
0.0 & 0.0 & 0.0 & 0.0 & 0.0 & 0.0 & 0.0 & 40.499 & -80.652 & 41.091 & -7.720 \\
0.0 & 0.0 & 0.0 & 0.0 & 0.0 & 0.0 & 0.0 & 0.0 & 8.100 & -10.018 & -8.652 \\
-2.241 & 32.747 & 0.0 & 0.0 & 0.0 & 0.0 & 0.0 & 0.0 & 0.0 & 23.866 & -49.475
\end{bmatrix}$$

$$B = \begin{bmatrix}
0.0 & 0.0 & 0.0 \\
0.00422 & 0.51258 & 0.0 \\
0.00340 & 0.41300 & 0.0 \\
0.00261 & 0.31732 & 0.0 \\
0.00129 & 0.17213 & 0.0 \\
0.00102 & 0.22340 & 0.0 \\
0.00129 & 0.28207 & 0.0 \\
0.00157 & 0.34423 & 0.0 \\
0.00184 & 0.40340 & 0.0 \\
0.00041 & 0.07022 & 0.0 \\
0.00183 & 1.58193 & 0.97192
\end{bmatrix}$$

$$D = \begin{bmatrix}
0.0 & 0.0 \\
0.0 & 0.0 \\
0.0 & 0.0 \\
0.0 & 0.0 \\
18.000 & 0.00016 \\
0.0 & 0.00102 \\
0.0 & 0.00129 \\
0.0 & 0.00157 \\
0.0 & 0.00184 \\
0.0 & 0.00041 \\
0.0 & -0.00095
\end{bmatrix}$$

Table 6.7 The controller matrices for the distillation column model of Shimizu and Matsubara (113)

$d_1=1$, $d_2=0$, $d_3=0$

$\mathbf{M}_0$ = diag (-56, -9, -10) and $\mathbf{M}_1$= diag (-15, 0, 0)

$$\mathbf{F} = \begin{bmatrix} -29945.6 & 70495.1 & -45357.7 & 00000 & 49055.5 & -6542.3 & -43470.7 \\ 176.05 & -414.44 & 266.66 & 00000 & -403.75 & 52.96 & 378.79 \\ -342.78 & 773.24 & -519.19 & 00000 & 749.26 & -123.05 & -657.74 \end{bmatrix}$$

Published by Shimizu and Matsubara (113)

$$\mathbf{F} = \begin{bmatrix} -29415.2 & 69750.13 & -44552.72 & 00000 & 48182.30 & -6055.5 & -43435.2 \\ 171.74 & -407.25 & 260.13 & 00000 & -396.68 & 49.85 & 376.82 \\ -332.51 & 760.5 & -507.29 & 00000 & 736.37 & 117.1 & 654.49 \end{bmatrix}$$

Computed on System 96 computer

$$\mathbf{G} = \begin{bmatrix} 53.47 & -5948.43 & 15.452 \\ -0.31 & 48.97 & -0.090 \\ 0.61 & -90.91 & 1.205 \end{bmatrix}$$

Computed on System 96 computer

$$\mathbf{G} = \begin{bmatrix} 54.42 & 6055.0 & 15.735 \\ -0.32 & 49.84 & 0.0925 \\ 0.623 & -92.48 & 1.209 \end{bmatrix}$$

Published by Shimizu and Matsubara (113)

==========

6.4.7 Remarks on the simulations for setpoint tracking

The simulation results have shown that the choice of $\mathbf{K}^*$ strongly determines the setpoint tracking performance of the decoupling and disturbance rejection controller. The appropriate values of the diagonal elements depend directly on the values of the closed loop poles assigned. The $\mathbf{K}^*$ must be chosen to satisfy Equation 6.23

$$C\,(-(A+BF))^{-1}B(B^*)^{-1}K^* = I$$

which is the steady state relationship between the outputs and the setpoints. The analytical and simulations results obtained showed that, for cases with $d_i = 0$ and $d_i = 1$, $\mathbf{K}^*$ must be chosen as $-\mathbf{M}_0$.to avoid steady state offset. This was confirmed by the simulations on the linearised state variable models of the distillation column and the model of Shimizu and Matsubara (113).

6.4.8 Using less than the minimum number of state variables that should be measured.

The procedure of Takamatsu and Kawachi (129) (Equation 6.12) gives the minimum number of state variables and the state variables themselves that must be measured to achieve complete decoupling control using the decoupling and disturbance rejection controller. The simulations that have been presented so far verified this as the desired control objectives were achieved. The simulations discussed here were done to examine what would happen if less than the minimum number of variables are fedback, since there is no guarantee that the variables will all be measurable in practice. This possibility was tested on model LM2 by examining the effect of not measuring each of the state variables, x_1, x_2, x_9 and x_{10}, on the quality of control. Simulations were performed for the setpoint tracking case using $\mathbf{M}_0 = \text{diag}(-5,-5)$.

Figure 6.19 shows the closed loop response when x_1 was not measured. The control actions were oscillatory at the initial stage causing initial oscillations in the outputs. The final value if x_1 showed an offset while x_{10} had no offset.

The absence of x_{10} measurement resulted in severe oscillatory control actions to be generated, as shown in Figure 6.20. This was expected since the entries $\mathbf{F}_2$ and $\mathbf{F}_{11}$ are affected by the pole assignments, so that these entries strongly determine the closed loop behaviour of the system.

The absence of either x_2 or x_9 also resulted in bad control, as shown in Figure 6.21 and 6.22. In both cases, saturation of the manipulated inputs occurred very quickly.

These results verified that these 4 state variables must be measured for the system to be controllable and that x_2, x_9 and x_{10} are more important than x_1 in achieving the control objectives in full. Thus, if in practice any of these variables cannot be measured, the decoupling and disturbance rejection control scheme cannot be applied successfully.

6.5 Application of the disturbance rejection control scheme to the column simulator

Section 6.4 discussed the application of the decoupling and disturbance rejection controller on the state variable models of the distillation column. Satisfactory results were obtained for both load disturbance rejection and setpoint tracking for many of the cases studied. This section discusses the application of the control scheme on the non-linear model of the distillation column, known as the column simulator. The control scheme was assessed for nominal performance on the column simulator for on-line application to be considered feasible. As mentioned in Section 2.2.4, nominal performance means stable performance of the control scheme on the model of the process. The performance of the controller on the column simulator would indicate how robust the controller is to non-linearities, as the controller is designed using linear state models obtained by linearising the model equations of the column simulator.

The simulations were performed with the controller designed using linearised state variable model LM2 with $\mathbf{M}_0$ = (-0.8, -0.8) specified. The sequence followed in the simulations is as follows:

(a) Control the top tray composition, x_1, to 0.85 using PI control,

(b) Ensure the the column simulator has reach steady state,

(c) Switch to disturbance rejection and decoupling control

and then

(d) Induce changes into the distillation system after some time duration.

A simulation was first performed with no disturbances induced into the distillation system after switching from PI control to the decoupling and disturbance rejection control scheme. Figure 6.23 shows the result that was obtained. Shortly after switching to disturbance rejection control the manipulated inputs moved quickly to their lower limits and remained at these limits. The closed loop system was clearly undesirable as the controller failed to maintain both x_1 and x_{10} at their initial values even though no load disturbances entered the system. This is contrary to what was

expected in that the outputs should stay at steady state until a disturbance enters the column.

This result is not easily explained as the column is a non-linear system, however non-linearity plays an important role in producing the undesirable behaviour. One possible explanation is that it is computer roundoff that produced changes in the manipulated inputs which in turn produced changes in the outputs, since at steady state the column simulator values are only affected by the computer roundoff. Eventually these round-off effects were amplified possibly due to the fact that the elements of the **F** matrices were large. Non-linear effects then came into play and prevented the controller from maintaining the outputs at their original values.

The controller behaved badly because of the significant differences between the linear model used to design the controller and the column simulator. The result in Figure 6.23 clearly demonstrated that the disturbance rejection control scheme could not tolerate the non-linearities in the column simulator; that is the controller was not robust to the non-linearities in the column simulator. If the controller were robust to the non-linearities, it would at least have been able to maintain the outputs at their initial values in the presence of the computer roundoff. On the basis of the poor performance of the controller on the column simulator, the disturbance rejection and decoupling control scheme is not applicable on the pilot plant distillation system.

The failure of the controller on the column simulator was consistent with the poor performance of the control scheme on the linearised models, where the controller designed on the basis of a model at one steady state performed badly on the model obtained at another steady state. This was because the region of validity of the linear model in approximating the column simulator is very small as was shown in Figures 5.14a and 5.14b. The result confirms the report by Doyle and Morari (177) and Morari (150) that neglecting of non-linearity in a model used for controller design can result in a controller that is too tight and hence poor performance on the non-linear system may result. In the case of the distillation column the effects of computer round off were amplified and this indicated the tightness of the controller as well as the limitation for on line application.

6.6 Concluding remarks on the simulation results of the decoupling and disturbance rejection control scheme

Application of the decoupling and disturbance rejection control strategy to the distillation column simulation has demonstrated the following. For the linear model :

a) A total of 6 state variables, the 1st, 2nd, 3rd, n-2 th, n-1-th and the n-th tray compositions needed to be measured for feedback for controller design to achieve complete decoupling control of the top and bottoms tray compositions.

b) Only two closed loop poles, one for each controlled output, need to be preassigned for desired closed loop response.

c) The disturbance rejection control scheme can completely remove the effects of feed composition disturbances from both the top and bottom tray compositions. The effects of feed flow disturbances can be suppressed from both outputs by choosing large, negative, poles.

d) Introducing the feedforward compensator $\mathbf{T_f}$ into the disturbance rejection control scheme degrades closed loop system dynamics. This shows that combining the feedforward compensator with state feedback for load disturbance rejection is not a good choice, as regards the distillation system modelled by the linearised state variable models.

e) For both setpoint tracking and load disturbance rejection, the decoupling and disturbance rejection control scheme performed better than multiple loop PI controllers. The disturbance rejection control scheme achieved complete decoupling control and returned the system to steady state in shorter times, and this time reduced as the magnitude of the poles were increased. In practice this

would mean significant reduction in off-specification products of the distillation column.

f) The proper value of $\mathbf{K}^*$ is strongly linked to the value of the closed poles assigned. The diagonal elements of $\mathbf{K}^*$ must always take the negative values of the corresponding poles in $\mathbf{M}_0$ to avoid offset in the final value of the corresponding setpoint. This condition does not hold in presence of non-linearities and indicates possible areas were difficulties will be met in practice.

g) From the simulation results presented earlier, the disturbance rejection and decoupling control scheme usually produced undesireable closed loop responses in the presence of non-linear effects in the distillation system. The approach was therefore not considered a good choice for on-line application on the pilot scale distillation column used in this work, since the column is non-linear.

The most significant limitation of the disturbance rejection and decoupling control scheme is the inability to handle non-linearities. Even small non-linear effects will cause offsets in the outputs and these cannot be eliminated as the controller is not equipped with integral action. This is a major obstacle in the application of the scheme to chemical systems, as chemical systems are usually non-linear systems. Control systems that are not robust to non-linearities will find limited application in the chemical industry.

To overcome the deficiency due to non-linearities, an adaptive form of the algorithm will be advantageous in that new $\mathbf{F}$ and $\mathbf{G}$ can be recomputed, or updated, as operating conditions of the process change. The frequency at which new controller matrices will need to be recomputed will depend on the degree of non-linearity of the system. An adaptive form of the control scheme also means that all the calculations in the synthesis procedure, including the procedure for finding the minimum number of states that should be measured, will have to be carried out each time new controller matrices are required. The computational effort needed for such a task will be

demanding and will increase greatly as the frequency that the new parameters are required increases and if the dimension of the system is large. All this still excludes the computational requirements of the method that will be used to obtain the new matrices A, B and D of the system each time new controller matrices need to be updated .

In simulation, the A, B and D matrices can be obtained by linearising the non-linear dynamic model itself around reference trajectories as the simulation progresses. The appropriate reference trajectory would be at the state the process is at the instants when the linearisation is to be done. Emphasis is put on the fact the the dynamic model itself should be linearised as this will minimise errors in the resulting linearised model. If, for example, an approximate non-linear model is used for the linearisation the control scheme will not be able to compensate for the errors between the approximate model and the "real" model.

By similar reasoning, in real applications it would also be inappropriate to use an approximate non-linear model for the linearisation as the controller may not be able to compensate for the error between the model and the process. A better approach would be to identify the system model on line. The estimation technique needed will be one that updates the A, B and D matrices with new coefficients using the process data available. The computational effort required by such an approach would be very high as the number of coefficients of the matrices would usually be large.

To identify all the coefficients of the system model accurately would also be difficult, particularly as the number of coefficients will be large compared to the number of measured variables that will be available. In the case the distillation column studied in this work, for example, only the feed flow, feed composition, reflux flow, reboiler input, top and bottom tray compositions will be available as measurements. These are five measurements compared to the total number of coefficients of the A, B and D matrices which are more than 30 (Tables 5.2a and 5.2b). The estimation technique that will be used will be a recursive technique similar to the recursive least squares method commonly used in adaptive control, as discussed in Section 2.9.5. To identify all the coefficients of A, B and D would require persistent excitation of the

column by the inputs and this excitation must be at the required degree which depends on the number of coefficients that are to be identified. If this is not satisfied, when the process is at steady state, for example, then some of the coefficients will be biased. Similar problems where discussed in Section 2.9.7 in relation to the application of parameter estimation techniques in adaptive control. The estimation technique used to obtain the A, B and D coefficients would also be susceptible to numerical problems as discussed in Jordan (185). For example, if a least squares technique is employed the covariance matrix may become illconditioned if the data used for estimation is not wel scaled.

Observability of the process at all times would be important considerations that must be addressed. This is an important consideration where a large number of coefficients need to be identified from much less measurements. Since it will be uneconomical to measure all the state variables of the distillation column, then a method is required which can produce estimates of the state variables from available process measurements. For this to be successful, the distillation system must be observable at all times; the conditions of observability has been stated in Section 2.3.1.

6.7 Addressing the problem of offset in the disturbance rejection and decoupling control scheme

The problem in question

A basic requirement of a control system is that it should have the ability to eliminate steady state offset; this requirement is secondary only to the requirement of closed loop stability. The discussions in Section 6.4 have shown that a major drawback of the disturbance rejection and decoupling control scheme is its inability to remove offsets, as the controller gives proportional control only. Some cases where offsets occurred when the control scheme was applied to the linear model of the distillation column are given as follows:

1) Offset in the bottom tray composition in the presence of feed flow disturbance (Figure 6.3)

2) Offsets in the top tray and bottom tray compositions when the feedforward compensation alone was applied in the presence of load disturbances (Figures 6.4 and 6.7)

3) Offsets in both outputs when $\mathbf{K}^* \neq \mathbf{M}_0$ in the setpoint tracking case (Figures 6.10 and 6.11)

4) Offsets in both outputs in the presence of model errors, which was non-linearities.

Shimizu and Matsubara (113) suggested the use of the feedforward compensation such as the compensator $\mathbf{T}_f$ to suppress the effects of feed flow disturbance on the bottom tray composition. This compensator was applied with and without the state feedback on the linear model of the column. The results in both cases, shown in Figures 6.4 and 6.5, showed clearly that offsets occurred in both outputs.

Approaches to solving the problem

The concept of proportional-plus-integral feedback is the most common approach used to counter steady state offsets in process control. It would be advantageous to equip the disturbance rejection and decoupling controller with the capability to deal with offset such as those obtained when the controller was applied on the linear model of the distillation system, as listed above. A linear state feedback multivariable controller which ensures that steady state offsets do not occur after load or setpoint disturbances could be developed or terms such as integral mode could be added to the disturbance rejection and decoupling control law (Equation 6.1). If any of this can be achieved it is then possible to avoid using the feedforward compensator $\mathbf{T}_f$ to attempt to remove offset in the bottom tray composition due to feed flow disturbance. The problem to address would then be the offset due to the remaining 3 cases, 1), 3) and 4) listed above.

It is possible to design state variable feedback controllers for linear multivariable systems that provide both disturbance rejection and servomechanism and ensure that no steady state offsets occur. Such design problems are dealt with by Preuss (208)

and Kimura (210). Only the approach used by Preuss will be review here, since he considers general control law of which the disturbance rejection and decoupling control law in Equation 6.1 is on such family of control laws.

The work of Preuss (208) was motivated by the fact that conventional state space controller design techniques are usually dedicated to the regulator problem. The object of the controller is to supply a control to take the plant from a non-zero state to a zero state; that is, to drive the plant output and its derivatives to zero when the plant is subjected to unwanted disturbances (Anderson and Moore (211)). Examples of these techiques are the modal control technique used by Davison (30), the pole assignment technique of Crossley and Porter (195) and the disturbance rejection technique of Wonham and Morse (178) used by Takamatsu et al. (130). All these have been mentioned in Section 2.4 through to Section 2.6. Typically, the controller is a state feedback controller which has proportional action only. It cannot deal with setpoint changes and cannot address offset as integral mode is absent. The decoupling and disturbance rejection technique used in this work has similar qualities but setpoint tracking is allowed for by using the constant prefilter, **G**, with the state feedback.

Preuss acknowledged that integral mode is the most popular way of eliminating offsets and his view is that a controller should, ideally, have both setpoint tracking and disturbance rejection capabilities. He, thus, proposed new methods for approaching the design of state variable feedback controllers that will meet the requirements of setpoint tracking and regulatory control, avoiding the use of integral action or setpoint prefilter. Starting from the control law of Equation 6.1, one approach considered by Preuss was to dispense with the prefilter such that the objective is to design the feedback control law

$$\mathbf{u} = \mathbf{R}\mathbf{x} + \mathbf{w} \qquad 6.39$$

where **R** is an m x n matrix. Comparing with Equation 6.1, the state feedback **R** is similar to the state feedback **F** in Equation 6.1, and the prefilter or precompensator, **G**, is replaced by the identity matrix, I, of appropriate dimension. The object is to design the state feedback **R** to meet the following requirements:

1) Asymtotical closed loop stability, that is, the eigenvalues of A + BR must have negative real parts.

2) Zero steady state errors in the outputs, that is, offset free response, in the presence of setpoint changes and load disturbances where the load disturbances can be either measured or unmeasurable.

The design of **R** for various objectives are given in the paper by Preuss (208). Such design methods would be appropriate for the linear model of the distillation column to deal with the offset that occurred in the bottom tray composition after feedflow disturbance when the decoupling and disturbance rejection controller was applied.

Preuss gave the necessary condition for the decoupling and disturbance rejection controller, Equation 6.1, to be able to achieve the requirements above as well as effect dynamical decoupling of the controlled system with the restriction that **G** = I. The condition is that B* in Equation 6.8 has necessarily to be of diagonal structure.

The results of the synthesis procedure of the decoupling controller in Equation 6.1 for the linear model of the distillation system (eg. Tables 6.1 and 6.2) shows, however, that B* is not of diagonal structure. It is therefore not possible for the controller to achieve the requirements of zero steady state errors in the presence of load disturbances and, alternatively or simultaneously, setpoint changes. In order to achieve the objectives, it is necessary to consider one of the design approaches presented by Preuss (208) or consider the addition of integral mode to the disturbance rejection and decoupling controller in Equation 6.1. The objective is that Equation 6.1 should be able to eliminate the offset that will arise when setpoint changes and feed flow disturbance are simultaneously occurring, as the simulation results on the linear model of the column have shown that feed flow disturbance resulted in offset in the bottom tray composition.

The use of integral action was preferred in this work rather than attempt to apply one of the methods proposed by Preuss. The reasons for this is given in the following.

In the first place, using any of the approaches of Preuss to obtain **R** in Equation 6.39 would require calculations which will be of the order of the calculations required to obtain **F** and **G** matrices in Equation 6.1. Secondly, the offset due to the model errors, which is non-linearities in the case in question, cannot be compensated for by the state feedback **R** alone. This is because **R** is designed for the linear multivariable system using the linear state variable model of the column.

The addition of integral mode to Equation 6.1, on the other hand equips the controller with the ability to eliminate offsets caused by unmeasurable load disturbances, non-linearities and other sources.

6.7.1 Incorporating integral mode into the disturbance rejection and decoupling control scheme

The addition of integral action was investigated to see whether it would extend the capabilities of the disturbance rejection and decoupling control scheme. It was first required to devise a way of introducing integral action into the decoupling and disturbance rejection control scheme and then apply it in this work.

In this work, the approach used to include integral action into the disturbance rejection and decoupling control scheme is on the basis of the conventional single input single output PI control system. An SISO PI controller in continuous time formulation is given by

$$u(t) = Kc\left(e(t) + \frac{1}{\tau}\int_0^t e(t)dt \right) \qquad 6.40a$$

where u is control input, τ_i is the integral time and Kc is the proportional gain. e(t) is the error signal given by

$$e(t) = y_s - y(t) \qquad 6.40b$$

where y is the controlled output and the subscript s denotes setpoint. Conventional controller design techniques, such as the Cohen and Coon method used in this work, are commonly used to obtain starting values of the parameters Kc and τ_i.

The representation of the decoupling and disturbance rejection control law in Equation 6.1,

$$\mathbf{u} = \mathbf{F}\mathbf{x} + \mathbf{G}\mathbf{w}$$

can be compared with the representation of a PI controller in Equation 6.39. The control law contains terms proportional to the state **x** and the setpoint **w**. It is therefore equivalent to proportional control action. Integral action can be included by adding an integral term similar to the integral term in the PI controller in Equation 6.40. This is done as follows

$$\mathbf{u} = \mathbf{F}\mathbf{x} + \mathbf{G}(\mathbf{w} + \mathbf{T}_I^{-1}\mathbf{h}) \qquad 6.41$$

The term $\mathbf{T}_I^{-1}\mathbf{h}$ is analogous to the integral term in the PI controller

$$\frac{1}{\tau}\int_0^t e(t)dt \qquad 6.42$$

The **h** is the integral of the error signal and is given by

$$\mathbf{h}_i(t) = \int_0^t \mathbf{e}_i(t)dt = \int_0^t (\mathbf{w}_i(t) - \mathbf{y}_i(t)) \quad \text{for i=1 to m} \qquad 6.43$$

and $\mathbf{T}_I$ is a diagonal matrix containing the integral times for each "control loop" i for i = 1 to m;

$$\mathbf{T}_I = \text{diag}\ (\tau_{i,1}, \tau_{i,2}) \qquad 6.44$$

From Equation 6.43 the following differential equations can be obtained:

$$d\mathbf{h}_i/dt = \mathbf{e}_i(t) = \mathbf{w}_i(t) - \mathbf{y}_i(t) \quad \text{for i = 1 to m}$$

$$\mathbf{h}_i(t) = 0 \text{ at } t = 0 \qquad 6.45$$

Equation 6.45 are m extra differential equations which are solved together with the system represented by Equations 6.2 and 6.3. Substituting Equation 6.41 into 6.2 gives the equation of the closed loop system as

$$d\mathbf{x}/dt = (\mathbf{A} + \mathbf{B}\mathbf{F})\mathbf{x} + \mathbf{B}\mathbf{G}\mathbf{w} + \mathbf{B}\mathbf{G}\mathbf{T}_I^{-1}\mathbf{h} + \mathbf{D}\mathbf{z}\mathbf{d} \qquad 6.46$$

The solution of the differential equations in Equation 6.45 give the **h** in the control law in Equation 6.41. The next problem was how to select the diagonal elements of **T**, which, by analogy with the PI controller, correspond to the integral times of each "control loop" i. In this work, values for these diagonal elements were obtained using the conventional single input single output controller design method that was used to assist the tuning of a PI controller. As mentioned earlier in the chapter, the Cohen and Coon Method (203) (Appendix A.2.2.1) was used in this work.

Incorporating derivative mode

A derivative mode can also be added to the control scheme, in a similar way the integral mode is added in Equation 6.41. With a derivative mode added, Equation 6.41 becomes

$$\mathbf{u} = \mathbf{Fx} + \mathbf{G}(\mathbf{w} + \mathbf{T}_I^{-1}\mathbf{h} + \mathbf{T}_D de/dt) \qquad 6.47$$

where $\mathbf{T}_D$ is a diagonal matrix containing the derivative times. The de/dt is defined by

$$de/dt = dw/dt - dy/dt = dw/dt - Cdx/dt \qquad 6.48$$

since $\mathbf{y} = \mathbf{Cx}$. For regulatory control only, $dw/dt = \mathbf{0}$. This is not so for setpoint changes. If, the setpoint changes are step inputs, which is the case used in this work, then

$$dw/dt = \infty. \qquad 6.49$$

To overcome this dw/dt can the approximated by

$$dw/dt = \Delta w/\Delta T \qquad 6.50$$

where $\Delta T = a\Delta Tc$ where a is an integer number which would determine the number of intervals over which $dw/dt \neq 0$. The value selected in this work was a = 2.

The derivative mode requires m extra equation to be solved and the selection of derivative times in $\mathbf{T}_D$. This extra overhead is quite smal compared to the increase in the computational overheads thatt would be incurred if Preuss's approach were to be used. The diagonal elements of $\mathbf{T}_D$ may also be chosen using SISO controller design techniques.

6.7.2 Significance of including integral mode

The way in which the integral and derivative modes has been introduced into the decoupling and disturbance rejection control scheme is approached from the point of view of analogy with a classical PI control. The question needs examining of whether by the inclusion of the integral term, $\mathbf{T}_I^{-1}\mathbf{h}$, and derivative term, $\mathbf{T}_D de/dt$, the resulting controller partially, or completely, looses its decoupling capabilities. That is,

does Equation 6.41 and 6.47 still posses decoupling property of the original controller, Equation 6.1.

There is, however, some benefit in using simple techniques to extend the capability of a multivariable controller such as the decoupling controller, from the practical application point of view: the inclusion of the integral and derivative modes did not involve rigorous mathematics and there is the possibility of using simple SISO controller tuning techniques to obtain starting values of the integral times in $\mathbf{T}_I$ and derivative times in $\mathbf{T}_D$. Furthermore, the implications in terms of practical applications would be great if the integral mode can indeed remove offset due to non-linear effects in the distillation column. This would mean increased possibility of applying the linear multivariable controller directly to the non-linear distillation system, as the integral mode has improved the robustness of the controller to non-linearities.

In a situation where distillation control objective is to reduce off specification product as the cost of off-specification products of the column is high, significant motivation exists to eliminate offset when the decoupling and disturbance rejection controller is being used. Therefore, even if the control scheme looses its decoupling properties, the financial benefits that can be obtained if the offset is eliminated could be much greater.

6.7.3 Application of the decoupling and disturbance rejection control scheme with integral and derivative action on the linear model of the distillation column

The proposed decoupling and disturbance rejection control scheme with integral action developed in Section 6.7.2 has been applied in some situations where offsets occurred when the disturbance rejection and decoupling control scheme (Equation 6.1) was applied on the linear model of the distillation column. The situations in which the proposed method was applied are as follows:

Case 1); where offsets in the bottom tray composition occurred in the presence of a 25% increase in the feed flowrate (Figure 6.3),

Case 2); where offsets occurred when $\mathbf{K}^* \neq -\mathbf{M}_0$ in setpoint tracking (Figure 6.10) and

Case 3); where offsets occurred in both the top tray and bottom tray compositions when the controller designed using model LM2 was applied on model LM1 in the presence of a 25% increase in the feed flow rate (Figure 6.9).

The decoupling and disturbance rejection control scheme with integral action was assessed using the $\mathbf{F}$ and $\mathbf{G}$ matrices obtained for the model LM2 using the pole assignments $\mathbf{M}_0$ = diag(-0.8, -0.8).

The diagonal matrix of the integral times was chosen as $\mathbf{T}_I$ = diag (3.0, 1.2), where the times are in minutes. These integral times correspond to the integral times used the multiple loop PI controllers for the top tray composition and the bottom tray composition PI control loops. In Section 6.4.4, the performance of this multiple loop PI control scheme for both disturbance rejection and setpoint tracking was compared with the decoupling and disturbance rejection control scheme without integral action (Equation 6.1).

Figure 6.24 shows the results obtained for Case 1) mentioned above. There was no offset in the final steady state value of the bottom tray composition as was present when the original decoupling and disturbance rejection control scheme without integral action was applied (Figure 6.3). The integral action improved the control of the bottom tray composition in that it removed the offset. This was, however, achieved at the expense of overall dynamic response of the closed loop system. The control inputs and controlled outputs exhibited oscillatory response, as should be the case when integral mode is introduced into a proportional controller; inclusion of integral mode to a controller with proportional action only increases the order of the overall system and thus makes it more sensitive. The oscillations were reasonably well damped and both outputs eventually settled at their original levels after 25 minutes.

The result shown in Figure 6.24 demonstrated that the proposed method of introducing integral action is worked satisfactorily in that the offset in the bottom tray composition was completely removed. What is also significant in the result is that the integral times in $\mathbf{T}_I$ where chosen as those of the PI controllers in the multiple loop PI

control system for the linear model. This demonstrated that the appropriate integral times for the proposed decoupling and disturbance rejection control scheme with integral mode can be selected using conventional controller design techniques for designing single loop controllers for linear systems, such as the Cohen and Coon method used in this work to assist the design of the multiple PI controllers for the linear model.

If the integral times in $\mathbf{T}_I$ are not carefully selected, the closed loop system may become unstable. The choice of the integral times in $\mathbf{T}_I$ would depend on the values of the pole assignments in a similar manner as the appropriate integral time will depend in the proportional gain in a PI controller. This is because the values of the poles assigned determine the speed of the closed loop response delivered by the disturbance rejection and decoupling control scheme. The closed loop response becomes faster as the magnitude of the is poles increased. This has been shown earlier in this chapter that the pole assignment of $\mathbf{M}_0$ = diag(-5, -5) gives faster response than when $\mathbf{M}_0$ = diag (-0.8, -0.8) is specified(Figure 6.3 and Figures 6.10 vs Figures 6.11). This effect of the pole assignments on the closed loop response delivered by the disturbance rejection and decoupling controller is analogous to the effect of increasing the proportional gain of a PI controller. For example, the closed loop response of an SISO linear first order system under proportional (P) control would increase as the proportional gain is increased.

Figure 6.25 shows that when the integral times in $\mathbf{T}_I$ were increased in value to $\mathbf{T}_I$ = diag (7.0, 5.0), the speed of the closed loop response of the linear model and the frequency of the oscillations of the outputs decreased accordingly. The oscillatory behaviour of the system decreased and the outputs settled at their setpoints in a slightly earlier time (20 minutes), compared with when $\mathbf{T}_I$ = diag (3.0, 1.2) was used. On the basis of this result it was decided to use $\mathbf{T}_I$ = diag (7.0, 5.0) in the decoupling and disturbance rejection control scheme with integral action. The latter choice is preferred as oscillatory behaviour is significantly reduced particularly in the response of the bottom tray composition.

Figure 6.26 shows the result obtained when derivative mode was added to the control scheme with integral mode compared with the result without derivative mode in Figure 6.25. The derivative times of $\mathbf{T}_D$ = diag (1.5, 1.0) was used. These times are approximately 10 times the derivative times computed for the top tray and bottom tray temperature PID controllers, in Table 5.6.The dynamic responses of the closed loop system was more sluggish than without the derivative mode. The most significant differences can be seen from the control inputs and the responses of the top tray composition. The overshoot is higher than without integral mode, but is lower in the case of the bottom tray composition.

Figure 6.27 shows the result for Case 2), which is for setpoint tracking where $\mathbf{K}^*$ $\neq$ $\mathbf{M}_0$. The figure compared the result for the controller with integral mode with when the control scheme is without integral action. The $\mathbf{K}^*$ was chosen as I and this choice has been shown in Figure 6.10 to result in offsets in both outputs for the case when $\mathbf{M}_0$ = diag (-0.8, -0.8). Slight oscillations of the outputs resulted but offsets did not result due to the integral action in the controller.

Figure 6.28 shows the result obtained when the control scheme with integral action was applied in Case 3). The integral action did not eliminate offset in this case. Instead it made the performance of the control scheme worse in that the control inputs simply saturated at their upper limits and the controlled outputs attained values which were unrealistic in practice, as compositions can have the maximum value of 1. This result demonstrated the greater sensitivity to non-linearities of the closed loop system when the control scheme was equipped with integral action compared with when integral action was not present. This greater sensitivity of the closed loop system is as a result of the integral action since adding integral action to a controller with proportional action only increases the sensitivity of the closed loop system, for example, oscillatory responses can be obtained of the integral times are chosen smal enough. This factor and the sensitivity to the model errors due to non-linearities, combined to produce an even more sensitive closed loop system. Therefore, the dynamic behaviour was therefore worse than without integral mode in the controller. It would have been an added bonus if the integral mode had successfully eliminated

this offset due to non-linearity, as non-linear systems are common in chemical processes.

6.7.4 Conclusions on the application of the decoupling and disturbance rejection with integral and derivative action on the linear model.

In this work, integral and derivative modes has been included into the decoupling and disturbance rejection control scheme. The approach followed to introduce the integral and derivative modes into the control scheme is based on the analogy with PI control. For each mode, an extra m differential equations need to be solved as a result of the introduction of the integral term, where the m is the number of controlled outputs.

One advantage of the method used to include two modes into the control scheme is that the appropriate integral and derivative times for each "control loop" can be selected using conventional controller design techniques used to assist the design of conventional SISO control systems for linear systems.

Simulation results on the linear model of the distillation column demonstrated that offsets are eliminated by the integral term, except offsets due to proces - model mismatch. The only disadvantage is the the decoupling properties of the original control scheme is partially lost by the addition of the integral and derivative modes.

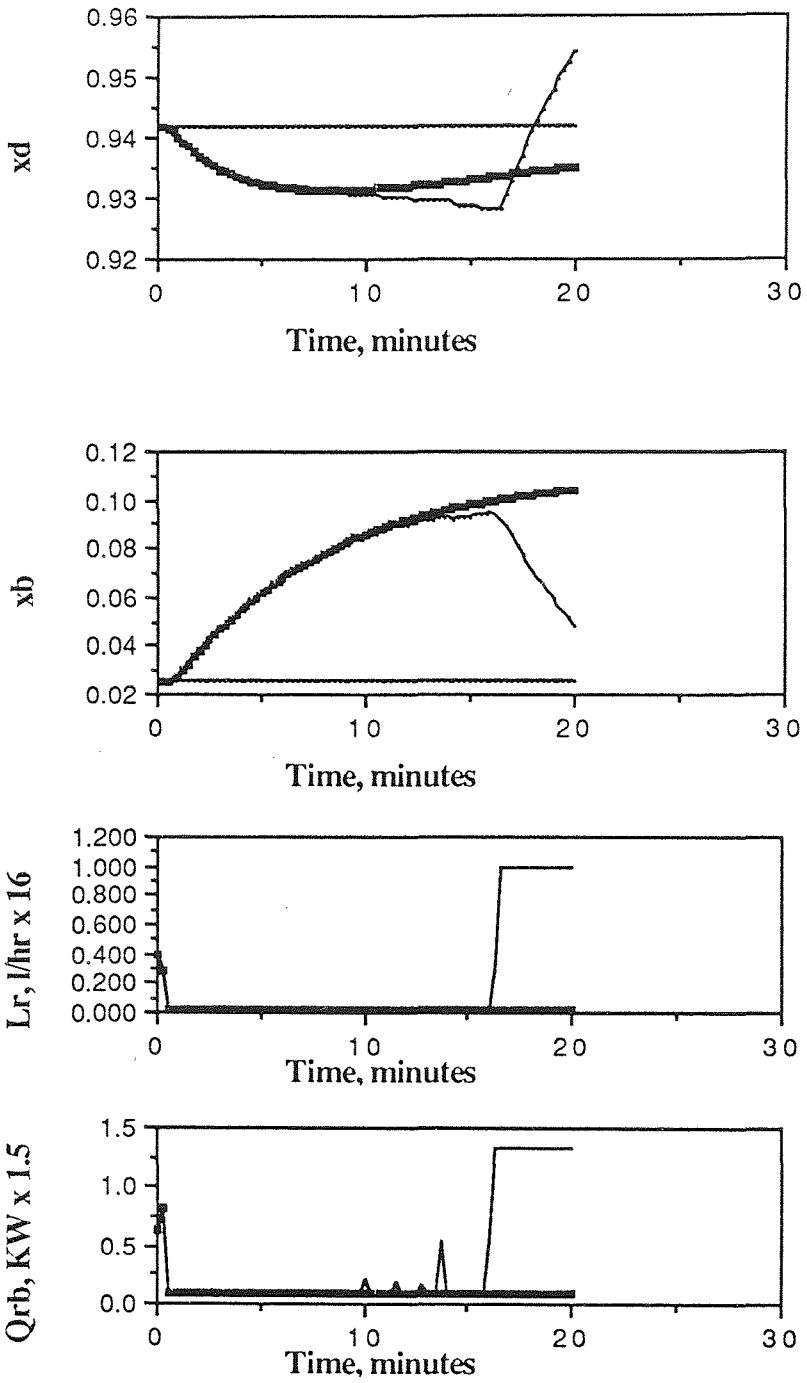

M_0 = diag(0.0, 0.0) single lines

M_0 = diag (-0.3, -0.3) thick lines

Figure 6.1. Load disturbance rejection - 25% increase in feed flow: Top and bottom products under control: M_0 = diag(0.0, 0.0) vs M_0 = diag (-0.3, -0.3)

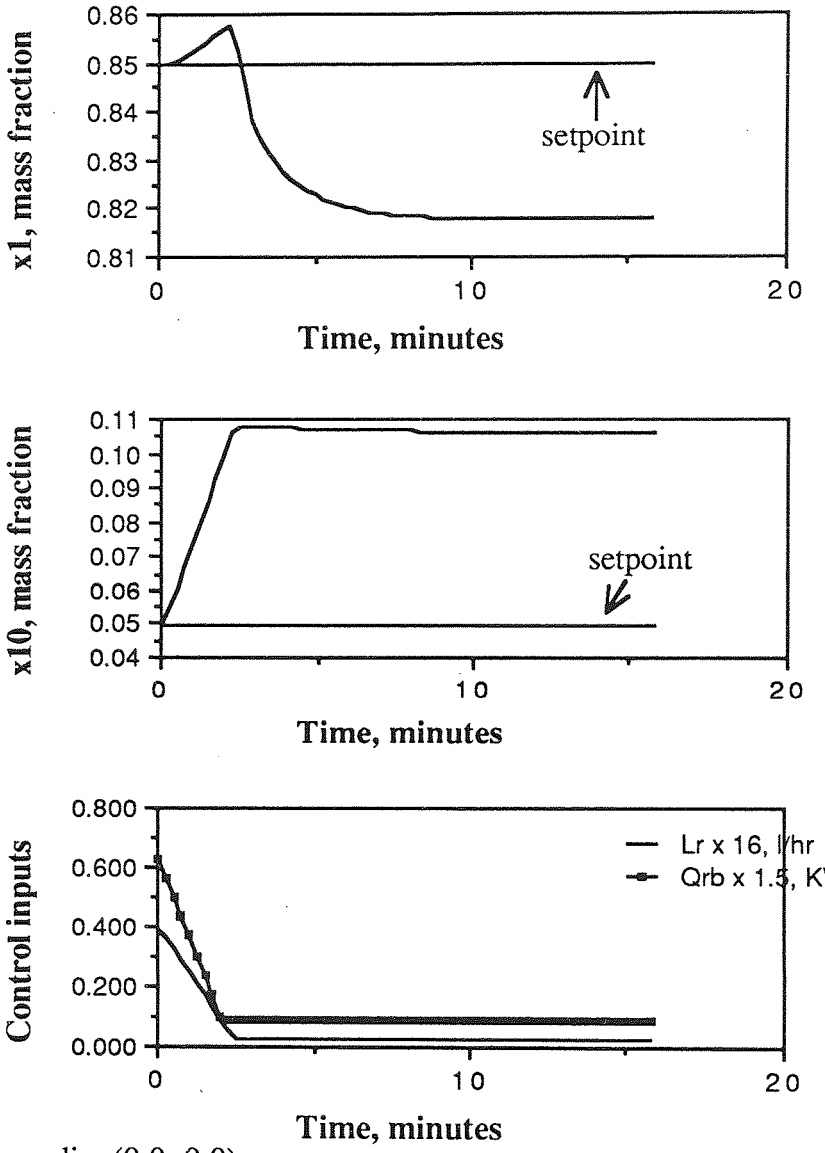

M_0 = diag(0.0, 0.0)

Figure 6.2. Load Disturbance rejection control - 25% increase in feed flow, Top tray and bottom tray compositions under control: Performance of an "integrator decoupled" system.

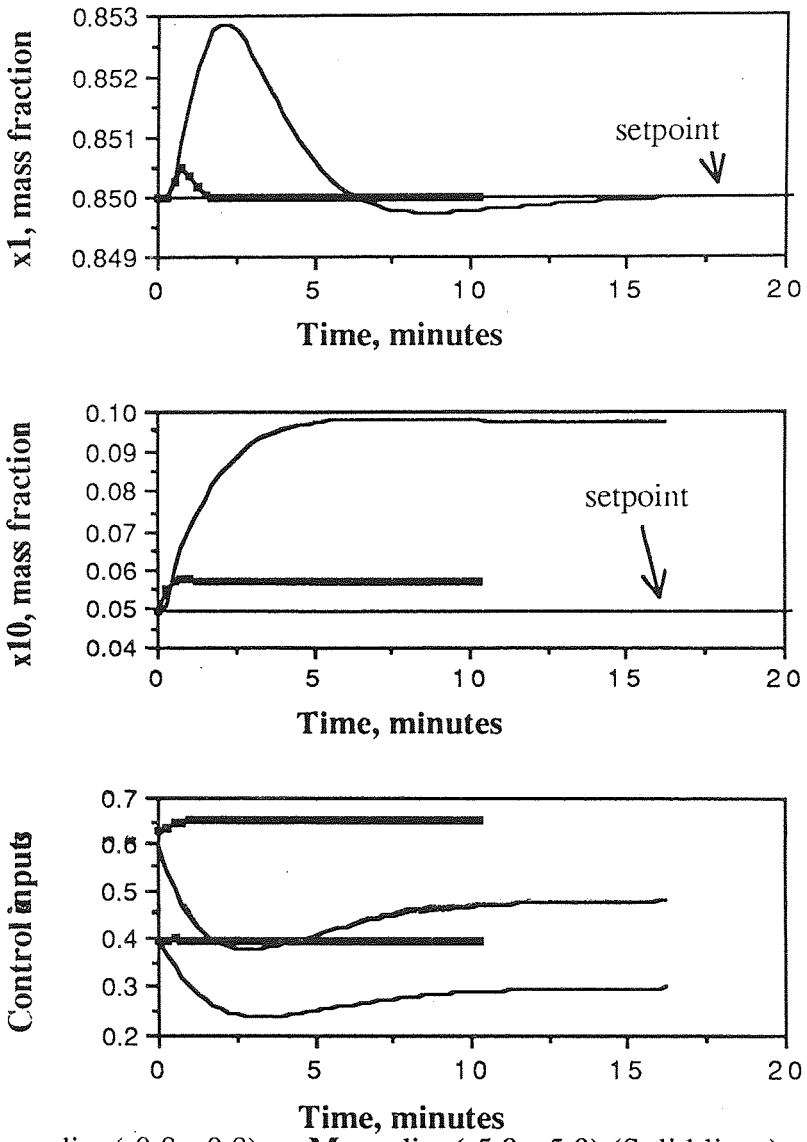

$\mathbf{M}_0$ = diag(-0.8, -0.8) vs $\mathbf{M}_0$ = diag(-5.0, -5.0) (Solid lines)

Figure 6.3. Load disturbance rejection - 25% increase in feed flow. Effect of pole assignments.

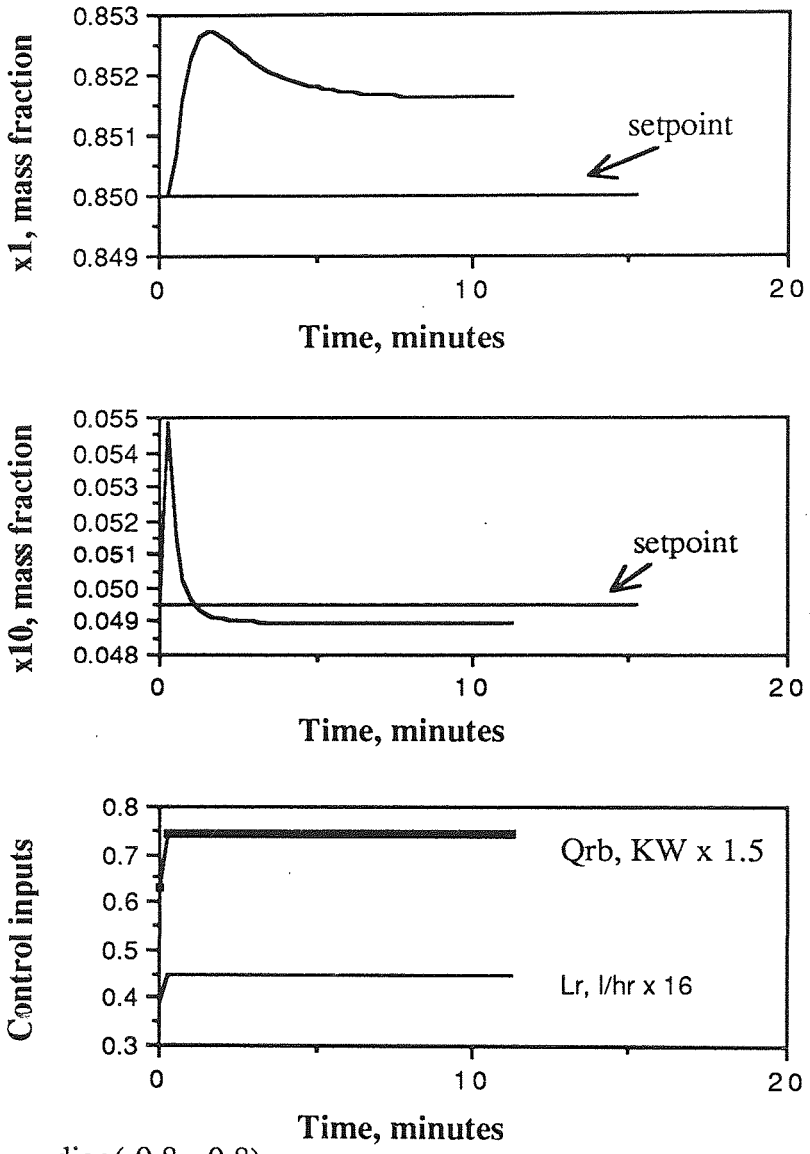

M_0 = diag(-0.8, -0.8)

Figure 6.4 Load disturbance rejection using the feedforward compensator, T_f. Load disturbance - 25% increase in feed flow

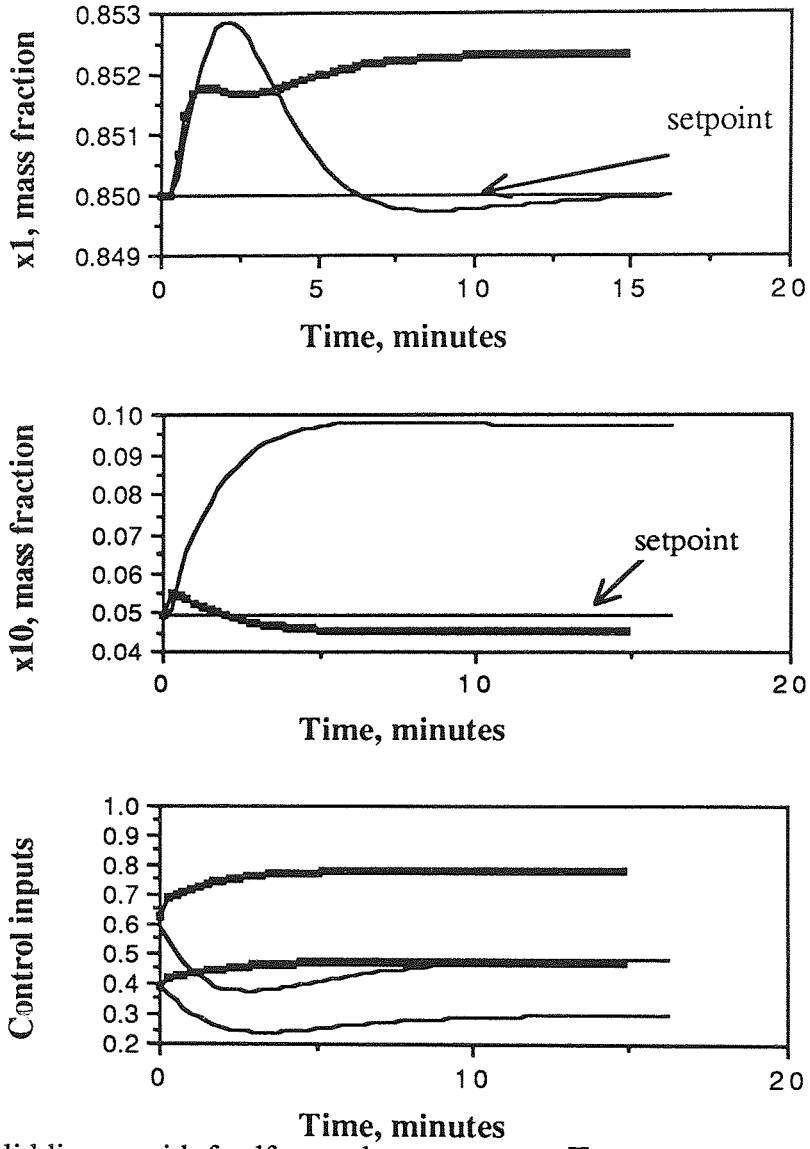

Solid lines - with feedforward compensator, T_f

Normal lines - state feedback alone

M_0 = diag(-0.8, -0.8)

Figure 6.5 Load disturbance rejection using the feedforward compensator, T_f, with state feedback. Load disturbance - 25% increase in feed flow

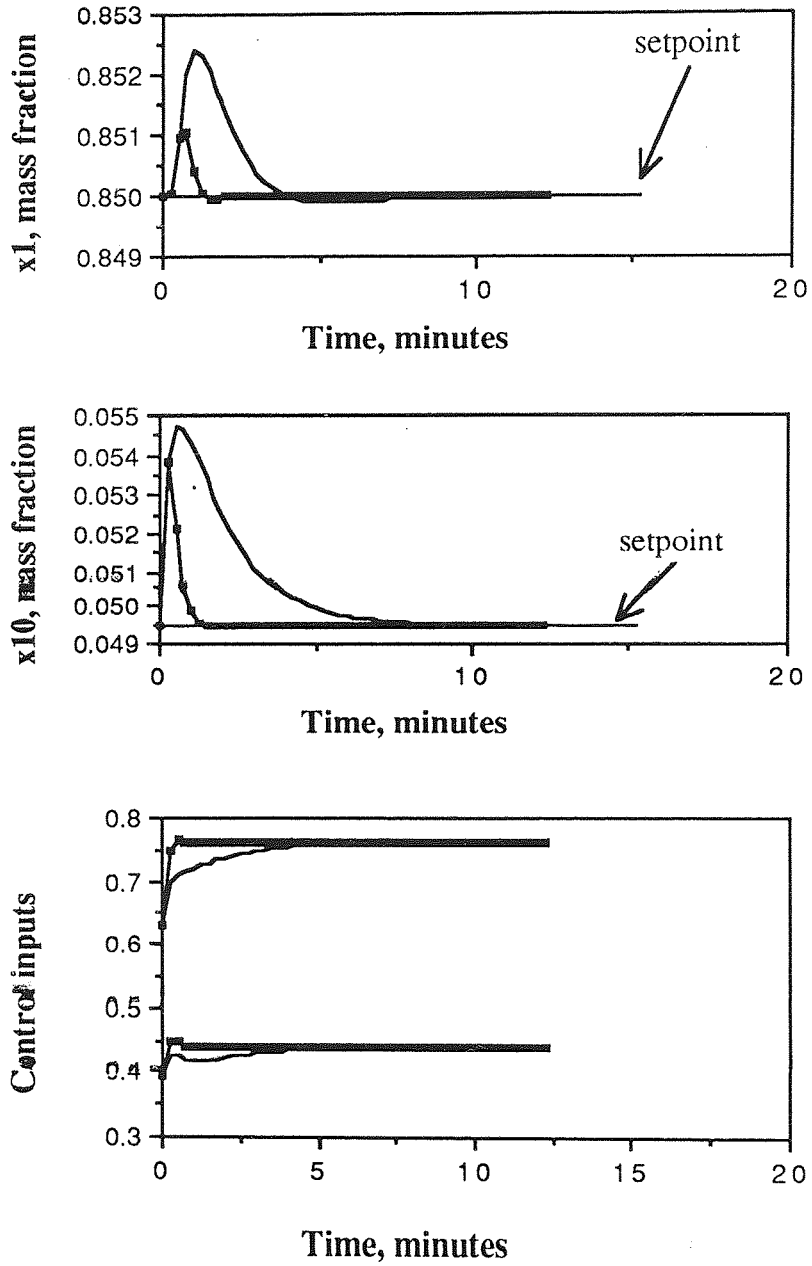

M_0 = diag(-0.8, -0.8) vs M_0 = diag(-5.0, -5.0) (Solid lines)

Figure 6.6 Load disturbance rejection - 25% increase in feed composition: Effect of pole assignments.

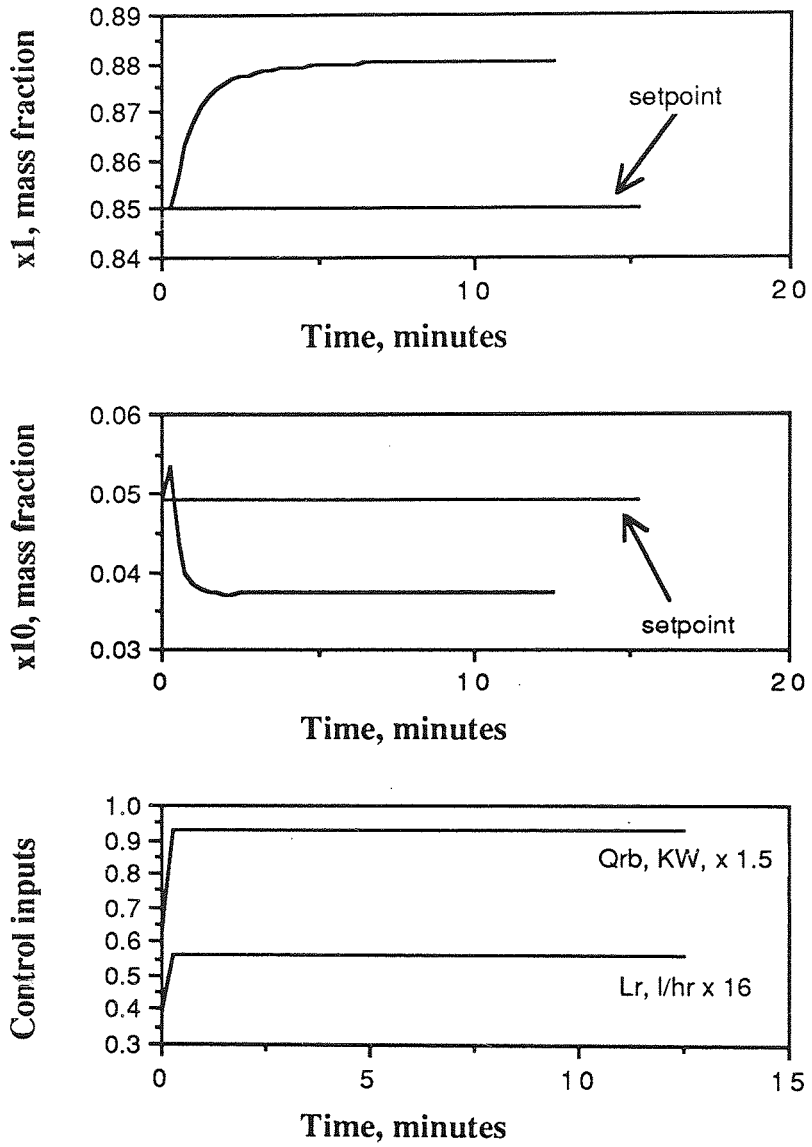

$\mathbf{M}_0$ = diag(-0.8, -0.8)

Figure 6.7 Load disturbance rejection using feed foward compensator, $\mathbf{T}_f$, alone. Load disturbance - 25% increase in feed composition

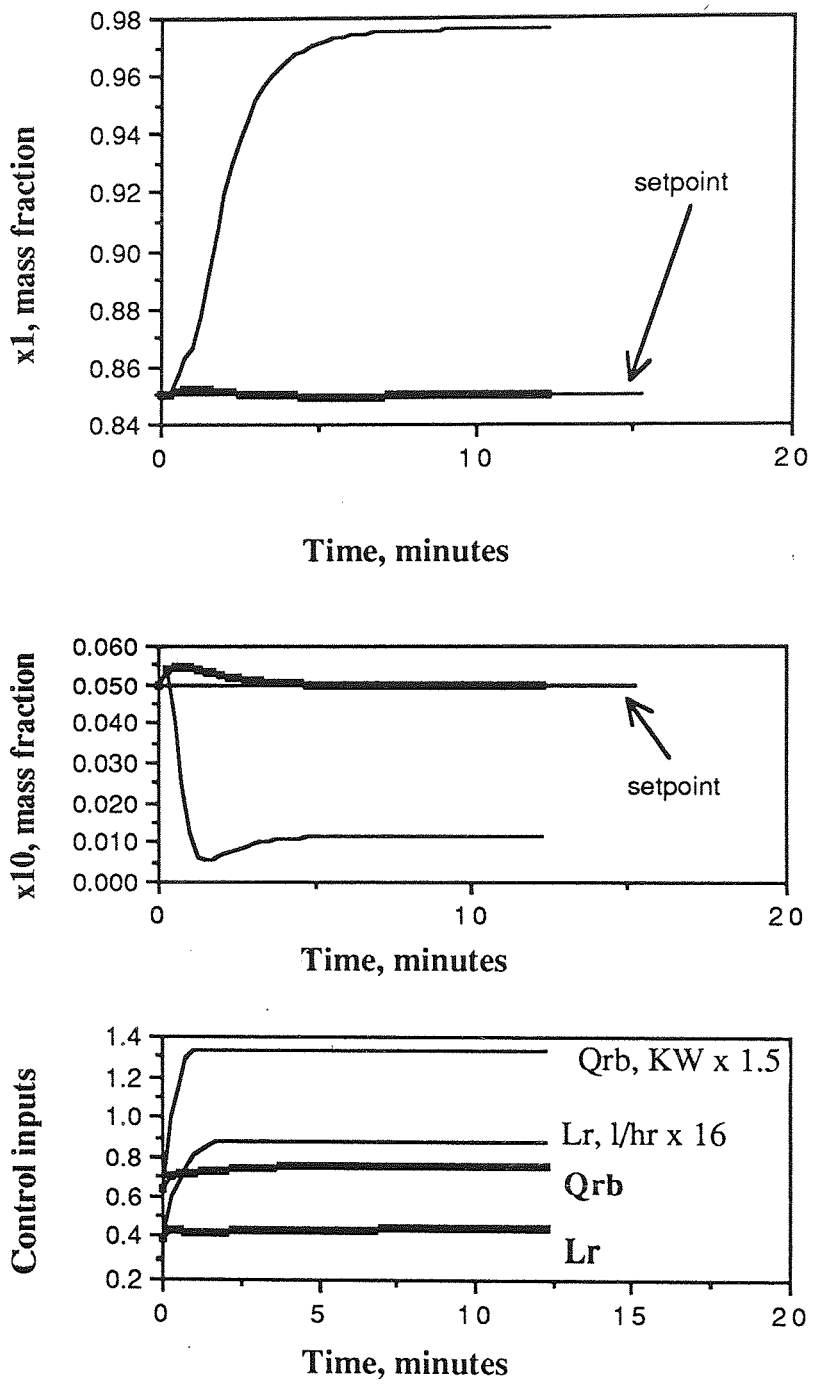

Normal lines - with feedforward compensator, T_f
Solid lines - state feedback alone
M_0 = diag(-0.8, -0.8)

Figure 6.8 Load disturbance rejection using the feedforward compensator, T_f, with state feedback. Load disturbance - 25% increase in feed composition.

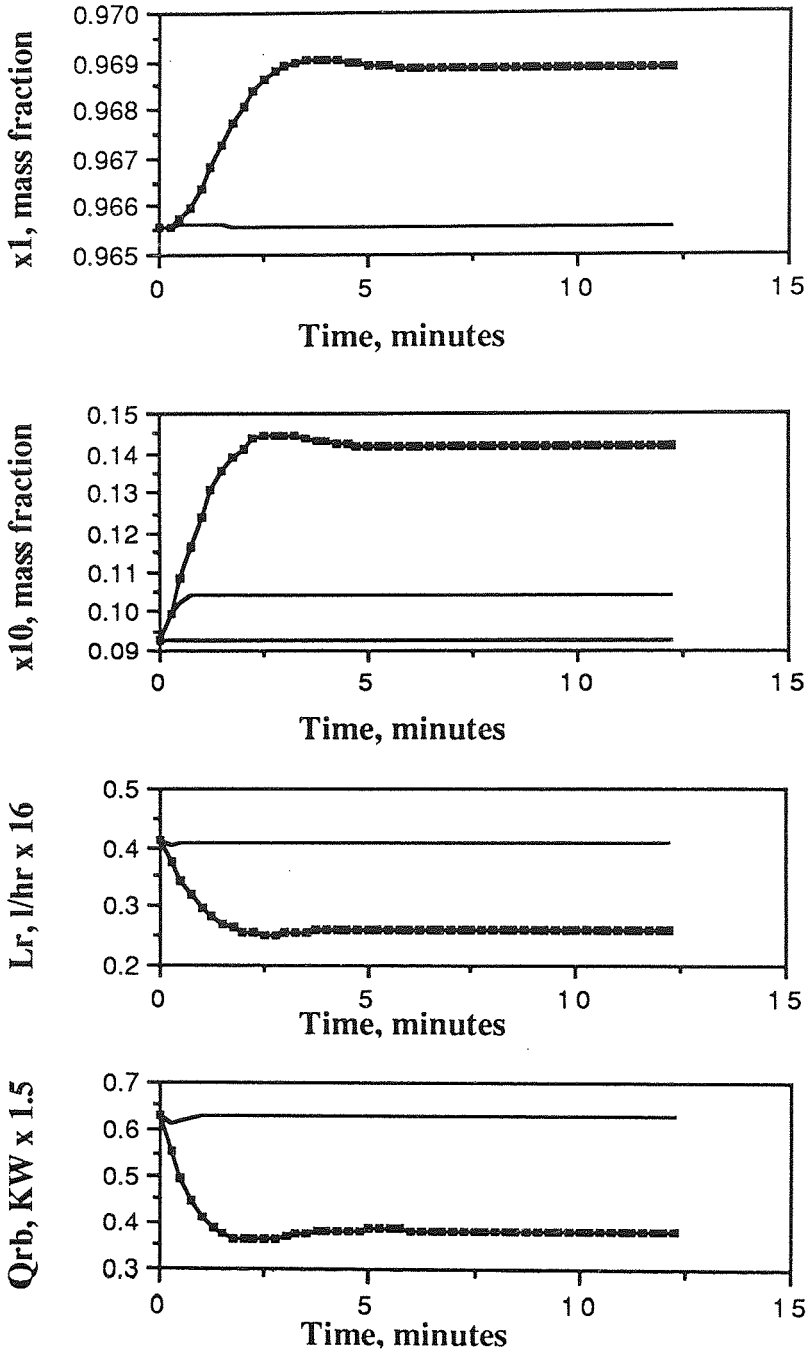

M_0 = diag(-5.0, -5.0) ;

Solid line - State feedback designed using model LM2 applied on model LM1
Normal line - State feedback designed using model LM1 applied on model LM1

Figure 6.9 Effect of non-linearities on the performace of the disturbance rejection controller: Load disturbance - 25% increase in feedflow.

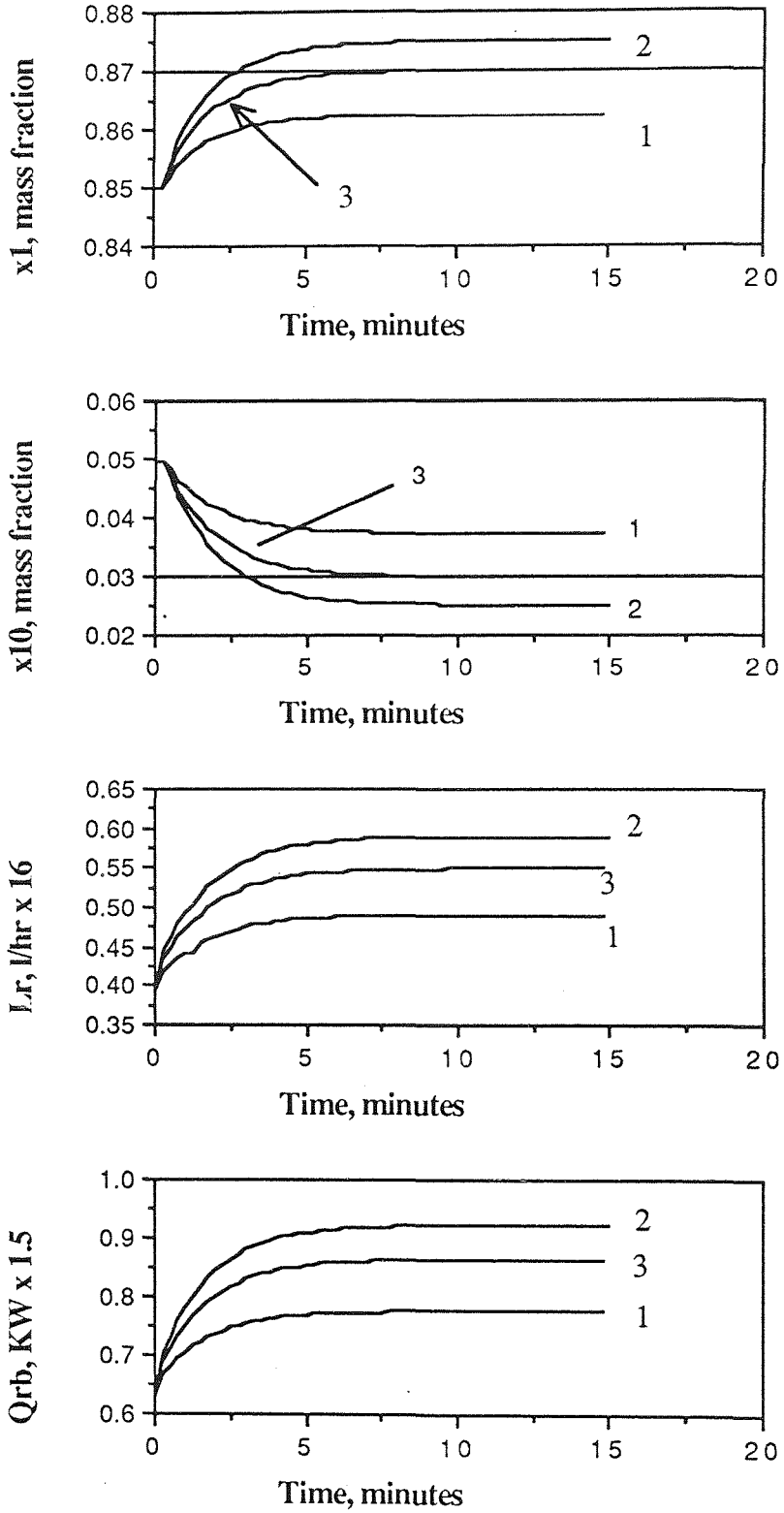

1 - K*= 0.5I; 2 - K* = I; 3 - K* = 0.8I

Figure 6.10 Setpoint tracking : M_0 = diag (-0.8, -0.8)

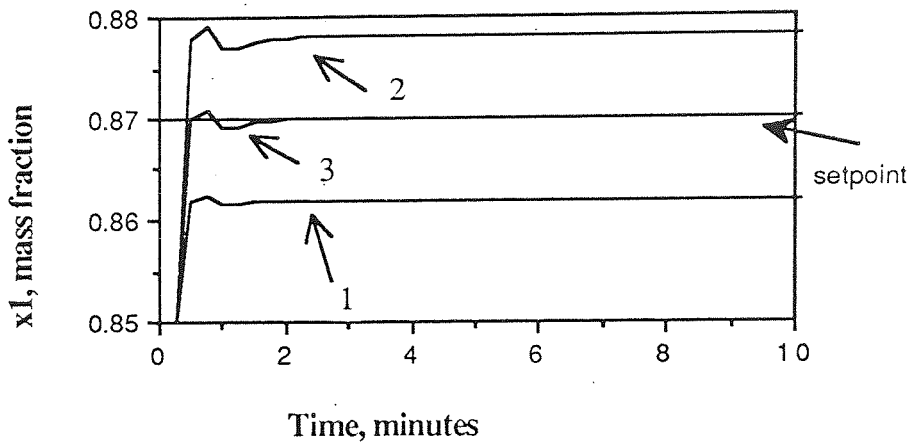

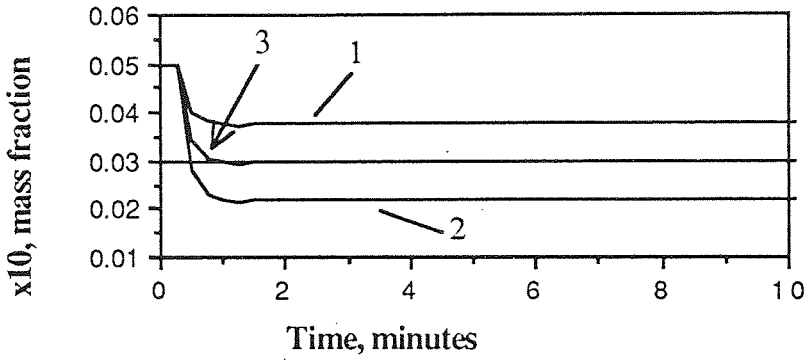

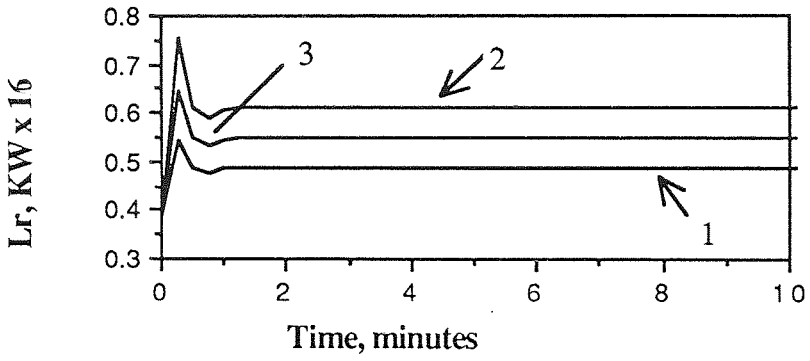

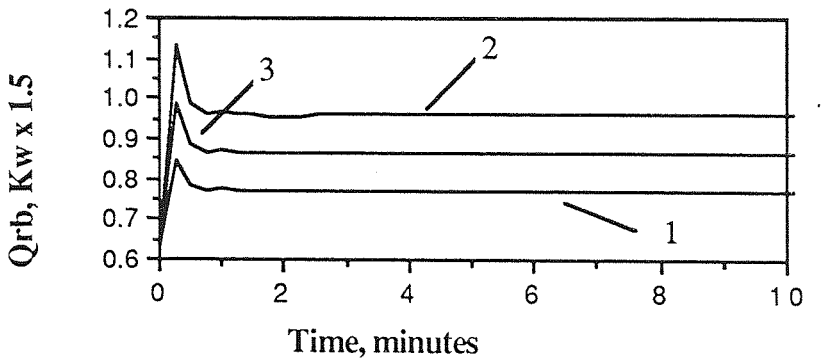

1 - K*= 3I; 2 = K* = 7I; 3 - K* = 5I

Figure 6.11 Setpoint tracking : M_0 = diag (-5, -5)

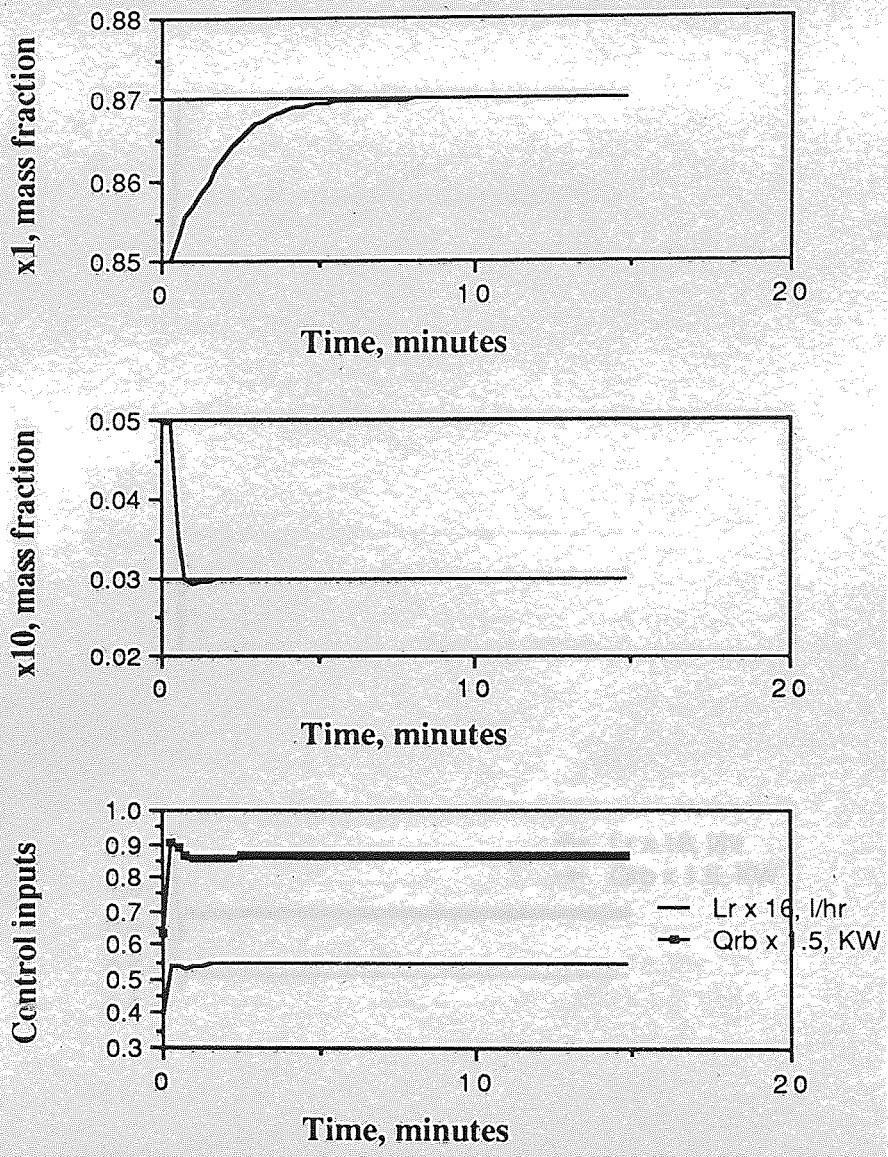

Figure 6.12 Setpoint tracking, $\mathbf{M}_0$ = diag (-0.8, -5), $\mathbf{K}^*$ = diag (0.8, 5)

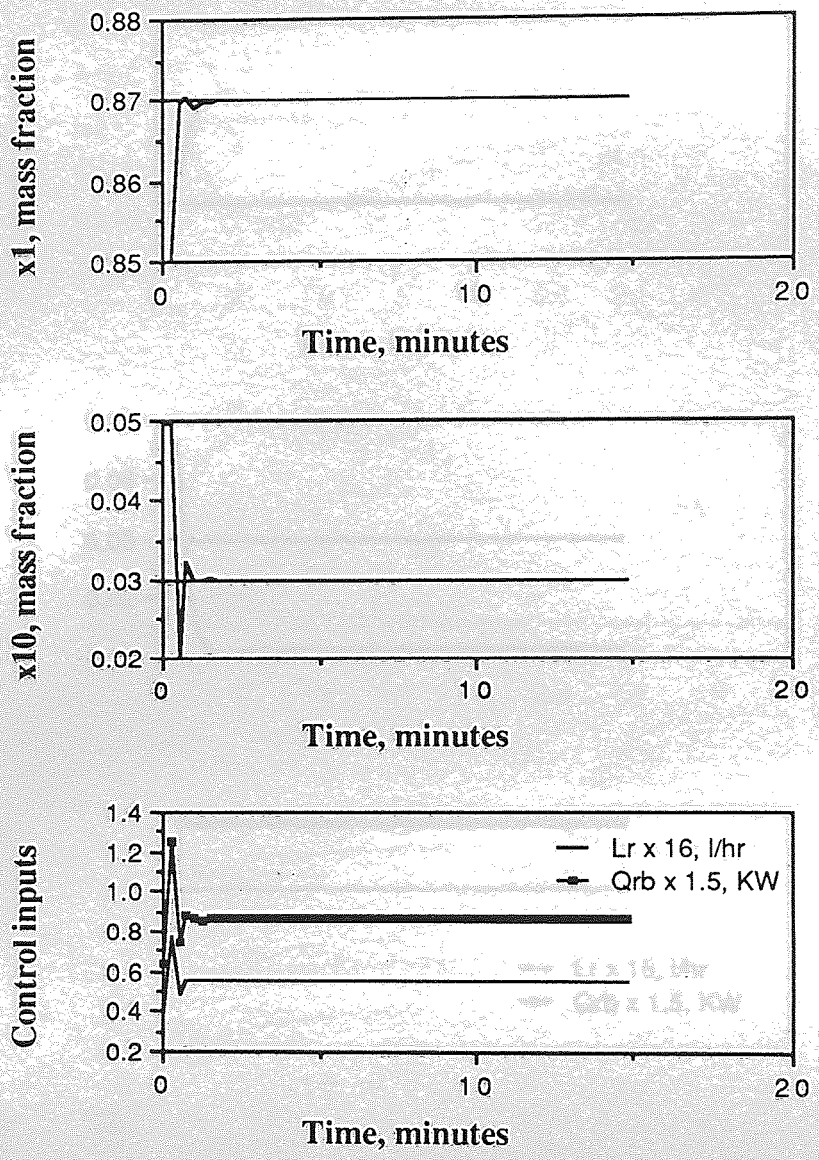

Figure 6.13 Setpoint tracking, $\mathbf{M}_0$ = diag (-5, -10), $\mathbf{K}^*$ = diag (5, 10)

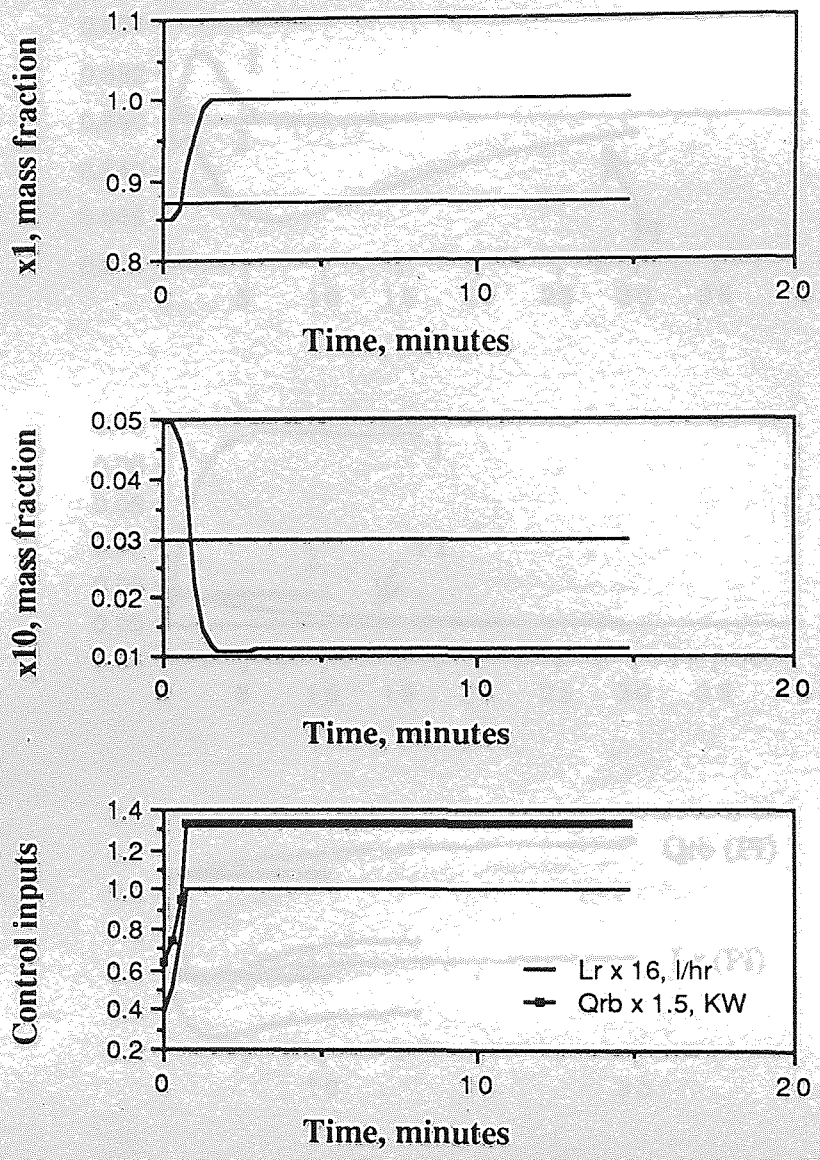

Controller design from model LM1 applied on model LM2

Figure 6.14 Setpoint tracking, $\mathbf{M}_0$ = diag (-5, -5); Effect of non-linearities.

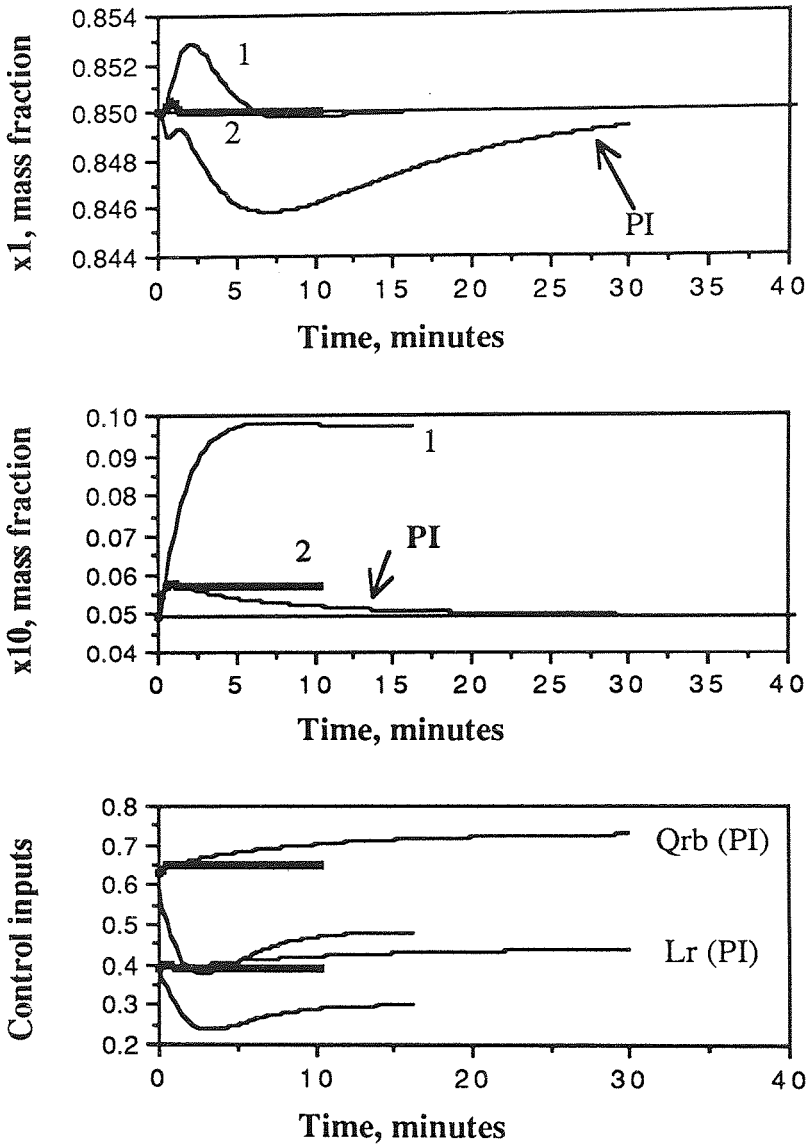

Figure 6.15 Comparison of multiple loop PI control with disturbance rejection control: Load disturbance rejection (25% increase in feed flow).

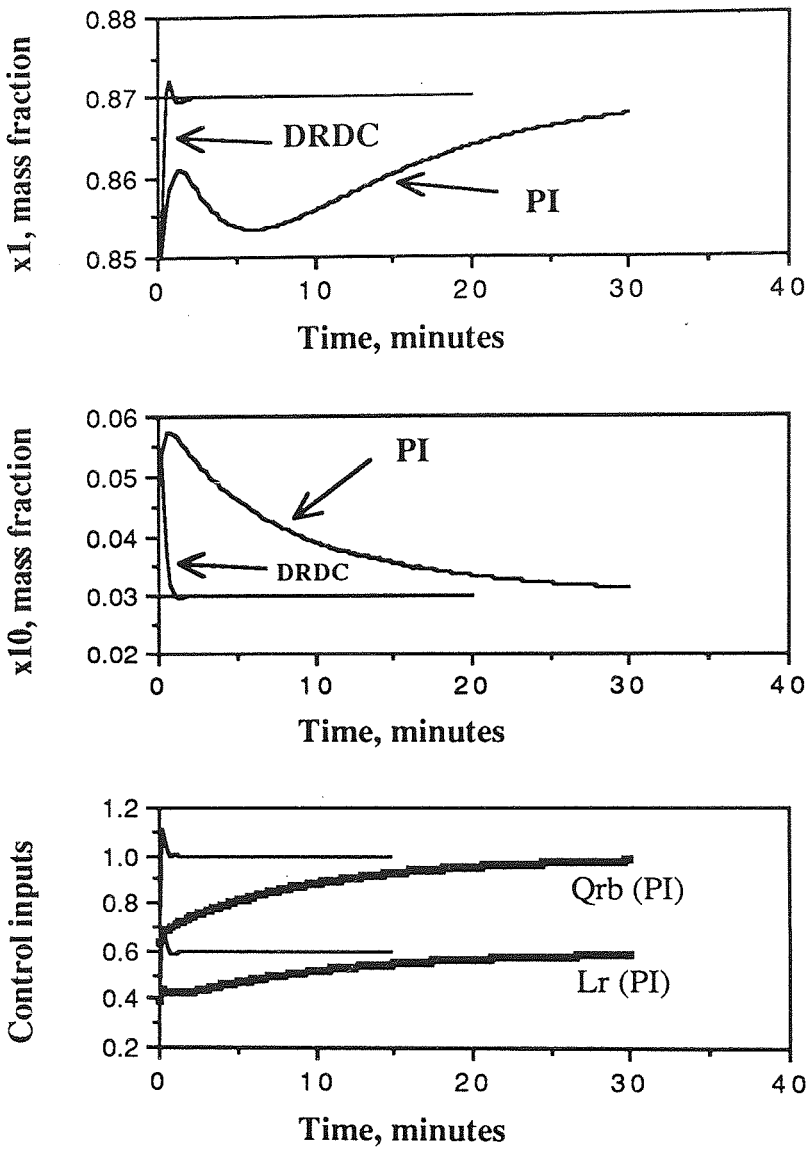

Load disturbance is 25% increase in feed composition

Figure 6.16 Comparison of multiple loop PI control with decoupling and disturbance rejection control: Setpoint tracking and load disturbance rejection, simultaneously.

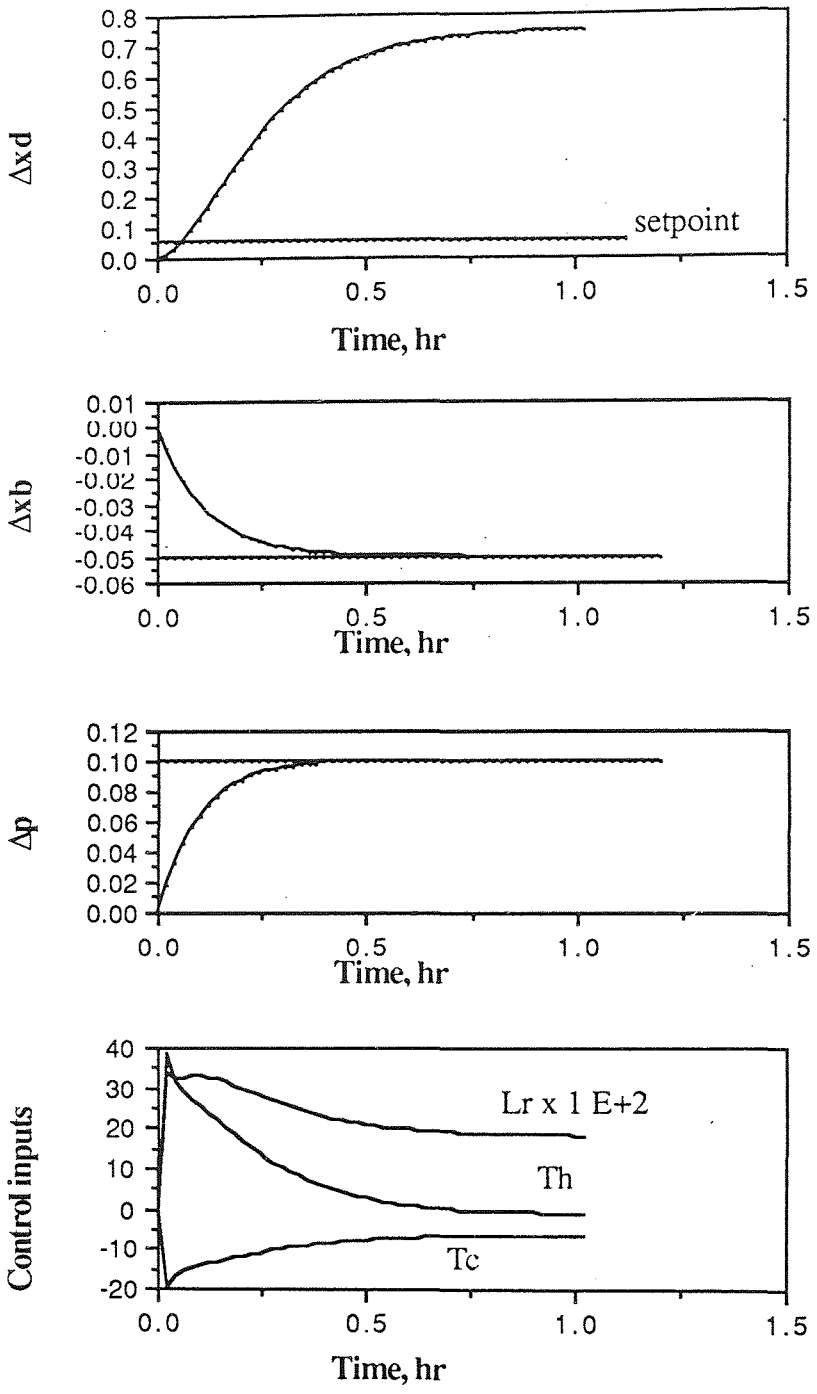

Figure 6.17 Application on the model of Shimizu and Matsubara (113): Setpoint tracking with $\mathbf{K}^*$ = diag (840, 9, 10)

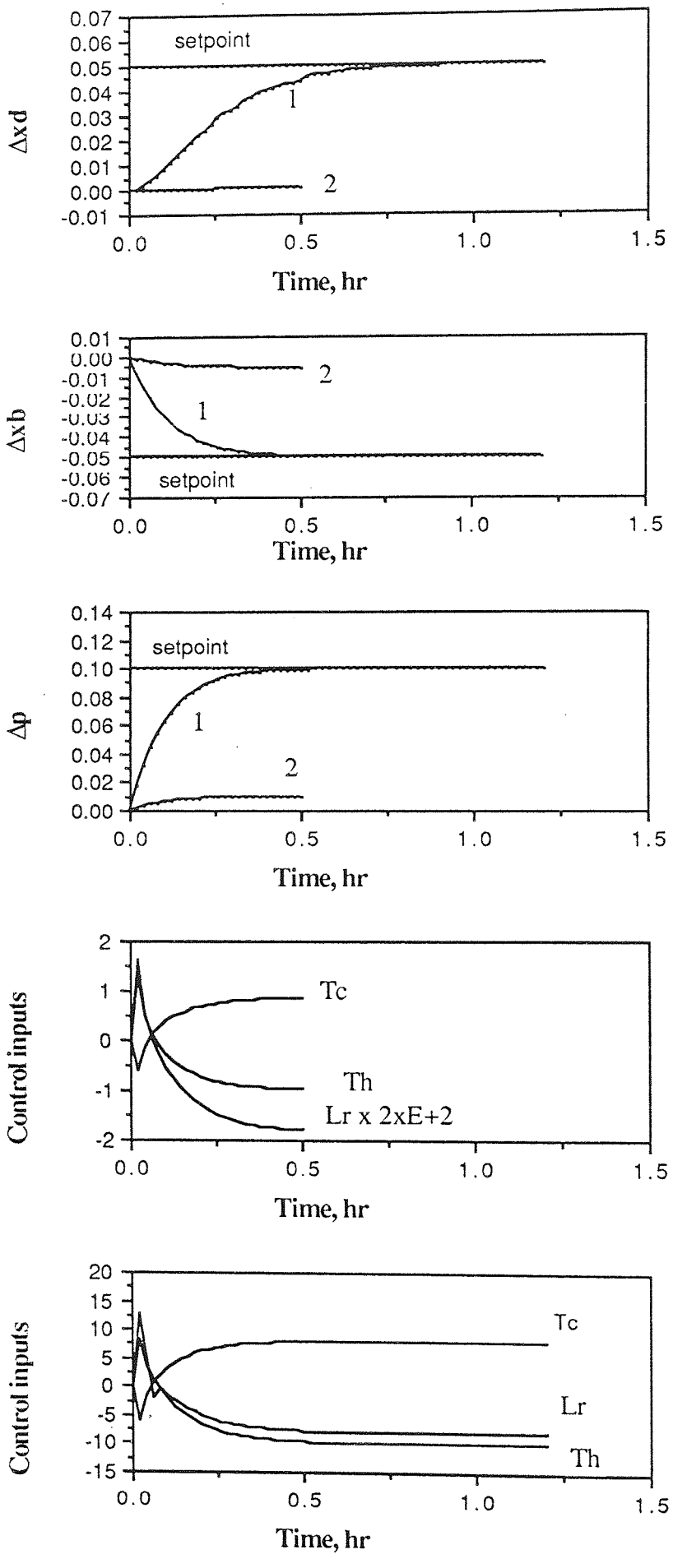

Figure 6.18 Application on the model of Shimizu and Matsubara (113): Setpoint tracking comparison of $\mathbf{K}^* = \text{diag}\,(56, 9, 10)$ and $\mathbf{K}^* = \mathbf{I}$

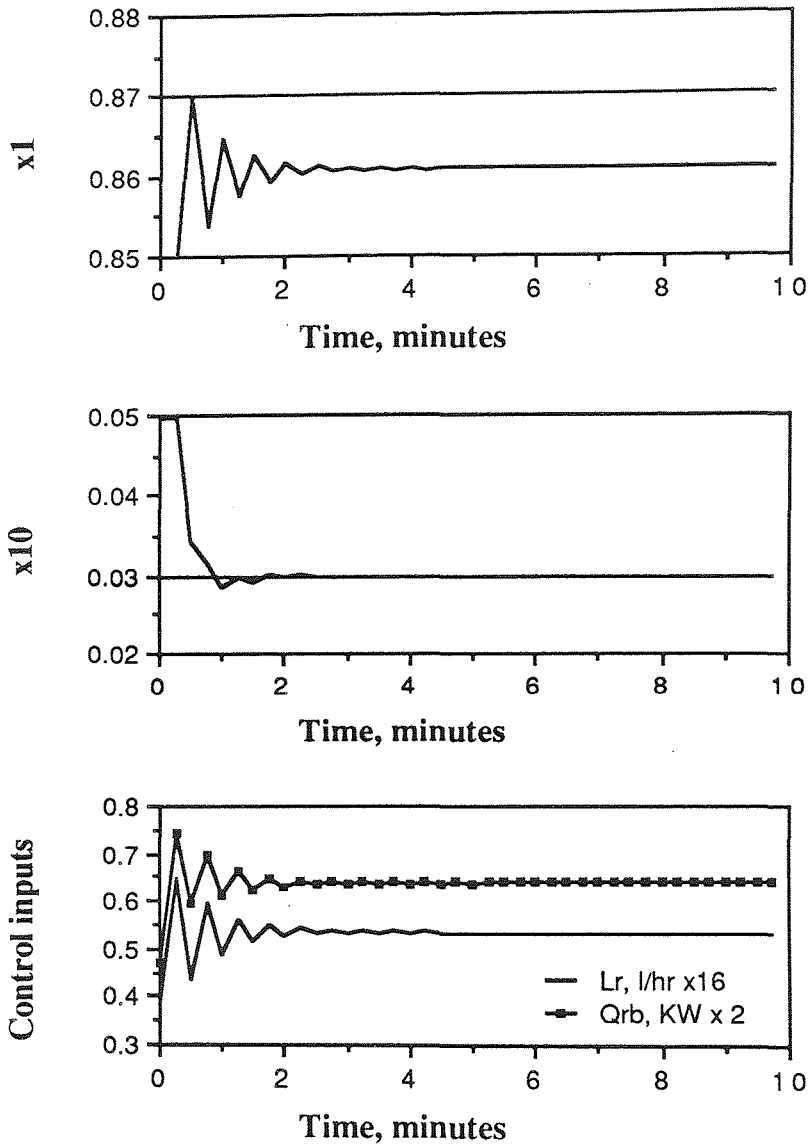

Figure 6.19 Effect of using less than the minimum number of state variables that should be measured: Top tray composition measurement not available.

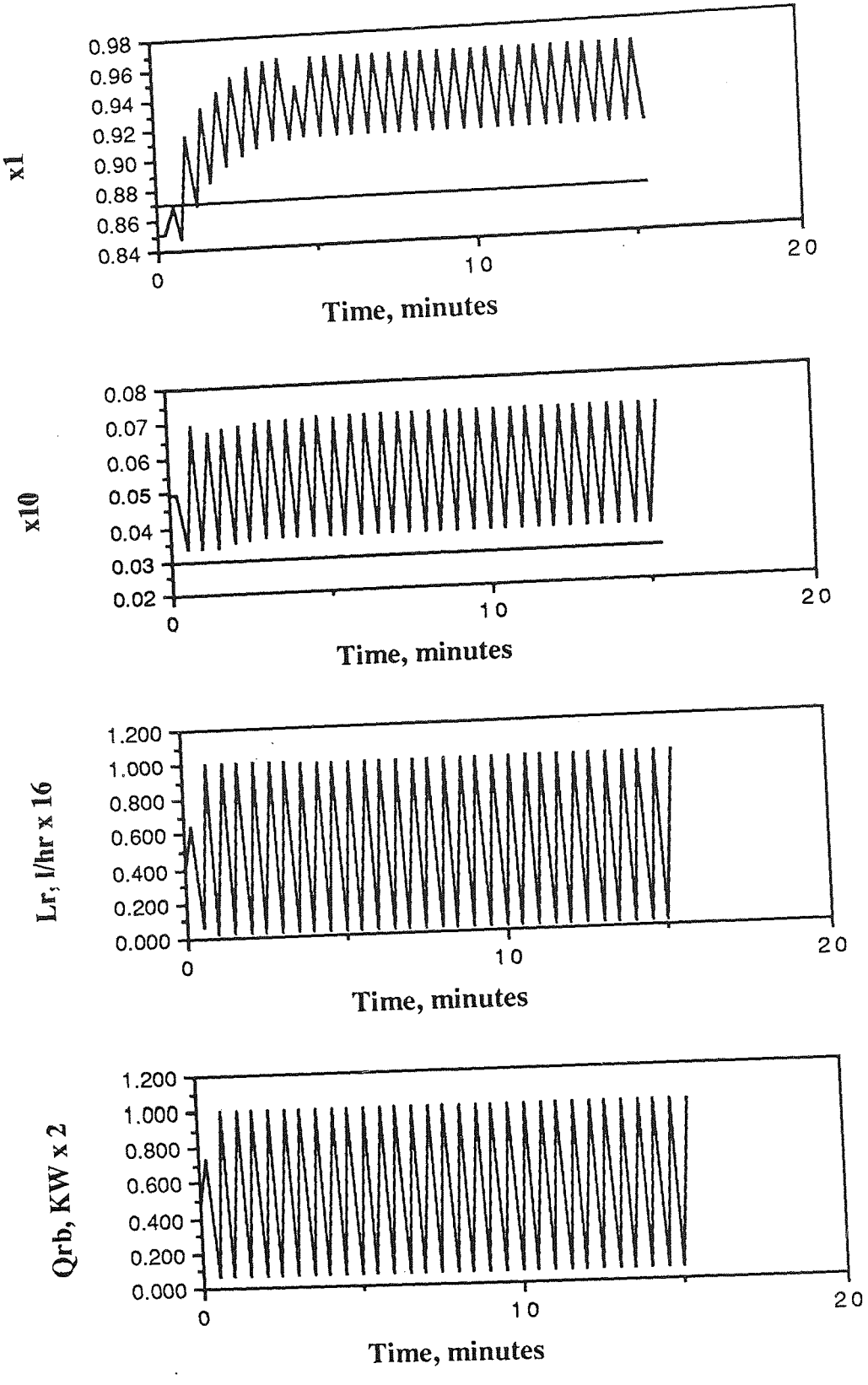

Figure 6.20 Effect of using less than the minimum number of state variable: Bottom tray composition measurement not available.

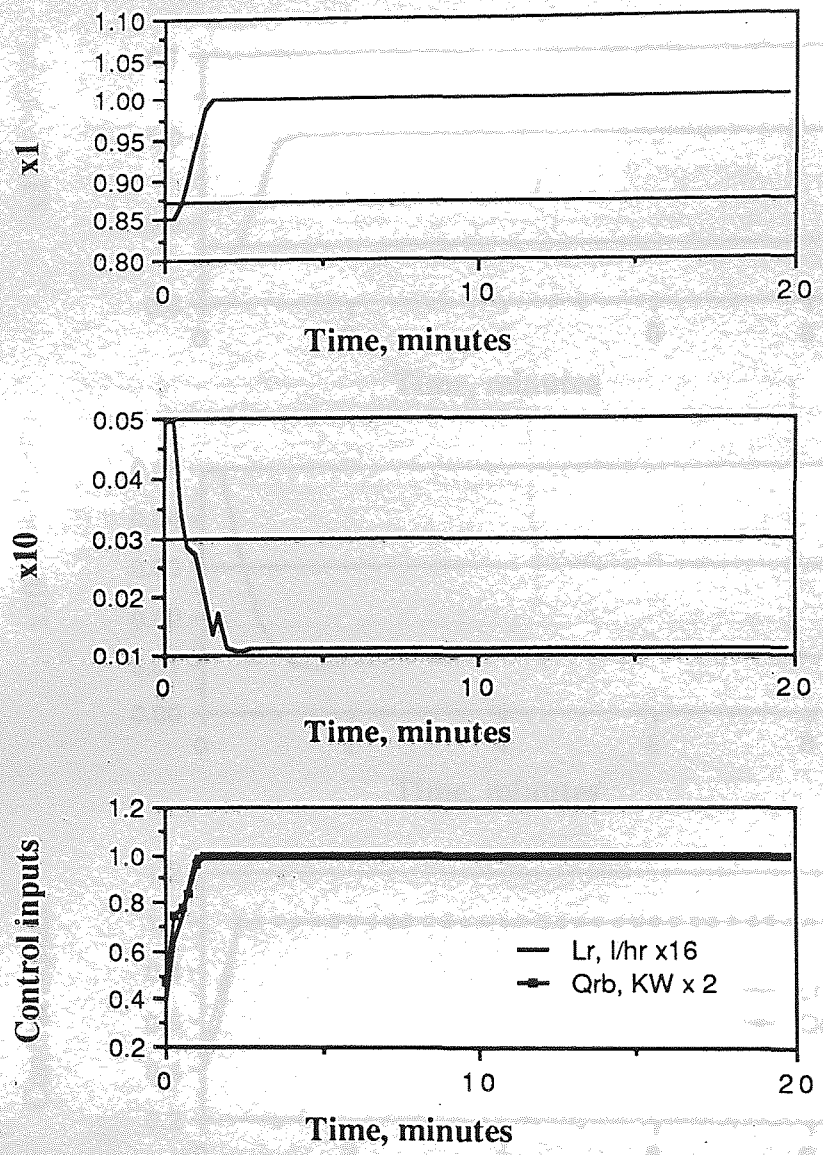

Figure 6.21 Effect of using less than the minimum number of state variable: Second tray composition measurement not available.

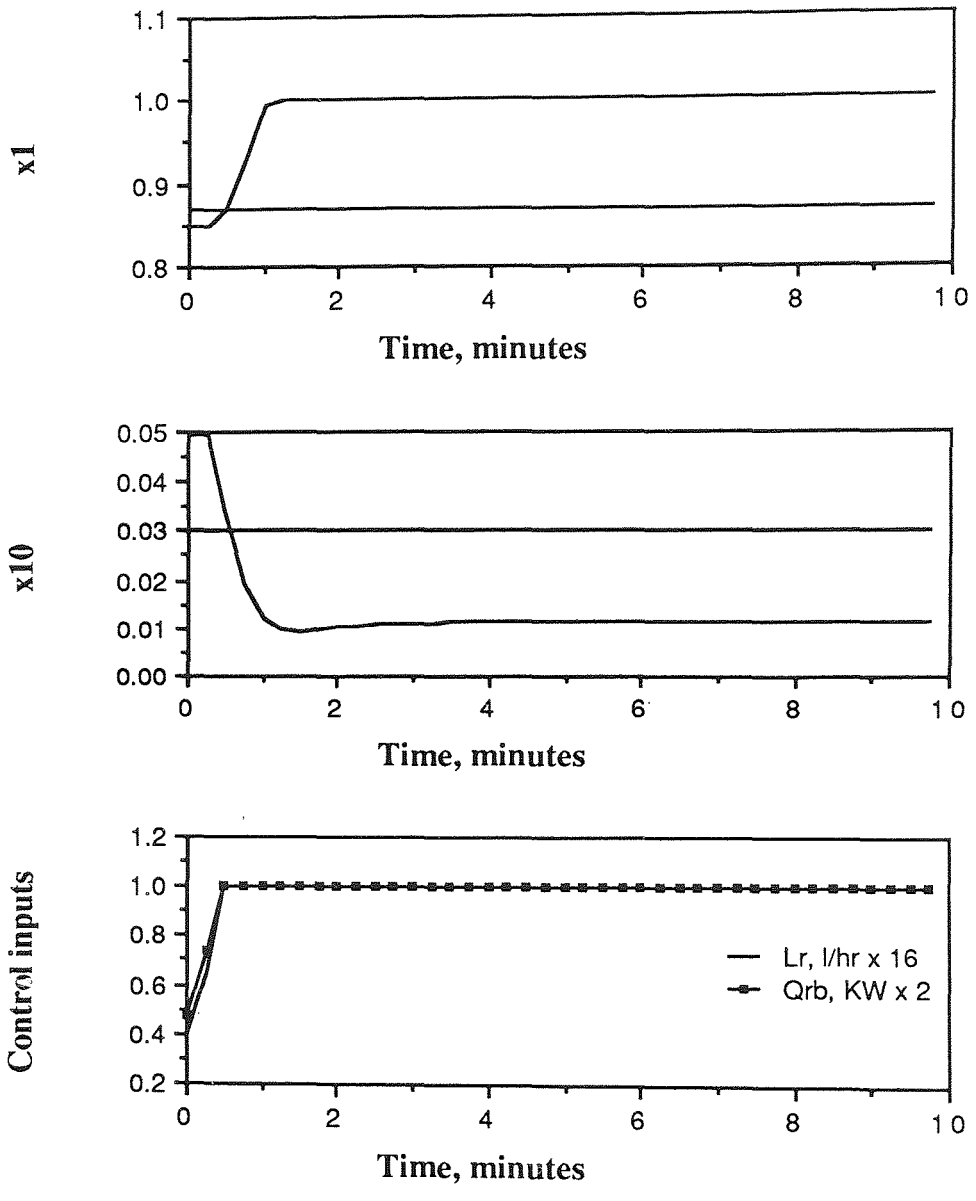

Figure 6.22 Effect of using less than the minimum number of state variable: Ninth tray composition measurement not available.

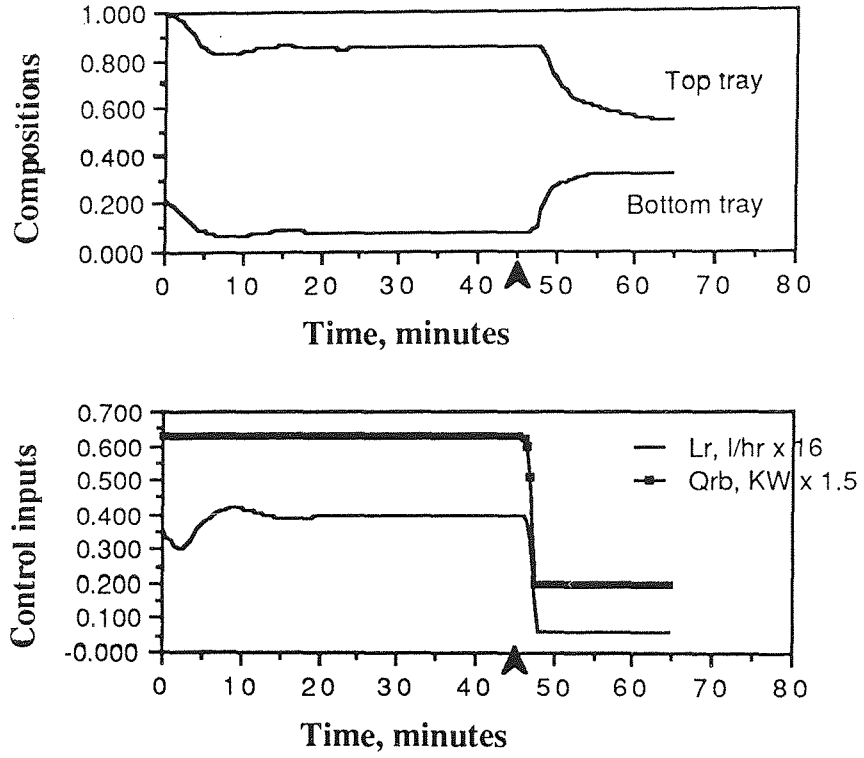

Arrow indicates point at which switch from PI to disturbance rejection control is made

Figure 6.23 Application of the disturbance rejection and decoupling control scheme on the column simulator.

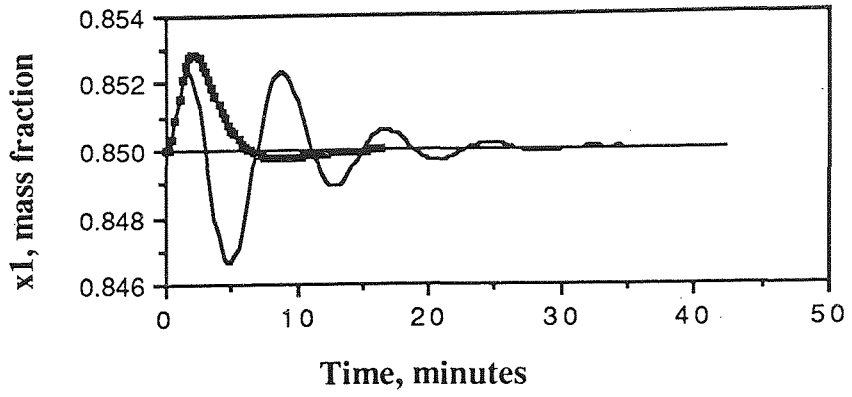

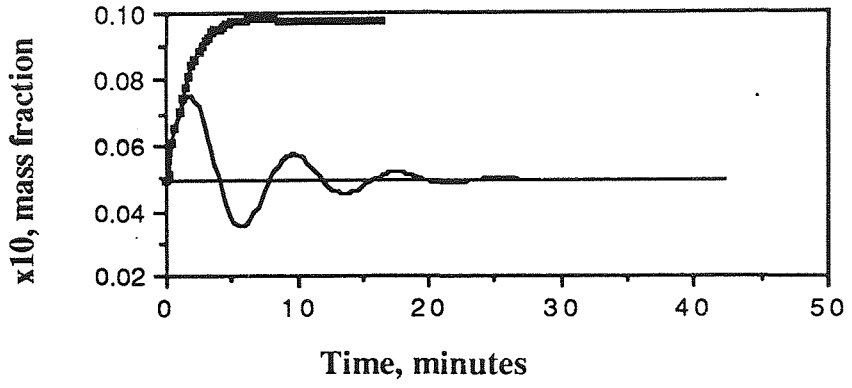

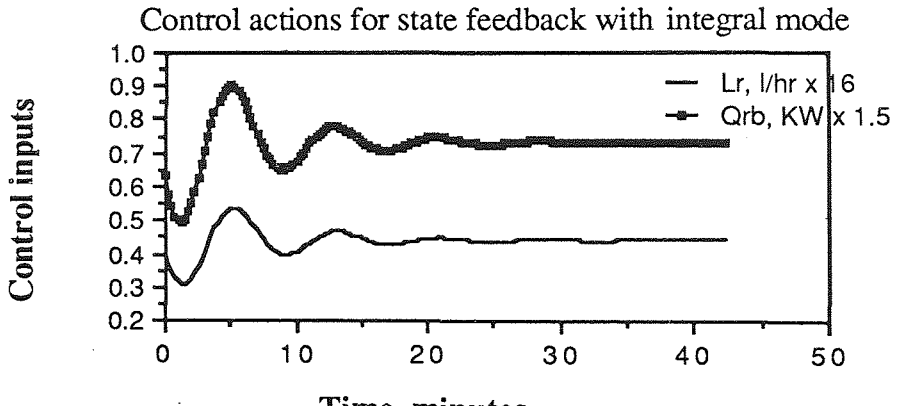

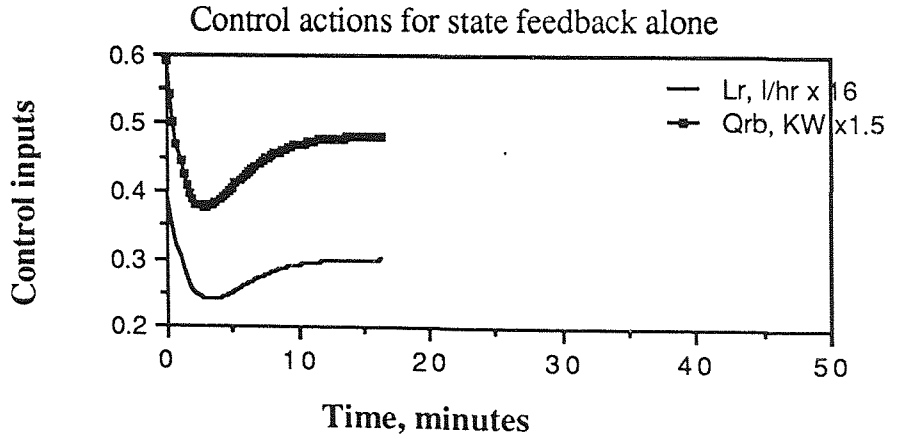

M_0= diag(-0.8,-0.8);T_I = diag (3.0, 1.2)

Figure 6.24 The performance of the decoupling and disturbance rejection conmtroller with integral mode for feed flow disturbance rejection

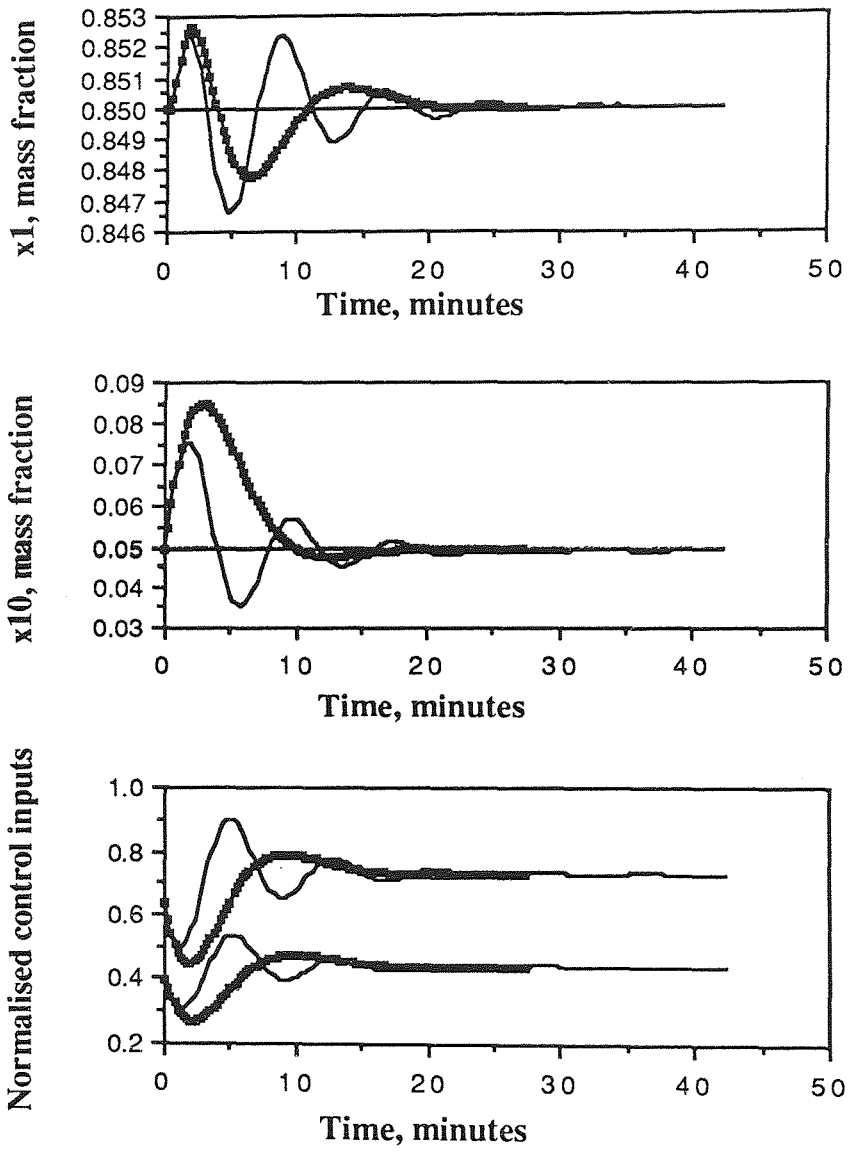

T_I = diag (3.0, 1.2) single lines

T_I = diag (7.0, 5.0) thick lines

M_0=diag(-0.8,-0.8)

Feed flow disturbance rejection

Figure 6.25 Effect of integral time on the performance of the decoupling and disturbance rejection controller with integral mode:

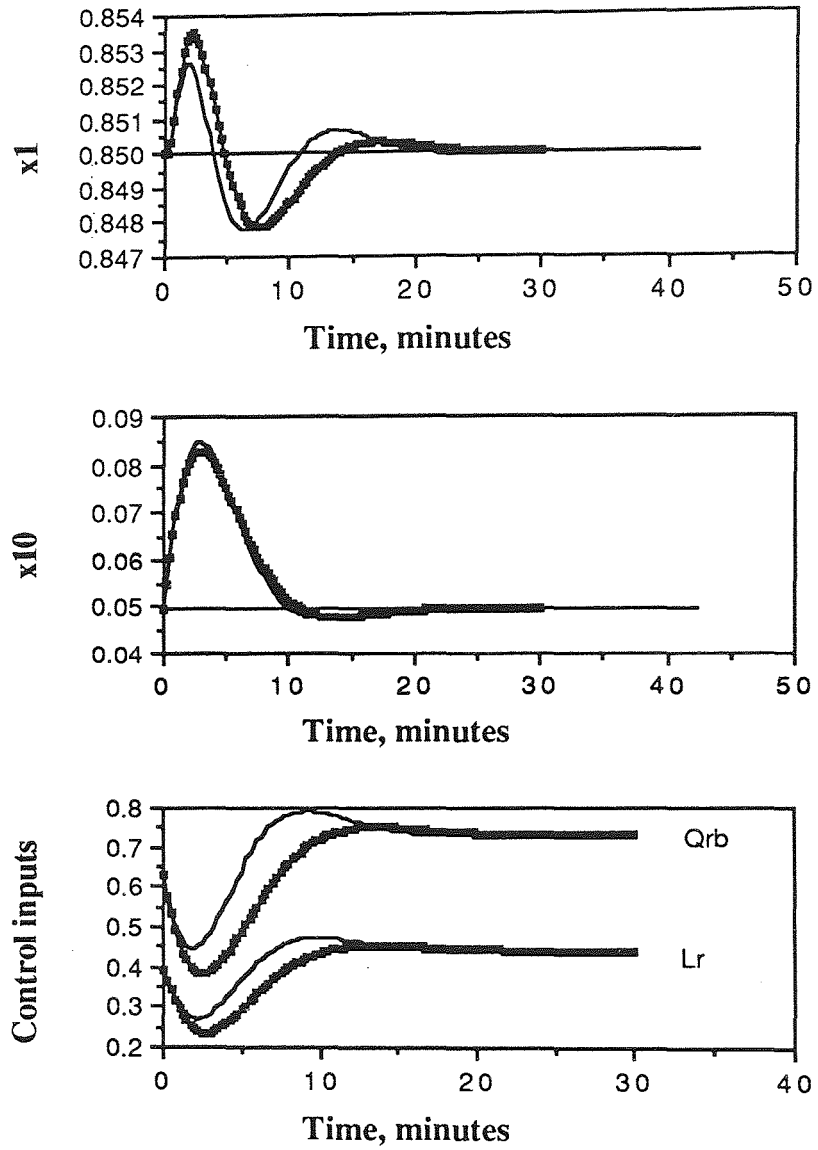

Normal lines - integral mode only included
Solid lines - integral plus derivative mode included

Figure 6.26 Effect of derivative mode on the performance of the disturbance rejection and decoupling controller with integral mode (Figure 6.25)

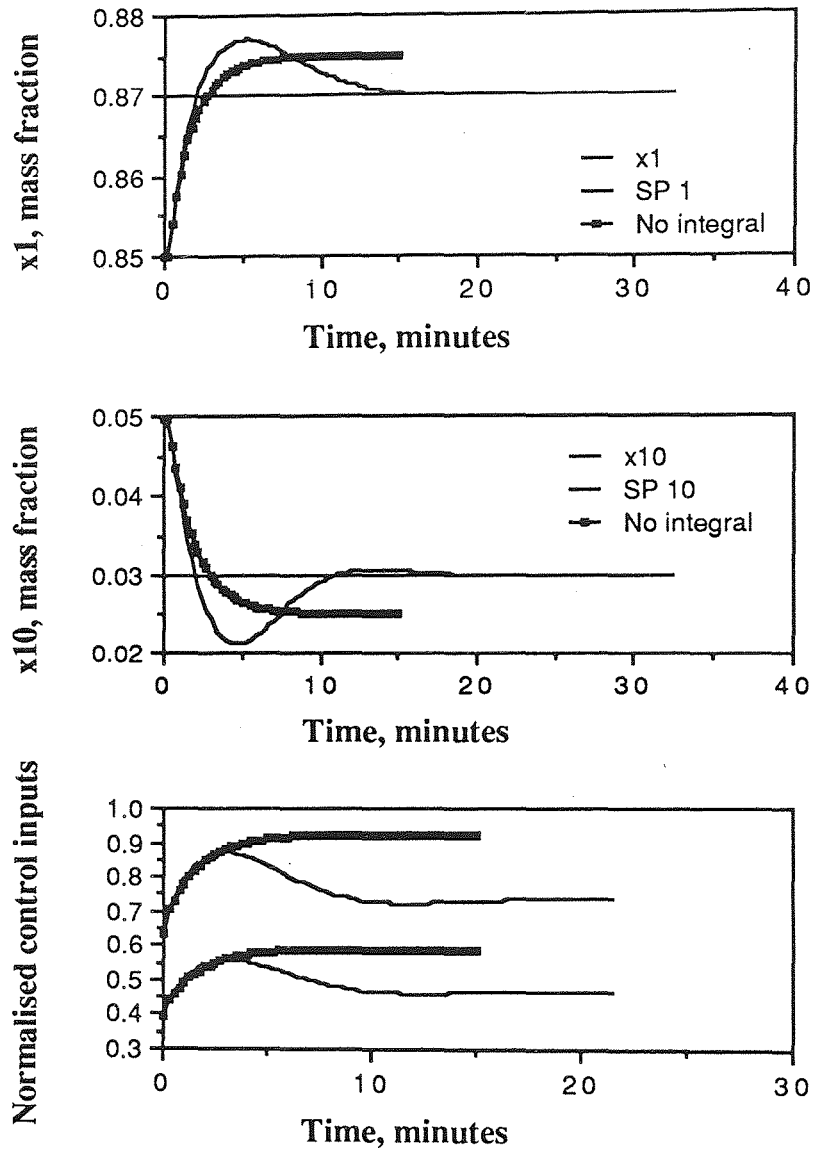

$\mathbf{M}_0$=diag(-0.8,-0.8) $\mathbf{K}^*$ = I and $\mathbf{T}_I$ = diag (7.0, 5.0)
Thick lines - No integral mode

Figure 6.27. Setpoint tracking; Use of integral action to remove offset due to wrong choice of $\mathbf{K}^*$

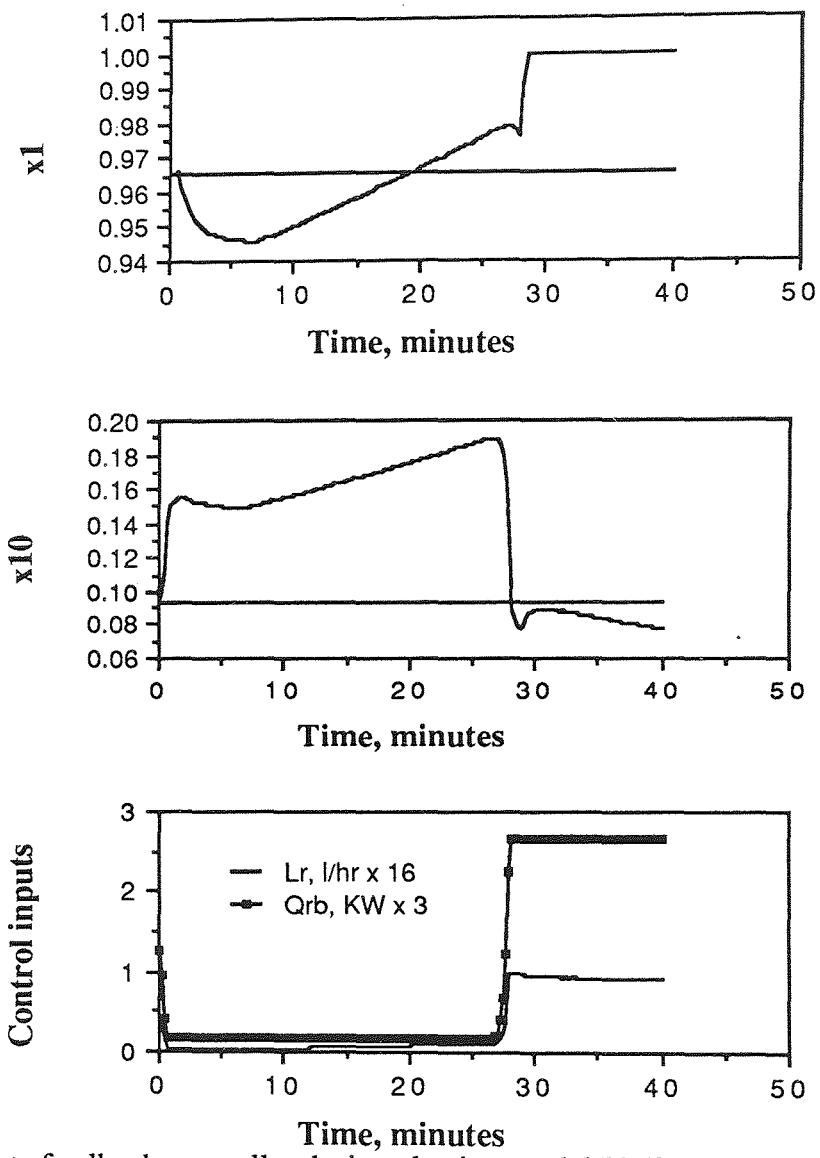

State feedback controller designed using model LM2 applied on model LM1.
For +25% feed flow disturbance

(Comparison with Figure 6.9 ; thick line trajectories)

Figure 6.28.Using integral action to attempt to remove offset due to non-linearity

CHAPTER SEVEN

Kalman Filtering Studies

7.1 Introduction

This chapter describes off-line Kalman filtering studies which were aimed at applying the Estimator Aided Feedforward control (EAFF) scheme of Daie (26) on the pilot plant distillation system. As discussed in Section 2.10.2, an extended Kalman filter functions as the estimator in the EAFF scheme to produce estimates of the top and bottom tray compositions from tray temperature measurements and other plant variables such as the feed flow and the reflux flow. The composition estimates are then used as the controlled variables for a multiple PI control system. Daie developed an EAFF for the distillation column which has been used in this research. As reported in Chapter 4, the column has been extensively modified in this work. Daie did not apply the EAFF control scheme on-line. This work was aimed to apply a modification of Daie's EAFF to the modified column.

As reported in the Section 2.10.1, Shaffii (115) attempted on-line implementation of the extended Kalman filter on the same distillation column and met with problems of computer memory limitations and excessive filter cycle time due to the computational load of the filter algorithm. Shaffii suggested simplifying the filter algorithm, and stressed that efforts should be directed at reducing the filter's execution time in order to enable real time application of the extended Kalman filter to be practical. Only then could the EAFF control scheme be practical for on-line application on the distillation column. This possibility was investigated in this work, as mentioned in Chapter 3. More powerful real time computing also relaxes the restriction on computational load and program memory requirements of the filter.

The linear state variable model of the column, model LM2 on Table 5.2b in Chapter 5, was used as the filter model. The use of the linearised state variable model in the design of the decoupling and disturbance rejection control was discussed in the previous chapter. The results demonstrated that it is not satisfactory to use the model

for controller design for the non-linear distillation system without incorporating a way for compensating for the non linearities neglected in the state variable model. The model may be limited as regards use for design of a state variable feedback controller for the distillation column, but it could be useful in the estimator to produce the required variables for implementing control. This possibility arises because there are some design parameters in the Kalman filter which can be adjusted to compensate for uncertainties in the filter model. These design parameters are the initial error covariance matrices and the system noise covariance matrix. How they are adjusted and how they affect the performance of a Kalman filter has been discussed in Section 2.10.1. Also uncertainties at different locations in the model could be addressed separately, as each diagonal element in the covariance matrices correspond to a differential equation in the state variable model.

7.2 The requirements of the Kalman filter

The main simplification made in the extended Kalman filter discussed in Section 2.10 was to use the linear state variable model of the distillation column as the filter model. The resulting simplified Kalman filter was required to satisfy the following requirements:

(i) Provide good estimates of the tray compositions particularly the top and bottom tray compositions which are the intended controlled variables.

(ii) The estimates should be free from static errors.

(iii) Provide good estimates of the measured inputs such as the feed flow, reflux flow and reboiler heat input.

If all these requirements are met then applying the EAFF scheme on the pilot plant distillation system could be considered. The interval of 30 seconds was chosen for the real time control of the column to allow for data logging, data storage control calculation. The "target" cycle time that the filter must meet was 15 seconds at the most, allowing 15 seconds for data logging, data conversion and control calculations.

7.3 Formulation of the Kalman Filter

The linearised state variable model of the column is

$$\mathbf{dx/dt} = \mathbf{Ax+Bu+Dzd} \qquad 7.1$$

The measured variables relate to the state variables as

$$\mathbf{y} = \mathbf{h(x)} \qquad 7.2$$

where A, B, D and **h** are, respectively, the state matrix, input driving matrix, disturbance matrix and the matrix relating the measurement vector **y** and the state vector **x**. The **h(x)** is non linear since the tray temperature relates to composition by a non linear relationship given by the vapour liquid equilibrium relationship. The **u** and **zd** are the vectors of the inputs and the disturbances, respectively. Assuming n is the number of states, m is the number of inputs, nd is the number of disturbances and nm is the number of measurements then **x**, **y**, **u** and **zd** are n x 1, r x 1, m x1 and p x 1 vectors, respectively. A, B, D and **h** are n x n, n x m, n x p and r x n matrices, respectively.

To minimise the computational overheads of the filter program, the reboiler drum and reflux drum composition were excluded as state variables in the filter model. Therefore, n = 10, m = 2 and nd = 2. The corresponding vectors, **x**, **u** and **zd** are given as

$$\mathbf{x} = [x_1, x_2, ..., x_n]^T$$

$$\mathbf{u} = [Lr, Q_{rb}]^T$$

$$\mathbf{zd} = [F, xf]^T$$

All the tray compositions and all the inputs in **u** and **zd** are to be estimated. Then the filter model can be reformulated as

$$\mathbf{dX/dt} = \mathbf{AX} \qquad 7.3$$

where $\mathbf{A} = \begin{bmatrix} A, B, D, \\ 0, 0, 0, \end{bmatrix}$ (n+m+p) x (n+m+p) matrix

$$\mathbf{X} = [\mathbf{x}^T, \mathbf{u}^T, \mathbf{zd}^T]^T$$

The measurement vector **y** will contain the measured tray temperatures as well as the measured inputs.

To evaluate the performance of the filter algorithm in the case of estimating the tray compositions, the tray compositions were required for comparison with the estimates produced by the filter. This was done using the non-linear relationship between the measured tray temperature and the composition on that tray for a binary system. This is given as

$$\underline{x}_1 = (P_T - P_1^0(T)) / (P_1^0(T) - P_2^0(T)) \qquad 7.4$$

where $\underline{x}_1$ is the mole fraction of the more volatile component (mvc), T boiling point of the liquid, P_T is the column pressure and $P_1^0(T)$ and $P_2^0(T)$ are the saturation vapour pressures of the mvc and the less volatile component (lvc), respectively. The relationship in Equation 7.4 is obtained from the following physical laws:

1) Raoults Law $\underline{x}_i P_i^0(T) = P_i$

2) Daltons law of partial presures $P_i = \underline{y}_i P_T$

3) Antoine relationship $\text{Log}_{10} P_i^0(T) = C1_i - C2_i/(C3_i - T)$

where P_i is the partial pressure exerted by the vapour of component i. The major error introduced in the calculation of the tray compositions from Equation 7.4 is due to pressure variations inside the column. The activity coefficients were omitted in the above equation for simplicity; simulations on the column simulator showed that they were close to one, for the chemical system used.

Since Equation 7.4 relates the measured tray temperatures to tray compositions through $\mathbf{h}(\mathbf{x})$ in Equation 7.2, the extended Kalman filter formulation was, therefore, retained. Equation 7.2 was linearised at every sampling interval. The deviations in the state and measured variables $\delta\mathbf{X}$ and $\delta\mathbf{y}$ were processed through the filter algorithm instead of the actual $\mathbf{y}$ and $\mathbf{X}$, where the symbol δ denote deviation from the last sampling instant.

7.3.1 Filter Equations

The discrete form of the Kalman filter was employed. The basic formulation of the Kalman filter has been presented in Section 2.10.1, Equations 2.123 to 2.128. For the non-linear distillation system the equations were formulated as follows:

Prediction step

$$\mathbf{X}^*(k+1, k) = \Phi(k+1, k)\, \mathbf{X}^*(k, k) \qquad 7.5$$

$$\underline{P}(k+1, k) = \Phi(k+1, k)\, \underline{P}(k, k)\, \Phi^T(k+1, k) + \underline{Q} \qquad 7.6$$

Estimation step

$$\underline{K}(k+1) = \underline{P}(k+1, k)\, \underline{M}^T(k+1)\, [\underline{M}(k+1)\, \underline{P}(k+1, k)\, \underline{M}^T(k+1) + \underline{R}]^{-1} \qquad 7.7$$

$$\delta\mathbf{X}\,\hat{}\,(k+1, k+1) = \delta\mathbf{X}^*(k+1, k) + \underline{K}(k+1)\, [\delta y(k+1) - \underline{M}(k+1)\, \delta\mathbf{X}^*(k+1, k)] \qquad 7.8$$

$$\underline{P}(k+1, k+1) = [I - \underline{K}(k+1)\, \underline{M}(k+1)]\, \underline{P}(k+1, k) \qquad 7.9$$

or

$$\underline{P}(k+1, k) = [I - \underline{K}(k+1)\, \underline{M}(k+1)]\, \underline{P}(k+1, k)\, [I - \underline{K}(k+1)\, \underline{M}(k+1)]^T + \underline{K}(k+1)\, \underline{R}\underline{K}(k+1)^T \qquad 7.10$$

where k denotes sampling instant. The $\delta\mathbf{X}^* = \mathbf{X}^*(k+1,k) - \mathbf{X}\,\hat{}\,(k,k)$ and $\delta y = y(k+1) - y\,\hat{}\,(k)$. The * and ^ denote prediction and estimate, and Φ denotes the transition matrix. The $\underline{Q}$ is the system noise covariance matrix, $\mathbf{E}[w\, w^T]$ where w is the vector of the noise affecting the system and $\mathbf{E}$ is the mathematical expectation operator. The $\underline{R}$ is the measurement noise covariance matrix given by $\mathbf{E}[v\ v^T]$ where v is the vector of the measurement noise. The $\underline{P}(k, k)$ is the covariance matrix of the error in $\mathbf{X}^*(k, k)$ and $\underline{K}(k + 1)$ is the filter gain matrix. The $\underline{M}(k)$ is the linearised measurement matrix given by

$$\underline{M}(k) = \partial\mathbf{h}\,(\mathbf{X}(k,k) / \partial\mathbf{X}(k,k)$$

such that

$$\delta y(k) = \underline{M}(k)\delta\mathbf{X}(k)$$

Equation 7.5 represents integration of $\mathbf{X}$ over the sampling interval Δt. This was done by integrating the filter model using the simple Euler method.

The transition matrix, Φ, is given as:

$$\Phi = (I + \mathbf{A}\, \Delta t) \qquad 7.11$$

The measurement matrix

$$\underline{M} = \partial\mathbf{h}\,(\mathbf{X}(k,k) / \partial\mathbf{X}(k,k) \qquad 7.12$$

contains the linearised forms of $\frac{dT_j}{dx_j}$, where j represents the tray number and x_j the composition of the more volatile component in tray j. For example, if the temperature of tray 7 is measured and it is the third measurement, that is, $y(3) = T_7$, then

$$\underline{M}(3, 7) = \frac{dT7}{dx7}, \qquad 7.13$$

The values of $\frac{dT_j}{dx_j}$ are obtained numerically by perturbing the function in Equation 7.4 with respect to T and then

$$\frac{dT_j}{dx_j} = 1 / \left(\frac{dx_j}{dT}\right). \qquad 7.14$$

7.3.2 The computational sequence of the filter algorithm.

The Kalman filter algorithm computational sequence is given in the following.

Step 1) Set k = 0, supply filter with state estimate X^(k,k), $\underline{Q}$, $\underline{R}$, and $\underline{P}$(0,0). Derive y^(k) form X^(k,k) and then compute measurement matrix $\underline{M}$(k+1) sing y^(k) as the reference trajectory to be used at the next sampling interval

Step 2) Start filter algorithm

Step 3) Compute the predicted state vector X*(k+1,k) at next sampling interval by integrating the filter process model from X^(k,k).

Step 4) Compute $\underline{P}$(k+1,k) from Equation 7.6

Step 5) Get process measurements y(k+1) and compute the state and the measurement deviations as

$$\delta X^*(k+1,k) = X^*(k+1,k) - X^\wedge(k,k)$$

$$\delta y(k+1) = y(k+1) - y^\wedge(k)$$

Step 6) Compute the filter gain matrix using Equation 7.7

Step 7) Compute estimate of the state deviations $\delta X^\wedge(k + 1, k + 1)$ from Equation 7.8 and then compute $\delta y^\wedge(k+1)$ as

$$\delta y^\wedge(k+1) = \underline{M}(k+1)\, \delta X^\wedge(k + 1, k + 1)$$

Step 8) Compute the state estimate and the estimate of the measurement vector:

$$X^\wedge(k+1, k+1) = X^\wedge(k, k) + \delta X^\wedge(k + 1, k + 1)$$

$$y^\wedge(k+1) = y^\wedge(k) + \delta y^\wedge(k+1).$$

These are now new reference trajectories.

Control actions should be computed and implemented at at this point.

For EAFF control the filter model integrates the estimates $\mathbf{X}\hat{}(k+1,k+1)$ up to the next sampling instant, k+2, to give $\mathbf{X}^*(k+2,k+1)$. Control is then based on the top tray and the bottom tray compositions contained in $\mathbf{X}^*(k+2,k+1)$.

Step 9) Compute new measurement matrix to be used at the next sampling instant using $\mathbf{y}\hat{}(k+1)$

Step 10) Compute $\underline{P}(k+1,k+1)$ using Equation 7.10

Step 11) Set k = k+1 and then jump to Step 2)

7.4 Off-line Kalman Filtering Studies

The software programs that perform the Kalman filtering are explained in Appendix A4 and listings are in Appendix A7. The whole package is written in Basic09 on the System 96.

Since the linearised state variable model used as the filter model is a rough approximation of the column simulator, it is therefore much less representative of the actual distillation column than the column simulator. The covariance matrices, $\underline{P}$ (0,0), $\underline{Q}$ and $\underline{R}$, are design parameters which can be adjusted to tune the filter to obtain the best filter performance possible. The elements of the $\underline{Q}$ matrix can be made larger to compensate for the model inaccuracies such as non linearities. Care must, however, be excercised in choosing these elements as the diagonal elements of the computed variances of the state variables elements of $\underline{P}(k,k)$ should not be too large in relation to the state variables otherwise the estimates may oscillate about the true states.

The state vector, $\mathbf{X}$, contains of

$$\mathbf{X} = (x_1, x_2, x_3, x_4, x_5, x_6, x_7, x_8, x_9, x_{10}, \text{Lr, Qrb, F, xf})$$

7.15

The measurements supplied to the filter are 5 tray temperatures and the four inputs, Lr, Qrb, F, xf. The measurement vector contains ;

$$\mathbf{y} = (T_1, T_2, T_7, T_9, T_{10}, \text{Lr, Qrb, F, xf}) \qquad 7.16$$

where the j in T_j denotes the tray. This large number of measurements were taken to partly compensate for the model inaccuracies. The top tray and the bottom tray temperatures, T_1 and T_{10}, were selected as measured variables because the liquid compositions on these trays would be the controlled variables. Although on-line measurement of the feed composition was not available, the feed composition was assumed measured in the filter because the feed was thoroughly mixed before the start of the experiment, as is reported in Appendix A1.3

In the filter model, Lr, Qrb and F have the units g/minute, joules per minute (J/min) and g/minute, respectively. They also have these units in the vector **X**. In the measurement vector **y**, these variables are in l/hr, KW and l/hr, respectively. To convert g/minute to l/hr, the liquid density was assumed to be constant at 1.5 g/cm^3. The measurement matrix $\underline{M}$ relating **y** and **X** handled the necessary conversions as is shown in Table 7.1.

Table 7.1 The Measurement matrix $\underline{M}$

Entry	Measurement
$\underline{M}(1,1) = \frac{dT_1}{dx_1}$	T_1, °C
$\underline{M}(2,2) = \frac{dT_2}{dx_2}$	T_2, °C
$\underline{M}(3,7) = \frac{dT_7}{dx_7}$	T_7, °C
$\underline{M}(4,9) = \frac{dT_9}{dx_9}$	T_9, °C
$\underline{M}(5,10) = \frac{dT_{10}}{dx_{10}}$	T_{10}, °C
$\underline{M}(6,11) = 0.04$	Lr, l/hr
$\underline{M}(7,12) = 1/60000.$	Qrb, KW
$\underline{M}(8,13) = 0.04$	F, l/hr
$\underline{M}(9,14) = 1.0$	xf, mass fraction

7.4.1 Results

Data from the experimental open loop step response tests shown in Figure 5.9 were used in these studies. The data were collected using sampling interval, Δt, of 30 seconds.

Estimation of the tray compositions

The estimation of the tray compositions, x_1, x_2, x_7, x_9, x_{10}, which had their corresponding tray temperatures measurements supplied to the filter will be discussed first. To represent reality, the initial values of some of the tray composition estimates supplied by the filter were deliberately made to be in error, or biased. The following set of covariance matrices were used:

$\underline{P}(0,0)$ = diag (0.01, 0.01, 0.05, 0.05, 0.05, 0.05, 0.01, 0.05, 0.01, 0.01, 100, 5000, 100, 0.01)

$\underline{Q}$ = diag (0.05, 0.05, 0.4, 0.4, 0.4, 0.4, 0.05, 0.1, 0.05, 0.05, 120, 10000, 120, 0.05)

$\underline{R}$ = diag (0.0001,0.0001,0.0001,00001,0.0001,0.4,10,0.4,0.01)

7.17

Figures 7.1a and 7.1b show the estimation of x_1 and x_2 and x_7, x_9 and x_{10} compared with their "actual" tray compositions, which are represented by the dashed lines. The estimates followed the trajectories of their true values quite well, but the biases in the initial values could not be removed. Only the estimates of x_1, with exact initial values, perfectly tracked the true values; the estimate and true values cannot be distinguished on the graph. Figure 7.1c shows the corresponding trajectories of the sizes of the gain matrix and the covariance matrix.

The trajectories of the baises between the estimated and true values are shown in Figures 7.2a and 7.2b. The biases stayed virtually constant except the relatively large amounts removed by the large step changes in the reflux flow, feed flow and reboiler heat input. Even then, the amount of bias removed from each estimate by each input change was quite small considering the sizes of the input changes.

The estimation of the tray compositions, x_3, x_4, x_5, x_6, x_8, which did not have their corresponding temperatures measured were unstable as the compositions became greater than 1, and the estimates overlapped with the other tray compositions. Figures 7.3a and 7.3b show the estimates for the x_3 and x_8, respectively. The corresponding diagonal elements of $\underline{P}(k,k)$ of these tray compositions at a steady state, t = 15 minutes, showed that the elements attained values greater than 1 throughout the time duration of the filtering exercise. These elements are indicated by ** below.

diag ($\underline{P}(k,k)$) = (2.003×10^{-7}, 1.912×10^{-7}, 151.2**, 1273.54**, 1466.86**, 258.59**, 6.83×10^{-2}, 2.98**, 2.26×10^{-1}, 1.73×10^{-7}, 122.98, 9.99, 123.22, 8.54×10^{-5})

These values "tell" the filter that the error between the estimated values of the tray compositions and the true values are greater than 1, which cannot be true since compositions in a distillation column can have the maximum value of 1. This resulted

in the bad filter performance as large corresponding gain elements were computed, as shown in Table 7.2.

The $\underline{P}(k,k)$ element corresponding to x_8 was much smaller compared with the other trays without temperature measurements. This is because the T_7 and T_9 above and below tray 8 were measured and that temperature measurements were more concentrated in the stripping section than in the enriching section.

Similar results were obtained when very small $\underline{P}(0,0)$ and $\underline{Q}$ elements

$$\underline{P}(0,0) = \text{diag}\ (0.01, 0.01, 0.0001, 0.0005, 0.0005, 0.0005, 0.0001, 0.0005, 0.0001, 0.0001, 100, 5000, 100, 0.01)$$

$$\underline{Q} = \text{diag}\ (0.05, 0.05, 0.0001, 0.0001, 0.0001, 0.0001, 0.05, 0.0001, 0.05, 0.05, 120, 10000, 120, 0.05) \qquad 7.18$$

were specified for the tray compositions. Figures 7.4a and 7.4b show the corresponding x_3 and x_8, respectively. The corresponding diagonal $\underline{P}(k,k)$ elements were smaller, but they were still greater than 1, except for x_8 (marked *** below) which is now less than 1.

$$\text{diag}\ (\underline{P}(k,k)) = (2.003 \times 10^{-7}, 1.9129 \times 10^{-7}, 15.399\ **, 117.29**, 129.07\ **, 25.0**, 9.7 \times 10^{-3}, 0.751**, 1.16 \times 10^{-3}, 1.37 \times 10^{-3}, 122.58, 9.99, 123.22, 8.536 \times 10^{-3}).$$

The estimation of x_8 was, however, still bad.

Table 7.2 Filter Gain Matrix at a steady state, t= 15 minutes

-4.4755 E -2	-3.3963 E-9	1.0402 E -10	-2.9066 E -11	-3.7762 E -10	3.7557 E -8	-1.3221 E -14	-8.5892 E -9	1.9645 E -9
1.4334 E -8	-4 3737 E -2	-8.0934 E -10	2.0348 E -12	-1.4962 E -10	8.5619 E -10	-1.1382 E -15	5.2636 E -11	-4.6566 E -10
6.4978 E -2	1.8382 E -1	-6.0826 E -2	9.4007 E -3	1.3912 E -1	2.6046 E -1	-4.0655 E -8	-1.1796 E -1	-1.2061
-1.8796 E -1	-2.9198 E-1	2.0715 E -1	-6.404 E -2	-4.8965 E -1	-5.2347 E -1	7.7842 E 08	2.6786 E -1	3.6769
1.9784 E -1	2.0418 E -1	-2.7776 E -1	1.3919 E -1	6.7962 E -1	5.0085 E -1	-9.871 E -8	-2.2893 E -1	-4.1880
-7.9576 E -2	-5.6619 E -2	1.676 E -1	-1.1902 E -1	-3.9999 E -1	-1.7847 E -1	4.9079 E -8	5.9801 E -2	2.0653
-1.0842 E -8	1.5155 E -10	-3.7053 E -2	-4.8671 E -12	5.1224 E -10	-8.0663 E -10	6.2984 E -16	5.0871 E -12	-3.725 E -9
5.9567 E -3	1.1332 E -3	1.4529 E -3	6.1282 E -2	8.6747 E -2	3.1180 E -2	-2.6669 E -9	1.7898 E -2	4.0130 E -3
1.4921 E -11	2.7623 E -12	2.9525 E -12	-3.3610 E -2	5.5830 E -10	5.4559 E -10	-1.1985 E -16	2.8645 E -10	1.1186 E -10
-2.5254 E -10	-3.531 E -11	-4.2624 E -11	4.9510 E -10	-3.0832 E -2	2.6216 E -9	-1.5754 E -15	1.6852 E -9	01.2155 E -9
-8.3838 E -2	1.1742 E -3	-2.9919 E -4	-1.5133 E -3	-8.4008 E -3	12.2980	7.5247 E -9	2.6054 E -3	-5.9073 E -3
2.9473 E -8	-5.5638 E -10	1.9389 E - 11	2.7287 E -10	5.1281 E -9	7.5247 E -9	9.9900 E -1	-6.6068 E -10	3.0502 E -10
1.9192 E -2	-2.7240 E -4	-3.3156 E -5	-9.3050 E -4	-5.4678 E -3	2.6053 E -3	-6.6066 E -10	12.3259	-2.7319 E - 3
-4.3371 E-6	-1.0944 E -6	-1.5648 E -6	-2.4967 E -7	3.9392 E -6	-5.9079 E -6	3.0504 E -13	-2.7315 E -6	8.5405 E -1

E - j → x 10^{-j}

Estimation of the parameters Lr, Qrb, F, and xf.

The best estimates of the measured Lr, Qrb, F were obtained using the covariance matrices of Equation 7.17. Figure 7.5 and 7.6 show the results for F and Lr, respectively. The estimates of Lr and F were good primarily because these variables were measured. The filter smoothed the measurements of F and Lr, but both overshoot their measured values after the large step changes. The Lr estimates subsequently exhibit oscillatory response.

The figures also show what happens when the corresponding Q elements of Lr, and F (marked ** below) were too small.

$\underline{P}(0,0)$ = (0.01, 0.01, 0.05, 0.05, 0.05, 0.05, 0.01, 0.05, 0.01, 0.01, 100, 10, 100, 0.01)

$\underline{Q}$ = (0.05, 0.05, 0.4, 0.4, 0.4, 0.4, 0.05, 0.1, 0.05, 0.05, 1**, 10, 1**, 0.05)

The filter now disregarded the measured values of these inputs and relied more on its inaccurate model to produced their estimates. The result was the poor tracking of F and Lr, as their estimates simply exhibited oscillatory behaviour with large amplitudes after there respective step changes. In the case of Qrb, smaller $\underline{P}(0,0)$ and $\underline{Q}$ elements was not too detrimental as shown in Figure 7.7. The overshoot was present after the set changes, but good estimates were produced within a short time.

Figure 7.8 shows what happens when xf was not measured, but was estimated as a state variable. The estimates produced were very oscillatory, as the trajectory was greatly affected by the changes in all the other inputs. This demonstrated that the xf must be measured to obtain stable satisfactory estimates of the variable. The same applied for the other inputs as well.

7.4.2 Discussion of the results

The Kalman filter was unable to give the following :

1) Remove the biases from the tray composition estimates,

2) Produce stable estimates of the tray compositions without tray temperature measurements and

3) Produce good estimates of the unmeasured feed composition,

This was because of the large inaccuracy of the filter model and that the sampling interval ΔT of 30 seconds is relatively long. The results demonstrated that the complete removal of biases in the tray composition estimates required the large changes in the inputs Lr, Qrb and F to be entering the system continuously. This requirement is a limitation since large changes in the inputs will not occur at, or near, steady state. Furthermore, in practice, the true values of the tray compositions will not be available since this is the primarily the reason why the filter was needed in the EAFF algorithm. Even when accurate knowledge of the tray compositions are available, biases will arise due to changes in operating conditions as the distillation column is non-linear.

7.4.3 Computational requirement of the Kalman Filter

The Kalman filter program presented in Appendix A7 and explained in Appendix A4 basically consists of matrix manipulation routines. The software was developed to handle a maximum of 15 state variables and 10 input measurements. This meant a large program memory requirement. The software required 6K for program storage and 12K for data storage. The size could be reduced but this was prevented by a limitation in Basic09. As reported in Chapter 4, the arrays and vector sizes must be explicitly declared in terms of the maximum possible size it will need during program execution. This limited the portability of the matrix manipulation routines so that the array and vectors in the package had to be declared in terms of the largest size which were 15 x 1 for vector and 15 x 15 for matrices.

Despite the large memory requirement of the filter algorithm, the ample memory on the System96 allowed all the program modules required to perform the off-line filtering studies to be in the computer memory. There was no need for program overlay as was required by Shaffii (115). Having said this, at run time, the filter program usually needed 60K of memory which is as large as the 64K limit that a single task can have on the System 96.

The filter cycle time was also excessive due to the computational load of the calculations involved. The filter required 72 seconds per cycle for 9 measurements and

14 state variables. This was more than twice the sampling interval of 30 seconds chosen for the control the the top and bottom tray compositions, and about 5 times the "target" interval of 15 seconds. Table 7.3 gives details of the times required by the major tasks in the filter algorithm. As expected, the filter cycle times dropped greatly with the number of measurements. These cycle times for the cases shown on Table 7.3 were still significantly longer than the maximum and target interval of 30 seconds and 15 seconds, respectively.

7.4.4 Conclusions and Recommendations

The conclusion that can be drawn from the off-line studies discussed above is that that the filter cannot be used for on-line application on the distillation column where the sampling time of 30 seconds is required for control and good estimates of all the required variables are needed. The filter failed to remove biases in the tray composition estimates except when the inputs and disturbances entered the column. It also produced unstable estimates of the tray compositions without associated tray temperature measurements and the cycle time required was too large.

The high inaccuracy of the filter model and the long sampling interval used were the major causes of the poor performance of the filter. For this model to be valid a much shorter sampling interval is necessary. The demand for computational power will then be more. All these factors were the reasons why further work regarding on-line application of EAFF scheme was not pursued.

It is suggested that a more accurate filter model such as the column simulator should be used for better performance of the filter to be achieved. The computational requirements would, however, increase significantly. The model reduction procedure suggested by Cho and Joseph (17,18,19) could useful in this respect. The procedure is based on the assumption that a separation column can be approximated by a distributed system in which the composition and flow profiles of the column can be represented as continuous variables along the length of the column. Thus the composition and flow profiles can be represented as the polynomials with respect to the length of the column. Cho and Joseph (18,19) have demonstrated that there

procedure could be used to reduce the order of a distillation column by a factor of 4 and still retain very good accuracy.

Table 7.3 Computer processing time required to perform the filter tasks.

(14 state variabes estimates - the 10 tray compositions, Qrb, Lr, F, and xf)

Task Computation of	Real time required in seconds
Covariance Matrix P(k+1,k)	14
Filter Gain K(k)	23
Covariance Matrix P(k,k)	25
Others**	10
Total	72
@Total for 8 measurements	62
@@Total for 6 measurements	45
@ 4 tray temperatures, Qrb, Lr, F and xf	
@@ 3 tray temperature, Qrb, Lr, F	
** Others - include integration of filter model at the prediction step, data storage, retrieval or real process data from floppy disk, and calculation of the measurement matrix .	

Figure 7.1a Estimation of the tray compositions corresponding to the tray temperatures measurements : Tray 1 and Tray 2

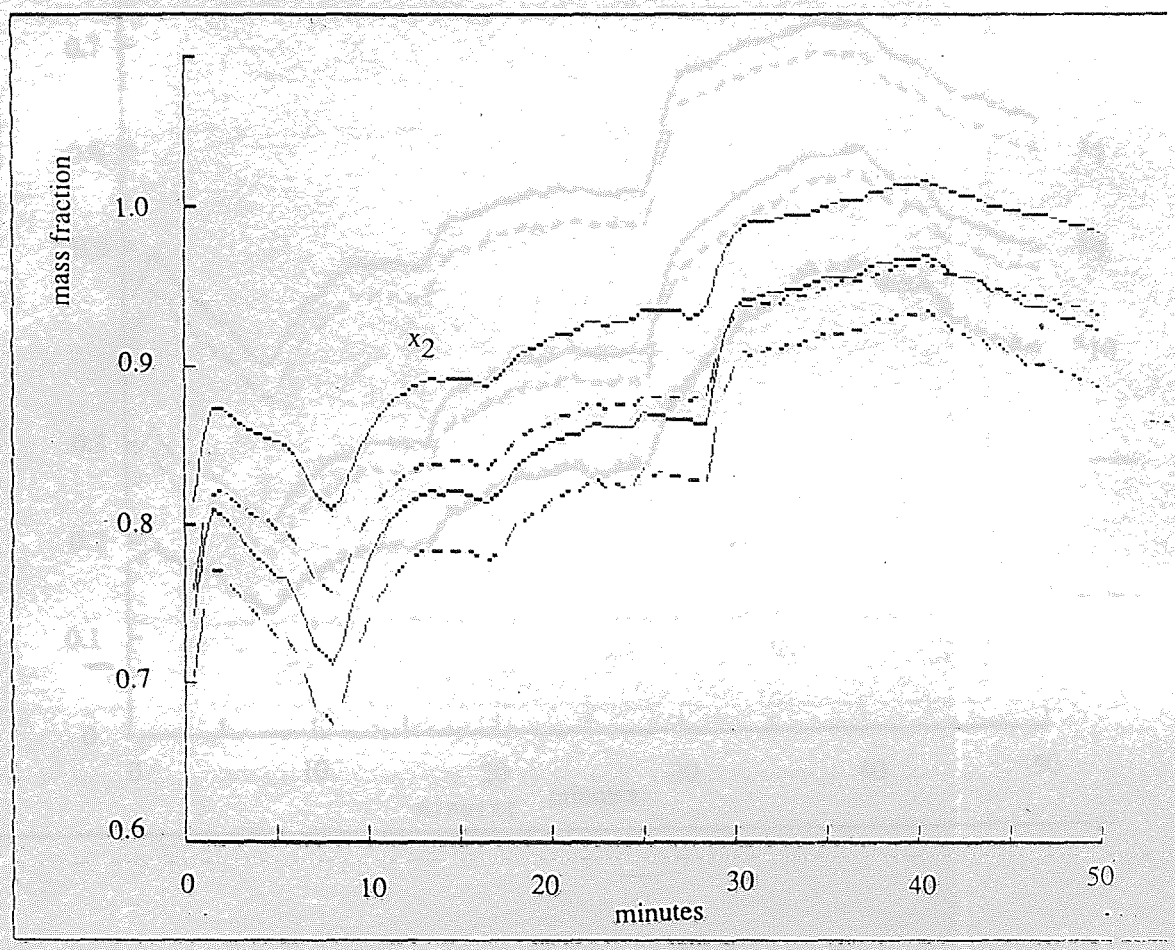

Figure 7.1b Estimation of the tray compositions corresponding to the tray temperatures measurements: Tray 7, Tray 9 and Tray 10

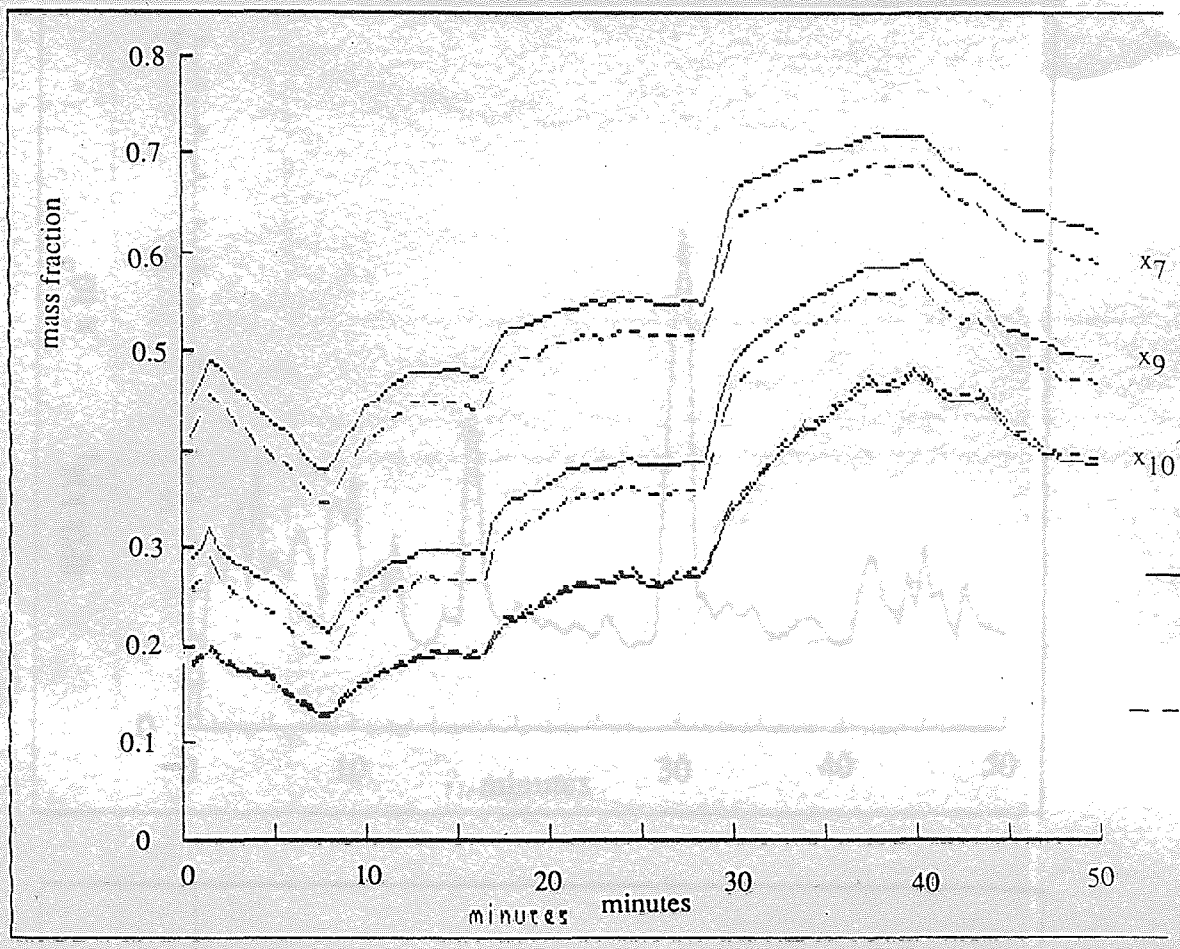

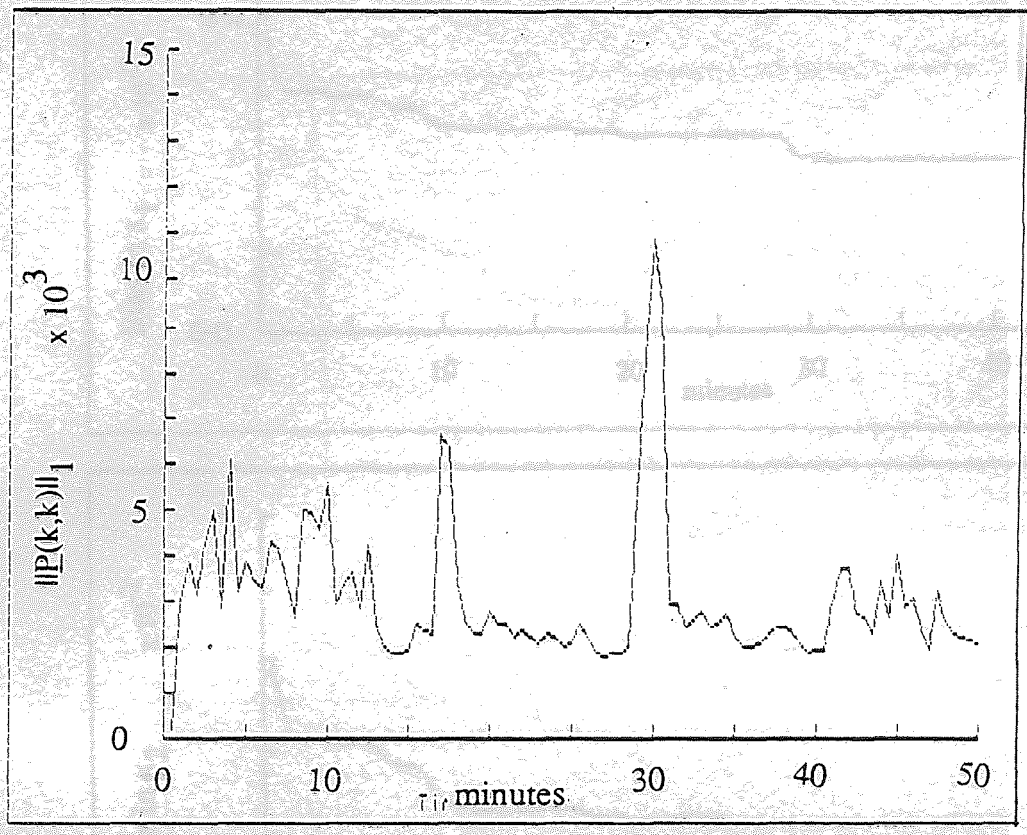

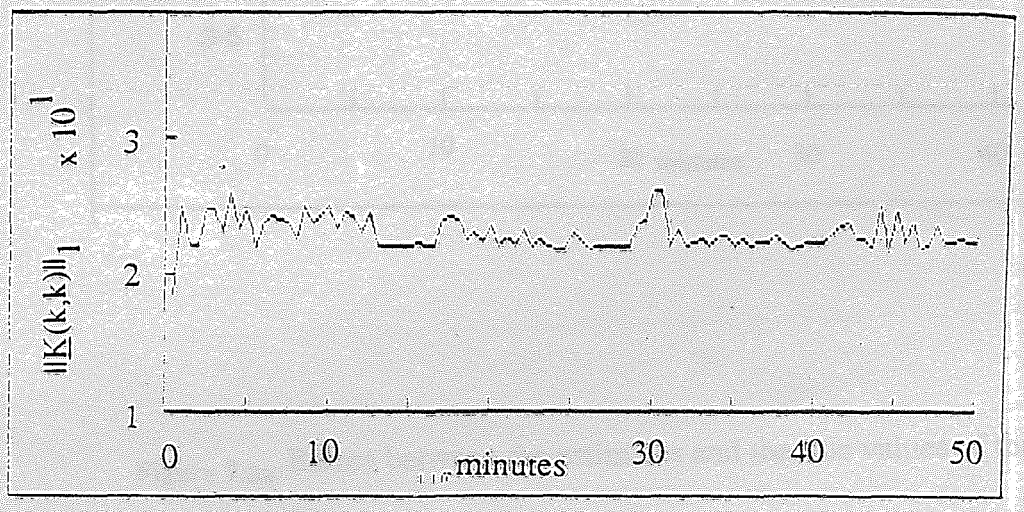

7.1c Trajectories of the 1- norms of the covariance and the filter gain matrices

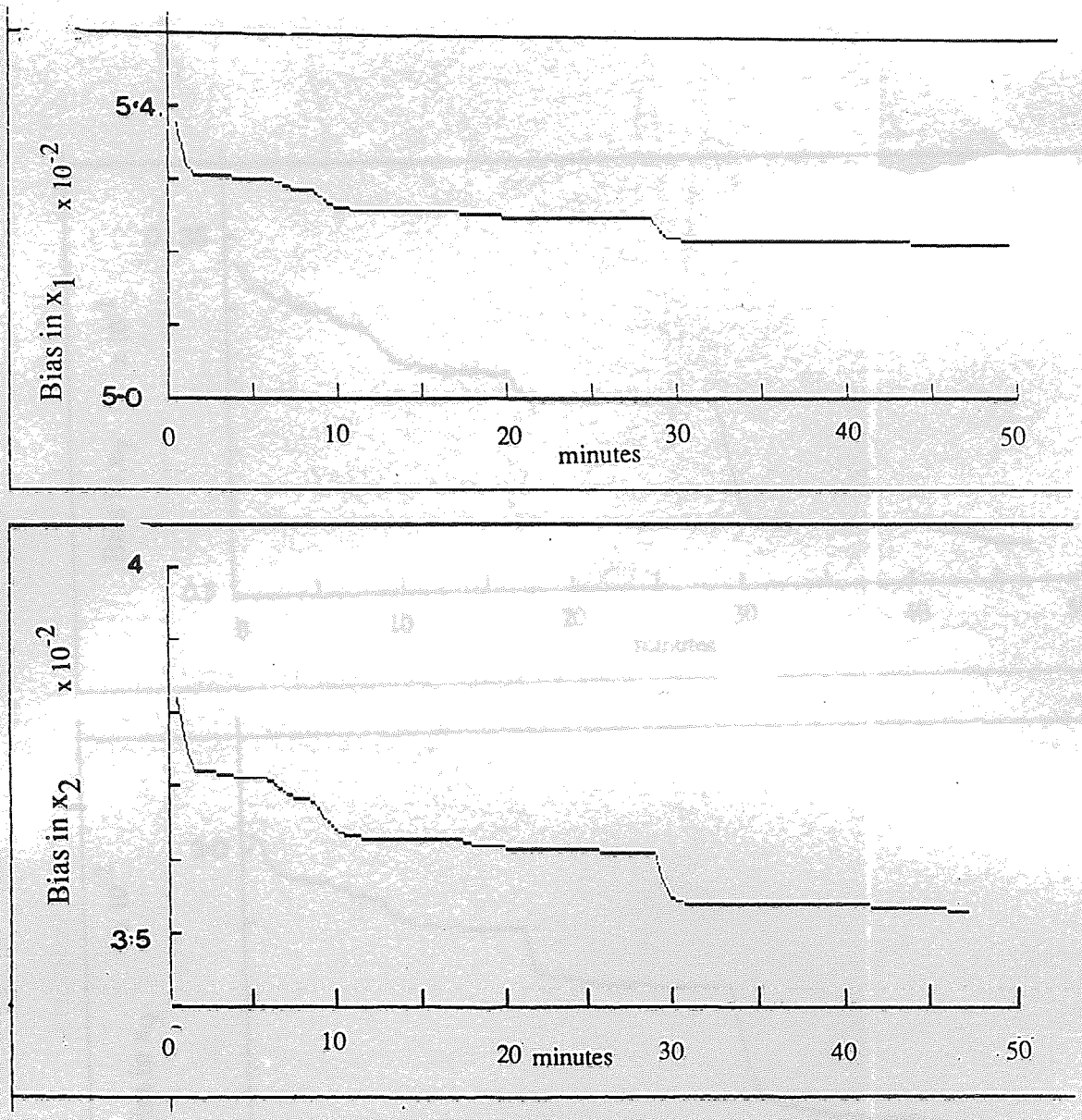

Figure 7.2a Baises between the estimates and the true values of the tray compositions: Tray 1 and Tray 2 .

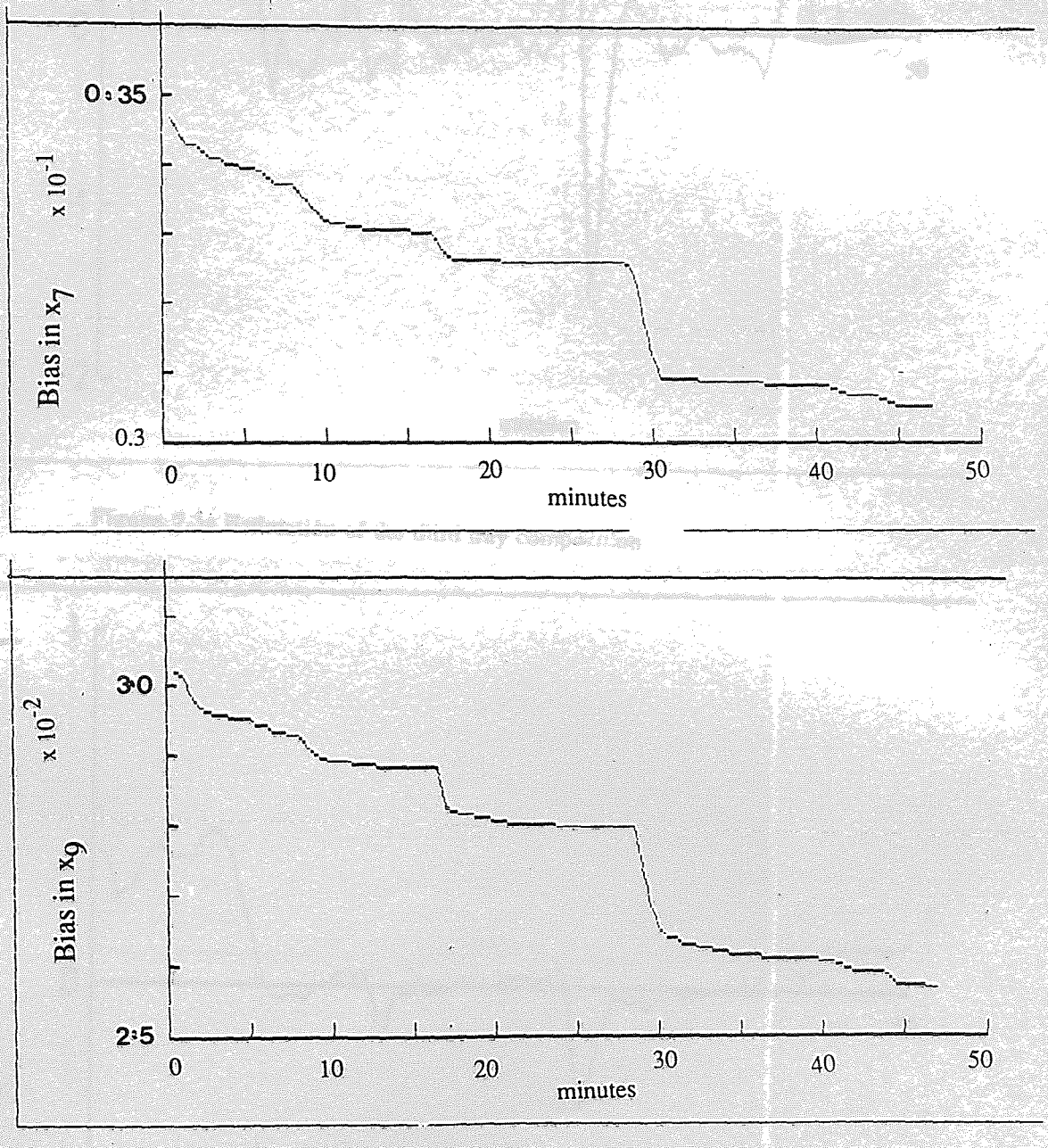

Figure 7.2b Baises between the estimates and the true values of the tray compositions: Tray 7 and Tray 9

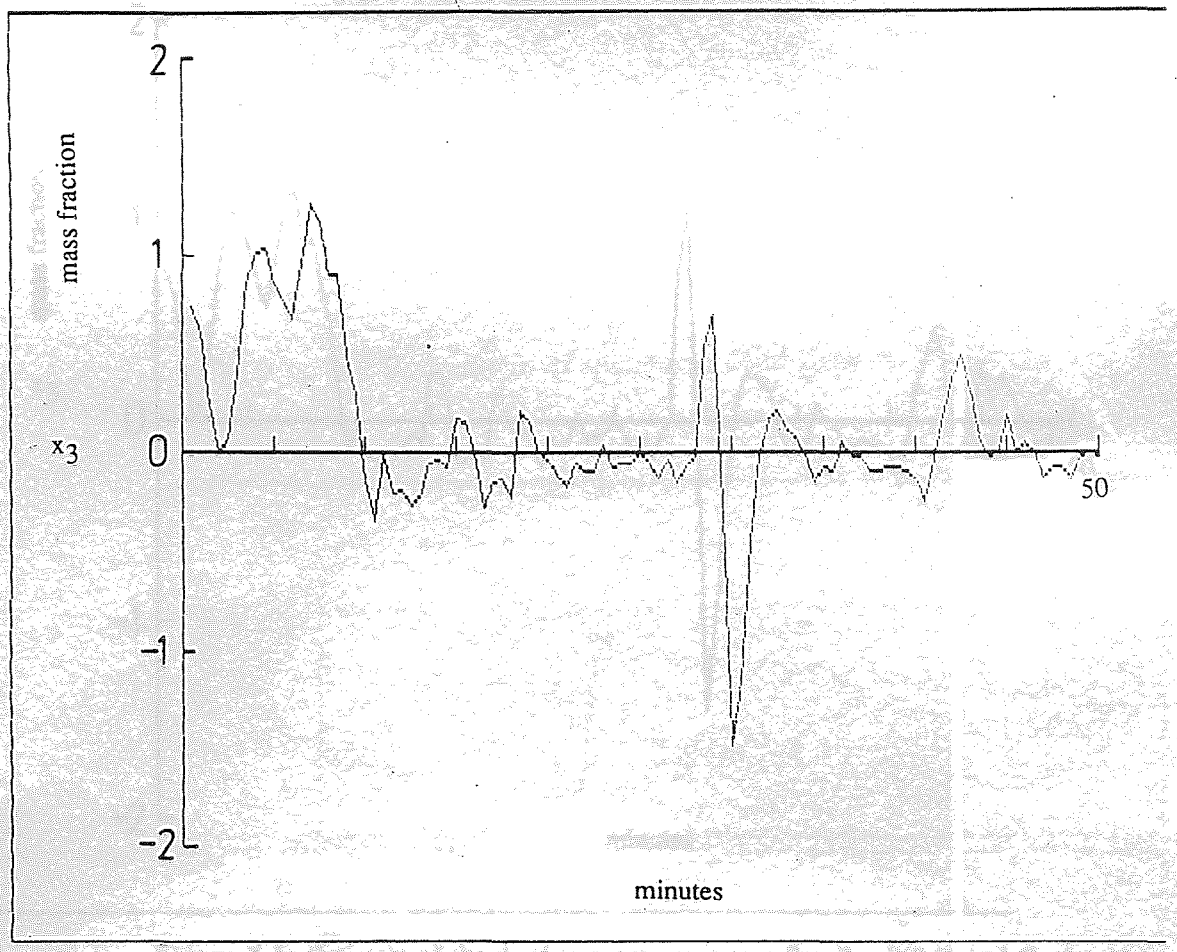

Figure 7.3a Estimation of the third tray composition

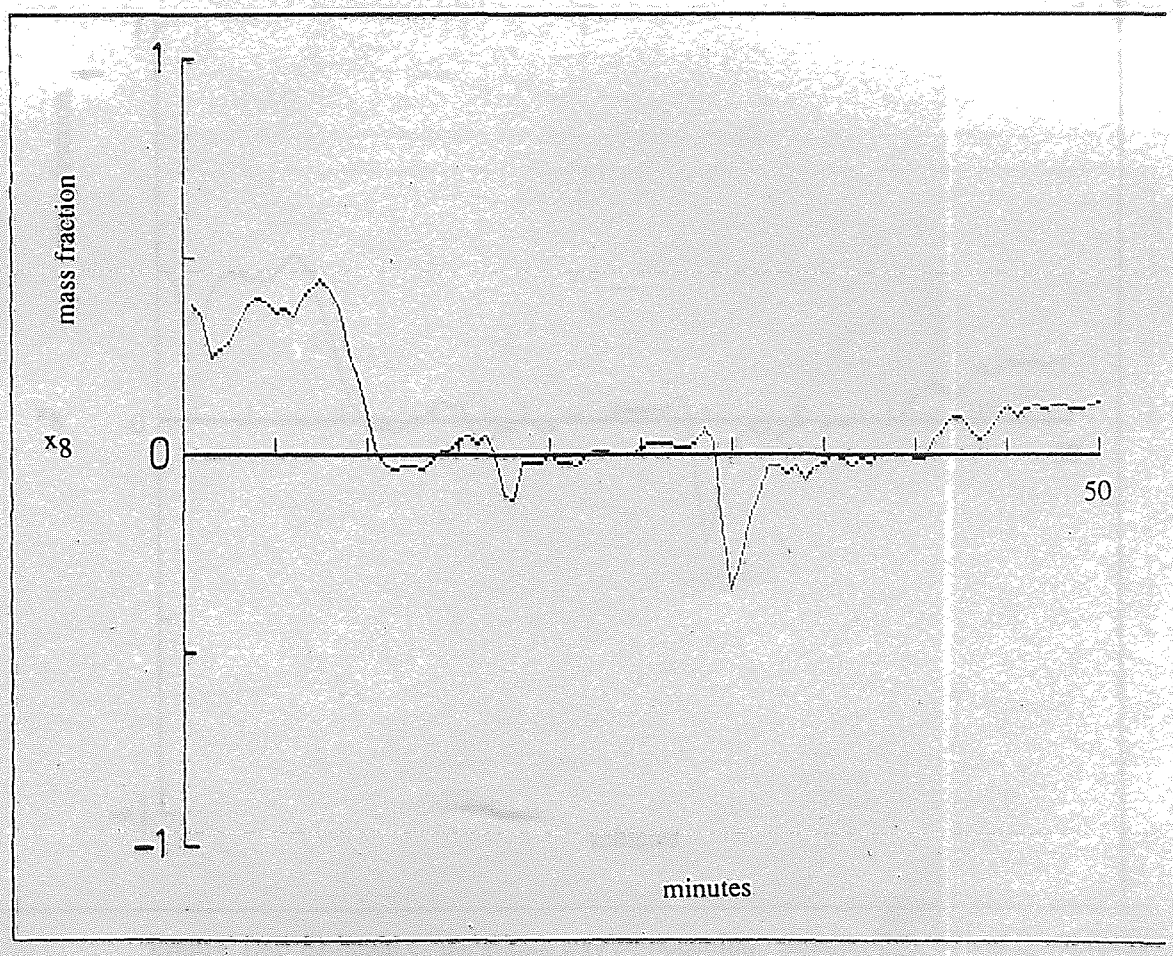

Figure 7.3b Estimation of eighth tray composition

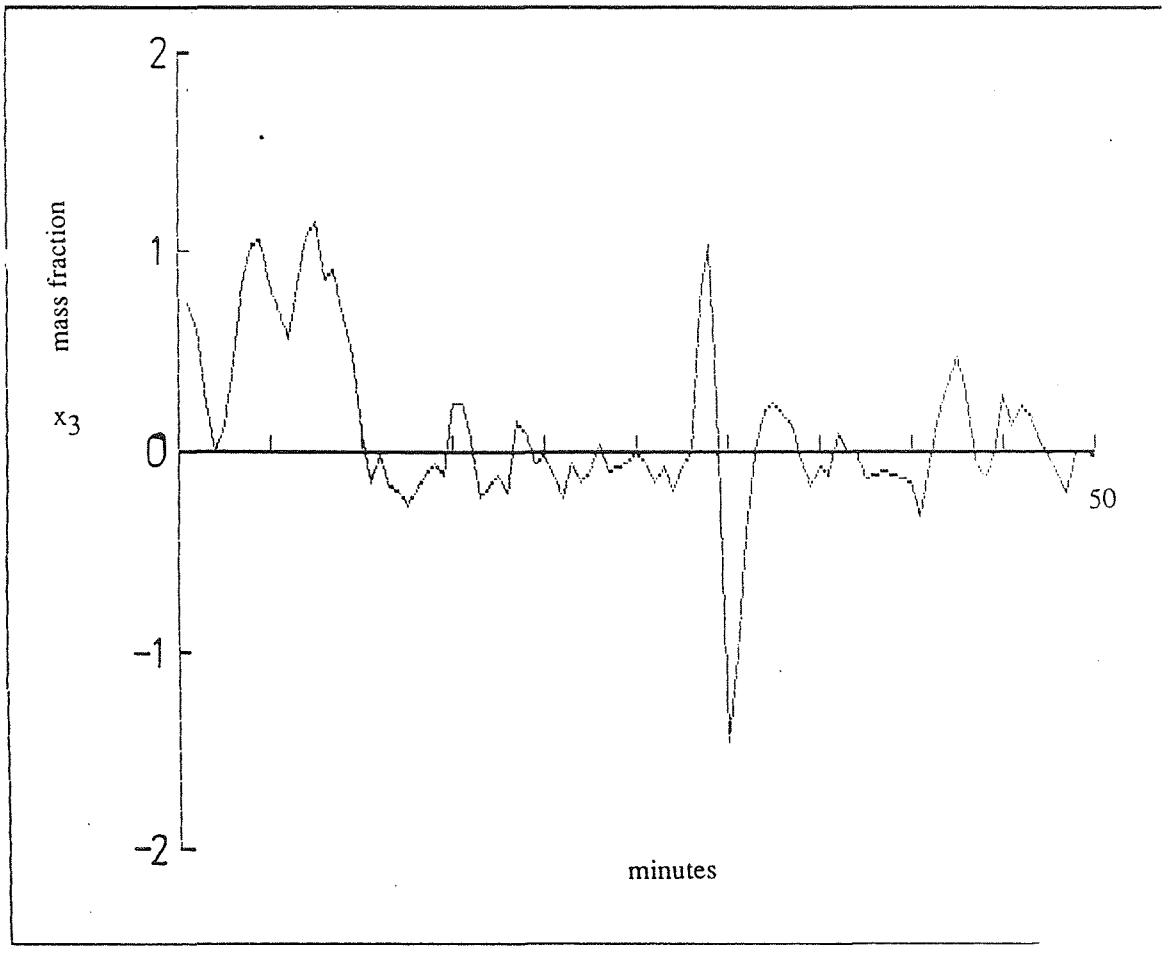

Figure 7.4a Estimate of the third tray composition : Smaller $\underline{P}(0,0)$ and $\underline{Q}$ elements for the tray compositions.

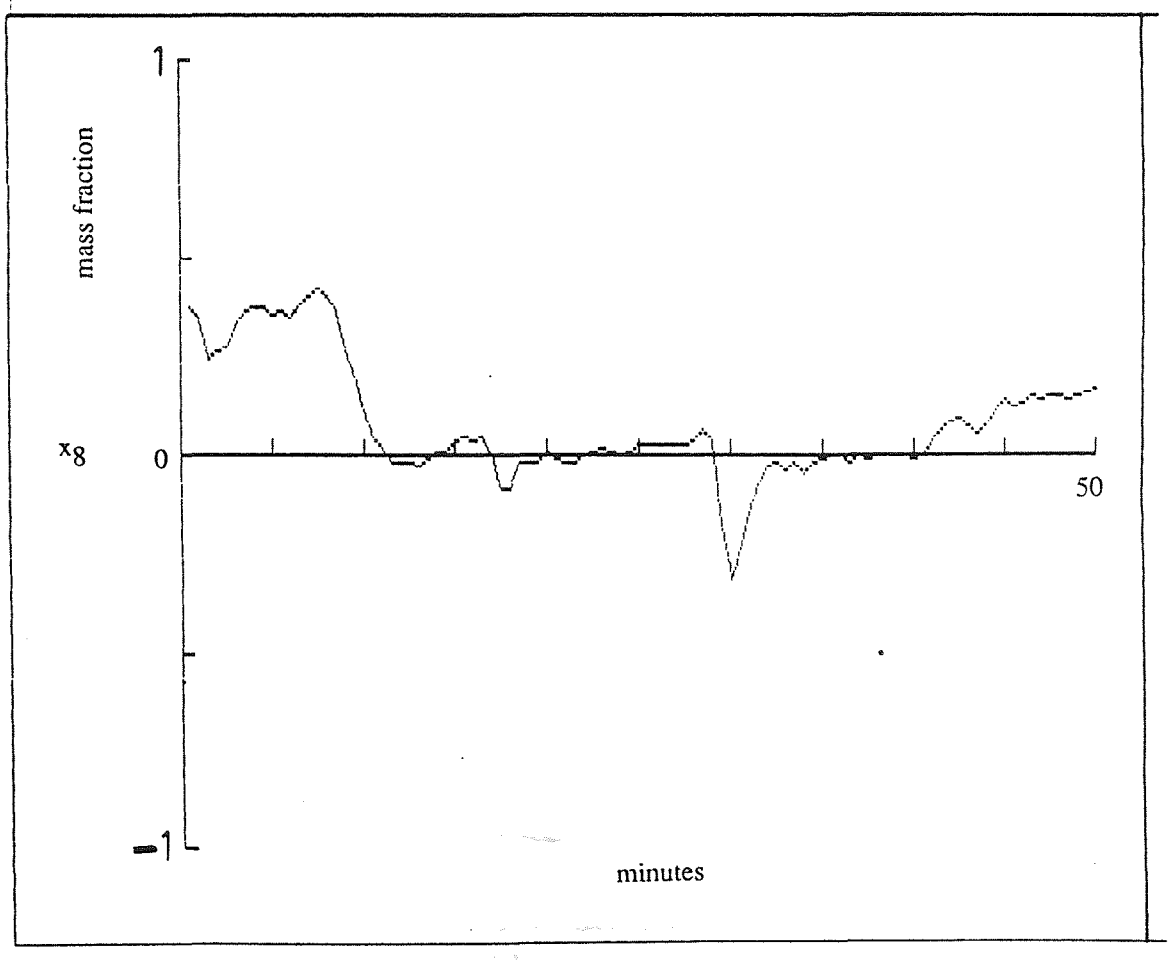

Figure 7.4b Estimate of the eighth tray composition : Smaller $\underline{P}(0, 0)$ and $\underline{Q}$ elements for the tray compositions without tray temperature measurements.

Figure 7.5 Estimation of measured feed flow

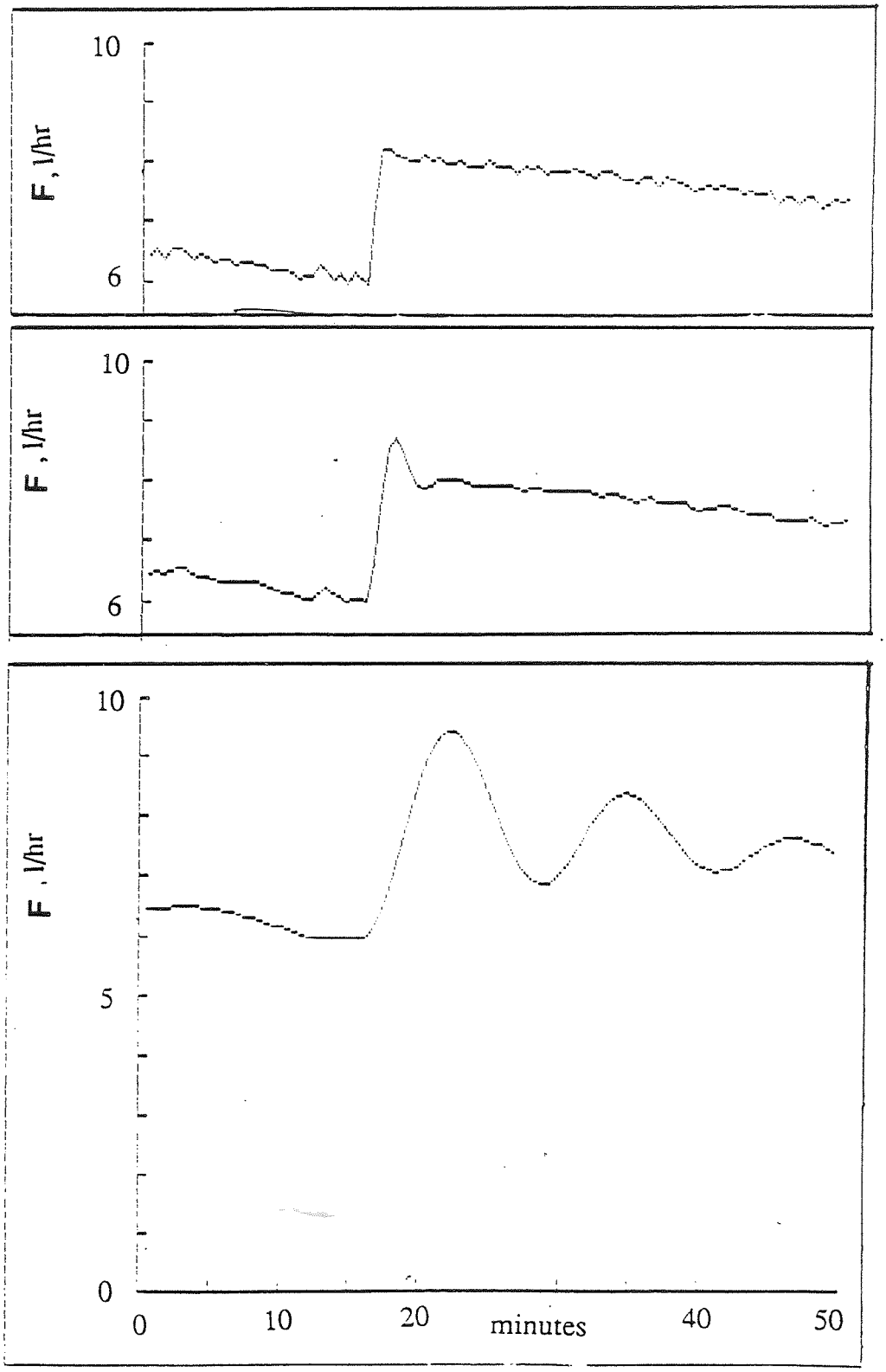

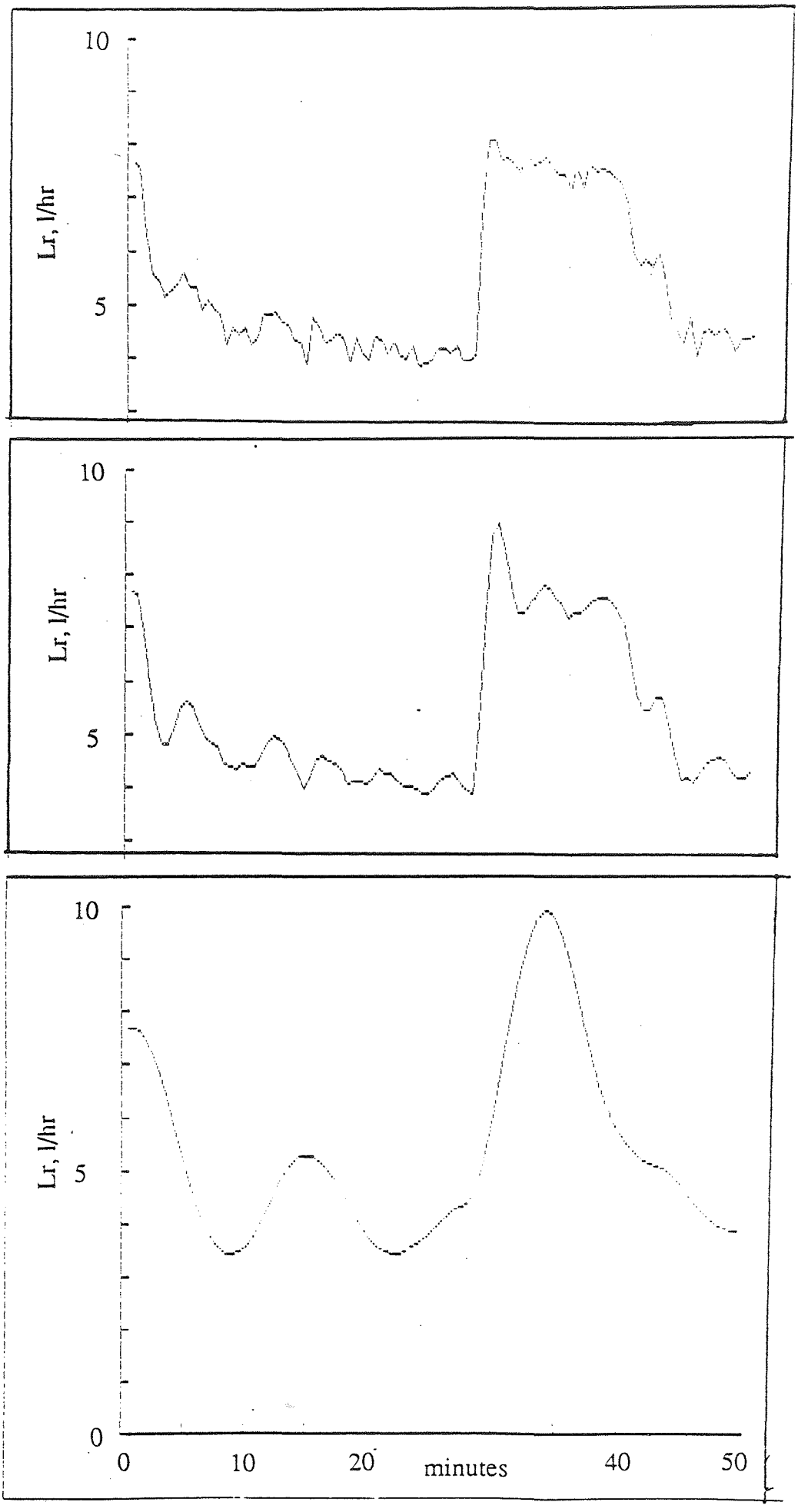

Figure 7.6 Estimation of measured reflux flow

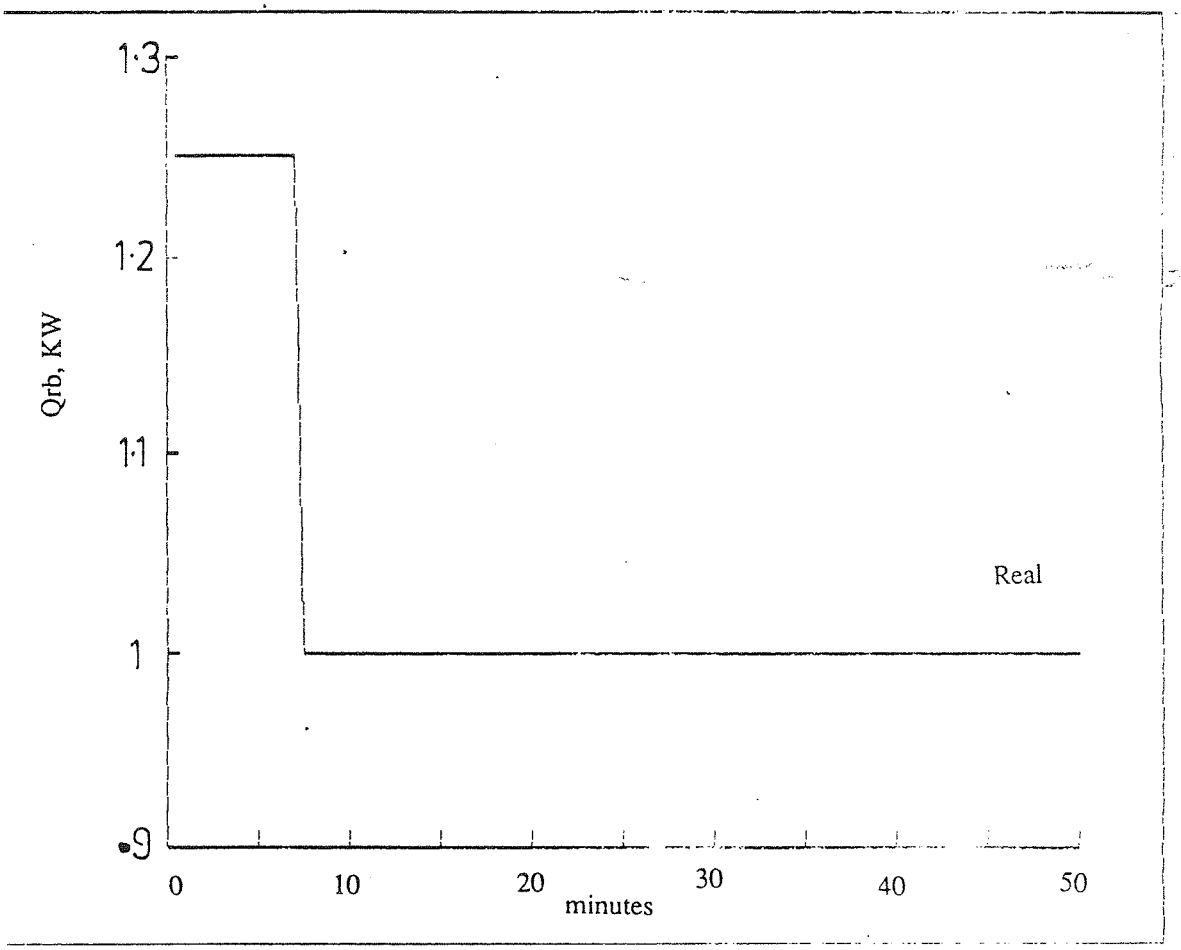

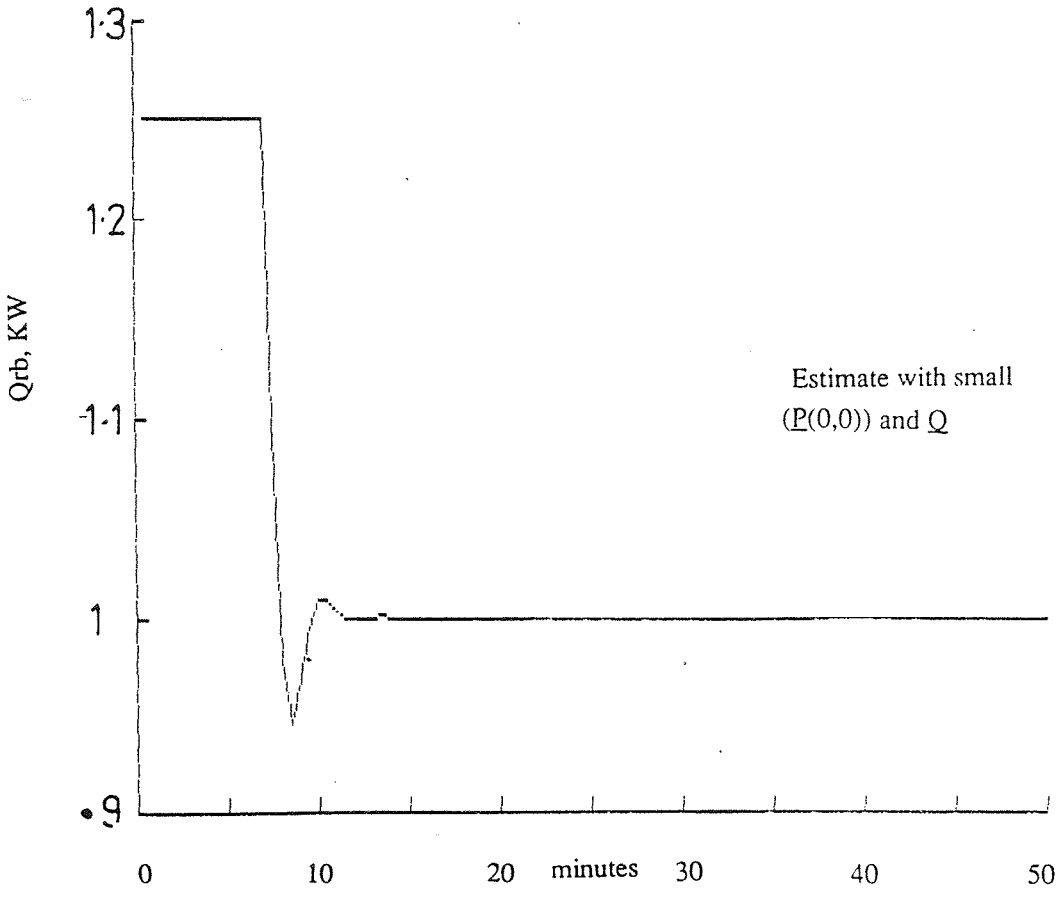

Figure 7.7 Estimation of reboiler heat input

Figure 7.8 Estimation of unmeasured feed composition